universität wien

MASTERARBEIT

Titel der Masterarbeit

„Towards a Complex of the Mycobacterial Proteasome“

verfasst von

Matthias Langer, BSc

angestrebter akademischer Grad

Master of Science (MSc)

Wien, 2015

Studienkennzahl lt. Studienblatt:	A 066 834
Studienrichtung lt. Studienblatt:	Masterstudium Molekulare Biologie
Betreut von:	Tim Clausen, PhD

TABLE OF CONTENTS

0. INDEX OF ABBREVIATIONS

APS	ammonium persulfate
Bpa	bacterial proteasome activator (Rv3780)
CP	core particle
CP_{T54V}	core particle containing the T54V mutation in the β-subunit
CP_{PL}	core particle containing the K52A (**p**ocket **l**ysine) mutation in the α-subunit
DMSO	dimethylsulfoxide
Dop	Deamidase of protein Pup (Pup deamidase/depupylase)
EM	electron microscopy
ID	intermediate domain (of Mpa)
Mpa	*Mycobacterium* proteasomal ATPase
Mtb	*Mycobacterium tuberculosis*
MWCO	molecular weight cut-off
n-CP	nascent core particle (prior to processing of the β-subunits)
NHS	N-hydroxy-succinimide
PafA	Proteasome accessory factor A (Pup-protein ligase)
***p*Bpa**	*para*-benzoyl-L-phenylalanine
PPS	Pup-proteasome system
PTA	phosphotungstic acid
Pup	prokaryotic ubiquitin-like protein
PVDF	polyvinylidene fluoride
RNS	reactive nitrogen species

RP	regulatory particle
STINT-NMR	Structural interaction nuclear magnetic resonance
Suc-LLVY-AMC	*N*-Succinyl-Leucine-Leucine-Valine-Tyrosine-7-amino-4-methylcoumarin
TB	tuberculosis
TEMED	tetramethylethylenediamine
UA	uranyl acetate
Ub	Ubiquitin

1. INTRODUCTION

1.1. Tuberculosis: epidemiology and significance

Worldwide, tuberculosis is the most lethal infectious disease after HIV/AIDS and the most lethal bacterial infectious disease altogether, with approximately one third of the entire world population latently infected by its causative agent *Mycobacterium tuberculosis.* Of an estimated 9 million people developing the disease in 2013, approximately 1.5 million died of it. Tuberculosis, despite the availability of a vaccine and the established treatment by combined antibiotic therapy, is still a major global health concern and is likely to remain so for the foreseeable future, even though the rate of new cases has been falling annually by 1.5% between 2000 and 2013 and the mortality rate has been reduced by 45% between 1990 and 2013.[1]

The relationship between tuberculosis and HIV infection has long been established as clinically significant. Of the 9 million people worldwide that developed tuberculosis in 2013, 13% (approx. 1.1 million) were found to be HIV-positive, with the vast majority of both cases and deaths (78%) occurring in sub-Saharan Africa.[1] HIV infection increases the probability of subsequent tuberculosis by more than an order of magnitude, from approximately 20-fold in countries with generalized HIV epidemics to approximately 37-fold in countries with low HIV infection rates.[2] Out of approximately 1.6 million AIDS-related deaths in 2012, 320.000 or 25% of those were due to tuberculosis, making tuberculosis the leading cause of death among AIDS patients.[3,4] While tuberculosis is primarily a disease of the lungs in most adults, a concomitant HIV infection can turn it into a systemic phenomenon.[5]

M. tuberculosis is transmitted in the aerosolized saliva or mucus of an infected person. The process is highly efficient, with only 5-10 colony forming units (CFUs) required to infect at least 95% of mice and the ID_{50} calculated at only 1.6 CFU.[6] When *M. tuberculosis* successfully infects a host, in the vast majority of cases (approximately 90-95%) the bacterium remains in a dormant stage that can last from weeks to several decades. This latent form of *M. tuberculosis* infection is difficult to detect, since symptoms are mild at best and often do not show at all. Although standard antibiotics (isoniazid, rifampicin, pyrazinamide and ethambutol) are effective in treating tuberculosis, the development of multidrug-resistant tuberculosis (MDR-TB) through incompletely administered antibiotics therapy poses an additional challenge for health services to overcome.[3,7]

M. tuberculosis is able to survive inside phagocytic phagosomes, an ability it shares with several other important pathogenic bacteria such as *Mycobacterium leprae* (the causative agent of Hansen's disease, i.e. lepra) *Legionella pneumophila, Listeria monocytogenes, Yersinia pestis, Bacillus anthracis* and *Streptococcus* sp.[8] Indeed, almost the entire life cycle of *M. tuberculosis* takes place inside the macrophages of the host.[9] During infection, the metabolism of *M. tuberculosis* is adapted to the conditions in the host, turning to fatty acids as its primary carbon and energy source. The metabolic pathways of the host macrophages themselves are manipulated, artificially enhancing their glucose uptake and inducing the formation of lipid droplets of triacylglycerol in the host cell that are subsequently taken up and used for storage by the bacterium.[10,11] This process is connected to the induction of the dormant state of *M. tuberculosis*, a stadium that can last for decades.[12]

M. tuberculosis' genome was sequenced in 1998, showing an unusually high amount of genes coding for lipogenetic and lipolytic enzymes.[13]

M. tuberculosis' high infectivity and lethality require a biosafety level 3 laboratory to safely perform experiments.[14] Its extraordinarily slow growth rate - with a doubling time of up to 24 hours - makes incubation times of several weeks necessary, several orders of magnitude higher than most other bacteria. Combined with other factors such as limited biomarkers, time-intensive treatment (and the resulting length of follow-ups) and high number of patients required for studies, this further complicates the development of anti-tuberculosis drugs.[15]

In recent years, its proteases have come to attention as promising targets for new therapeutic molecules. Most significantly, a 2003 study showed that the proteasome of *M. tuberculosis* is essential for resistance against reactive nitrogen intermediates (RNIs) such as nitric oxide, which are used for immune defense by the macrophages it infects.[16] Thus, an inhibitor specifically targeting the proteasomes of *M. tuberculosis* could conceivably sensitize it to RNIs and allow the macrophages to clear the infection. Other proteases such as the subtilisin-like mycosins (important for secretion pathways that allow the manipulation of and escape from macrophages), HtrA (essential for some aspects of virulence), the signal peptidases LepB and LspA as well as ClpP (involved in protein degradation and turnover) have also been cited as potentially useful in this regard.[17,18]

Proteasome inhibitors such as the boronic acid-dipeptide bortezomib (approved for the treatment of multiple myeloma), are unspecific and inhibit the host proteasomes alongside those of the infecting bacteria, causing cytotoxic effects. The growth of *M. tuberculosis* can however be halted by oxathiazol-2-one compounds, which specifically deactivate its active site threonine by cyclocarbonylation and whose affinity for eukaryotic proteasomes is only 0.1% of that for those of *M. tuberculosis.*[18-20]

1.2. The eukaryotic proteasomal system

Protein degradation by proteases is an essential mechanism found in all three biological domains, with all intracellular proteins and many extracellular ones being subject to a continuous cycle of synthesis and degradation.[21] Misfolded proteins, whether due to mutation or spontaneous misfolding, as well as proteins that were damaged by heat or oxidative stress, tend to aggregate. Protein aggregates can be inherently cytotoxic and have been conclusively linked to neurodegenerative diseases such as Alzheimer's and Parkinson's disease.[22]

Protein degradation, being an irreversible process, must be tightly controlled both in regard to the selection of proteins to be degraded as well as the timing of degradation. This necessitates a precise system of marking, recognizing and destroying the substrate. In eukaryotes, this is accomplished by covalent linkage of the marker protein ubiquitin (Ub) to the substrate – usually to lysine residues - and the subsequent recognition of the Ub tag by the proteasome, a multi-subunit complex containing several proteolytically active sites that cleave the substrate into oligopeptide fragments. The entirety of these processes is referred to as the ubiquitin-proteasome system (UPS).[23-25] In some cases, the proteasome can degrade substrates without them having to be ubiquitinated.[26]

The eukaryotic proteasome is a complex of approximately 2.6 MDa consisting of two subcomplexes, the 20S core particle (CP) and the 19S regulatory particle (RP) that together make up the 26S proteasome.[1] The 20S core particle is a cylindrical complex to which 19S regulatory particles are bound to at one or both ends. The ubiquitinated substrate is bound, deubiquitinylated, unfolded and translocated by the regulatory particle into the core particle, where it is ultimately degraded.[24] Both the 19S and the 20S complex are in turn made of a large number and variety of subunits (which, especially in the 19S regulatory particlem perform specialized functions such as ubiquitin binding, ATP hydrolysis and deubiquitinylation).[24] In total, the eukaryotic 26S proteasome consists of at least 33 different subunits, at least 19 in the 19S regulatory particle and 14 in the 20S core particle (of which two copies each are present).[24]

The 26S proteasome is the largest and most complex member of a family of proteases that is distinguished by the presence of at least one AAA (ATPases associated with various/diverse cellular activities) protein.[27] The AAA-ATPase recognizes the ubiquitin-tagged substrate and unfolds it, then translocates it into the catalytic section of the proteasome where it is degraded.[24] Other, external and non-proteasomal ubiquitin receptors such as Rad23, Dsk2, and Ddi1 also bind to ubiquitin and direct it towards the proteasome.[28]

The mechanism by which substrates are tagged with ubiquitin is complex and has a much simpler equivalent in prokaryotes (see section **1.3** for a description of the comparable processes in *Mycobacterium tuberculosis*). It consists of a system of three proteins: the ubiquitin-activating enzymes (E1s), the ubiquitin-conjugating enzymes (E2s) and the ubiquitin ligase enzymes (E3s).[23] Ubiquitin itself is a small, 76-residue protein forming a distinctive β-fold which has been found in several other proteins not involved in protein degradation.[29] These proteins are sequentially active, linking ubiquitin to the target in a series of intermediate steps. First, the E1 covalently binds to the C-terminal end of ubiquitin with one of its cysteine residues. E2 then takes over the thioesterified ubiquitin and binds to both E3 and the substrate, which allows E3 to link ubiquitin to one of the target's lysine residues by its carboxyl tail.[30]

Ubiquitin itself contains seven non-consecutive lysine residues, which, combined with its N-terminus, allow up to eight other ubiquitin monomers to bind to it and form polyubiquitin chains.[30] The eventual fate of the substrate is dependent upon the specific type of linkage – for example, the minimal required signal for degradation in the proteasome consists of a tetraubiquitin chain connected by the lysines 48 of the monomers.[31] A lysine 63-connected tetraubiquitin chain, in contrast, does not serve as a degradation tag but as a signal for the substrate to be used in various non-proteolytic pathways like DNA damage tolerance, inflammation, protein trafficking and protein synthesis.[32] Heterogeneous, branched chains consisting of several different types of lysine links have also been found.[33]

[1] Both designations refer to the sedimentation coefficient of the complexes, expressed in Svedberg units (S).

1.2.1. The 20S core particle

The 20S core particle (CP) is the proteolytic component of the proteasomal system. It is a self-compartmentalized, multi-catalytic protease whose general structure is conserved across eukaryotes, bacteria and archaea, even though the level of complexity is higher in eukaryotes than it is in prokaryotes.[24,34,35]

In eukaryotes, the core particle is a cylindrical, multi-subunit complex responsible for the degradation of substrates. It consists of four axially stacked heptameric rings, two α- and two β-rings. Each α-ring is made of seven distinct α-type subunit proteins (α_1-α_7) and conversely, each β-ring is made of seven distinct β-subunits (β_1-β_7). A double β-ring is capped by an α-ring on each side, forming a barrel-shaped $\alpha_{1\text{-}7}\beta_{1\text{-}7}\beta_{1\text{-}7}\alpha_{1\text{-}7}$[2] structure (**Fig. 1.2.1.1**) of approximately 150 Å in height and 115 Å in diameter.[36] The core particle is divided into two anterior chambers formed by the α-rings and a central catalytic chamber formed by the β-rings, in which the substrate is degraded. [24,37] Access to the central chamber is possible through the pore or gate created by the α-rings. However, in the initial state, the openings into the core particle are closed off by the highly conserved N-terminal tails of some α subunits.[38,39] The position of these tails is not fixed but fluctuates between the open and the closed configuration, with a higher probability of the former.[40]

This blockage of the proteasomal gate can be released by conformational changes induced by the binding of an activator protein (or activator protein complex) like the 11S complex, PA26, PA28 or PA200.[41-45]. In yeast, the opening of the gate is triggered by the binding of the 19S regulatory particle. A component of the 19S RP, the Rpt1-6 ring, specifically the ATPase domain of the Rpt2 subunit, binds to the 20S CP's α-ring and causes a structural shift that ultimately displaces the α-rings' N-terminal tails and therefore opens the gate . This process is ATP-dependent.[41,46] So far, every ATP-dependent protease with known structure has been found to be autoinhibited in its default state,[27] likely in order to avoid uncontrolled proteolysis.

The catalytic sites of the 20S CP are located on the interior side of the β-rings, preventing interactions with the cytoplasm and increasing the efficiency of proteolysis by concentrating the sites in a small volume. Each 20S core particle has a total of six active catalytic sites, one on each of the β_1, β_2, and β_5 subunits of the two β-rings.[34,47] The subunits all use a nucleophilic N-terminal threonine as the active site residue.[48] The sites are, however, selective for specific residues: β_1 is responsible for postglutamyl peptide hydrolase (PGPH)/caspase-like (cleaves after acidic residues) activity, β_2 for tryptic (cleaves after basic residues) activity and β_5 for chymotryptic (cleaves after hydrophobic residues) activity.[47] Substrates are cut into short peptides with a median length of five amino acids.[49,50]

In newly synthesized subunits, the catalytic threonines are contained within the N-terminal region and are preceded by a propeptide which protects the active site residues from N_α-acetylation.[51] This necessitates the removal of the propeptide before they can become active, which occurs by autocatalytic cleavage[52,53] assisted by at least one chaperone, the proteasome maturation factor Ump1.[54] The autocatalytic processing of the active subunits is independent from each other.[55]

[2] Usually simplified to α_7-β_7-β_7-α_7

Apart from Ump1**,** the eukaryotic 20S proteasome has at least two other chaperone complexes that assist in its assembly: the Pba1-Pba2 (proteasome biogenesis–associated) dimer and the Pba3-Pba4 dimer.[54,56,57] Ump1 associates with the nascent core particle (n-CP) and is captured inside the central chamber once the complex forms from the two α_7-pre-β_7 double rings (α_7 - pre-β_7 - pre-β_7 - α_7). There, it ensures the proper and timely processing of the pre-β7 subunits. Once the propeptides have been cleaved off and the reactive sites have been exposed, Ump1 is degraded as the first substrate of the mature 20S CP.[54] Both Pba1 and Pba2 have the HbYX motif as their C-terminal end (see section **1.4.1**).[58] Pba3-Pba4 is involved in the interaction between two α-subunits necessary for the formation of the α-ring.[57]

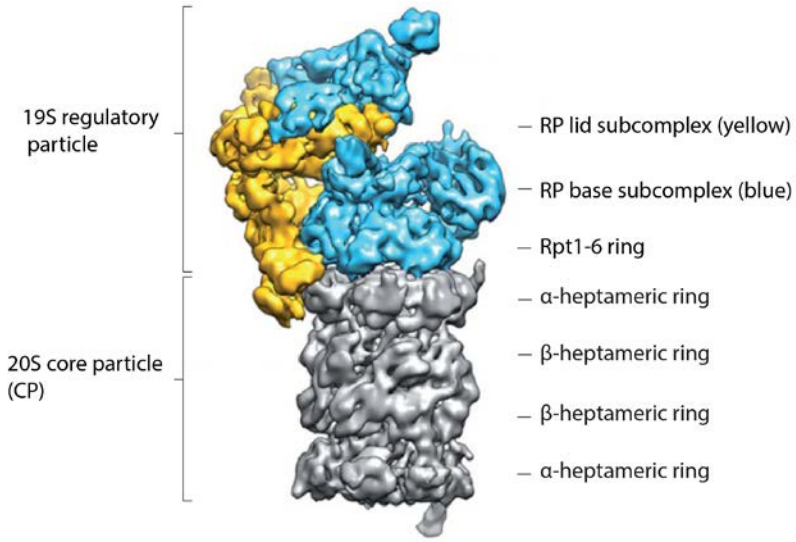

Fig. 1.2.1.1 the eukaryotic 26S proteasome complex, shown with one 19S regulatory particle bound to the 20S core particle. The base of the regulatory particle contains the heterohexameric Rpt-ATPase ring. The 20S core particle shows the conserved α_7-β_7-β_7-α_7 architecture also found in prokaryotes and archaea. Adapted from [24].

Additionally, the proteasome activator BLM10 (also called BLM3, related to PA200 in humans) has been implicated as a chaperone involved in 20S core particle assembly.[59] BLM10 binds to the core particle with its C-terminal tail, using the same binding sites that the 19S regulatory particle's Rpt ATPases also use. Like Pba1 and Pba2, the C-terminal tails of BLM10 end in an HbYX motif (YYX).[60] The binding of BLM10 to the 20S proteasome triggers an opening of the gate and thereby enhances the proteolytic activity.[60]

1.2.2. The 19S regulatory particle

The 20S core particle of the proteasome alone can only degrade unstructured proteins or small peptides. With a diameter of 13 Å, its pore is too narrow for anything but extended loops to fit through the gate. Larger protein substrates must therefore first be unfolded before they can be taken in and degraded by the core particle.[39] Since the core particle itself lacks this ability, external CP-associated ATPases provide the mechanical force required to unfold the substrate, allowing a loose end or loop to be threaded into the central chamber of the CP where it can be cleaved.[61,24] In the eukaryotic proteasome, these ATPases are part of a larger complex, the 19S regulatory particle (RP), which is bound to one or both ends of the CP cylinder.[24] The RP consists of two subcomplexes, the lid and the base[3](see **Fig. 1.2.1.1**)[24].

The base of the RP is in direct contact with the CP and contains ten distinct subunits: the heterohexameric **r**egulatory **p**article A**T**Pases Rpt1-6 and the **r**egulatory **p**article **n**on-ATPases Rpn1, Rpn2 , Rpn10 and Rpn13.[24] Each of the six Rpt subunits is a unique protein that assembles into a ring structure in a defined order (1-2-6-3-4-5).[24] Rpn1 and Rpn2 are the largest single subunits in the proteasome and most likely serve as structural support and scaffolding for the binding of substrates and other factors. Rpn10 and Rpn13 are mono-and polyubiquitin receptors.[62] The RP is not always completely aligned with the CP, being axially offset by as much as 30 Å and set at an angle of 5-10° relative to the α-ring.[63] It is assumed that only two to four of the Rpt subunits can bind ATP, engage the CP and function as the gate-opening trigger simultaneously. The "wobble" model explains the angle between the RP and the CP by postulating that the ATPase interacts with the CP's α-ring by alternate binding of ATP-bound Rpt subunits, leading to the RP being tilted to the side of the currently engaged subunits. The simultaneous model, in contrast, assumes that some subunits have a designated role in binding the CP and opening the gate while bound to ATP, while the other subunits unfold the substrate. In this case, the RP would be stably bound to the CP and aligned with its axis and surface.[64]

The Rpt1-6 ring directly binds to the core particle's α-ring, unfolds the substrates and translocates them into the CP for degradation, hydrolyzing ATP in the process.[24] The interaction between Rpt and the CP is mediated by Rpt's C-terminal tails, which insert into pockets formed by the interfaces between the subunits of the α-ring.[65,66] Three of the six Rpt subunits, Rpt2, Rpt3 and Rpt5, have a conserved HbYX (hydrophobic amino acid – tyrosine – any amino acid) motif on their C-terminal tails. This motif is essential for the binding of Rpt to the CP α-ring and is discussed in greater detail in section **1.4.1**. However, only Rpt3 and Rpt5, but not Rpt2, are required for the interaction of the RP to the CP. The non-HbYX-motif-containing Rpt subunits (Rpt1, Rpt4 and Rpt6) are not essential for the interaction, although truncating Rpt6 by its last three C-terminal residues destabilizes the RP-CP complex.[67] Rpt3, in turn, is not required for triggering the gate opening mechanism of the CP.[68]

It has been suggested that during the assembly of the regulatory particle, the CP serves as a scaffold or a template for the formation of the base subcomplex. An intermediate form of the base called BP1 exists during the assembly process, containing Rpn1, Rpt2, Rpt3, Rpt5 and the chaperone Hsm3. It is

[3] The established nomenclature of "lid" and "base" is somewhat misleading because the "base" is not below but lateral to the "lid" and interacts with both the lid and the CP.

thought that Rpt4 and Rpt6 bind to each other first and are then bound by the BP1 complex in turn, which creates the mature Rpt ring.[69]

The lid subcomplex of the 19S RP consists of nine subunits of the Rpn family: Rpn3, Rpn5-9, Rpn11, Rpn12 and Rpn15. These units are grouped into two modules: Module 1 (Rpn5 / Rpn6 / Rpn8 / Rpn9 / Rpn11) binds to both the base subcomplex of the RP and α-ring of the CP, while module 2 (Rpn3 / Rpn7 / Rpn12 / Rpn15) is bound to module 1. Both modules are connected to each other by Rpn11.[63] Although its precise function is unknown, Rpn7 of module 2 has been demonstrated to be essential for the stability of the 26S proteasome.[70,71]

1.3. The mycobacterial proteasomal system

Although all eukaryotes and archaea have 20S proteasomes, among bacteria they are found in only the phyla *Actinobacteria* - of which *Mycobacterium tuberculosis* is a member - and *Nitrospira*.[50] In these two groups, the proteasomes are highly conserved.[72,73] Many other bacteria use the heat shock protein complex HslVU, a less complex homolog of the proteasome, instead. HslVU consists of the protease heat shock locus V (HslV) and the ATP-dependent unfoldase HslU. HslV is homologous to the catalytic β-subunits of the 20S-proteasomes and HslU is related to the ATPase ClpX, one of a number of equivalent alternative bacterial protease systems such as Lon and FtsH.[74,75] It has been suggested that the actinobacteria are evolutionary predecessors to the archaea, which would make the actinobacterial proteasome the ancestor to both the archaeal and eukaryotic proteasomes.[76]

Similar to the ubiquitinylation system in eukaryotes, some bacteria use an equivalent system of tagging proteins that are to be degraded. Although the cell has a number of small non-proteasomal proteases the main work of proteolysis in these bacteria is performed by proteasomes. The basic principle is the same in both eukaryotes and bacteria: a small protein is covalently linked to the substrate and the tag is recognized by the protein degradation machinery, which then cleaves the substrate into peptides. In bacteria such as *M. tuberculosis*, the tagging protein is Pup (prokaryotic ubiquitin-like protein). Like ubiquitin, Pup is covalently attached to lysine residues of target proteins, however, in contrast to ubiquitin, poly-pupylation has never been observed.[77-79]

Other systems of protein tagging exist. In *E. coli*, errors in translation that lead to incompletely expressed proteins - typically, stalled ribosomes resulting from mRNAs lacking stop codons - can lead to attachment of a C-terminal 11-residue tag (AANDENYALAA) that is recognized and degraded by the cytoplasmic ClpP-ClpA or ClpP-ClpX protease complex. In contrast to the ubiquitin and Pup pathways, this so-called SsrA tag (named after the tmRNA that codes for the tag) is linked to the target proteins co-translationally, while both ubiquitin and Pup are linked to their targets post-translationally. [80,81]

Although the actinobacterial proteasome is structurally similar to the eukaryotic one and the pupylation mechanism in actinobacteria is equivalent to the function of ubiquitin in eukaryotes, the similarities end beyond that. Pup itself is not related to ubiquitin at either the structural or the sequence level and the protein degradation system itself is different between eukaryotes and

actinobacteria. While in eukaryotes almost all protein degradation is performed by the ubiquitin system, actinobacteria have several chaperone protease systems existing in parallel with the PPS.[29]

1.3.1. Pup as the mycobacterial equivalent to ubiquitin

Pup is a 64-amino acid, 6.9 kDa protein that is partially disordered in its unbound form and comprises two distinct domains, one of which is bifunctional.[29,82] In its unconjugated form, it is most likely highly unstable and is rapidly degraded.[50,83,84] In actinobacteria, the linkage of Pup to the substrate is performed by a single enzyme, PafA (proteasome accessory factor A). The ligation is a three-step process nonetheless, since two modifications to Pup by PafA are necessary before it can be connected to the target.[77] First, Pup's C-terminal glutamine must be deamidated to glutamic acid by Dop (deamidase of Pup).[85] After the C-terminal glutamate has been deamidated, its γ-carboxyl group is phosphorylated by PafA. Then, a nucleophilic attack by the ε-amino group of the target lysine forms a peptide bond between Pup_{Glu} and the substrate.[77,86] Several *Actinomyces* species were shown to use a variant of Pup that has a native C-terminal glutamate and therefore does not need to be deamidated by Dop for ligation, however, these species still produce Dop as well. This discovery suggested a second function for Dop, which was indeed found and identified as depupylase activity, i.e. removing Pup tags from substrates. PafA and Dop are homologous sequentially as well as structurally.[29,87,88]

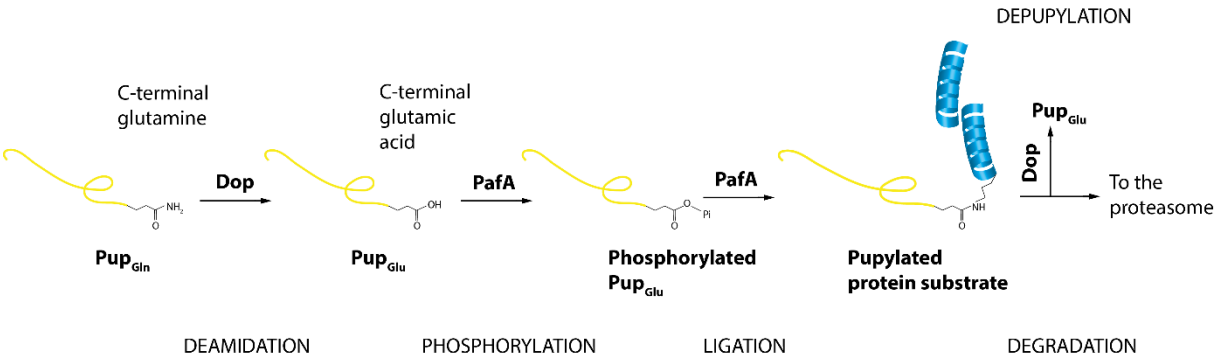

Fig. 1.3.1.1. The Pup/Dop/PafA/proteasome system. The C-terminal glutamine of Pup is deamidated by Dop, allowing PafA to first phosphorylate and then ligate the deamidated Pup to a lysine residue in the targeted substrate protein. Pup then binds to the proteasomal ATPase Mpa, where it is unfolded and degraded together with the substrate. Alternatively, Dop can function as a depupylase and recycle Pup by removing it from the substrate before degradation. Adapted from [29,89] and [50].

The precursor-Pup (Pup-Glu or Pup-GGQ) is not degraded by the proteasome but interacts with Mpa nonetheless, showing that the initial contact between Pup and Mpa does not depend on whether Pup terminates in glutamine or glutamic acid. In-cell STINT-NMR analysis has demonstrated that the interaction of Pup with the holoproteasome is stronger than the interaction of Pup with Mpa alone[90], which could indicate subtle conformational changes of Mpa when it binds to the 20S CP.

Pup's structure, as far as it can be distinguished due to its inherent disorder, contains three distinct sections. Its N-terminus (residues 1-21) is unstructured, but the central residues (21-51) tend to form an α-helix which is stabilized once bound to Mpa. The C-terminus (52-64) is unstructured when bound to Mpa[90] but forms a small α-helix when binding PafA. The C-and the N-terminus, although disordered, take part in the interaction to Mpa together with the central α-helix. Within the Mpa-binding central domain there is a 9-amino acid segment that also serves as a PafA binding site (**Fig. 1.3.1.2**). Pup can simultaneously interact with Mpa on one side and PafA on the other.[91] Its C-terminus is highly conserved, while its N-terminus is variable among the actinobacteria.[29]

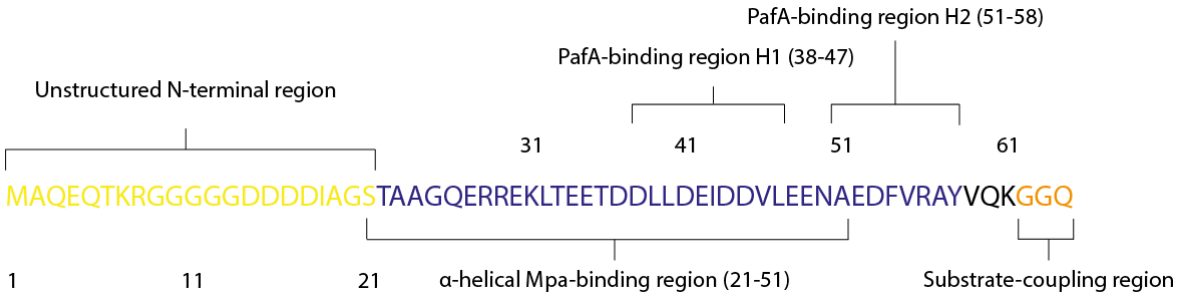

Fig. 1.3.1.2. Primary structure and domains of Pup from *M. tuberculosis*. The GG sequence of the substrate-coupling region is highly conserved across the actinobacteria and occurs at the C-terminus of ubiquitin as well.[92] Adapted from [91].

The gene organization to code for the proteasome and its associated proteins is conserved in actinobacteria. *pup* and the proteasomal genes (*prcB* and *prcA*) are combined in an operon, the genes for the Pup-deamidase (*dop)* and the AAA unfoldase (*arc*, or *mpa* in *M. tuberculosis*) are located upstream, the Pup-ligase gene *pafA* downstream of the operon (**Fig. 1.3.1.3**).[29]

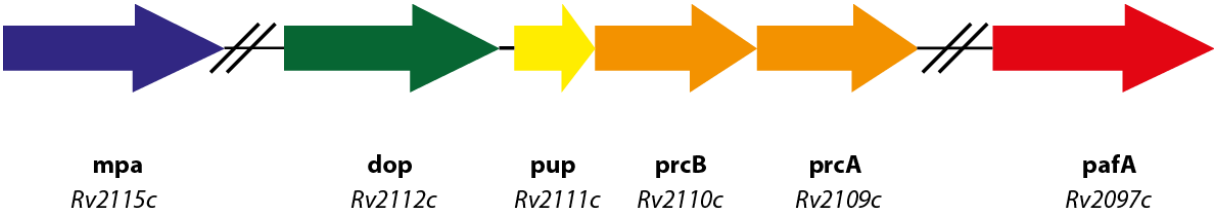

Fig. 1.3.1.3. Organization of the proteasome gene locus of *M. tuberculosis* strain H37Rv. *mpa*: mycobacterial proteasomal ATPase. *dop*: deamidase of Pup. *pup:* proteasomal ubiquitin-like protein. *prcB/A:* proteasome core protein B/A. *pafA*: proteasome accessory factor A. Additional genes located between *mpa* and *dop* as well as between *prcA* and *pafA* are not shown. Downstream of *pafA* are the *pafB* and *pafC* genes (not shown) which were shown to be co-transcribed with *pafA* but do not play a role in the pupylation pathway.[93] Adapted from [29] and [50].

1.3.2. The 20S core particle

The general structure of the proteasome is conserved in all three domains of life.[94] Like that of the eukaryotic proteasome, the 20S core particle (CP) in actinobacteria is a cylindrical complex (716 kDa in *M. tuberculosis*) composed of four heptameric α and β rings, stacked in the order α_7-β_7-β_7-α_7.[37,95] Its overall structure and dimensions, at approximately 150 Å in length and 110 to 115 Å in diameter, are very similar to the eukaryotic core particle.[50] Contrary to the eukaryotic proteasome, however, the rings in *M. tuberculosis* are homomers: each α- or β-ring consists of seven identical subunits expressed from only one gene: *prcA* for α-subunits and *prcB* for β-subunits.[96] The β-rings form the central chamber and contain the catalytic sites, while the α-rings at both ends serve as a gate into the CP.[96] The *M. tuberculosis* core particle shares 65% sequence identity (for both subunit types) with that of the closely related actinomycete *Rhodococcus* and 32% sequence identity with that of the archaeon *Thermoplasma*.[50]

The entrances or gates into the mycobacterial core particle on the ends of the cylinder are normally blocked by N-terminal residues of the α-rings' subunits[37], similar to those of the eukaryotic proteasome.[41] However, while the eukaryotic proteasomes' gates are completely closed by the N-terminal tails in the default state, those of prokaryotes retain a small opening.[34,47] Electron microscopy has shown that the occluding structure slightly protrudes above the gates in the α-rings, preventing unregulated access to the catalytic chamber.[96] In mycobacterial proteasomes, deletion of the α-subunits' N-terminal octapeptide increases the activity 14-fold by opening the gate.[96]

When the β-subunits are synthesized, they contain an N-terminal propeptide as their residues 1-57 and the active site threonine at position 58. The propeptides therefore have to be cleaved off to expose the catalytic residue, analogous to the process in eukaryotes and other actinobacteria.[96] During the formation of the β-rings in *Rhodococcus*, the propeptides double the area of contact between the subunits and thereby promote the assembly.[97] In *M. tuberculosis,* this process has a unique characteristic: deleting the propeptides from the β-subunits altogether does not cause any difference in the assembly compared to the wild type.[96] In *M. tuberculosis*' case, the propeptides therefore seem to act as a thermodynamical barrier rather than promoting the formation of the

complex.[37,96] The prcB$_{T54V}$/CP$_{T54V}$ mutant, where one the β subunits' threonine at the site of the autocatalytic processing (at position 54 in *Streptomyces griseus*, which was used in this study) is mutated, cannot cleave its propeptides at all (see section **2.4**). The CP$_{T54V}$ mutant produces non-processed CP complexes that are structurally almost identical to those of the wild type due to the propeptides folding inward, with the only difference being the increase in circumference (which, in electron microscopy, makes them indistinguishable from the wild type complexes, as seen in section **3.8**).[98]

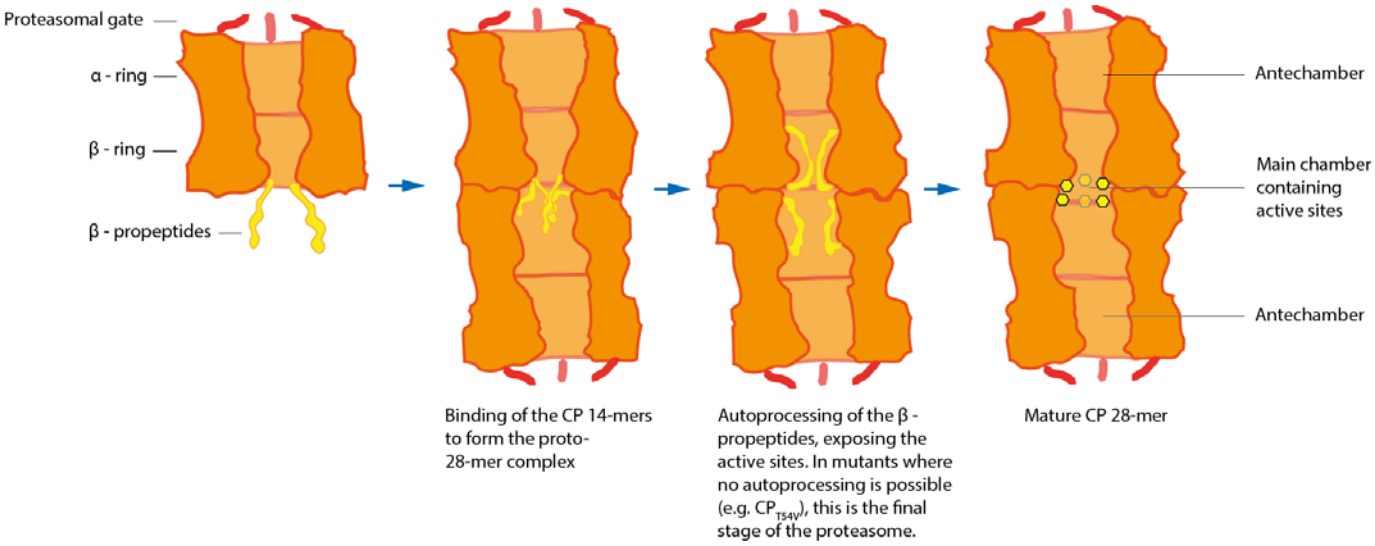

Fig. 1.3.2.1. Assembly of the CP 28-mer and autocatalytic processing of the β-propeptides.

The assembly of the α –subunits into the heptameric α-rings in *M. tuberculosis* requires the co-expression of both prcA and prcB from a single vector with a separate promotor for each gene[37,96], similar to the requirements in *Rhodococcus*.[99] In contrast, in the archaeon *Thermoplasma* the formation of α-rings is independent from the presence of β-subunits.[100]

In vivo, the two halves of the proteasomes seem to effect an autoprocessing function that cleaves the β propeptide and allows function. An incubation temperature of 37°C is necessary for expression in *E. coli* for the proteasome to function, alternatively, mutants where these peptides are deleted can produce functional proteasomes at room temperature.[96]

It has recently been shown that both PrcA and PrcB can be phosphorylated, and that these phosphorylations influence the activity as well as the assembly of the proteasomal complex. Proteasomes containing PrcA phosphorylated by PknB show an increase in proteolytic activity. PrcA is sequentially phosphorylated on three threonine residues (T84, T202 and T178) by the kinase PknB. T178 and T202 are located on the surface of PrcA, but T84 is located on the inside of the α-ring, near the interface of the α- and β rings. Since T178 and T202 are accessible from the outside but T84 is

not, the phosphorylation of T84 must take place even before the assembly of the half-proteasome. After T84 is phosphorylated, changes in the hydrogen bond structure between T84 and T202 most likely position the latter for PknB to engage, which in turn causes rearrangements that allow the final phosphorylation of T178.[101]

The pocket lysine mutant CP_{K52V} has the lysine in the α-subunits' binding pocket replaced, which was shown to abolish the binding of the Mpa tails in previous experiments in our lab. The effect of this mutation was analyzed in this study (see section **3.2** and **3.4**). Mutations within the Walker A (K299Q) and B (D371A, E372A) motifs of Mpa inhibit its ATPase activity *in vitro*, with the Walker A mutation also showing a reduction in ATP binding capacity. However, the mpa607 mutant, which lacks the C terminal amino acids tyrosine and leucine, is attenuated in mice comparably to an *mpa* null mutant, even though the ATPase activity of mpa607 is only slightly lower than in the wild type.[16,102,103] This suggests that the C terminus of Mpa plays a vital role in the assembly of the Mtb proteasome. Another protein kinase, PknA, can phosphorylate both the CP α subunit and the unprocessed CP β subunit of the half-proteasome, thereby hindering the assembly of the holoproteasome by affecting the autocatalytic activity of the CPβ propeptides. In contrast, the phosphorylation of CP α by PknB does not influence the assembly of either the unprocessed half- or the holoproteasome. The reduced production of functional holoproteasomes also reduces *M. tuberculosis*' resistance to reactive nitrogen species, but increases its resistance to hydrogen peroxide between 2-or 3-fold. Since the H_2O_2 level in macrophages rises as soon as one hour after infection with *M. tuberculosis* but the level of RNS such as nitric oxide only starts to rise 72 hours after the infection[104], it is possible that phosphorylation by PknA serves to enhance *M. tuberculosis*' resistance against short-term H_2O_2 stress.[101]

The open-gate mutant of the 20S proteasome, in which eight residues are deleted from the α-subunit's N-terminus (*prcA*Δ(2-9)), forms a complex together with the β-subunits that lacks the protuberant structure at the α-ring gates but is otherwise indistinguishable from the wild type 20S-proteasome. The peptidolytic activity of the open-gate mutant (using the fluorogenic peptide Suc-LLVY-AMC as a substrate), however, is 14 times higher than in the wild type[96], which demonstrates the effectiveness of the gate closing residues in preventing even small substrates from being degraded in an uncontrolled manner.

The mycobacterial proteasome can degrade a wide range of oligopeptide substrates, even though it only contains a single type of catalytic site on its β-subunits. The topology of its substrate-binding site exhibits composite characteristics of the amino acid-specific catalytic β1, β2, and β5 substrate-binding sites in the 20S proteasome of *Saccharomyces*. This allows *M. tuberculosis* to cleave several different substrate types: it has chymotryptic (cleaves after a hydrophobic residue), tryptic (cleaves after a basic residue) or PGPH/caspase-like (cleaves after acidic residues) ability.[34,48,50,55,96] Among the eubacteria, the tryptic and PGPH/caspase activity is unique to *M. tuberculosis* – all other known bacterial proteasomes only show chymotryptic activity, due to the limitation to a single type of catalytic site.[96]

1.3.3. The AAA-ATPase Mpa

In *M. tuberculosis*, the ATPase ability required to unfold and translocate the substrate into the CP is provided by Mpa (mycobacterial proteasomal ATPase), a 67.4 kDa protein forming ring-shaped homohexameric complexes that bind to both ends of the CP.[105] The Mpa ring is therefore the structural equivalent of the eukaryotic 19S RP base's heterohexameric Rpt1-6 ring, but also performs functions that in the 19S RP are left to specialized subunits that are not part of the ring itself (Rpn1/2/10/13), such as recognizing and binding Pup and the substrate.[24] The Mpa hexamer recognizes the Pup-tag attached to the substrate, unfolds the tagged protein and threads it through the central pore into the main chamber of the CP, where both Pup and the substrate are degraded (in contrast to eukaryotic proteasomes, where ubiquitin is not degraded).[105,106]

Mpa is most similar to the ATPase ARC (ATPase forming ring-shaped complexes) of the closely related actinomycete *Rhodococcus erythropolis,* sharing with it 82% of its sequence. Like Mpa, ARC forms hexameric (and potentially dodecameric) complexes.[107,108] Mpa also has a close resemblance to the eukaryotic p97/valosin-containing protein (VCP).[102] Mpa is homologous to members of the AAA-ATPase family and contains the canonical Walker A and B motifs as well as the so-called second region of homology (SRH). In particular, Mpa is homologous to the ATPases that form part of the eukaryotic 19S-proteasome complex.[102] Mutation studies have confirmed that the ATPase activity of Mpa is dependent on the Walker motifs.[102]

Mpa can be broadly divided into four domains with distinct functions (**Fig. 1.3.3.1**):[109,110]

- the N-terminal coiled-coil domain (residues 1-96) that binds to Pup
- the interdomain (residues 97-245) that is responsible for the hexamerization of Mpa
- the AAA-ATPase domain (residues 246-609)
- a C-terminal tail domain

The structures of the coiled-coil and the interdomain have been resolved on the atomic level, but the precise structure of the ATPase domain is presently unknown, as is the extreme N-terminus of the coiled-coil domain. EM studies have shown the Mpa hexamer to be an asymmetrically-shaped complex 11.5 nm in height and 8-12.5 nm in diameter.[102] X-ray crystallography studies of the subdomains revealed that in the hexamer, six negatively charged glutamines (Glu145) are located at the entrance of the central channel while the channel itself is positively charged. In it, three layers consisting of (in descending order) six arginines, six lysines and six histidines form a gradually constricting tunnel that narrows from 28 Å inside the arginine ring at the entrance to 15 Å at the bottom layer (see **Fig. 1.3.3.3**). The surface of Mpa is negatively charged on its side but has several ositive areas on its top, which likely function as part of a substrate-binding site.[109]

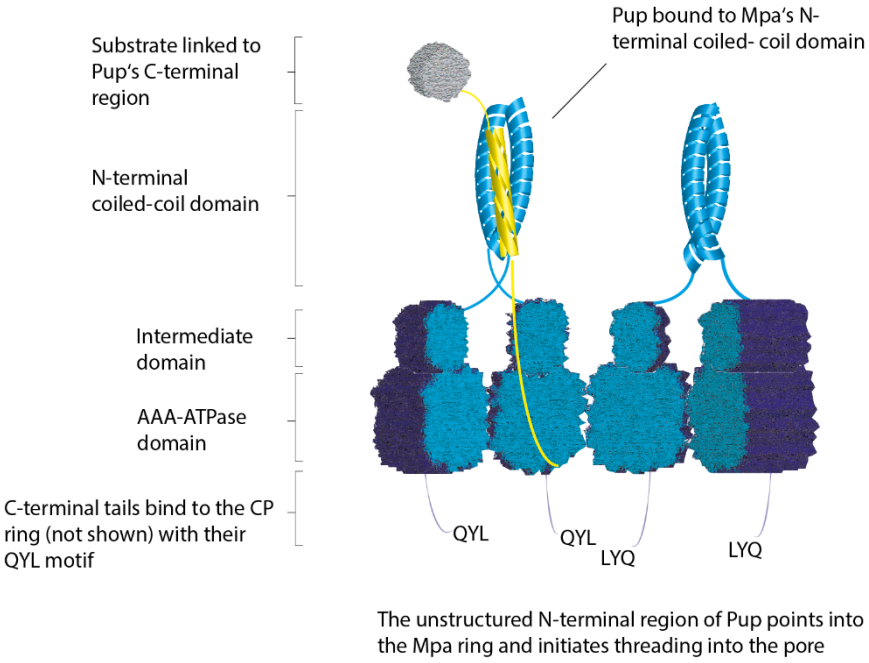

Fig. 1.3.3.1: Schematic cutaway illustration of Pup (yellow) bound to the Mpa ring (blue). Pup's N-terminal region enters the opening of the Mpa ring and interacts with the pore loops of the AAA-ATPase domain, which triggers the translocation into the complex and the unfolding of both Pup and the substrate.

The N-terminal coiled-coil domain of Mpa recognizes and binds to the central C-terminal region (residues 21-58, see **Fig. 1.3.1.2.**) of Pup.[111]. The C-terminal domain of Pup is partially unstructured (akin to the N-terminal domain) and forms an α-helix, using Mpa's coiled-coil domains as a template.[110] NMR studies have shown that the disordered N-terminal region of Pup does not take part in the binding to Mpa, however, it is essential for substrate degradation. Strong evidence has been found that the N-terminal domain, when Pup is bound to Mpa, extends through the Mpa pore beyond the interdomain, interacts with the AAA pore loops and initiates unfolding of the substrate (**Fig. 1.3.3.1**).[105] Mpa pulls on Pup to initiate unfolding of substrate proteins and to drag them toward the catalytic 20S-proteasome chamber.[105]

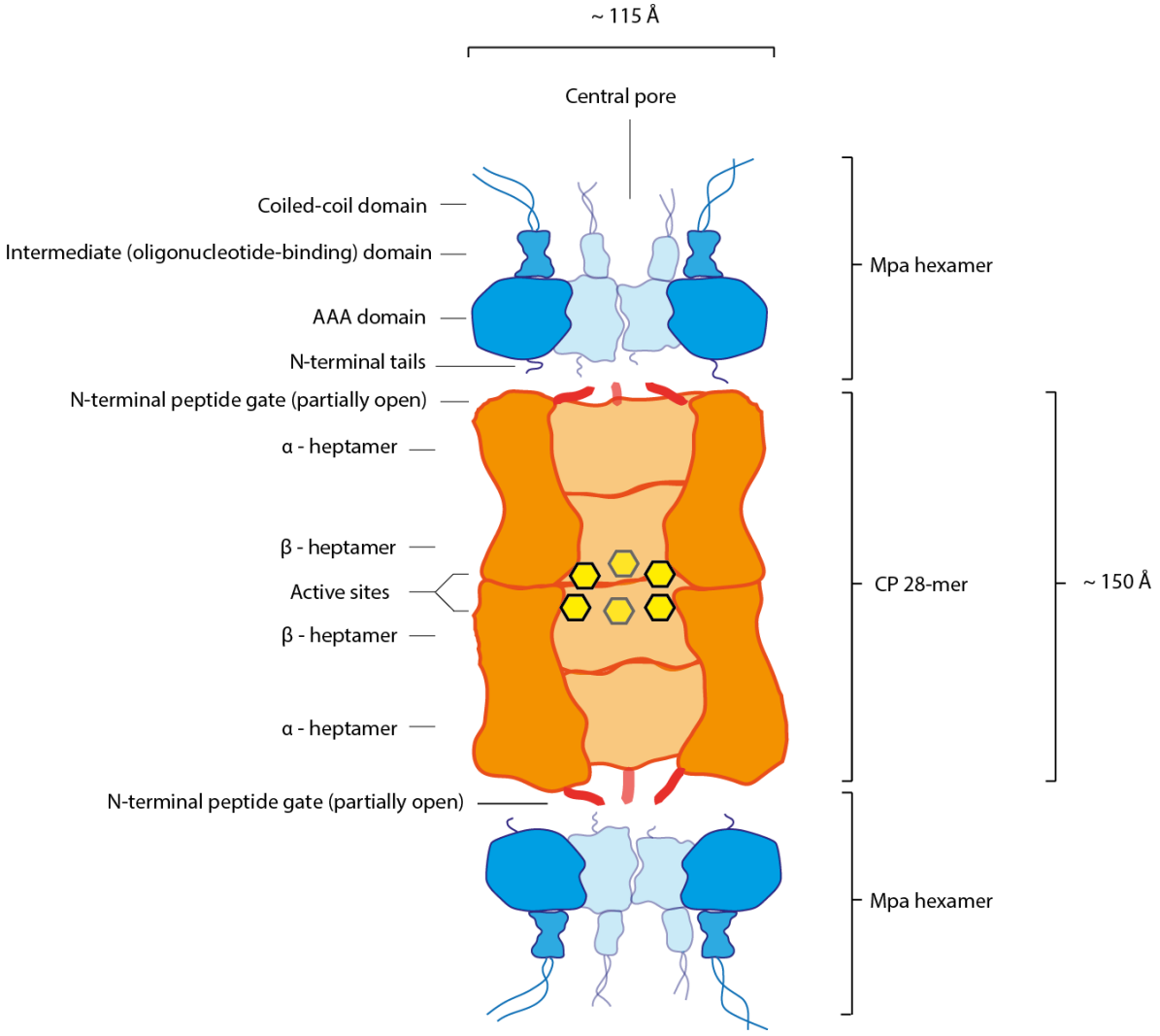

Fig. 1.3.3.2. Binding of Mpa to the CP 28-mer. Adapted from [98] and [110].

The interdomain of Mpa bridges the N-terminal coiled-coil-domain and the C-terminal ATPase domain. It contains a double oligonucleotide-binding fold, a characteristic that has also been found in an archaeal regulatory particle in a single-fold variant[63] as well as in a bacterial regulatory particle as tandem double OB folds.[112] As both these domains form hexamers like Mpa does, hexameric OB rings are likely a unique characteristic of proteasomal ATPases in general.[112] The interdomain is essential to Mpa's function since it is necessary for the formation of the Mpa hexamer from individual Mpa molecules. The interdomain can hexamerize both as part of full-length Mpa and as an isolated domain, forming the ring that comprises the structure of the 19S regulatory particle. The AAA domain as an isolated protein is unstable and does not hexamerize, requiring the stabilizing influence of the interdomain. It has been suggested that the interdomain functions as a sort of scaffold or platform that serves as a basis for the mechanical force generated by the ATPase in order to unfold the substrate.[109]

The side of the interdomain hexamer surface is strongly negatively charged but the top has several positively charged areas. Since the top of the interdomain hexamer correlates to the nucleotide/sugar-binding sites of other OB fold proteins, this could imply a role in the binding of the substrate for the interdomain.[109]

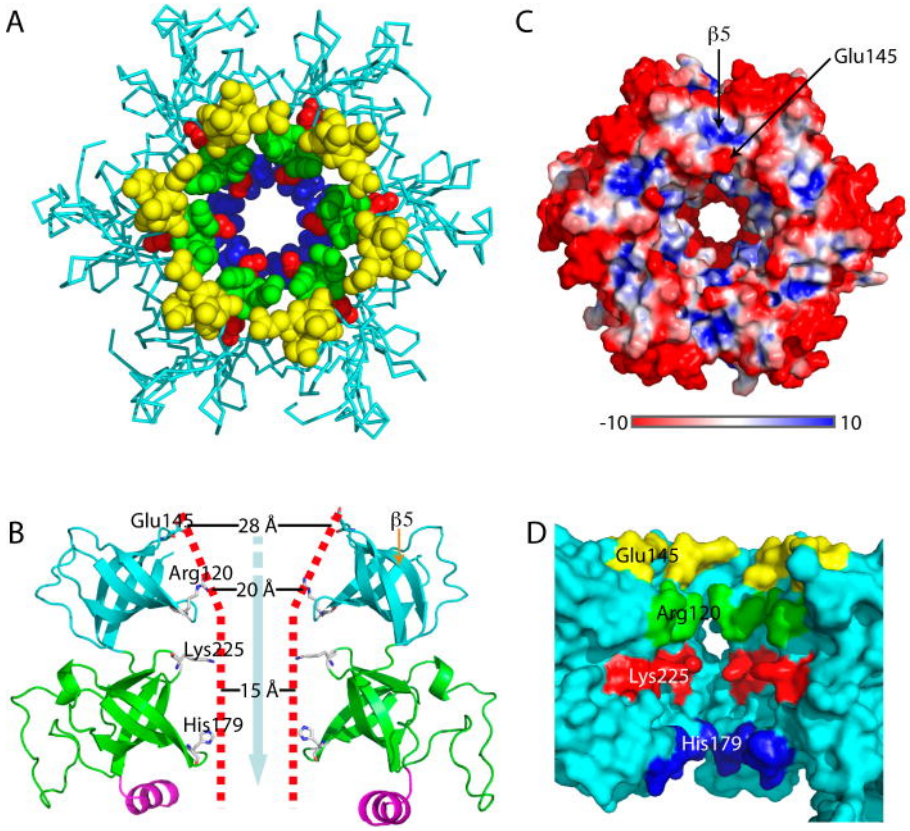

Fig. 1.3.3.3. Crystal structure of the Mpa interdomain hexamer. (A) Top view, looking down the central channel. The residues of the four β-hairpins lining the pore are shown as ball-and-stick models in different colors. Yellow: Glu145. Green: Arg120. Red: Lys225. Blue: His179. (B) Cross-section in side view. The four residues are indicated. The central channel constricts in a funnel-like manner from 28 Å at the entrance to 15 Å at the bottom interface with the CP's α-ring (not shown). The arrow shows the path of the peptide through Mpa towards the CP. (C): Top view, looking down the central channel, showing the surface charge distribution. The substrate-binding site in the OB-fold above the β5-strand and the negatively charged Glu145 are indicated. (D) Surface-view cross section, showing the central channel and the four channel-lining residues in the same color scheme as in (A). From [109].

The interaction between Mpa and the CP occurs between the extreme C-terminal residues of Mpa and the N-terminal domain of the α-ring of the CP (**Fig. 1.3.3.2**). The binding of archaeal and eukaryotic ATPases to the 20S core particle requires the insertion of the ATPases' C-termini into clefts or pockets on the surface of the α-ring of the core particle, formed at the interface of the α-subunits.[113] This, in turn, opens the proteasomal gate by rearranging the N termini of the α-

subunits.[114] The last three residues of the C-terminal tail (QYL) resemble the highly conserved hydrophobic-tyrosine-X (HbYX) motif found in both eukaryotes and archaea (see section **1.4.1** for a detailed discussion).[58,114,115]

Mpa also plays a role in the depupylation of substrates. *mpa* mutants accumulate the pupylated protein Ino1 that is otherwise almost undetectable in both wild type and proteasome deletion strains.[69] Mpa has also been shown to enhance the depupylation of substrates *in vitro*. It has been proposed that this is the result of the unfolding of the substrate by Mpa, which allows Dop to access and cleave the peptide bond between Pup and the target protein more easily.[92,116,117]

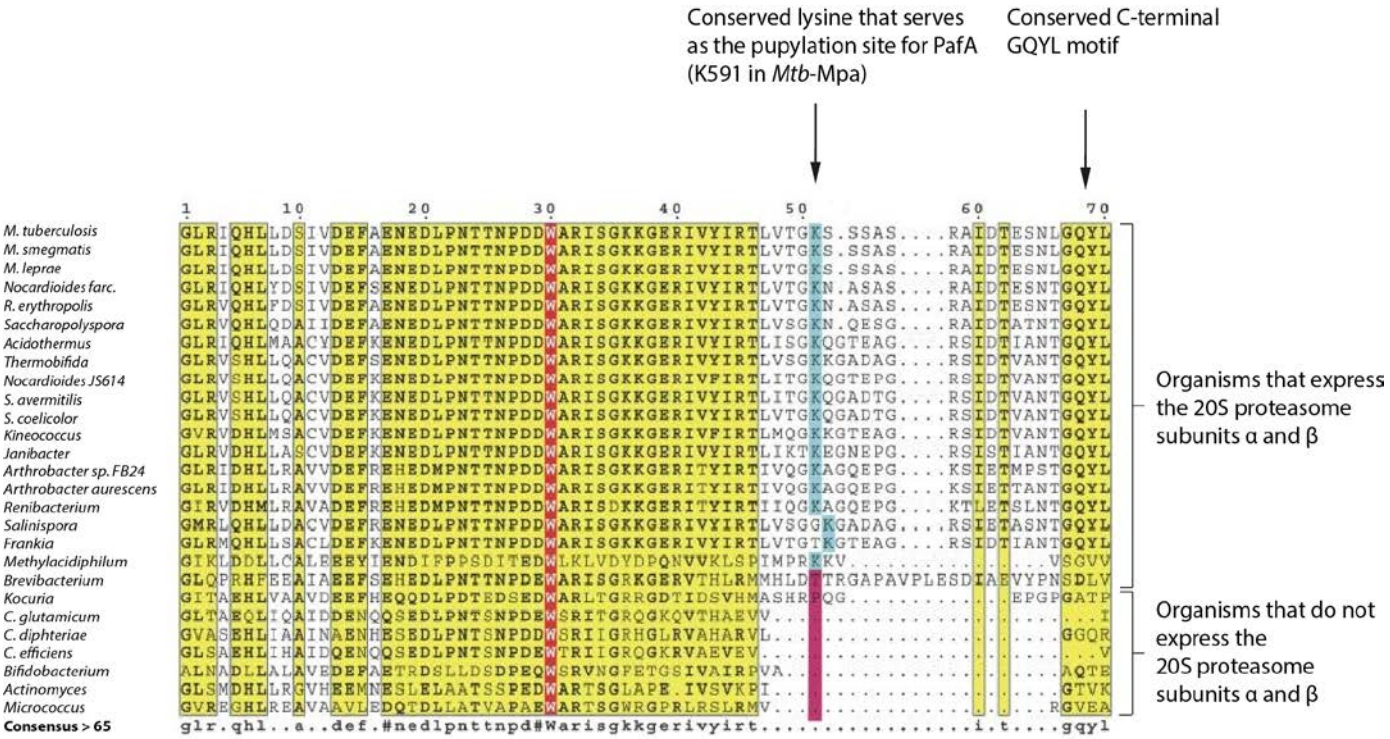

Fig. 1.3.3.4. Comparison of the last 70 residues of mycobacterial Mpa (line 1) and those of homologous proteins from other actinobacteria. In bacteria that express the 20S-proteasome subunits α and β, the pupylation target lysine is conserved, but it is absent in those organisms that do not express the subunits. The C-terminal GQYL motif is also conserved in 90% of those actinobacteria that express the 20S-proteasome subunits but not in others. Adapted from [118]

As with other proteasome substrate proteins, Mpa itself can be pupylated at a lysine residue (K591) by PafA. This C-terminal residue is highly conserved across a variety of actinomycetes expressing the proteasomal α and β subunits, but is absent in Mpa homologues of organisms that do not express proteasomal genes (**Fig. 1.3.3.4**). Unlike the ubiquitinylation process, pupylation mostly results in monopupylated Mpa, which is unable to bind to the proteasome core due to Pup's location close to the C-terminal QYL motif. Pupylation of the Mpa hexamer destabilizes it and causes it to ultimately

dissociate into its component subunits, which cannot unfold substrates on their own. However, pupylation of the hexamer alone does not decrease its unfoldase activity as long as the hexamer remains intact. Depupylation by Dop restores the ability of Mpa to bind to the proteasome, making pupylation a fast and easily reversible way of controlling Mpa's function. [118]

Remarkably, the pupylation of free Mpa hexamer causes it to lose its ATPase ability. This effect is likely based on the binding of Pup to Mpa's N-terminal coiled-coil domain while linked to the C-terminal lysine 591, as using a Pup mutant that is unable to interact with the coiled-coil domain (Pup_{39S40S}) does not influence the hydrolysis of ATP.[118]

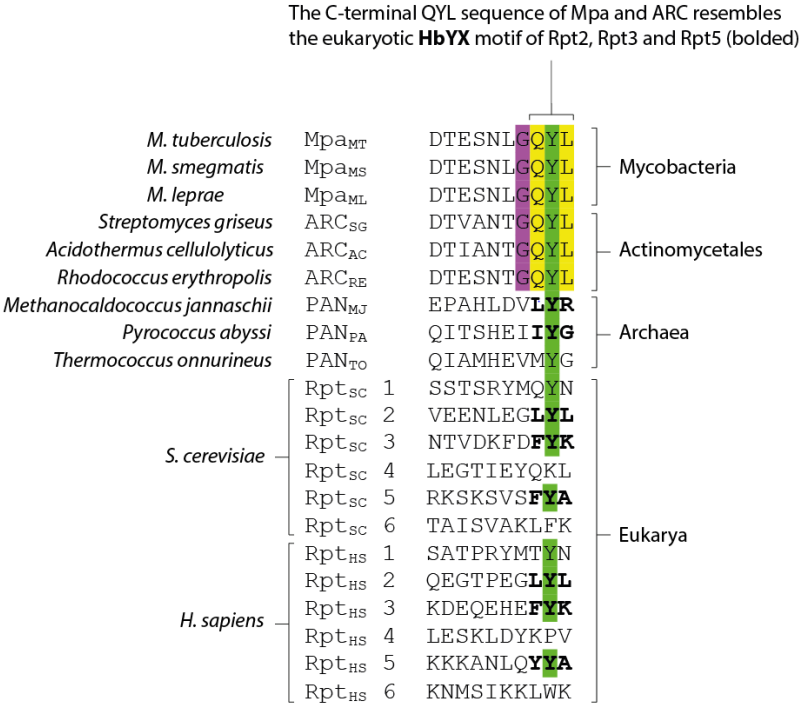

Fig. 1.3.3.5. Comparison of the last 10 C-terminal residues of Mpa from *M. tuberculosis* with those of *M. smegmatis, M. leprae,* actinobacterial ARC (including that of *S. griseus* used in this study), archaeal PAN and Rpt1-6 from *S. cerevisiae* and *H. sapiens*. Purple: conserved Q in Mpa of *M. tuberculosis* and ARC of *S. griseus*. Yellow: conserved QYL motif in Mpa of *M. tuberculosis* and ARC of *S. griseus* (compare with Fig. **1.3.3.2**). Green: conserved tyrosine in Mpa and Rpt. Bolded: conserved HbYX motif in Rpt. In both *S. cerevisiae* and *H. sapiens*, only Rpt 2, 3 and 5 terminate in the HbYX motif.

1.3.4. The bacterial proteasome activator Bpa

A recent study identified a previously unknown protein interacting with the 20S proteasome, making it, together with Mpa, the second proteasomal interactor found to date. A search for genes coding for the HbYX motif in the genome of *M. tuberculosis* found a protein (designated Rv3780), which contains as its C-terminus the conserved GQYL sequence also found in Mpa. Apart from this motif, the sequences of Rv3780 and Mpa are nonhomologous. Rv3780 was subsequently shown to assemble into homohexameric rings (analogous to Mpa) and bind to the outer α-rings of the CP barrel, competing with Mpa for binding and thereby inhibiting the degradation of pupylated substrates. Paradoxically, the presence of Rv3780 was also demonstrated to increase the peptidase activity of the 20S proteasome approximately two-fold when L-Suc-LLVY-AMC is used as a substrate. Thus, Rv3780 was named Bpa (bacterial proteasome activator). The gene is located far away from the locus of the other proteasomal genes, in a region where no other proteasome-associated genes are found. [119]

Since it lacks ATPase ability, Bpa cannot unfold proteins and is therefore unable to replace Mpa as the 20S proteasome-associated unfoldase. However, the 20S proteasome gains the ability to degrade β-casein – which intrinsically resembles an unfolded protein due to exposed hydrophobic residues - when only Bpa but not Mpa is present, showing that Bpa can stimulate proteolytic activity as long as the substrate does not need to be unfolded first. This might point to Bpa's role in the degradation of non-native or defective proteins. [119]

Like Mpa, Bpa does not readily interact with the 20S CP unless the open-gate CP mutant, where the first 7 N-terminal residues of the α-subunits are deleted, is used instead of the wild type. In this case, stable complexes can be formed from recombinant Bpa, Δ7NprcA and prcB, where Bpa binds to the top of the core particle's α-ring and is likely axially aligned with it. So far, only core particles with one Bpa bound to one side have been seen in EM. [119]

The binding of Bpa to CP was demonstrated to be dependent on the C-terminal HbYX-like motif QYL. However, pull-down assays showed that the interaction between Bpa and the CP barrel *in vitro* is weak to nonexistent and can only be reliably replicated when the open-gate proteasome mutant (Δ7PrcAB) is used. [119] This indicates that the assembly of the Bpa-CP complex *in vivo*, like that of the Mpa-CP proteasomal complex, requires yet another unidentified factor. Bacterial two-hybrid analysis showed that Bpa can interact not only with fully formed 20S proteasomes but in principle also with free CPα rings, although the existence of these is contentious. Small amounts of Bpa were found associated with half-proteasomes (a $CP\alpha_7$ ring plus an unprocessed $CP\beta_7$ ring) in a pull-down assay, prompting the question whether Bpa itself could be involved in the maturation of the 20S proteasome – however, no effect on the processing of CPβ could be found.[119]

1.4. The eukaryotic and the mycobacterial proteasome systems compared

Both eukaryotic and prokaryotic proteasomes share a general structure of heptameric, axially stacked rings capped by regulatory/unfoldase particles. However, both the core particle and the regulatory particles differ fundamentally in their internal architecture, with the eurkaryotic proteasome being significantly more complex than its prokaryotic counterpart. While the eukaryotic 26S proteasome can be isolated as a cohesive complex, this has not yet been achieved in either prokaryotes or bacteria.[50] Differences are not only found in the makeup of the proteasomes themselves but also in their associated proteins. In contrast to the intrinsically disordered Pup, Ubiquitin is a very stable protein whose compact β-grasp fold is used by several other, functionally unrelated proteins.[23,85] Pup and ubiquitin share no common features apart from their C-terminal diglycine motif.[92]

1.4.1. The HbYX motif

All proteasomal activators that bind to the 20S CP do so by inserting their C-terminal tails into intersubunit pockets on the surface of the CP's α-ring. The HbYX (hydrophobic amino acid – tyrosine – any amino acid) motif is a recurring and conserved feature of these proteins, forming the last three C-terminal residues of the tails. It is conserved in the ATPases Rpt2, Rpt3 and Rpt5 of the eukaryotic 19S RP and the archaeal PAN (proteasome-activating nucleotidase). In eukaryotes, the ATPase hexamer is formed by the Rpt1-6 subunits which are arranged in a 1-2-6-3-4-5 order.[120] Thus, the HbYX motif is present in alternate subunits, with the non-HbYX-containing Rpt1, Rpt6 and Rpt4 monomers between them. Other proteasomal activators, such as the eukaryotic Blm10 and PA28/11S, also bind to the CP in the described manner but do not contain the HbYX motif.[58] In mycobacteria, the proteasomal ATPase Mpa does not terminate in the HbYX motif but in QYL, which is highly conserved in its own right across multiple actinobacterial species (see **Fig. 1.3.3.4** and **1.3.3.5**). This QYX motif also occurs in Rpt 1 of *S. cerevisiae* as QYN.[114]

The HbYX motif has been demonstrated to be essential for the binding of the regulatory particles to the 20S core particles. It has also been shown that a seven-residue peptide (the last seven C-terminal residues of PAN, Rpt 2 or 5) containing the HbYX motif is sufficient to trigger the opening of the core particle's gate.[114] Deleting the two C-terminal residues from Mpa (Y and L) abolishes *M. tuberculosis*' resistance to nitric oxide completely, providing evidence for the critical function that the HbYX motif plays in the interaction of the ATPases with the core particle.[16,103] Despite the importance of the motif, its presence does not necessarily indicate a critical function. Although the eukaryotic RP subunits Rpt2, Rpt3 and Rpt5 all contain the motif, only Rpt3 and Rpt5 are essential for the binding of the RP to the CP.[67]

The penultimate tyrosine of HbYX in particular is essential for the interaction between the regulatory particles/ATPases and the 20S proteasome. In *M. tuberculosis*, replacement of it by even another aromatic amino acid such as phenylalanine (Mpa_{Y608F}) causes hypersensitivity to RNI on a level comparable to the *mpa* null mutant.[90] The tyrosine is conserved across the overwhelming majority of proteasome-containing bacteria as well as in most archaeal and some eukaryotic 19S-ATPase subunits.[103,118]

The HbYX motif in general and the penultimate tyrosine in particular can be a target for post-translational modification. The eukaryotic ATPase Cdc48 (p97/valosin-containing protein in mammals) terminates in a canonical HbYX motif, in this case LYG. The tyrosine was shown to be phosphorylated in a cell-cycle-dependent manner, which triggers transport into the nucleus. A mutant where the tyrosine was replaced by glutamate exhibited behavior as if the tyrosine were constitutively phosphorylated.[103,121,122] In *M. tuberculosis*, replacing the tyrosine with glutamic acid (Mpa_{Y608E}) to simulate phosphorylation by introducing a negative charge also causes hypersensitivity on par with the *mpa* null mutant.[123]

The binding sites for both PAN and Rpt2/3/5 on the 20S core particle are not located on the α-subunits themselves but are formed by the interfaces of the subunits.[65,66] Even the eukaryotic proteasomal activator protein PA26, which does not contain the HbYX motif, binds to these intersubunit pockets.[42] Although an atomic-level resolution structure of the Mpa-CP complex has yet to be produced, it is reasonable to assume that this is the case in Mpa as well. The gate opening mechanism in eukaryotes has been shown to be dependent on the carboxyl group of the last residue X. Introducing a mutation at this point does not negatively affect the opening, but altering the carboxyl group itself does.[114] When the HbYX motif binds to the intersubunit pockets on the α-rings' surface, its terminal carboxyl group form a salt bridge with the ε-amine of a conserved lysine residue inside the intersubunit pocket (the so-called pocket lysine).[66]

1.4.2. The 20S core particle

Structurally, the eukaryotic and the mycobacterial 20S core particles are almost identical. Both consist of four stacked heptameric α- and β- rings forming a hollow cylinder, in which the catalytic sites are located on the interior side of the inner β- rings, which are in turn capped by the outer α-rings. Their size is comparable as well, however, the rings of the eukaryotic CP are formed by seven unique α- or β-subunits each, while in *M. tuberculosis,* the rings are homoheptamers coded for by only one gene per ring: *prcA* for the α- and *prcB* for the β-subunits (see section **1.3**).[50]

An important difference between the eukaryotic and the prokaryotic proteasomes is that in eukaryotes, the central opening of the 20S α-rings is completely occluded by the α-rings' N-terminal tails (although the tails' orientations fluctuate between the closed and the open state, overall they are more likely to be in the former), while in prokaryotes it is partially open, forming a distinct channel into the inner chamber with a diameter of 2-3 nm.[34,37,47] EM studies have suggested that this is the result of the prokaryotic N-terminus being intrinsically disordered, and that this is the case in *M. tuberculosis* as well.[43,96,124] The occluding sections of the α-rings are conserved in eukaryotes, containing an YDR motif that is absent in bacterial proteasomes. It is possible that the lack of this motif is the reason for the partially open gate in prokaryotes.[41,125]

1.4.3. The ATPases

The ATPases of eukaryotes (Rpt1-6), archaea (PAN) and actinobacteria (ARC/Mpa) share a common structure both regarding their assembly as hexamers and concerning their internal architecture, despite the eukaryotic ATPase forming a subcomplex of the much larger regulatory 19S regulatory particle while both PAN and ARC/Mpa function as stand-alone units.[126] All three have an N-terminal coiled-coil domain, an oligonucleotide/oligosaccharide-binding (OB) domain, the AAA-ATPase domain and a C-terminal domain that forms tails with which the ATPase hexamer binds to the 20S core particle. This combination of N-terminal coiled-coil and OB domains is unique to the proteasomal ATPases. Both PAN and ARC/Mpa contain a critical and highly conserved proline at the link between these two domains, which, due to the proline's ability to switch between *cis* and *trans* configurations, enables the formation of the coiled-coil structures by dimerization of the N-terminal α-helices.[24,120,127].

1.5. The interaction between Mpa and the CP in the mycobacterial proteasome complex

Although the composition of the mycobacterial proteasome complex has been well established as the regulatory/unfolding ATPase Mpa bound to the 20S core particle, the two subcomplexes have been found to have essentially no interaction *in vitro.* The open-gate mutant of the CP (CP_{OG}), where the CPα subunit is truncated by its first eight N-terminal residues - thereby removing the occlusion from the entrance to the central chamber of the 20S core particle – is in principle able to form a complex with wild-type Mpa in the presence of 1mM ATPγS, but only approximately 2% of the core particles do so. When using the N-terminal Mpa deletion mutant Mpa_N97Δ (which removes the double alpha helices required to bind Pup), this number increases to 15%.[102,109] It has been suggested that either unidentified additional factors are necessary for the binding, or that recombinant Mpa/CP exhibits an altered conformation of their N-termini due to lacking assembly factors.[29]

The conserved structure of the bacterial, archaeal and eukaryotic holoproteasome complexes includes a fundamental discrepancy: the hexameric ATPase rings bind to the heptameric 20S α-rings, as is the case with Mpa and the 20S-CP in *M. tuberculosis* (**Fig. 1.3.3.2**). This circumstance is yet to be explained in terms of their interaction as well as in the evolutionary reason behind it. It has been suggested that in eukaryotes and archaea, the simultaneous engaging of all or most of the intersubunit pockets by the ATPase tails is unnecessary for binding and even unlikely.[65,128] A similar mechanism could be in place in the mycobacterial proteasome, where some of the six C-terminal Mpa tails could bind to the pockets on the α-rings' surface while others would be left free.

Intriguingly, in the eukaryotic proteasome, of the six C-terminal tails of the heterohexameric Rpt1-6 ring (arranged in the order 1-2-6-3-4-5), only three (2, 3 and 5) possess HbYX motifs, forming an alternating sequence (see section **1.4.1**)[67,120]. While two of the HbYX-containing tails (Rpt2 and Rpt5) are essential for binding, two of the non-HbYX-containing tails do not contribute to the interaction to the CP at all and the third (Rpt6) does so only partially. This reduction in the number of potential interactors provides a solution to the symmetry mismatch that could conceivably also apply to the

mycobacterial proteasome. Since Mpa's C-terminal tails do not terminate in the HbYX motif but in QYL (see sections **1.3.3** and **1.4.1)**, it is possible that the mechanism that allows Mpa to bind to the core particle despite the QYL motif – for example post-translational modification of the glutamine – only engages some of the tails while leaving others unaltered. Since only two out of six Rpt subunits are essential to the assembly and stability of the complex in eukaryotes, the Mpa hexamer could similarly be modified on only two or three of its tails, which could then attach it to the core particle. Considering that Mpa is a homohexamer, the modification mechanism could likely not distinguish between the individual tails and might modify them at random, unlike the Rpt1-6 ring where the subunits assemble in a defined order.

The *mpa607* mutant, where the last two residues of mpa (tyrosine and leucine) are deleted, exhibits hypersensitivity against nitric oxide and is attenuated in mice to the same level as the null mutant. This confirms the importance of the conserved QYL motif in binding to the 20S proteasome.[16,103] Using oligopeptides corresponding to the last 25 C-terminal residues of Mpa, ITC experiments in our laboratory showed that the same deletion abolishes the binding of the peptide to the 20S CP (see section **1.7**).

1.6. The role of the mycobacterial proteasome in defense against the host

The significance of the mycobacterial proteasome in the defense against the host immune system, in particular against the acidified nitrite produced by the macrophages it infects in the latent stage, has long been established. In fact, *mpa* and *pafA* were originally found by screening the virulent *M. tuberculosis* strain H37Rv (the attenuated strain is H37Ra) for genes that grant resistance against reactive nitrogen intermediates (RNIs). Mutants with insertions in *mpa* (Rv2115c) and *pafA* (Rv2097c) were attenuated in mice and hypersensitive against acidified nitrate *in vitro.*[16]

How *M. tuberculosis* circumvents the host immune response is not well understood, though intriguing results have been published. The proteasomal complex of *M. tuberculosis* plays a critical part, with knockout mutants defective for the proteasomal genes being recognized and eliminated by the host immune system. The 20S core particle of *M. tuberculosis* is required for optimum growth but not essential for its survival. Deletion or silencing of both *prcA* and *prcB* resulted in a phenotype that was impaired in its growth but otherwise viable. This defect is more pronounced on solid agar plates than in liquid medium.[129,130] In fact, the PPS might not even be required for the survival of the bacterium under normal conditions. It is known to play a crucial role in the defense of Mtb against the host immune system, in particular when *M. tuberculosis* is taken up by host macrophages. Additionally, it is also necessary under starvation conditions, where it is used for the recycling of proteins in order to provide the amino acids necessary for the adaptation of the proteome to the new requirements.

Mutants of Mtb with the *prcA* and *prcB* genes either deleted or silenced were hypersensitive to nitrosative stress *in vitro* and showed cell counts of less than 0.001% of the wild type. Surprisingly, when complementing the deletion mutant with the *prcAB*-T1A genes, which express a complete but proteolytically inactive version of the proteasome, resistance against nitric oxide and reactive nitrogen intermediates was restored to wild type levels together with the growth rate both in vitro

and *in vivo*.[75] Thus, whatever the function of the proteasome regarding protection against the host immune system might be, the simplest and most intuitive hypothesis, namely that the proteasome degrades bacterial proteins damaged by reactive nitrogen species (RNS) that would otherwise accumulate and kill the cell, cannot be the only explanation. For permanent survival in the host, however, active proteasomes are a necessity.[75] Since both replication and RNS resistance are restored by the inactive proteasome but persistent infection is still hindered, this suggests that there seem to be long-term host immune responses that require proteolysis to overcome.

The parallel Clp mechanism (consisting of the ClpP1, ClpP2 and ClpX proteases) has been shown to be essential for *M. tuberculosis in vitro*[131], indicating a shared responsibility of the two systems between housekeeping functions and those required during infection.

1.7. Previous results from our laboratory

In our previous experiments, instead of the *mpa*, *prcB* and *prcA* genes of *M. tuberculosis*, the equivalent genes *arc*, *prcB* and *prcA* of the related actinomycete *Streptomyces griseus* (strain JCM 4626 / NBRC 13350) were used. ARC (**A**TPase **f**orming **r**ing-shaped complexes) has 68% sequence identity with Mpa, is slightly shorter (588 residues in ARC, 608 in Mpa) and theoretically slightly more stable (instability index: 35.22 for ARC, 36.44 for Mpa as calculated by ExPASy ProtParam) than Mpa.[132] It is identical in its function to Mpa and contains the same C-terminal QYL sequence (see **Fig. Fig. 1.3.3.5**). Since ARC is also an alternative name for the mycobacterial Mpa, *S. griseus*' ARC will be called Mpa in this study.

When purifying Mpa with SEC, three distinct forms of Mpa can be seen: aggregates, dodecamers and hexamers. When purifying recombinant His_6-tagged Mpa with a NiNTA column, the removal of the nucleotides by adding EDTA prior to SEC significantly improves the purity, removing almost all aggregates and dodecamers. The formation of aggregates is not influenced by salt or protein concentration, the composition or the pH of the buffer, the presence of ATP or its analogues or reducing agents such as TCEP or DTT.

In another experiment, the 20S CP was able to degrade the short fluorogenic peptide Suc-LLVY-AMC by itself, without the assistance of bound Mpa. Together with the Mpa substrate experiment described above, these observations support the established view that 20S CP alone can take up and cleave small peptides and unstructured proteins but requires the associated ATPases to unfold larger substrates. The ATPase activity of Mpa was confirmed by introducing a debilitating mutation (E330Q) into Mpa's Walker B motif. In an unfolding assay using the Pup-luciferase fusion protein, the mutant showed no activity at all while the wild type was active.

A previous study showed that recombinant Mpa and the 20S CP only interact very weakly *in vitro*, and that the complex is not stable enough to be purified by SEC.[109] This result was confirmed in our experiments. No complex formation could be seen with SEC and no degradation of the substrate Pup-PanB could be detected when combining wild type Mpa and wild type CP. A series of ITC experiments were performed to test the influence of mutations in the C-terminal tails of Mpa on the interaction with the 20S CP. Synthetic oligopeptides corresponding to the last 25 or 26 residues of Mpa from *Streptomyces griseus* were used to compare the binding ability of the wild type peptide to

that of several mutants. Most importantly, the Mpa_{Q586F} mutant had its C-terminal QYL sequence converted into a canonical HbYX motif by exchanging the Q with F, creating a sequence equivalent to the FYK/FYA of *S. cerevisiae* Rpt3/5 and FYK of *H. sapiens* Rpt3. ITC measurements showed that this mutation significantly enhances the binding of Mpa to the 20S proteasome, by a factor of 5 compared to the wild type ($K_{D\ WT}$ = 100 µM, $K_{D\ Q586F}$ = 20 µM). Why Mpa does not use the HbYX motif even though it would markedly improve the interaction is unknown. When the last two residues of the QYL were deleted entirely, no binding between the Mpa peptide and the 20S CP could be detected at all. Compared to the findings of Darwin et al. where this mutation caused hypersensitivity of *M. tuberculosis* against nitric oxide, this provides further evidence for the critical role that the YL plays in the interaction between the Mpa hexamer and the 20S CP.

Experiments in our lab showed that the full-length Mpa_{Q586F} mutant can bind stably to the wild type 20S CP *in vitro*, enabling the size exclusion purification of the complex and the putative identification by EM of a 20S CP bound by one Mpa hexamer at each end. However, this stable interaction can only be achieved when mpa_{Q586F}, *prcB* and *prcA* are combined on a single plasmid, the so-called tricistronic expression construct triC (mpa_{Q586F} - *prcB*His_6 – *prcA*) under the control of a single promotor. The resulting 20S CP exhibits an interesting behavior: although its general structure is identical to conventionally produced 20S CP, its β-subunit propeptides are not cleaved during the assembly and can easily be distinguished from processed β-subunits by SDS-PAGE. Thus, the triC-CP represents the intermediate form of the 20S CP (see **Fig. 7A**), with the β-subunit propeptides remaining folded inside the central chamber. Structurally, this is of little importance, since the resulting CP barrel is almost identical to that of the mature type, except that its radius is 1.5 Å larger. The tricistronic construct was used extensively in the course of this study (see sections **3.6 - 3.10**).

2. MATERIALS AND METHODS

2.1. Reagents and other chemicals

All reagents and chemicals used were purchased from Sigma-Aldrich, Fluka or Roche Life Sciences unless otherwise stated and were of the highest grade available. Antibiotics were purchased from Sigma-Aldrich.

2.2. Buffers, solutions, media and antibiotics

Commonly used buffers are listed here; specialized buffers such as those used for recombinant protein purification are listed in the corresponding section. All buffers were filtered through a Pall Aerodisc 0.2 µm filter and degassed with a vacuum pump for at least 20 minutes. Percentages refer to mass concentrations (grams per milliliter) unless stated otherwise.

SDS-PAGE loading buffer:	80 mM Tris-HCl (pH =6.8) 2% SDS 10% glycerol 0.02% bromophenol blue 50 µl/mL 2-mercaptoethanol
SDS-PAGE running buffer:	25 mM Tris-HCl (pH = 8.3) 200 mM glycine 0.1% SDS
10x TAE buffer:	0.4 M Tris-HCl (pH = 8) 0.2 M acetic acid 10 mM EDTA-Na_2 salt
10 x TBS buffer:	200 mM Tris-HCl 1.5 M NaCl
DNA loading buffer:	30% glycerol 0.25% bromophenol blue 0.25% xylene cyanol

LB medium (pH = 7):	10 g tryptone 5 g yeast extract 10 g NaCl
Staining solution for SDS-PAGE:	2.5 g Coomassie Brilliant Blue R-250 450 mL ethanol 100 mL acetic acid 450 mL water
Destaining solution for SDS-PAGE:	250 mL ethanol 80 mL acetic acid 670 mL water
Lysozyme*:	50 mg/mL
DNAse I*:	1 mg/mL
Ampicillin*:	50 mg/mL
Tetracyclin*:	5 mg/mL

*Stored at -20°C.

2.3. Bacterial strains

Host strain	*Genotype*
BL21 (DE3)	F^- ompT gal dcm lon hsdS_B(r_B^- m_B^-) λ(DE3 [lacI lacUV5-T7 gene 1 ind1 sam7 nin5])
DH5α	F^- endA1 glnV44 thi-1 recA1 relA1 gyrA96 deoR nupG Φ80d*lacZ*ΔM15 Δ (*lacZYA- argF*) U169, hsdR17(r_K^- m_K^+), λ–

2.4. Plasmids

Name	*Genes*	*Description*
5a	*prcA-prcB*His_6	CPα and C-terminal His_6-tagged CPβ
$5a_{T54V}$	$prcA\text{-}prcB_{T54V}His_6$	CPβ propeptide mutant
$5a_{PL}$	$prcA_{K52V}\text{-}prcB His_6$	CPα pocket lysine mutant
5b	*prcA-prcB*-Strep II	Strep II-tagged core particle
5c	*mpa*His_6	C-terminally His_6-tagged Mpa
5d	His_6*Mpa*	N-terminally His_6-tagged Mpa
5dtriC	*mpa-prcB*-His_6*prcA*	Holoproteasome: Mpa + 5a
$5dtriC_{Q586F}$	$mpa_{Q586F}\text{-}PrcB\text{-}His_6 prcA$	Holoproteasome: Mpa_{Q586F} + 5a
$5dtriC_{Q586pBpa}$	$mpa_{Q586pBpa}\text{-}PrcB\text{-}His_6 prcA$	Holoproteasome containing *p*Bpa
pDULE-ABK	p*Bpa-RS/tRNA*$_{CUA}$	Plasmid to introduce *p*Bpa into Mpa

The pDULE-ABK plasmid was developed to allow the incorporation of the photoreactive unnatural amino acid *para*-benzoyl-L-phenylalanine (*p*Bpa) into recombinant proteins. *p*Bpa, as a member of the benzophenone group, can be induced by UV radiation to form a covalent bond with adjacent C-H groups (see **Fig. 2.4.1**) and is therefore highly useful for protein-peptide or protein-protein interaction studies.[133,134]

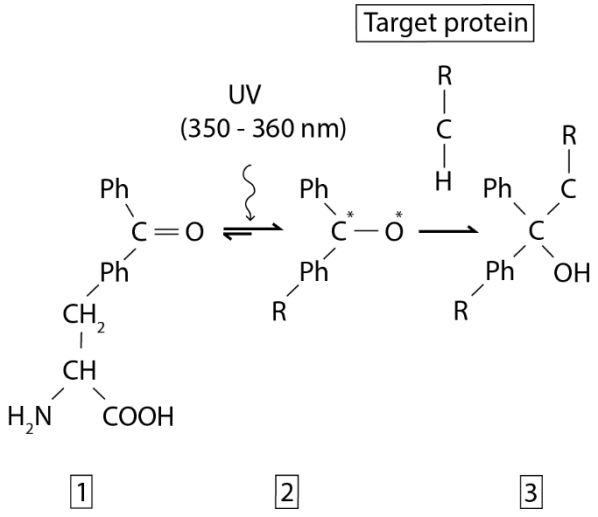

Fig. 2.4.1. Photochemical mechanism of UV-induced *p*Bpa crosslinking. **(1)** When *p*BpA is irradiated by UV radiation of 350-360 nm wavelength, it forms a diradicaloid **(2)** that interacts with weak C-H α-bonds of target proteins within approximately 3 nm. **(3)** The diradicaloid forms a covalent bond with the target protein. Ph: phenyl group. R: rest of *p*Bpa. Adapted from [134].

pDULE-ABK codes for two genes, one for a tRNA ($tRNA_{CUA}$), the other for an aminoacyl-tRNA synthethase (*p*Bpa-RS). These form a so-called orthogonal tRNA pair/aminoacyl-tRNA synthethase pair ("orthogonal" in the sense of "as opposed to the standard genetic code") that specifically links *p*Bpa to the $tRNA_{CUA}$ and inserts it into the nascent protein. $tRNA_{CUA}$ contains the CUA anticodon that recognizes the amber codon TAG. TAG normally functions as a stop codon but can be overridden and used as a regular codon by amber suppressor tRNAs such $tRNA_{CUA}$ used in pDULE-ABK. When co-transforming pDULE-ABK with a gene containing the amber mutation ($Mpa_{Q586pBpa}$ in this study), the $tRNA_{CUA}$ is charged with *p*Bpa by the specialized aminoacyl-tRNA synthethase and incorporates *p*Bpa into the nascent protein at the amber codon, which would otherwise be read as a stop codon.[133,135] The pDULE-ABK plasmid was generously provided by Dr. Peter Schultz.

The *mpa, prcA* and *prcB* genes used were those of the actinobacterium *Streptomyces griseus* (NBRC 13350) which have been established as a viable and stable model for the *M. tuberculosis* proteasomal complex in previous experiments in our lab (see section **1.7.**)

2.5. Transformation of chemically competent *E. coli*

In a 1.5 mL Eppendorf tube 2 µl of plasmid solution were added to 30 µl chemically competent bacteria (produced in-house), gently mixed and kept on ice for 15 minutes before heat shocking at 42°C for 90 s. Bacteria were them again put on ice for 5 minutes. 350 µl LB medium without antibiotics was added and the tube incubated for 1 h at 37°C under gentle shaking. Subsequently they were used either to inoculate liquid LB medium or plated on LB-agar plates containing 50 µg/mL ampicillin.

2.6. Preparing chemically competent *E.coli* with the calcium chloride method

To express the pDULE-RBK plasmid (see section **2.4**) in order to produce *p*Bpa-containing protein (see section **2.9)**, BL21(DE3) E. coli were made chemically competent with the $CaCl_2$ method. All steps were performed on ice and using ice-cold solutions unless indicated otherwise.

100 mM $CaCl_2$ solution was prepared and filtered through a sterile Aero 0.2 µm membrane. An overnight culture of BL21(DE3) was used to inoculate 50 mL LB medium that was incubated at 37°C until an OD_{600} of between 0.3 and 0.4. Incubation was then stopped and the culture was transferred into two pre-cooled 50 mL Falcon tubes, kept on ice for 10 minutes and then centrifuged at 4000 rpm for 7 minutes. The supernatant was removed and the pellet resuspended in 10 mL 100 mM $CaCl_2$ solution, then centrifuged at 3500 rpm for 7 minutes, then the supernatant was again removed and the pellet resuspended in 10 mL $CaCl_2$ solution as before. The cells were then kept on ice for 30 minutes and centrifuged at 3500 rpm for 5 minutes. Finally, the supernatant was removed and the pellet was resuspended in 1 mL $CaCl_2$ solution + 15% glycerol, the cells divided into 30 µL-aliquots, flash-frozen in liquid nitrogen and stored at -80°C. To use the transformed competent cells, a sterile

inoculation loop was used to scrape cells directly from the frozen aliquots and streak them on LB-agar plates containing 25 µg/mL tetracyclin.

2.7. Expression of recombinant proteins in *E. coli*

After transformation as described above, 150 mL of LB + 50 µg/mL ampicillin was inoculated with the entire and grown overnight at 37°C under constant shaking at 180 rpm. Of these overnight cultures 25 mL were used the next day to inoculate 2 L of LB + Amp for the main cultures each. These were then incubated at 37°C and 180-200 rpm until an OD_{600} between 0.9 and 1 and then induced with 0.5 mM IPTG. The induced cultures were incubated either for 3 h at 37°C (expression of CP) or for 6 h at 25°C (expression of Mpa alone or the entire proteasome complex). Cells were harvested by centrifugation at 4000 rpm for 20 minutes in a Beckmann Coulter J6M centrifuge using a JS-4.2 rotor, resuspended in 0.9% NaCl solution, transferred into Falcon tubes and again centrifuged for 45 minutes at 3000 g. The liquid supernatant was discarded, cell pellets were weighed, shock frozen in liquid nitrogen and stored at -20°C.

2.8. Expression of selenomethionine-containing recombinant Mpa in *E. coli*

All buffers and components were either autoclaved or filtered sterilely.

10 x MinA buffer:	105 g K_2HPO_4
	45 g KH_2PO_4
	10 g $(NH_4)_2SO_4$
	5 sodium citrate tribasic dihydrate
	Filled up to 1000 mL with water
MinA medium:	100 mL 10 x MinA buffer
	1 mL 1 M $MgSO_4$ (autoclaved)
	480 µL 1% thiamine
	10 mL amino acid mix I (4 mg/mL of all amino acids except T, W, F and M)
	10 mL amino acid mix II (4 mg/mL of T, W and F)
	40 mL selenomethionine (1 mg/mL)
	10 mL 20% glucose (autoclaved)
	50 mg ampicillin
	Filled up to 1000 mL with water

BL21 (DE3) were transformed with 5c plasmid and grown as an overnight culture in LB + ampicillin as usual. 25 mL of the overnight cultures per liter of SeMet expression were centrifuged and resuspended in 10 mL MinA medium. Main cultures were grown at 37°C until OD_{600} = 0.9 and

induced with 0.5 mM IPTG as usual. Immediately after induction, the temperature was lowered to 28°C and the cultures were grown overnight at 180 rpm. Harvesting was done as usual.

2.9. Expression of recombinant *p*Bpa-containing Mpa

To determine the optimal conditions for the expression of $Mpa_{Q586pBpa}$, test expressions were set up at different temperatures (18°C, 25°C) and at different IPTG concentrations (0.1 M , 0.5 M). *E.coli* BL21 (DE3) [pDULE] (see **2.5**.) were transformed with the $5c_{Q586pBa}$ plasmid as usual. Overnight cultures were used to inoculate LB containing 1 mM *p*Bpa (from 1 M *p*Bpa stock solution dissolved in 1 M NaOH) that were induced with 0.1/0.5 mM IPTG as usual (see **2.6.**), the temperature was then set to 18/25/37°C and the culture incubated overnight in the dark (using a shaker with the window covered with aluminium foil) at 180 rpm. Samples of 25 mL each were taken at 1, 3 and 6 hours after induction, centrifuged, shock frozen and stored at -20°C as with normal harvests. The incubation was finished the next day, approximately 18 hours after induction.

2.10. Batch purification of His_6-tagged proteins

To purify His_6-tagged proteins, the following buffers were used:

Start buffer:	50 mM monobasic sodium phosphate hydrate ($NaH_2PO_4 \cdot H_2O$) 300 mM NaCl
Wash buffer:	50 mM monobasic sodium phosphate hydrate ($NaH_2PO_4 \cdot H_2O$) 300 mM NaCl 25 mM imidazole
Elution buffer:	50 mM monobasic sodium phosphate hydrate ($NaH_2PO_4 \cdot H_2O$) 300 mM NaCl 500 mM imidazole

The expression cultures were lysed with 1 mL primary amine-free Merck Millipore BugBuster Extraction Reagent per 25 mL of culture according to the manufacturer's instructions. Lysed samples were then centrifuged for 30 minutes at 13000 rpm, the supernatant was transferred into a fresh tube and 300 µL Qiagen Ni-NTA Superflow suspension (previously washed three times with Ni-NTA start buffer) were added. The samples were then incubated at 4°C for 30 minutes under rotation, transferred to a 96-well fritted plate, washed once with start buffer and twice with wash buffer by centrifuging. To elute the protein, 75 µL elution buffer were added and the plate centrifuged again.

2.11. IMAC purification of recombinant proteins

All protein purification steps were performed on ice or at 4°C unless stated otherwise. Purification was performed on Amersham Bioscience ÄKTA Explorer machines. Absorbance was measured at 280 nm. His_6-tagged recombinant proteins were purified using the following buffers:

Start buffer (pH_{RT} = 8):	50 mM monobasic sodium phosphate hydrate ($NaH_2PO_4 \cdot H_2O$) 300 mM NaCl (150 mM for low-salt variant) 10 mM imidazole
Elution buffer (pH_{RT} = 8):	50 mM monobasic sodium phosphate hydrate ($NaH_2PO_4 \cdot H_2O$) 300 mM NaCl (150 mM for low-salt variant) 250 mM imidazole

Frozen cell pellets were thawed in warm water. 1 mL of cold start buffer was added per gram of pellet, in addition to 2 mL lysozyme solution, 1 mL of DNAse I solution, 0.5 mL of 0.5 mM PMSF and two tablets of Roche's EDTA-free cOmplete protease inhibitor per pellet (previously dissolved in 1 mL cold start buffer). After gentle manual mixing by inversion, cells were incubated on ice for 45 min, then sonicated with a SONICATOR MODEL at 60% power/1 second pulse/0.3 seconds pause (for CP purification) or 60% power/1 second pulse/1 second pause (for Mpa purification) with the sonication container submerged in ice water. After sonication, the lysate was centrifuged for 30 minutes at 18,000 rpm in a Sorvall RC 3B centrifuge using an SS-34 rotor. The supernatant was decanted and a sample was taken from the debris pellet.

The supernatant was loaded onto a GE HisTrap HP 5 mL Ni-Sepharose column (previously equilibrated with at least 5 column volumes of start buffer) at a flow rate of 1 mL/min. The column was washed with 100% start buffer after loading until the absorbance was below 300 mAU, then the column was washed with 30% elution buffer until the absorbance was below 200 and the protein eluted with 100% elution buffer. Different gradient steps were tested but did not result in significantly purer protein, at the cost of lower yield. Fractions were analyzed with SDS-PAGE and those containing the desired protein were concentrated with Sartorius Vivaspin columns (MWCO 10.000 for CP and 30.000 for Mpa). Purified proteins were shock frozen in liquid nitrogen and stored at -80°C if no further purification was required.

After the elution of the desired protein, the columns were washed with elution buffer for 5 column volumes, then washed with water for another 5 volumes and stored in 20% ethanol.

2.12. Size exclusion chromatography purification

All protein purification steps were performed on ice or at 4°C unless stated otherwise. Purification was performed on Amersham Bioscience ÄKTA Explorer machines. Specialized buffers and SEC procedures are described in the corresponding section. For general purification of proteins, the following buffer was used:

SEC buffer (pH_{RT} = 8): 50 mM monobasic sodium phosphate hydrate ($NaH_2PO_4 \cdot H_2O$)
300 mM NaCl

Proteins were concentrated as described above and loaded onto a GE Superose 6 XK16/70 column previously equilibrated with one column volume of SEC buffer through a 2 mL injection loop. Flow rates were in the range of 0.5-1 mL/min. Fractions were analyzed with SDS-PAGE and those containing the desired protein were concentrated with Sartorius Vivaspin columns (MWCO 10 kDa for CP and 30 kDa for Mpa) to a reasonable concentration and amount, shock frozen in liquid nitrogen and stored at -80°C.

Buffer exchange was performed with a GE Healthcare HiPrep 26/10 Desalting column.

2.13. Laemmli-SDS-PAGE

To analyze proteins, Laemmli-SDS-polyacrylamide gel electrophoresis (SDS-PAGE)[136] was used. 12% gels were cast according to the following recipe:

Component	*Separating gel*	*Stacking gel*
1.5M Tris-HCl (pH = 8.8)	20 mL	-
0.5M Tris-HCl (pH = 6.8)	-	7.5 mL
Polyacrylamide solution	32 mL	4.5 mL
Water	28 mL	17.4 mL
10% SDS	800 µl	300 µl
10% APS	400 µl	300 µl
TEMED	40 µl	30 µl

As a high-resolution alternative in the higher mass area, 10% gels were also used, with 26.4 mL polyacrylamide and 32.8 mL water and all other components equal.

Immediately after casting the separating gel, a layer of water-saturated tert-Butanol ($\frac{1}{3}$ water, $\frac{2}{3}$ butanol shaken and left to separate into water and butanol phases) was applied to the top to level

the upper edge. After the separating gel polymerized, the tert-Butanol was discarded and the stacking gel was cast.

Protein samples were mixed 1:1 with SDS-PAGE loading buffer, heated to 95°C for 2 minutes and loaded. Gels were run at 200-220 volts until the dye front reached the lower edge, then stained with Coomassie Brilliant Blue solution (by heating in a microwave for 30 seconds) and destained. As a marker, Thermo Scientific PageRuler Prestained Protein Ladder was used unless otherwise indicated.

2.14. Silver staining

All steps were performed on a shaker at room temperature unless otherwise indicated. SDS-PAGE gels were transferred directly from the electrophoresis apparatus into a glass chamber and fixed for one hour in 40% ethanol, 10% acetic acid. Gels were then washed with 30% ethanol for 2 x 20 minutes, then with water for another 20 minutes. Gels were sensitized in fresh 0.02% Na_2SO_3, washed with water for 3 x 20 seconds and subsequently soaked in cold $AgNO_3$ at 4°C for 20 minutes. After washing with water for 3 x 20 seconds, the gels were transferred into a new glass chamber, washed again with water for one minute and developed in fresh 3% Na_2CO_3, 0.05% formalin until the staining was sufficient. The staining was then terminated by washing with water for 20 seconds and soaking in 5% acetic acid afterwards. Gels were stored in 1% acetic acid after washing with water for 3 x 10 minutes.

2.15. Protein concentration measurements: Bradford assay and NanoDrop

BioRad Protein Assay solution was diluted 1:5. 995 µl of this solution was mixed with 5 µl of the protein solution. Absorption was measured at 595 nm with a photometer. Protein concentration was determined with a standard curve constructed according to the manufacturers' instructions.

A Thermo Scientific NanoDrop 1000 spectrophotometer was also used to determine protein concentration according to the manufacturer's instructions. Values for the molar absorbance coefficient ε were taken from the Swiss Institute of Bioinformatics' ProtParam tool based on the presence of aromatic amino acids and their absorbance at 280 nm. [137]

2.16. Isothermal titration calorimetry (ITC)

During the assembly of the holoproteasome (Mpa-CP) complex, the C-terminal tails of Mpa bind to pockets on CP's surface, likely formed by the interface of the CPα-subunits.[66] Mpa's C-terminal tails end in the highly conserved QYL motif, resembling the HbYX motif that is found in the analogous Rpt proteins of humans and *S. cerevisiae* (see section **1.4.1**). The understanding of this binding process between the tails of Mpa and the pockets of CP is therefore important for the understanding of the complex assembly as a whole.

To simulate the binding of Mpa to the CP, the C-terminal tails can be synthesized as oligopeptides of varying length. Seven-residue peptides terminating in the HbYX motif are sufficient to bind to the CP and trigger the opening of the gate for both eukaryotic and archaeal proteasomes.[114] Previous ITC experiments in our lab had used peptides corresponding to the last 25 or 26 residues of *S. griseus*' Mpa (which also end in the GQYL motif) and its CP for the same purpose. Mutant variations of these peptides had shown that the replacement of the QYL motif's glutamine with a hydrophobic amino acid such as phenylalanine (the Q586F mutant) or leucine (Q586L) resulted in stronger binding of the peptide to the CP 28-mer compared to the wild type peptide, with an approximate K_D of 20 µM for both the Q586F and the Q586L mutant versus an approximate K_D of 100 µM for the wild type (see also section **1.6**). In both cases, a single-site model was fitted (**Table 1,** peptides 4, 9 (with CP_{WT}) and 10). ITC studies from our lab had also demonstrated that deletion of the YL residues completely abolished binding to the CP, confirming earlier results using proteasome systems of *M. tuberculosis*.[123] Why Mpa and ARC do not contain the eukaryotic HbYX motif but only the related QYL sequence, when the canonical HbYX would markedly improve its binding ability, is a question that has yet to be answered. It is conceivable that a higher affinity for CP would actually negatively influence the function of the proteasome pathway, for example by premature assembly of the holoproteasome. It would necessarily follow that this problem has been solved in eukaryotes.

The Q586F mutant peptide (peptide 9) was used in this study to analyze potential binding to the open-gate variant of the CP In the open-gate mutant, the first seven N-terminal residues of CPα are deleted, removing the peptides that block the entrance into central channel and increasing its proteolytic activity by an order of magnitude.[96] This deletion, for reasons that are still unclear, also allows the *in vitro*-interaction of Mpa and CP (see section **1.3.2**).

The photoreactive non-natural amino acid para-Benzoylphenylalanine (*p*Bpa) can be used to crosslink interacting proteins or peptides. When irradiated with ultraviolet light between approximately 350 and 360 nm, it forms covalent bonds with carbon-hydrogen bonds within 3 Å of its carbonyl oxygen.[133] Thus, proteins or peptides containing *p*Bpa will be permanently linked to their binding partners, as long as the site of interaction is located within the maximum distance from the *p*Bpa residue. To test the feasibility of photocrosslinking *p*Bpa-containing full-length Mpa to CP, ITC was performed with four pBpa-containing 26-amino acid peptides, corresponding to the last 25 or 26 amino acids of Mpa's C-terminal domain. *p*Bpa was used either as a replacement for the HbYX phenylalanine of the Q586F mutant (peptide 20: Q586*p*Bpa), in addition to the Q586F mutation (peptide 21: Q586F Y587*p*Bpa, peptide 33: V581*p*Bpa Q586F, peptide 34: T584*p*Bpa Q586F) or as a second variant that did not contain the Q586F mutation (peptide 22: L588*p*Bpa). These were used to test whether the use of *p*Bpa instead or in addition to the previously introduced hydrophobic amino acids would alter the improved binding characteristics of the and hence whether they could subsequently be used for establishing a stable, cross-linked full-length Mpa : CP complex. In addition, the non-*p*Bpa mutants Q586W *(*peptide 31), Q586F L588A (peptide 16) and Q586F L588E (peptide 17) were tested as a comparison to the *p*Bpa peptides.

Peptides were dissolved in either reaction buffer or pure DMSO since not all peptides were equally soluble. The purified CP_{WT} or CP_{OG} used for the ITC was transferred into reaction buffer by centrifugation in Sartorius Vivaspin columns (MWCO: 10.000 Da) and exchanging of buffer at least three times, unless the last purification step had already been performed in reaction buffer.

ITC reaction buffer (pH = 8): 50 mM Tris-HCl
150 mM NaCl
20 mM $MgCl_2$
1 mM TCEP

Solutions in reaction buffer of 250 µM (peptides 20 and 22), 500 µM (peptides 9, 21 and 31) or 1000 µM (peptides 17, 33 and 34) were prepared. Except for peptide 31, none of the peptides could be completely dissolved. For peptides 9, 20, 21 and 22, the solution was centrifuged and the supernatant was used for the ITC after the concentration had been determined by NanoDrop.

Peptides 16, 17, 31, 33 and 34 could not be dissolved in reaction buffer alone at all even after shaking at 37°C, 1000 rpm for 30 minutes. For these peptides, a 10 mM stock solution in pure DMSO was prepared and then diluted to 1 mM with reaction buffer to the required volume, i.e. a final DMSO concentration of 10%. The same amount of DMSO was added to the solution containing the CP.

ITC was performed with a MicroCal VP-ITC MicroCalorimeter. Samples were degassed and temperature-equilibrated with a ThermoVac Sample Degasser/Thermostat. All measurements were performed at 26°C with 20 injections, 120 seconds spacing without and 180 seconds with DMSO. Data analysis was performed using MicroCal Origin 7.0 software.

Peptide	Sequence	Variant
4	TLVTGKQGADTGRSIDTVANTGQYL	Wild type
9	TLVTGKQGADTGRSIDTVANTG**F**YL	Q586F
10	TLVTGKQGADTGRSIDTVANTG**F**YL	Q586L
16	WTLVTGKQGADTGRSIDTVANTG**F**Y**A**	Q586F L588A
17	WTLVTGKQGADTGRSIDTVANTG**F**Y**E**	Q586F L588E
20	WTLVTGKQGADTGRSIDTVANTG***pBpa***YL	Q586*pBpa*
21	WTLVTGKQGADTGRSIDTVANTG**F*****pBpa***L	Q586F Y587*pBpa*
22	WTLVTGKQGADTGRSIDTVANTG**F**Y***pBpa***	Q586F L588*pBpa*
31	WTLVTGKQGADTGRSIDTVANTG**W**YL	Q586W
33	WTLVTGKQGADTGRSIDT***pBpa***ANTG**F**YL	V581*pBpa* Q586F
34	WTLVTGKQGADTGRSIDTVAN***pBpa***G**F**YL	T584*pBpa* Q586F

Table 1: List of C-terminal 25- or 26- residue Mpa peptides tested with ITC for their binding to either CP_{WT} or CP_{OG} (only with peptide 9). Mutant residues are bolded, the HbYX motif is underlined. For peptides 16 – 34, an N-terminal W residue was added in order to enable spectroscopic quantification.

2.17. Affinity chromatography

Affinity chromatography to isolate anti-Mpa and anti-CP antibodies from rabbit serum was performed with a GE Healthcare 1 mL HiTrap NHS-activated HP sepharose column. The following buffers were used, in addition to reagents that are listed in the protocol:

Coupling buffer (pH = 8):	20 mM HEPES 150 mM NaCl
Blocking buffer (pH = 8.3):	0.5 M acetic acid 0.5 M NaCl
Wash buffer (pH = 7.4):	1 x PBS[4] 0.1% Tween 20

For anti-Mpa antibody purification, Walker B-mutant Mpa (Mpa_{WB}) was used as a ligand to bind the antibody. For the anti-CP antibody, wild type CP was used. Both proteins were first buffer-exchanged into coupling buffer and then used according to the protocol.

The column was washed with 1 mM ice cold HCl and immediately, 1 mL of the ligand solution (Mpa_{WB} or CP) was injected. The column was closed and incubated at room temperature for 30 minutes. 10 mL blocking buffer were injected to saturate unbound NHS groups, a sample was taken and the column was again closed and incubated at room temperature for 30 minutes. The column was washed with 10 mL 10 mM Tris-HCl (pH = 8), then washed with the following buffers, listed in order of usage:

10 mL 0.1 M glycine (pH = 2)
20 mL 10 mM Tris (pH = 8)
10 mL 0.1 M glycine (pH = 2)
10 mL 10 mM Tris (pH =8)
20 mL PBS (pH = 7.4)

The rabbit serum containing the anti-Mpa and anti-CP antibodies was thawed on ice and diluted with 2x PBS to 50 mL (approximately 1:1). The column was connected to a GE Healthcare Äkta Explorer FPLC machine, the serum was applied to the column using the sample pump, collected and recirculated to bind the antibody. After the second run, the column was washed with 100 mL wash buffer (100 column volumes), then with 30 mL PBS and finally with 7 mL 10 mM Tris (pH = 8).

To elute the antibody, fractionation tubes containing 200 µL 1M Tris, pH = 8 were prepared. 0.1 M glycine (pH = 2.6) was slowly injected into the column with a 1 mL syringe and fractions of

[4] (supplied by the in-house media kitchen as 10 x PBS)

approximately 1 mL (including the Tris) were collected. In total, 11 (anti-CP) and 12 (anti-Mpa) fractions were collected and their concentrations measured with NanoDrop at the IgG settings. The fractions of highest concentrations were collected, pooled and dialyzed against 1x PBS + 10% glycerol in a 3.5 kDa cutoff membrane over night at 4°C.

2.18. Western blotting

Western blots were performed according to the semi-dry protocol, using the following buffers:

Blotting buffer:	50 mM Tris-HCl 380 mM glycine 0.1% SDS 20% methanol
Blocking buffer:	1 x TBS 3% Sigma-Aldrich bovine serum albumin 1 mM EDTA 0.05% Tween 20

Primary antibody (rabbit anti-Mpa or anti-CP IgG):	diluted 1:1000 in 1 x TBS + 3% BSA
Secondary antibody (mouse anti-rabbit IgG antibody coupled to horseradish peroxidase):	diluted 1:10000 in 1 x TBS + 5% milk powder

PVDF membranes were soaked in methanol to activate them, then placed on Bio-Rad blotting paper. Gels were then placed on the membranes and another piece of blotting paper was put on top. The entire stack was soaked in blotting buffer and the current was set to 0.1 A per gel and run for approximately 60 to 70 minutes, until the voltage had increased from 6 V at the beginning to 12 to 15 V. The gels were removed, the membranes were placed in blocking buffer and incubated on a shaker for 1 hour at room temperature. Afterwards, they were washed with 1 x TBS for 3 x 15 minutes and the primary antibody was applied, then the membranes were shaken either for 1 hour at room temperature or overnight at 4°C. The triple TBS washing step was repeated, the secondary antibody was added and incubated while shaking at 4°C. Finally, the membranes were washed with TBS + 0.1% Tween 20 for 4 x 15 minutes. The blot was developed with the Amersham ECL Plus Western Blotting Detection system according to the manufacturer's instructions. Amersham Hyperfilm ECL films were used with varying exposure times depending on the intensity of the signal.

2.19. Growth of *Streptomyces griseus* cultures

Streptomyces griseus cultures were used for pull-down experiments with lysate and grown on or in ISP2 medium (10 g/l malt extract, 4 g/l yeast extract, 4 g/l glucose). Sterile ISP2-agar plates were prepared, a -80°C glycerol stock of *S. griseus* was streaked out on them and the plates were then incubated at 26°C for 72 hours. Precultures were inoculated in 3 x 150 ml ISP2 medium and shaken at 26°C, 180 rpm for 72 hours. Two of the precultures were pooled, 60 ml of this and 60 ml of the remaining preculture were used to inoculate 3 x 2 l liquid ISP2 medium. These main cultures were then again incubated at 26°C, 180 rpm for 72 hours. Harvesting was performed as usual (see section **2.7**).

2.20. Pull-down assays from *Streptomyces griseus* lysate

Although the Mpa and CP subunits of the proteasome complex can be recombinantly expressed, they have not been demonstrated to interact *in vitro* unless mutants are used, and even then the level of interaction is very low. In the co-immunoprecipitation experiment (section **2.21**) it was attempted to isolate the proteasome complex from the cell lysate of *Streptomyces griseus* using Mpa- and CP-specific antibodies. Here, the Mpa-CP holoproteasome was to be pulled from *S. griseus* cell lysate by using its component proteins as bait. Hexahistidine-tagged Mpa and CP were bound to Qiagen NiNTA-agarose beads, then added to the *S. griseus* cell lysate to immobilize the proteasomal subunits, which were then to be eluted by a conventional imidazole buffer (compare with section **2.11**). Mass spectroscopy of the pull-down elutions was performed to test whether binding of Mpa or CP occurs *in vivo* and if so, whether Mpa's C-terminal tails (in particular the HbYX-like QYL motif) are modified post-translationally.

Buffers used:

Pull-down start buffer (pH = 8):	50 mM sodium phosphate monohydrate ($NaH_2PO_4 \cdot H_2O$) 150 mM NaCl
Pull-down wash buffer 1 (pH = 8):	50 mM sodium phosphate monohydrate ($NaH_2PO_4 \cdot H_2O$) 150 mM NaCl 10 mM imidazole
Pull-down wash buffer 2 (pH = 8):	50 mM sodium phosphate monohydrate ($NaH_2PO_4 \cdot H_2O$) 150 mM NaCl 25/40 mM imidazole
Pull-down elution buffer (pH = 8):	50 mM sodium phosphate monohydrate ($NaH_2PO_4 \cdot H_2O$) 150 mM NaCl 150 mM imidazole

S. griseus cultures were grown and harvested as described in section **2.19** and lysed using a French press (2 kbar), with the lysate reapplied twice. The lysate was then centrifuged for 30 minutes at 38700 g as described in section **2.19**. Qiagen NiNTA agarose beads were washed and equilibrated in start buffer. 45 µg of bait protein (either CP or Mpa, Hsp104 as a negative control) were mixed with 15 mg of the lysate and incubated at 4°C for 2 hours in Falcon tubes on a shaker. 50 µL of the NiNTA beads were added and the lysate was again incubated for 10 minutes at 4°C. After centrifugation, the supernatant was removed (the flow-through fraction), the beads were washed with 100 µL of wash buffer 1, the supernatant was removed and the step repeated (wash fraction 1 and 2). Next, the washing was repeated with 100 µL of wash buffer 2 twice as before (wash fraction 2 and 3), then once with wash buffer 3 (wash fraction 4). Finally, the elution was performed by centrifuging and removing the wash buffer, adding 50 µL elution buffer to the beads, mixing carefully by pipetting up and down and repeating once. Therefore, two elution fractions per pulldown were produced (elution 1 and 2). Samples for SDS-PAGE gels were taken from the supernatant at every step.
For mass spectrometry, the elution fractions were transferred into 50µl 20 mM Tris-HCl buffer using Vivaspin spin columns (MWCO: 5 kDa). Hsp104 was used as a control protein together with purified Mpa and CP. Untreated lysate was used as a reference sample.

2.21. Co-immunoprecipitation from S. griseus cell lysate

Despite the well-established model of the Mpa-CP proteasome complex of *M. tuberculosis*, the interaction between Mpa and the CP has so far proved to be elusive *in vitro.* To test this interaction *in vivo*, two co-immunoprecipitation (Co-IP) experiments were performed, in which anti-Mpa or anti-CP antibodies were used to bind Mpa or CP in *S. griseus* cell lysate. If the Mpa or CP that were bound by the antibody had been part of the holoproteasome, the complex as a whole could conceivably be isolated.

Protein A-coupled magnetic DynaBeads® from Life Technologies were used to couple anti-Mpa (c = 1.2 mg/mL) or anti-CP antibodies (c = 0.98 mg/mL). The Co-IP was performed according to the manufacturer's instructions unless otherwise noted. Two approaches per protein were used: *directly* and *indirectly*. In the direct approach, the antibodies were coupled to the beads, then added to the lysate, where they would interact with Mpa or CP. In the indirect approach, the free antibodies were added to the lysate, allowed to bind their respective target protein and only then coupled to the beads. In both methods, the antibodies were removed from the beads by an acidic elution buffer, then analyzed by SDS-PAGE and silver staining.

Buffers used:

Reaction buffer (pH = 7.4):	1 x PBS 0.02 % Tween 20
Elution buffer: (pH= 2.8):	50 mM glycine
Wash buffer: (pH =7.4):	1 x PBS

50-150 µg of antibodies in solution were diluted with reaction buffer to 200-600 µL. For the direct approach, 50 µL of the washed and equilibrated beads were mixed with the antibodies and 1-10 mL of the lysate and then incubated for 2 hours at room temperature under rotation. For the indirect approach, the antibodies were added to 1-10 mL of the lysate without the beads, incubated for 2 hours at room temperature as before, the beads were added and incubated for 10 minutes under rotation. Washing steps and the elution were performed according to the manufacturer's instructions.

2.22. Photocrosslinking of Mpa's C-terminal tail peptides and the CP

The photoreactive non-natural amino acid *para*-benzoyl-L-phenylalanine (*p*Bpa) can be induced by near-UV radiation to form covalent bonds with proteins or peptides in its vicinity, making it useful to study peptide-protein or protein-protein binding. When irradiated at wavelengths of 350-360 nm, the carbonyl oxygen of *p*Bpa's benzophenone group reacts with carbon-hydrogen bonds within 3-4 Å and forms a covalent bond.[138] Here, *p*Bpa-containing peptides equivalent to the last 25 residues of Mpa's C-terminal tails were crosslinked to purified CP 28-mers, simulating the binding of full-length Mpa to the CP *in vivo*. In addition to the wild type CP (CP_{WT}), the pocket lysine mutant of CP (CP_{K52A} = CP_{PL}) was used. CP_{PL}'s α-subunit contains the K52A mutation, which replaces a lysine in the binding site on the surface on the α-ring. Results from our lab have shown that this lysine is essential for the binding of the C-terminal tails of Mpa in these pockets, and the CP_{PL} therefore is unable to interact with Mpa or its tail peptides. In both *S. griseus* and *S. cerevisiae*, the pocket lysine mutations inhibit the processing of the CPβ-propeptide, even though there is no direct contact between the binding sites of the α-ring and the β-subunits. Nonetheless, the assembly of the holoproteasome is not influenced by this mutation and the unprocessed β-subunits are incorporated in the CP just as they are in the wild type (see also section **1.3.2**).[139]

In previous ITC experiments (see section **2.16**) two peptides corresponding to the last 25 amino acids of Mpa's C-terminal tails, each containing a *p*Bpa residue at different positions, had been selected for the crosslink with the CP. Both included an additional N-terminal tryptophane to allow spectroscopic quantification (bold: mutant residues, underlined: HbYX motif):

Peptide 20 (Q586*p*Bpa): WTLVTGKQGADTGRSIDTVANTG***pBpa***YL
Peptide 33 (V581*p*Bpa): WTLVTGKQGADTGRSIDT***pBpa***ANTG**F**YL

10 mM stock solutions of the peptides dissolved in 100% DMSO were used at a final concentration of 100 µM. CP_{WT} and CP_{PL} were washed 3x with crosslinking buffer in a Vivaspin column (MWCO: 30 kDa) to exclude nonspecific crosslinking with Tris contained in the original size exclusion respective ion exchange buffers.

Crosslinking buffer (pH_{RT} = 8): 20 mM $NaH_2PO_4 \cdot H_2O$
150 mM NaCl

The concentration of CP_{WT} and CP_{PL} was then determined with a NanoDrop spectrophotometer. Per reaction, an amount of approximately 50 µg of each CP 28-mer was used in a volume of 100 µl. At

maximum, one peptide could bind to each of the α-subunits of the CP, irrespective whether this would indeed correspond to the situation *in vivo*. Since each CP 28-mer contains 14 α-subunits, the effective concentration (C_E) was then calculated as 14 times the true CP concentration.

C_E [CP_{WT}]: 0.6 µM x 14 = 8.4 µM
C_E [CP_{PL}]: 2.5 µM x 14 = 35 µM

Crosslinking was performed for 45 min in a 96-well Nunclon plate with a volume of 100 µl per reaction, using a Blak-Ray B-100SP UV lamp emitting at 365 nm, slightly higher than the recommended wavelength of 350-360 nm. The plate was kept on ice during the crosslinking and positioned at a distance of approximately 2 cm below the lamp. Samples of 15 µl each were taken at 0, 15, 30 and 45 min and immediately denatured in 15 µl SDS-PAGE loading buffer.

2.23. Test expression of $Mpa_{Q586pBpa}$

ITC experiments with peptides corresponding to the last 25 C-terminal residues of Mpa (see section **2.16**) had shown that introducing the Q586F mutation, which creates a canonical HbYX motif, enables the peptide to bind to the α-subunits of the CP. A variant of the HbYX motif in peptides containing the Q586*p*Bpa (peptide 20) mutation (*i.e.* the exchange of the Q codon with the amber codon TAG), which allows the introduction of the photoreactive amino acid derivative *p*Bpa, was also demonstrated to have the same effect on binding. The V581*p*Bpa Q586F (peptide 33) variant also interacted with the CP, but with less affinity than peptide 20.

Photocrosslinking experiments with the two peptides (see section **2.22**) had shown that although the V581*p*Bpa Q586F variant produces crosslinked peptide-CP complex, the yield is lower than that of peptide 20. Therefore, the Q586*p*Bpa mutation was chosen as the basis of producing full-length pBpa-containing Mpa, *i.e.* $Mpa_{Q586pBpa}$. To determine the optimal conditions for the expression of full-length $Mpa_{Q586pBpa}$, test expressions were set up at different temperatures (18°C/25°C/37°C); each induced at a different IPTG concentration (0.1 mM and 0.5 mM, respectively). $CaCl_2$-competent *E.coli* BL21 (DE3) [pDULE] were transformed with the $5c_{Q586pBa}$ plasmid as described in section **2.5** and used to inoculate overnight cultures of 100 mL LB + 25 µg/mL tetracycline. These were then used to inoculate expression cultures of 100 mL LB + 5 µg/mL tetracycline + 1 mM *p*Bpa (from 1 M *p*Bpa stock solution dissolved in 1 M NaOH), which were induced with 0.1/0.5 mM IPTG at OD_{600} = 0.8 – 0.9 as usual (see **2.6.**). The temperature was then set to 18/25/37°C and the culture incubated overnight in the dark at 180 rpm. An additional set of two control cultures at 25°C was induced with 0.1 M and 0.5 M IPTG but did not have *p*Bpa added, while a third control culture at 18°C was neither induced nor had *p*Bpa added.

Samples of 25 mL each were taken at 1, 3 and 6 hours after induction, centrifuged, shock frozen and stored at -20°C. The incubation was stopped 18 hours after induction. After a final sample had been taken, the 25-mL samples were thawed and lysed with Merck Millipore amine-free BugBuster extraction reagent (1 mL per sample). The lysed samples were centrifuged at 13,000 rpm for 10 minutes and the supernatant was transferred into a fresh tube. Qiagen NiNTA Superflow resin was washed in NiNTA start buffer (50 mM $NaPO_4$, 300 mM NaCl, pH_{RT} = 8) three times, 300 µl each were

added to the samples and incubated under rotation at 4°C for 30 minutes. The samples were transferred to a 96-well Nunclon plate, washed once with start buffer and twice with wash buffer (NiNTA start buffer + 25 mM imidazole). Finally, the protein was eluted with 75 µl elution buffer (NiNTA start buffer + 500 mM imidazole). 15 µl of each elution fraction was analyzed by SDS-PAGE and Western blotting with rabbit anti-Mpa antibody (diluted 1:10,000, generated by Gramsch Laboratories) and mouse anti-rabbit HRP IgG antibody (diluted 1:10,000, generated by Thermo Scientific/Pierce Antibodies) using the Pierce HCL Western blotting substrate as described in section **2.18.**

2.24. Photocrosslinking of full-length $Mpa_{Q586pBpa}$ to CP_{WT}

To produce full-length His_6-$Mpa_{Q586pBpa}$, *E.coli* BL21(DE3) [pDULE] (see section **2.4**.) were transformed with the $5c_{Q586pBpa}$ plasmid and used to set up overnight cultures of 100 ml LB + 25 µg/mL ampicillin + 5 µg/mL tetracycline as usual. 25 mL of these cultures were used to inoculate 2 L LB + 50 µg/mL ampicillin + 5 µg/mL tetracycline + 1 mM *p*Bpa (from 1 M *p*Bpa stock solution dissolved in 1 M NaOH). After incubation in the dark at 37°C, 180 rpm up to OD_{600} = 0.9, the cultures were induced with 0.5 mM IPTG and shaken at 25°C, 180 rpm for 6 hours. Cells were harvested as described in section **2.7**, shock frozen and stored at -20°C.

The purification of His_6-$Mpa_{Q586pBpa}$ was performed with a 5 mL GE HisTrap NiNTA column as described in section **2.11,** except that an elution buffer gradient of 10%/20%/30%/40% was used to elute the protein. The hexamer was purified by SEC on a GE Superose 6 XK16/70 column as described in section **2.12** using Tris-free crosslinking buffer (20 mM monobasic $NaH_2PO_4 \cdot H_2O$, 150 mM NaCl, pH = 8) instead of SEC buffer. Purified hexameric fractions were combined and concentrated in GE VivaSpin columns (MWCO = 30 kDa).

The crosslinks were performed as described in section **2.21** with effective concentrations of

$$C_E\,[Mpa_{Q586pBpa}] = 6 \times 99\ \mu M = 594\ \mu M$$
$$C_E\,[CP_{WT}] = 7 \times 95.7\ \mu M = 670\ \mu M$$

i.e. a ratio of approximately 0.9 : 1 with an irradiation time of 20 minutes (Fig. **3.5.1.**). For subsequent crosslinks, an $Mpa_{Q586pBpa}$: CP ratio of 2.5 : 1 or 1 : 1 was used (**Fig. 3.5.2 - 3.5.4**). To test the potential effects of nucleotides on the binding of $Mpa_{Q586pBpa}$ to CP, the non-hydrolyzable ATP analogue AMPPNP and $MgCl_2$ (10 mM for both, diluted from 100 mM stock solutions in crosslink buffer) were added. Western blots were performed as described in section **2.9.**

2.25. *Strep*-Tactin purification of crosslinked *Strep*-II-tagged Mpa peptide - CP complex

The exceptional affinity of the coenzyme biotin (vitamin B_7) to the avian protein avidin or its bacterial equivalent streptavidin ($K_D = 10^{-14}$ - 10-15 M) has long been utilized in protein purification and detection, and variants of both biotin and avidin/streptavidin with improved characteristics for specialized applications have been developed.[140] The *Strep*-tag II by IBA is an artificial eight-amino acid sequence (WSHPQFEK) with a high affinity towards *Strep*-Tactin, a recombinant variant of streptavidin. Thus, the *Strep*-tag II is the functional peptide equivalent to biotin, but has a significantly lower affinity to *Strep*-Tactin than biotin has to streptavidin ($K_{D\ Strep\text{-tag II: }Strep\text{-Tactin}}$ = 10 µM). The *Strep*-tag II's affinity to *Strep*-Tactin is, however, higher than its affinity to natural streptavidin ($K_{D\ Strep\text{-tag II: Streptavidin}}$ = 72 µM). Due to its small size and chemical inertness it can be used as a protein or peptide tag without influencing the structure or the activity of the tagged protein.[141,142]

Desthiobiotin, a derivate of biotin lacking its sulfur atom and therefore its thiophene ring, binds reversibly to *Strep*-Tactin (K_D = 10-11 M) and can be eluted from it. Desthiobiotin can therefore be used as a tagging molecule in protein purification as well and can be displaced from streptavidin by either biotin or HABA (2-(4-Hydroxyphenylazo)benzoic acid). The latter is used to regenerate the column material and is not normally used to elute bound proteins.

To explore the possibility of purifying the crosslinked full-length $Mpa_{Q586pBpa}$ - CP complex (see **section 2.21** for the description of the crosslinking process) by pulling down desthiobiotin- or *Strep*-tagged Mpa, it was attempted to isolate the Mpa C-terminal peptide - CP complex first. Two Mpa-tail peptides containing either an N-terminal desthiobiotin or an N-terminal *Strep*-tag II (WSHPQFEK) and the Q586*p*Bpa mutation were used to crosslink to CP:

Desthiobiotin-Peptide 20 (Q586*p*Bpa): desthiobiotin-TGKQGADTGRSIDTVANTG***p*Bpa**YL

Strep*-tag-II-Peptide 20 (Q586*p*Bpa):** WSHPQFEK-TGKQGADTGRSIDTVANTGp*Bpa**YL

To test whether the desthiobiotin tag would influence the binding ability of the peptide when the K52A mutation was present, CP_{PL} was used to crosslink the peptide in addition to CP_{WT}. CP_{WT} and CP_{PL} were transferred into crosslink buffer by washing on a Vivaspin 500 (10 kDa MWCO) three times. Per reaction, an amount of approximately 50 µg of each CP 28-mer was to be used in a volume of 100 µl. As each peptide could maximally bind to an α-subunit and each CP 28-mer contains 14 α-subunits, the effective concentration (C_E) was the actual concentration as measured with NanoDrop x 14: C_ECP_{WT} = 0.62 µM, C_ECP_{PL} = 0.7 µM.

The desthiobiotin peptide was used at a concentration of 100 or 200 µM, diluted from a 10 mM stock solution (peptides dissolved in 100% DMSO). Crosslinking was performed for 45 min in a 96-well Nunclon plate with 100 µl volume of each reaction, the plate was ice-cooled during the crosslinking and positioned at a distance of approximately 2 cm at a right angle to the lamp. Samples of 15 µl each were taken at 0, 15, 30 and 45 min and immediately denatured in 15 µl SDS-PAGE loading buffer.

For the crosslink using the desthiobiotin-tagged peptide 20, C_E = 138 µM of the CP_{WT} 28-mer and 200 µM of the peptide were used. The crosslink was prepared as described and the purification performed on an IBA StrepTactin spin column according to the manufacturers' instructions. 200 µl of the crosslink mix containing approximately 100 µg of the CP complex were purified, less than the maximum capacity of 150 µg of protein per column. For the elution, 150 µl of 2.5 mM biotin, 2.5 mM desthiobiotin and 1 mM HABA buffers were used successively. After the last elution, the column matrix material was removed from the column, mixed 1:1 with SDS-PAGE loading buffer and analyzed by SDS-PAGE.

Elution buffer (pH = 8):	100 mM Tris/HCl
	150 mM NaCl
	1 mM EDTA
	2.5 mM biotin or desthiobiotin

In addition, commercial 2 mM biotin elution buffer as supplied by the manufacturer was used.

The crosslink for the *Strep* II-tagged peptide 20 was set up with an excess of 200 µM of *Strep*-II-tagged peptide 20 over C_E = 124 µM CP_{WT} 28-mer and performed as described above. 400 µl of the crosslink mix, containing approximately 100 µg of the CP complex were purified per column. After the purification, the complex was successively eluted with 150 µl each of 2.5 mM biotin and 2.5 mM desthiobiotin elution buffer.

The crosslinked complexes were applied to IBA *Strep*-Tactin spin columns and purified according to the manufacturer's instructions, using the recommended buffers for washing. All purification steps were performed at 4°C. For the elution, 2.5 mM biotin and 2.5 mM desthiobiotin buffers were used instead of the recommended 2 mM desthiobiotin buffer, with the concentrations of the other components kept as indicated in the manufacturer's manual.

SEC was performed with the purified *Strep*-II tag- peptide-CP complex on a GE Healthcare Superose 6 3.2/300 column at room temperature using standard SEC buffer (50 mM $NaH_2PO_4 \cdot H_2O$, 300 mM NaCl, pH = 8) and a flow rate of 0.035 µl/min. The concentration of the elution fractions was determined by a Bradford assay as 0.25 mg/mL, corresponding to a CP 28-mer concentration of 0.35 µM. 2 x 100 µl were pooled, concentrated to 35 µl (*i.e.* to a concentration of 1.43 mg/mL) with a Vivaspin sample concentrator (MWCO: 50 kDa) and injected into the SEC column via a 25 µl loop.

2.26. Crystallisation studies of wild type and selenomethionine-Mpa

Although the N-terminal coiled-coil domain and the interdomain of Mpa have been resolved to atomic level by X-ray crystallography[109], the structure of its AAA-ATPase domain and its extreme C-terminal end are not yet known (see section **1.3.3.**) Although trials were conducted in our lab, experience has shown that Mpa is difficult to crystallize and has not yet given usable diffraction data. To refine crystallization strategies for Mpa, five commercial crystal screen solution kits were used to crystallize purified wild type Mpa and the selenomethionine-containing variant of Mpa (SeMet-Mpa):

- JBS Classic 1-4 (Jena Bioscience)
- JBS Classic 5-8 (Jena Bioscience)
- MIDAS (Molecular Dimensions)
- Morpheus HT-96 Green Screen (Molecular Dimensions)
- Wizard 1 (Emerald BioSystems)

All screens were used in duplicate, one plate was stored at 4°C and the other at 19°C. Mpa was purified by NiNTA- and size exclusion chromatography as previously described, concentrated on a Vivaspin concentrator (MWCO = 5000 Da) to 18.1 mg/mL (as measured with NanoDrop spectrophotometer). 96-well plates (100/200 nl of protein solution + 100 nl of buffer in the reservoir per well) were prepared with TECAN, Art Robbins Crystal Phoenix and a TTP Labtech Mosquito robots and stored in a Rigaku Minstrel HT monitoring system at 4°C or 19°C. 10 mM $MgCl_2$ and 10 mM AMPPNP were added to the Mpa samples.

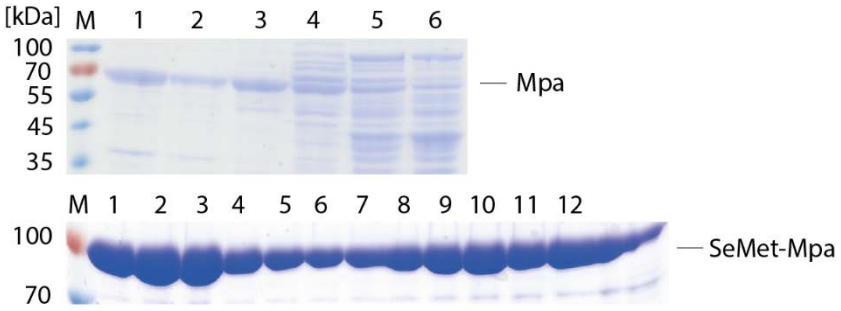

Fig. 3.13.1. SEC purification of NiNTA-purified wild type Mpa (top) and SeMet-Mpa in GE Healthcare Superose 6 XK16/70 columns using standard SEC buffer. Wild type Mpa partially disintegrated (fractions 4-6) and only fractions 1-3 were used.

2.27. Electron microscopy

To analyze the binding of the recombinant Mpa variants $Mpa_{Q586pBpa}$ (as part of the photocrosslinked $Mpa_{Q586pBpa}$ – CP complex, see section **3.4**) and Mpa_{Q586F} (as part of the tricistronic Mpa_{Q586F} – CP complex, see section **3.6**) to the core particle, electron microscopy of the SEC-purified complexes was performed. In addition, the structure of the unprocessed CP_{T54V} 20S core particle (see section **1.3.2**) was also analyzed by electron microscopy. Test staining was performed with 2% uranyl acetate (UA) and phosphotungstic acid (PTA, pH = 7.2), applied to the samples for 30 seconds. PTA was found not to stain the complex at all, resulting in diffuse and grainy backgrounds without visible protein. Therefore, 2% UA was used for all subsequent TEM. Samples were diluted from 1:10 to 1:100 with buffer before usage. Sample concentrations are given in section **3.7**.

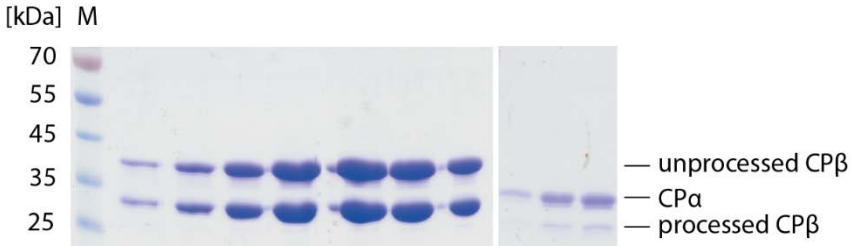

Fig. 2.22.1. SEC purification of CP_{T54V} (left) and wild type CP (right) on GE Healthcare Superose 6 XK16/70 columns using standard SEC buffer.

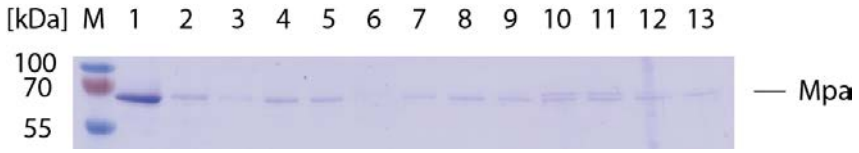

Fig. 2.22.2. SEC purification of Mpa on a GE Healthcare Superose 6 XK16/70 column using standard SEC buffer after NiNTA. Fraction 7 was used for EM (c = 0.03 mg/mL).

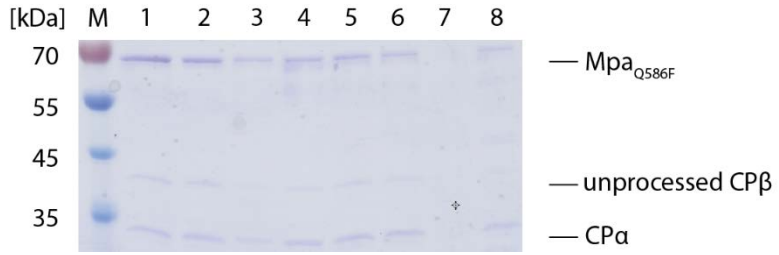

Fig. 2.22.2. SEC purification of tricistronic Mpa_{Q586F} – CP complex in a GE Healthcare Superose 6 3.2/300 column using 50 mM MES (pH = 6) buffer + 2 mM ATPγS after NiNTA. Fraction 7 was used for EM (c = 0.03 mg/mL).

A photocrosslinked complex of $Mpa_{Q586pBpa}$ and Strep II-tagged CP (*prcA-prcB-Strep II*) was prepared as described in section **2.24** with a ratio of 2.5 : 1 $Mpa_{Q586pBpa}$ to $CP_{Strep\ II.}$ The complex was purified on a StrepTactin spin column as described in section **2.25** and then purified by SEC using a GE Healthcare Superose 6 XK16/70 column in standard SEC buffer. Complex fractions were pooled (c = 21.1 mg/mL) and diluted 1:100 for EM (c = 0.2 mg/mL).

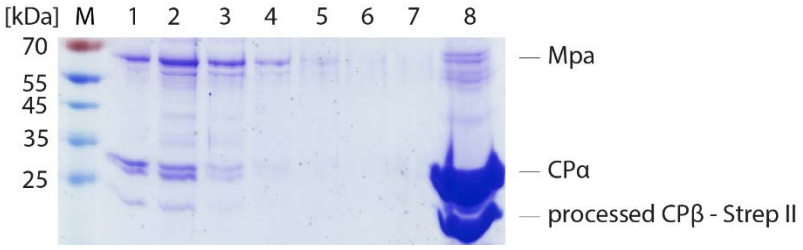

Fig. 2.22.3. SEC purification of photocrosslinked $Mpa_{Q586pBpa}$ – CP-Strep II complex in a GE Healthcare Superose 6 XK16/70 column using standard SEC buffer. Lane 8 contains the pooled complex fractions that were used for EM (c = 21.1 mg/mL).

To test the effect of repeated SEC on the tricistronic complex, EM was performed on samples taken from the second of two purifications on a GE Healthcare Superose 6 XK16/70 column and then a GE Healthcare Superose 6 3.2/300 column using 50 mM MES (pH = 6) buffer + 2 mM ATPγS (see section **3.6.5**).

2.28. Mass spectrometry

To analyze the results of the pulldown assays (see section **2.20**), samples were submitted for in-house mass spectrometry. From pulldowns using either Mpa_{WT} or CP_{WT} as bait, 50 µL of the elution fractions were taken. To avoid the binding of the imidazole present in the elution buffer to the reversed phase, the samples were desalted by dialysing them with a membrane column in 20 mM Tris-HCl for 3 hours, changing the buffer once.

As controls, purified samples of approximately 2 µg Mpa and 1 µg CP, respectively, were submitted after transferring into 20 mM Tris-HCl buffer in the way described above.

2.29. Pup-Luciferase unfolding assay

Although the $Mpa_{Q586pBpa}$ – CP complex can be created *in vitro* relatively easily by UV-photocrosslinking (see section **2.24**), it is uncertain whether $Mpa_{Q586pBpa}$ retains its unfolding ability as part of the artificial holoproteasome. To determine whether the crosslinking of $Mpa_{Q586pBpa}$ to CP would increase the unfolding ability of $Mpa_{Q586pBpa}$, an unfolding assay using the bioluminescent protein luciferase coupled with Pup was performed. If $Mpa_{Q586pBpa}$ is active as part of the crosslinked complex it could bind Pup and then unfold the luciferase, leading to a measurable decrease in bioluminescence compared to the control and allowing a comparison between the activity of free and crosslinked $Mpa_{Q586pBpa}$.

As a substrate, His_6-tagged firefly Pup-luciferase fusion protein (total molecular weight: 73.7 kDa) was used to measure the decline in flurorescence upon unfolding of the luciferase by Mpa, and, if present, the difference between crosslinked Mpa-CP complex and Mpa and CP alone.

Final concentrations:	1.25 µM $Mpa_{WT/Q586pBpa}$ or crosslinked $Mpa_{Q586pBpa}$- CP complex
	15 µM luciferin
	20 µM Pup-luciferase
	10 + 10 mM ATP

A mastermix of buffer, luciferin, Pup-luciferase and the first addition of ATP (10 mM) was prepared according to the above concentrations to a volume of 100 µl – [$Mpa_{WT/Q586pBpa}$ or crosslinked Mpa-CP complex] – [ATP] and incubated at room temperature for 25 minutes. After 25 minutes, $Mpa_{WT/Q586pBpa}$ or crosslinked Mpa-CP complex was added together with the second addition of ATP, adding up the total volume to 100 µl. The measurement was performed immediately afterwards with a BisTek Synergy H1 Hybrid Reader at room temperature without shaking. Light produced by the oxidation of luciferin to oxyluciferin was measured at 580 nm for 30 minutes with one measurement every 23 seconds.

2.30. Pup-PanB substrate degradation assays

An adapted version of the assay described by the Weber-Ban group[105] was performed to test whether the crosslinked $Mpa_{Q586pBpa}$ complex would show any increased ability to degrade the substrate compared to its free components $Mpa_{Q586pBpa}$ and CP. As a substrate, the previously identified Mpa substrate PanB (ketopantoate hydroxymethyltransferase) was used. PanB was identified as a substrate for the proteasome in a previous study[143] and was used here as a fusion protein of Pup and PanB.

Reaction buffer (pH =7.5):	50 mM HEPES
	10 mM $MgCl_2$
	1 mM DTT

Reactions:	0.2 µM $Mpa_{Q586pBpa}$-CP complex or free $Mpa_{Q586pBpa}$ and CP 1 µM Pup-PanB or PanB 40 nM phosphocreatine salt 0.4 U/mL creatine phosphokinase 5 mM ATP

All reactions were mixed in 1.5 mL Eppendorf tubes and incubated at 26°C and 300 rpm. Samples were taken at 0, 1, 2, 4, 6 and 16 hours after the start of the reaction and analyzed by SDS-PAGE.

2.31. Fluorescent substrate degradation assays

As in sections **2.24** and **2.25**, the ability of the crosslinked $Mpa_{Q586pBpa}$ complex to degrade a substrate was tested, using the peptide Succinyl-LLVY-AMC. When Succinyl-LLVY-AMC is hydrolyzed by the proteasome, AMC (7-Amino-4-methylcoumarin) is released and can be induced to fluoresce. The intensity of this fluorescence can then be used to determine the level of proteolytic activity.[144] Ubiquitin-coupled AMC can be used for the same purpose with eukaryotic proteasomes.[145]

Buffer:	50 mM Trizma base 150 mM NaCl 10% glycerol 20 mM $MgCl_2$ 1 mM DTT
Substrate:	Suc-LLVY-AMC, final concentration 5 µM

A master mix of 16 x substrate (prepared from 10 mM Suc-LLVY-AMC stock by Bachem) and buffer was prepared, crosslinked complex or non-crosslinked Mpa + CP or buffer was added to a concentration of 100 nM and incubated on shaker at 37°C, 300 rpm in the dark. After 1 hour, the reaction was stopped by adding 200 µL 20% SDS. Measurements were done with a Horiba Jobin Yvon FluoroMax-4 spectrofluorometer. The excitation was set at 360 nm and the emission at 460 nm.

2.32. Stability of the proteasome

2.32.1. Influence of pH on the stability of the proteasome

The wild type proteasome of *M. tuberculosis* has never been successfully reconstituted *in vitro* from its component subcomplexes due to the limited interaction between Mpa and the CP. The open-gate mutant of the CP (CP_{OG}), where the first eight N-terminal residues of the CPα subunit are deleted, has been demonstrated to interact with Mpa, but even then the affinity is very low: approximately 2% of the CP_{OG} forms a complex with wild-type Mpa and 15% with the N-terminal deletion mutant Mpa_N97Δ (see section **1.5**).[109] Unlike its eukaryotic and archaeal equivalents Rpt and PAN, the C-terminal tails of Mpa do not end in the canonical HbYX motif but in QYL.[58,114] When the QYL sequence is converted to an HbYX motif by replacing the glutamine with a hydrophobic amino acid such as phenylalanine (the Q586F mutation), Mpa_{Q586F} can bind to the CP *in vitro* (see section **3.1** – **3.5**).

Previous experiments in our lab demonstrated that the formation of the proteasomal complex is possible when co-expressing mpa_{Q586F}, *prcA* and *prcB* in *E. coli*. By combining the three genes on a single tricistronic plasmid under control of one promotor (mpa_{Q586F}-*prcB-*His_6-*prcA)* the subunits self-assemble into the holoproteasome complex. The hexahistidine tag located on the C-terminus of the CPβ subunit allows IMAC purification of the CP complex with Mpa_{Q586F} bound to it.

Contrary to the wild type proteasome, the N-terminal propeptide of the CPβ subunit is not cleaved during the assembly and the CPβ subunit therefore remains in the unprocessed state. This effect is similar to that of the T54V mutation in *S. griseus* ($CP\beta_{T54A}$) and of the pocket lysine mutation ($CP\alpha^5_{K66A}$ and $CP\alpha^6_{K62A}$ in *S. cerevisiae*), which in yeast also abolishes the autoprocessing of the β-propeptide.[139] Unlike the yeast proteasome, where the assembly of the CP is blocked by the presence of the β-propeptide and requires the proteasome-associated protein Ecm29 to incorporate the unprocessed β-subunits[139], the recombinant tricistronic complex forms normally. Presumably, the β-propeptide remains folded inside the chamber akin to the intermediate state of the wild type CP (see section **1.3**). As seen in figure **3.6.1.1,** the complex can be isolated easily and to a high degree of purity using the standard NiNTA purification method (see section **2.11**).

The tricistronic complex can be be further purified using SEC, however, it was found to disassemble during a second SEC purification, most likely due to the decreasing concentration. In this experiment, it was attempted to determine whether stabilizing buffer conditions exist, and if so, whether the proteasome could be stabilized permanently. The optimal pH of *M. tuberculosis*' Mpa has been cited as between 7.4 – 7.5[102], but to the author's knowledge no studies exist regarding the optimal pH of the proteasome as a whole. In addition, electron microscopy was performed on the purified complexes to investigate whether the presence of the unprocessed CPβ-subunit could influence the tendency of the CP 28-mer to bind Mpa_{Q586F}.

In the first experiment, the stability of the tricistronic complex during SEC under various pH conditions was tested using four buffers:

Buffer 1 (pH = 6): 50 mM MES, 75 mM NaCl

Buffer 2 (pH = 7): 50 mM $NaH_2PO_4 \cdot H_2O$, 75 mM NaCl

Buffer 3 (pH = 8): 50 mM TrisHCl, 75 mM NaCl

Buffer 4 (pH = 9): 50 mM CHES, 75 mM NaCl

The proteasome complex was expressed and harvested using the tricistronic plasmid (*mpa*$_{Q586F}$*-prcB-His*$_6$*-prcA*) as described in section **2.5** and **2.7**. The complex was purified on a GE HisTrap 5 ml NiNTA column using low-salt versions of the start and elution buffers as described in section **2.11.** Sonication was performed on 60% power for 3 minutes. 20 µl of the purified complex were added to 20 µl of each buffer to test for precipitation, then centrifuged for 1 minute at 17,000 g. 30 µl of the supernatant were injected through a 25 µl loop into a GE Superose 6 3.2/300 column at room temperature and a flow rate of 0.04 mL/min.

2.32.2. Influence of salt concentration on the stability of the proteasomal complex

In the previous experiment, the optimal pH value of the buffer used for the stable purification of the tricistronic holoproteasome (the Mpa$_{Q586F}$ – CP complex) was determined (see section **3.6.1**). To further narrow down the optimal buffer conditions, NiNTA-purified tricistronic complex was subjected to SEC in a GE Healthcare Superose 6 3.2/300 column as before, using 50 mM MES (pH = 6) buffer with a range of sodium chloride concentrations (0, 75, 150, 300 and 500 mM). The purified complex used for the tests was taken from the same pooled fractions that were used for the pH tests. Samples were tested for precipitation as described in section **2.12.** 30 µl of the supernatant were injected through a 25 µl loop at a flow rate of 0.05 – 0.065 mL/min at room temperature.

2.32.3. Influence of nucleotides on the stability of the proteasomal complex

To test whether nucleotide binding to the AAA-ATPase Mpa$_{Q568F}$ would influence the stability of the tricistronic proteasome complex, a series of SEC purifications using the salt-free 50 mM MES (pH = 6) buffer selected in the previous two experiments in the presence of ATP sodium salt, ADP and the non-hydrolyzable ATP analogs ATPγS and AMPPNP were performed.

NiNTA-purified tricistronic complex was prepared as described in section **2.5** and **2.7**. The complex was purified on a GE HisTrap 5 ml NiNTA column using low-salt versions of the start and elution buffers as described in section **2.11.** 30 µL of the complex were mixed with 30 µL of the 50 mM MES

(pH = 6) buffer and centrifuged for 1 minute at 17,000 g. Prior to the injection, 2 mM of ATPγS, ATP sodium salt, ADP, AMPPNP or 1 mM ATPγS + 1 mM ATP dissolved in 50 mM MES (pH = 6) buffer were added to the samples and centrifuged for 10 minutes at 17,000 g to avoid injecting any precipitated protein. 30 µl of the supernatant (final concentrations were injected through a 25 µl loop into a GE Superose 6 3.2/300 column pre-equlibrated with 50 mM MES (pH = 6), containing 2 µM of the nucleotide(s).

2.33. Binding of Pup-GFP and Pup-PanB to the proteasome complex

After establishing the buffer conditions most favorable to the stability of the Mpa_{Q586F}-CP proteasome complex, it was tested whether the tag protein Pup would bind to the complex under these conditions. Two recombinant hexahistidine-tagged fusion proteins were used: Pup-GFP (33.8 kDa) and Pup-PanB (40 kDa), the fusion of the Pup tag to the bacterial 31.9 kDa protein PanB (ketopantoate hydroxymethyltransferase). PanB was identified as a substrate for the proteasome in a previous study.[143] *In vivo*, PanB forms octamers or decamers[146,147], and results from our lab have indicated that recombinant Pup-PanB expressed in *E. coli* assembles into higher oligomers of approximately 700 – 800 kDa. Both proteins were supplied purified by NiNTA-IMAC. Pup-GFP was further purified by SEC using a GE Healthcare Superdex 75 10/300 and SEC buffer as described in section **2.11.**

The purified tricistronic Mpa_{Q586F} –CP complex (see section **2.12**) was diluted 1:1 with 50 mM MES (pH = 6) + 2 mM ATPγS, gently mixed and centrifuged for 10 minutes at 17,000 g to remove potentially precipitated protein. Purified Pup-GFP or Pup-PanB was also diluted with the same buffer and centrifuged as described, then added to the complex (final concentrations: Mpa_{Q586F} – CP: 11 µM, Pup-GFP: 29.6 µM, Pup-PanB: 27.6 µM). After mixing, the sample was again centrifuged for 10 minutes at 17,000 g. 30 µl of the supernatant were injected via a a 25 µl loop into a GE Healthcare Superose 6 3.2/300 column pre-equilibrated with 50 mM MES (pH = 6) + 2 µM ATPγS buffer at a flow rate of 0.05 mL/min.

3. RESULTS AND DISCUSSION

3.1. Isothermal titration calorimetry (ITC)

Although the peptide and protein solutions containing DMSO were prepared with high accuracy to prevent differences that would lead to dilution heat when injecting the peptide into the cell, the sensibility of the instrument was high enough to detect even the irregularities caused by the inherent error of the micropipettes. Most measurements using peptides dissolved in DMSO therefore were influenced by fluctuations arising from discrepancies in the DMSO concentrations between the peptide and the protein solution, which masked the true binding spikes and rendered some of the measurements unusable. A solution of pure reaction buffer supplemented with 10% DMSO injected into the same solution in the cell also showed heat spikes. Future experiments will have to take this high sensitivity into account and include dialysis of both the peptide and the protein in the same DMSO-containing solution rather than adding DMSO to both, even when high-precision pipettes are used.

The binding of peptide 9 (Q586F) (**Fig. S1**, top left) to the open-gate CP was broadly comparable to that of the previous experiment using wild-type CP (data not shown). However, no clear conclusion could be drawn from the curve regarding either the affinity or the number of binding sites. The previously established single-site model is supported by the initial rise in binding enthalpy [kcal/mole of injectant] at a molar ratio (MR) of peptide to CP of around 1 – 1.5, but the drop at 4 MR and second rise at 5 MR suggests either irregularities or sequential two-site binding. The latter is unlikely, given that the open-gate deletion in PrcA would have to cause such a fundamental change in the binding behavior of the peptide, however, this possibility cannot be excluded. It is more probable that this curve shape is due to a random fluctuation and the peptide binds to the open-gate mutant on a single site as well. No model could be fitted to the curve regardless of the binding site parameters.

Peptide 16 (Q586F L588A, dissolved in DMSO due to insolubility in buffer alone) (**Fig. S1**, top right) was notable for its very high binding heat and enthalpy, the highest of all tested peptides together with peptide 33 (V581*p*Bpa Q586F, also dissolved in DMSO. **Fig. S2**, bottom right). This was likely due to dilution heat caused by a difference in the DMSO content of the peptide solution and the CP solution. Intriguingly, the curve of peptide 16, like that of peptide 9, also shows a shape that could be interpreted as being caused by sequential two-site binding. Here however, the molar ratio at both potential binding events is several times higher than that calculated for peptide 9 for unknown reasons. Furthermore, the first slope is small and very poorly resolved, making it difficult to distinguish it from a random outlier. It therefore is likely that there was no true two-site binding and that the single-site model is correct. As in peptide 9, no model could be fitted to the curve under any parameters.

The binding behavior of peptide 17 (Q586F L588E, not shown) could not be analyzed due to the high dilution heat caused by the discrepancy in DMSO content between the peptide and the protein solution. This resulted in the calculated enthalpy to be positive and in a decrease over the course of the titration, which would normally indicate an endothermic reaction. This, however, is highly

unlikely considering that none of the previous experiments using the Q586F mutant showed this behavior, and it is implausible that the L588E mutation alone could be the cause of such a fundamental change.

The first *p*Bpa peptide to be tested, peptide 20 (Q586*p*Bpa), showed that using *p*Bpa instead of phenylalanine as the replacement for the Q586 allows binding of the peptide to CP as well. Although no model could be fitted to the curve, the number of binding sites can be estimated at between 1 and 2 for the entire CP 28-mer. The binding heat itself is low (approximately 0.33 µcal/s for the first peak), but not significantly less than that of peptide 9 (Q586F), its non-*p*Bpa equivalent (approximately 0.48 µcal/s for the first peak). The finding that *p*Bpa can be used to alter the ARC/Mpa peptide's QYL sequence to create the canonical HbYX motif, thereby enabling binding of the peptide to the CP, formed the base for the photocrosslinking experiments detailed in section **3.2.**

Peptide 21 (Q586F Y587*p*Bpa) did not show any binding to the CP at all, demonstrating again the critical importance of the penultimate tyrosine (see section **1.4.1**).[118,123] Considering that *p*Bpa, although structurally related to tyrosine, contains an additional benzoyl group linked to its benzyl ring and is therefore bulkier, this might demonstrate the precise interaction required between Y587 and the binding pocket of CP. As previously mentioned in section **2.15**, previous ITC experiments in our lab had confirmed that deletion of the YL residues completely abolished binding between the peptides and the CP.

Peptide 22 (L588*p*Bpa) did not bind to the CP as expected, lacking the necessary Q586F or Q586*p*Bpa mutation. The interaction between the wild type C-terminal peptide of Mpa and the CP was demonstrated in our lab to be very weak, consistent with other studies that found no direct interaction between Mpa and CP of *M. tuberculosis*.[109] The replacement of the C-terminal L with a hydrophobic amino acid has not yet been attempted and is unlikely to have any influence on the interaction, given that the residue at this position is not conserved. *In vitro* studies have shown that deleting the YL residues completely abolishes the binding of Mpa to the proteasome, and it is conceivable that the replacement of L588 by *p*Bpa lowers the affinity of the C-terminal tails for the CP even below that of the wild type.[1, 16]

Peptide 31 (Q586W), in which a variant of the HbYX motif was established by introducing tryptophane instead of phenylalanine, showed binding to the CP, but only with a low affinity. The same pseudo-double-sigmoid curve shape as with peptide 9 (**Fig. S1**, top left) could be present, but the heat spikes are too low (below 0.3 µcal/s and therefore less than one tenth of the average value recommended by the manufacturer) and do not have enough variance between them to accurately distinguish between outliers and a true trend. Predictably, no model could be fitted to the curve regardless of the parameters chosen.

Peptide 33 (V581*p*Bpa Q586F) was dissolved in DMSO due to its insolubility in the buffer alone. Although the curve indicates that binding took place - consistent with the previously established result that the Q586F mutation allows the interaction between peptide 9 and CP - the comparatively high peak values indicate that the DMSO percentages of the solutions were not exactly matched, causing dilution heat. It is possible that the V581*p*Bpa mutation negated the binding enabled by the Q586F mutation and that the spikes are entirely caused by the DMSO discrepancy, but unlikely considering the distance between the two residues. Nonetheless, this experiment is of limited value

because the existing binding heat was most likely artificially increased or masked by the DMSO artifact.

The ITC experiment using peptide 34 (T584*p*Bpa Q586F), also dissolved in DMSO, showed an unexpected phenomenon that most likely disqualifies it for further analysis: although the heat spikes are comparable to those of peptide 9 (**Fig. S3**, top left), the binding enthalpy turns positive at a molar ratio of ligand to protein of approximately 2, which would indicate an endothermic reaction. It is possible that this is an effect of the mismatched DMSO concentration between the two solutions and the resulting dilution heat, although the reason why this should shift the calculated enthalpy towards the positive is unknown. Although a two-site model could be fitted to this curve, the errors are larger than the values for both the binding sites and the affinities. It is possible that a two-site model would be a valid explanation for Mpa/ARC's binding to CP, but considering the extremely poor accuracy of the calculated values there is little to support it. The question whether the binding sites of CP are allosteric is intriguing, but so far there is no indication of it and more precise ITC experiments will have to be conducted to determine whether this is the case.

MicroCal, the manufacturer of the ITC apparatus, recommends a minimum of 10 µcal per injection and an average of at least 5 µcal per injection over the entire experiment, neither of which was reached by any of the peptides. Only peptide 9 even reached 5 µcal with the first injection and none of the others' initial spikes were above 3 µcal, with most of them significantly lower. It is therefore possible that the values in general were too low to be accurately measured, although binding undoubtedly occurred with peptides 9, 20 and 31 and could be distinguished easily from those where no binding occurred at all, such as peptide 21.

Of all the peptide mutants tested, peptide 20 (Q586*p*Bpa) proved to be the most promising in regards to its potential to be used for photocrosslinking. The formation of a non-canonical HbYX motif by replacing Q586 with *p*Bpa was demonstrated to allow binding of the peptide to CP in the same way as the Q586F mutation does, indicating that the tail/binding site interaction is tolerant of variations in the structure of the residue at this position as long as it contains an aromatic side chain. Peptide 20 was therefore chosen as the primary peptide in the photocrosslinking experiments. In addition, peptide 33 (V581*p*Bpa Q586F) was selected as a back-up peptide. Contrary to peptide 20, in peptide 33 the *p*Bpa residue is located outside the HbYX motif created by the Q586F mutation, which could influence the photocrosslinking process.

Peptide	Sequence	Variant
4	TLVTGKQGADTGRSIDTVANTGQYL	Wild type
9	TLVTGKQGADTGRSIDTVANTG**F**YL	Q586F
10	TLVTGKQGADTGRSIDTVANTG**F**YL	Q586L
16	WTLVTGKQGADTGRSIDTVANTG**FYA**	Q586F L588A
17	WTLVTGKQGADTGRSIDTVANTG**FYE**	Q586F L588E
20	WTLVTGKQGADTGRSIDTVANTG***p*Bpa**YL	Q586*p*Bpa
21	WTLVTGKQGADTGRSIDTVANTG**F*p*Bpa**L	Q586F Y587*p*Bpa
22	WTLVTGKQGADTGRSIDTVANTG**FY*p*Bpa**	Q586F L588*p*Bpa
31	WTLVTGKQGADTGRSIDTVANTG**W**YL	Q586W
33	WTLVTGKQGADTGRSIDT***p*Bpa**ANTG**F**YL	V581*p*Bpa Q586F
34	WTLVTGKQGADTGRSIDTVAN***p*Bpa**G**F**YL	T584*p*Bpa Q586F

Peptide	N	K [L/mol]	ΔH [kJ/mol]	ΔS [J/K]
4	0.68 ± 0.48	$1.05 \times 10^4 \pm 1.84 \times 10^4$	-870.3 ± 1239	15.5
9 (bound to CP_{WT})	0.108 ± 0.069	$2.89 \times 10^4 \pm 7.77 \times 10^4$	$-1.759 \times 10^4 \pm 1.250 \times 10^4$	-38
9 (bound to CP_{OG})	n.a.	n.a.	n.a.	n.a.
10	0.136 ± 0.311	$1.24 \times 10^4 \pm 8.10 \times 10^4$	$-1.163 \times 10^4 \pm 2.931 \times 10^4$	-20.1
16	n.a.	n.a.	n.a.	n.a.
17	n.a.	n.a.	n.a.	n.a.
20	n.a.	n.a.	n.a.	n.a.
21	n.a.	n.a.	n.a.	n.a.
22	n.a.	n.a.	n.a.	n.a.
31	n.a.	n.a.	n.a.	n.a.
33	n.a.	n.a.	n.a.	n.a.
34	N1: 0.160 ± 0.249 N2: 0.318 ± 0.614	K1: 3.09×10^5 $\pm 1.33 \times 10^7$ K2: 2.17×10^3 $\pm 3.40 \times 10^5$	ΔH1: -1.543×10^4 $\pm 3.01 \times 10^4$ ΔH2: -8.394×10^4 $\pm 1.71 \times 10^8$	ΔS1: -26.4 ΔS2: -265

Table 2. Top: List of C-terminal 25- or 26- residue Mpa peptides tested with ITC for their binding to either CP_{WT} or CP_{OG} (only with peptide 9). Mutant residues are bolded, the HbYX motif is underlined. For peptides 16 – 34, an N-terminal W residue was added in order to enable spectroscopic quantification.

Bottom: Peptides listed in the upper table with binding parameters determined by ITC. N: binding stoichiometry (number of binding sites per CP 28-mer). K: binding constant. ΔH: binding enthalpy. ΔS: binding entropy. Peptides 4, 9 (with CP_{WT}) and 10 were tested in previous experiments and were included for comparison.

3.2. Photocrosslinking of Mpa's C-terminal tail peptides and the CP

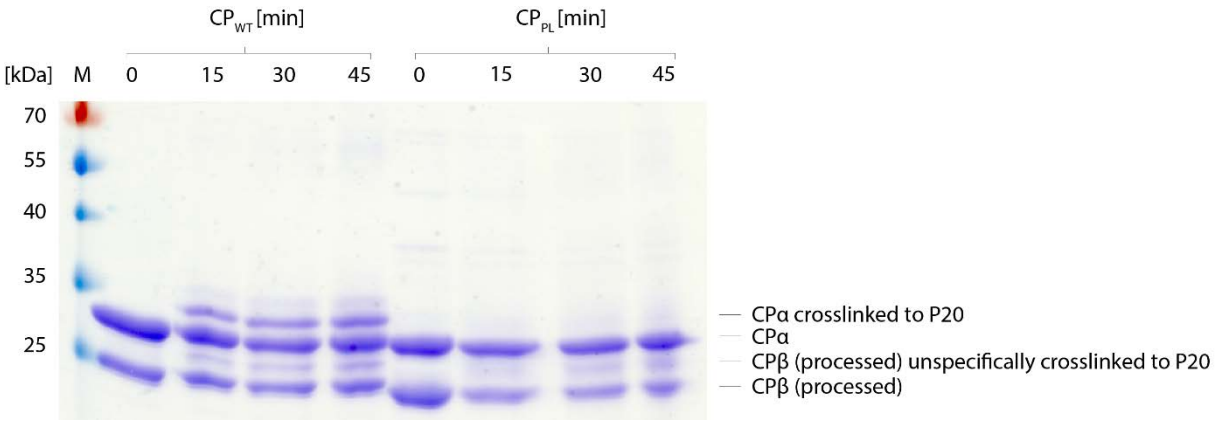

Fig. 3.2.1: 199 µM CP$_{WT}$ and 248 CP$_{PL}$ (effective concentrations) photocrosslinked with 100 µM peptide 20. Samples taken at indicated time points before and during crosslinking.

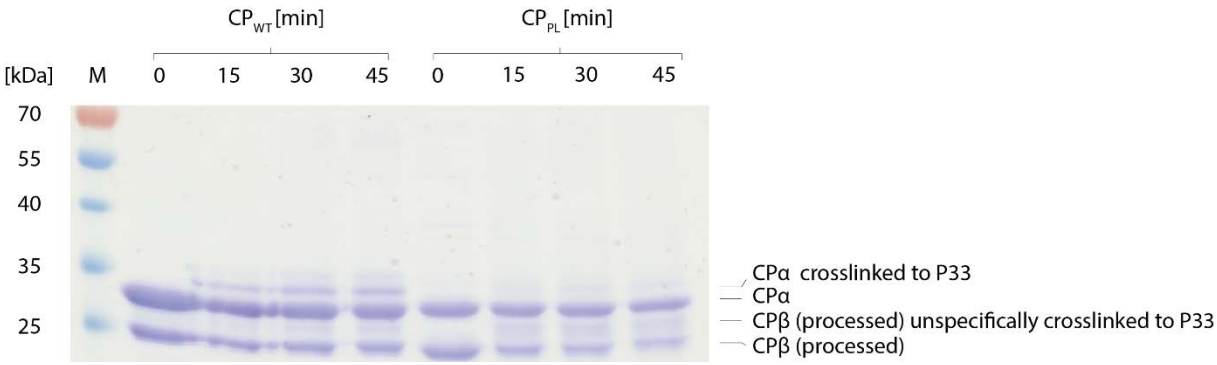

Fig. 3.2.2: 199 µM CP$_{WT}$ and 248 µM CP$_{PL}$ (effective concentrations) photocrosslinked with 100 µM peptide 33. Samples taken at indicated time points before and during crosslinking.

As shown in **Fig. 3.2.1** and **Fig. 3.2.2**., the crosslinking of the *p*Bpa-containing peptides to CP α was successful and a clear size shift of the crosslinked α-subunits can be seen. The percentage of *p*Bpa-peptide crosslinked per reaction has been cited to be as high as 50 - 100%[138], with the yield achieved here less than the lower limit. Although estimations are difficult, approximately $\frac{1}{3}$ to half of the α-subunits were crosslinked with peptide 20 and approximately $\frac{1}{5}$ with peptide 33, even after 45 minutes of irradiation. There does not seem to be a significant change in the amount of crosslinked protein over time after 15 minutes of UV exposure, although in the case of peptide 20 (**Fig. 3.2.1)**, the intensity of the corresponding band slightly increases between 30 and 45 minutes. The amount of the unspecifically crosslinked β-subunits does increase over time, as seen in both peptide crosslinks, however, the efficiency is significantly lower than that of the specific interaction. The ratio

of unspecific crosslinking to the α-subunit of CP_{WT}, the α -subunit of CP_{PL} and the β-subunits of both does not differ significantly between the two peptides.

Although the effiency of the crosslink was expected to be lower than that cited in the literature, the fact that the amount of crosslinked complex did not increase with the irradiation length could be indicative of an underlying characteristic of the complex. In eukaryotes, the interaction between the Rpt1-6 subunits of the 19S regulatory particle and the CP is dependent on only two of the six C-terminal tails, Rpt3 and Rpt5, both of which terminate in the HbYX motif. A third subunit, Rpt2, also includes the HbYX motif and binds to the CP but is not essential for the interaction (see sections **1.2.2** and **1.4.1**). A fourth subunit, Rpt6, which does not contain the HbYX motif, nonetheless has been demonstrated to interact with the CP and to contribute to the stability of the binding between the complexes. Rpt1 and Rpt4 have not been conclusively demonstrated but are presumed to bind to the CP.[67,114]

Thus, out of a total of six subunits in the RP, only four bind to the CP and only two of those are essential for the binding. It is is reasonable to assume that the interaction of the Mpa tails with the CP in *S. griseus* and *M. tuberculosis* parallels this behaviour, and it is possible that the binding of one or several of the Mpa tails induces a conformational change in the CP which prevents the rest of the binding sites from being engaged. The symmetry mismatch between the hexameric Mpa and the heptameric CP might also prevent the binding of all six C-terminal Mpa tails.

The pocket lysine mutant CP_{PL} shows no crosslinking of the peptides to CP α above the background level caused by unspecific binding, and even less unspecific crosslinking than that to CP β, which should not have binding sites for the peptide at all. This is further evidence that the pocket lysine is indeed necessary for the binding of Mpa to CP, and that the crosslinking process is specific. Considering its higher yield of crosslinked complex compared to peptide 33, peptide 20 (Q586*p*Bpa) was selected as the basis for the expression of full-length *p*Bpa-containing Mpa, *i.e.* $Mpa_{Q586pBpa}$.

3.3. Test expressions of full-length Mpa$_{Q586pBpa}$

As seen in **Fig. 3.3.1** (top left), expressing Mpa$_{Q586pBpa}$ at 18°C does not lead to usable amounts of protein even at high IPTG concentration. The higher expression temperatures of 25°C and 37°C, in comparison, yield reasonable amounts after 6 hours. There is a significant amount of impurities in the samples, showing that the batch purification using the NiNTA Superflow resin was expectedly inferior to the NiNTA-FPLC column purification.
Although the over-night expression resulted in high amounts of protein, considering wild type Mpa is normally expressed at 30°C for 6 hours the closest conditions for Mpa$_{Q586pBpa}$ expression were chosen, i.e. 25°C for 6 hours.

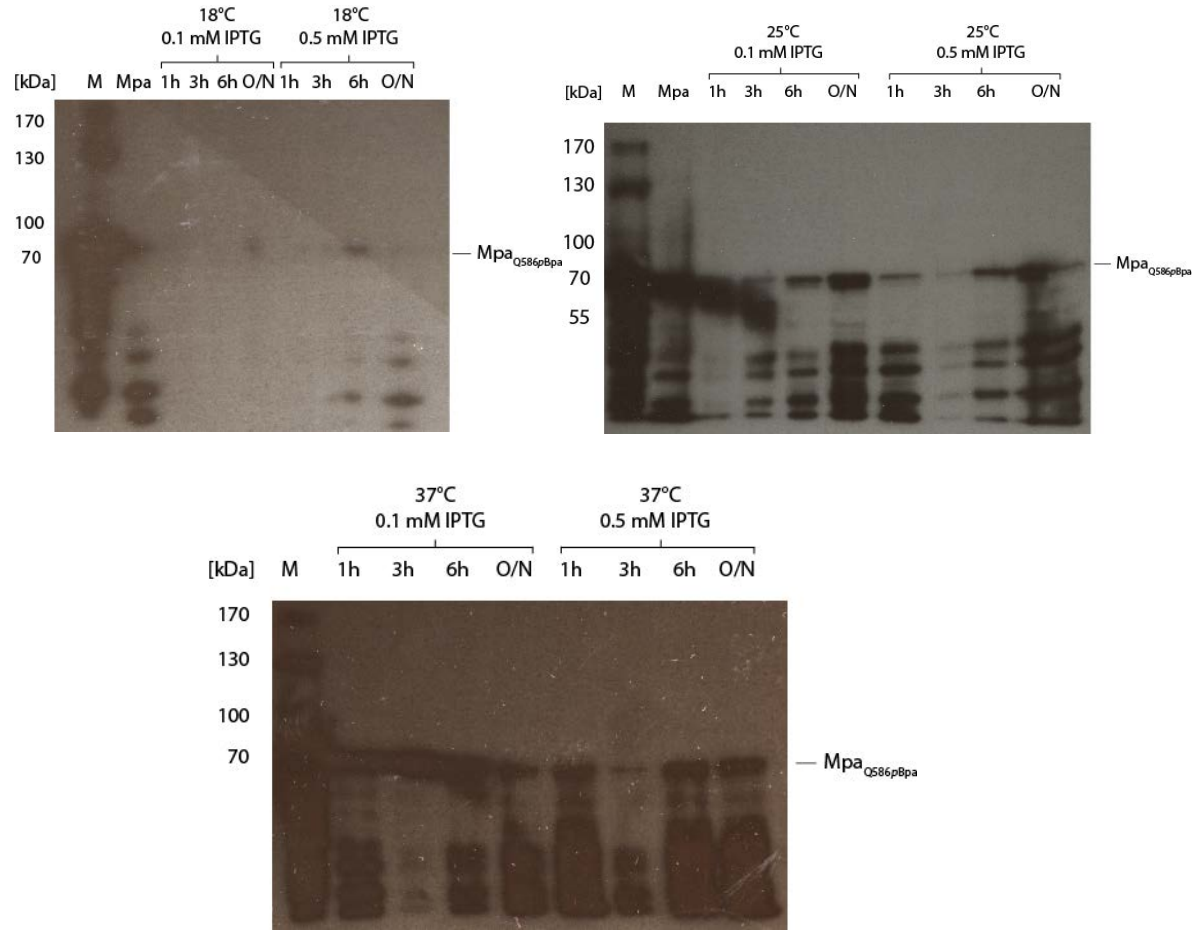

Fig. 3.3.1: Comparison of Western blots with anti-Mpa antibody (1:10,000) of Mpa$_{Q586pBpa}$ test expressions at 18°C (top left), 25°C (top right) and 37°C (bottom) and IPTG concentrations of 0.1 mM or 0.5 mM.

3.4. Photocrosslinking of full-length $Mpa_{Q586pBpa}$ to CP_{WT}

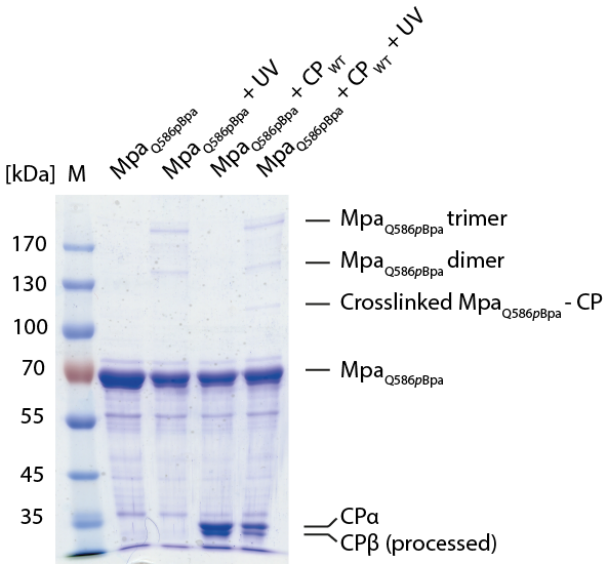

Fig. 3.4.1: Crosslinking of full-length $Mpa_{Q586pBpa}$ to CP_{WT} at a ratio of 0.9:1.

As seen in **Fig. 3.4.1**, the crosslinking process can also be performed with full-length protein. Only after irradiating $Mpa_{Q586pBpa}$ together with CP, but not when irradiating $Mpa_{Q586pBpa}$ alone, a new band appears between 100 and 130 kDa, indicating that it represents the crosslinked $Mpa_{Q586pBpa}$-CP complex. However, the size is inconsistent with an Mpa monomer (65.1 kDa) linked to an CPα monomer (29.5 kDa), which should form a complex of 94.6 kDa, well below the approximately 120 kDa seen here. In yeast, the binding pocket is formed by the interface of two α-subunits[139], and if the same applies to *S. griseus* this result could be interpreted as $Mpa_{Q586pBpa}$ interacting with both subunits and being crosslinked to both. However, the sole carbonyl group of *p*Bpa, upon UV exposure, generates an oxygen diradical that can only form a single bond.[148] It is also possible that the apparent difference in size is due to warping of the gel, as seen around 35 kDa. Although a crosslinked $Mpa_{Q586pBpa}$ dimer (130.2 kDa) would also be of the approximate same size, this 120 kDa band is not visible when crosslinking $Mpa_{Q586pBpa}$ alone in the absence of the CP.

In contrast, the bands at approximately 140 kDa and above 170 kDa both appear after irradiating $Mpa_{Q586pBpa}$ alone. They therefore very likely consist of two (2 x 65.1 kDa = 130.2 kDa) and three (3 x 65.1 kDa = 195.3 kDa) crosslinked $Mpa_{Q586pBpa}$ monomers, respectively. It is possible that higher-order $Mpa_{Q586pBpa}$ oligomers can be photocrosslinked, but the limitations of the gel used here preclude the visualization of such large complexes. Whether the structure of the crosslinked $Mpa_{Q586pBpa}$ units resembles the wild-type, i.e. the C-terminal tails were crosslinked to each other while the interdomains formed the oligomers, or if the tails interacted with and were bound to random sites on the surface of their adjacent monomers is unknown. Crosslinking is in any case highly inefficient, with less than 10% of the $Mpa_{Q586pBpa}$ forming the bond and the rest remaining free.

To verify that the new band produced by the crosslink consists indeed of $Mpa_{Q586pBpa}$ and the CP linked together, as well as to test whether the ratio of $Mpa_{Q586pBpa}$ to the CP during the crosslink influences the efficiency, new photocrosslinks were performed at an $Mpa_{Q586pBpa}$: CP ratio of either 1:1 or 2.5:1. The reactions were analyzed by Western blotting using rabbit anti-CP antibodies (diluted 1:10,000). 10 mM AMPPNP and 10 mM $MgCl_2$ were added to test the influence of nucleotide binding to the crosslink (**Fig. 3.4.2 A** and **B**)**.**

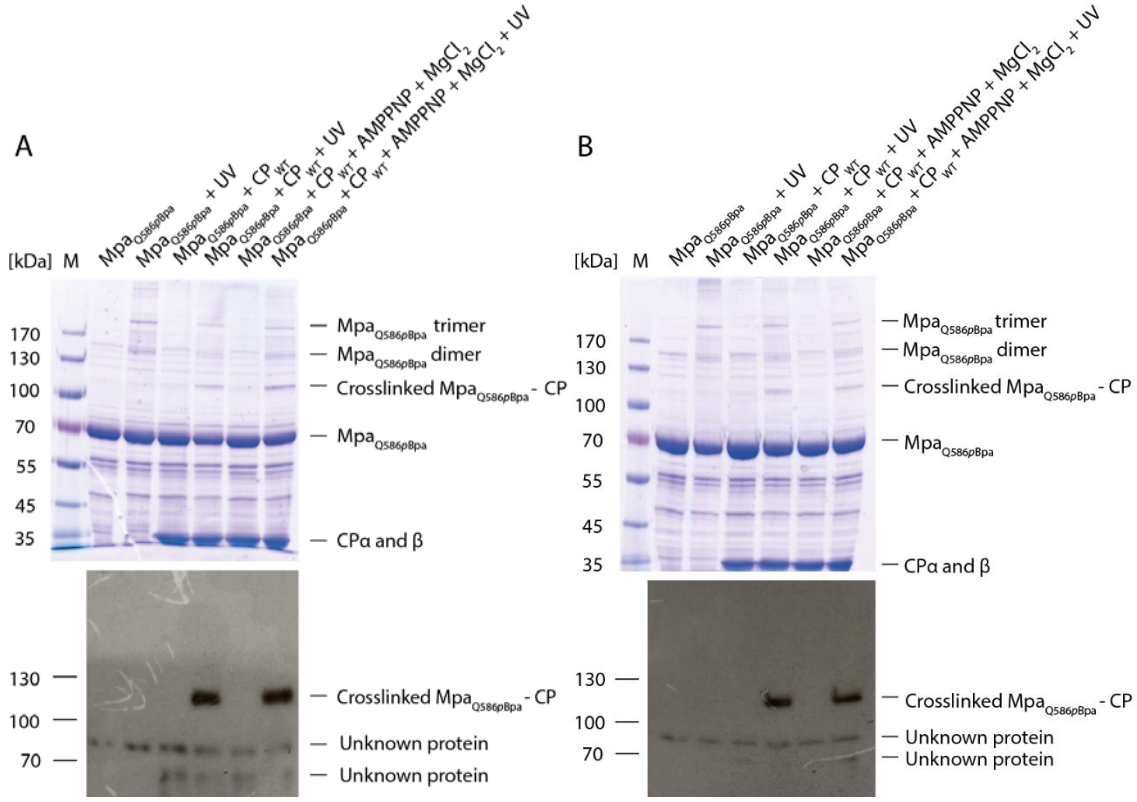

Fig. 3.4.2 A: Coomassie-stained SDS-PAGE gel (top) and Western blot using rabbit anti-CP antibody diluted 1:10,000 (bottom) of the crosslinking of $Mpa_{Q586pBpa}$ to CP_{WT} at a ratio of 1:1. AMPPNP and $MgCl_2$ were added to test the influence on the crosslinking efficiency. **B:** Coomassie-stained SDS-PAGE gel (top) and Western blot using anti-CP antibody diluted 1:10000 (bottom) of the crosslinking of full-length $Mpa_{Q586pBpa}$ to CP_{WT} at a ratio of 2.5:1.

In the Western blots, the anti-CP antibody unspecifically reacted with a contaminating protein of approximately 85-90 kDa present in the purified $Mpa_{Q586pBpa}$ solution as well as an additional protein of approximately 65 kDa in the purified CP solution. Although the size of the latter corresponds almost exactly to $Mpa_{Q586pBpa}$, this band is not visible in the lanes containing pure $Mpa_{Q586pBpa}$ and must therefore be an unrelated contamination.

Despite these unspecific interactions, the intensity of the signal was significantly higher for the band at 120 kDa than for the contaminants. This indicates that CP is indeed present and provides strong

evidence that the 120 kDa band must be the result of an $Mpa_{Q586pBpa}$ – CP crosslink rather than a dimerization of $Mpa_{Q586pBpa}$. The ratio of $Mpa_{Q586pBpa}$ to CP does not seem to have an influence on the efficiency, nor does the presence of AMPPNP and $MgCl_2$. Western blots using anti-Mpa antibody (diluted 1:10,000) were performed as well but did not give usable results due to high background signals.

To test whether the binding of $Mpa_{Q586pBpa}$ is a specific event that engages the pockets on CPα's surface (which had already been established for the tail peptide in section 3.2, compare **Fig. 3.2.1 and 3.2.2**) and not merely unspecific aggregation during the crosslink, it was repeated with the CP pocket lysine mutant (CP_{PL}, *i.e.* the K52A mutant).

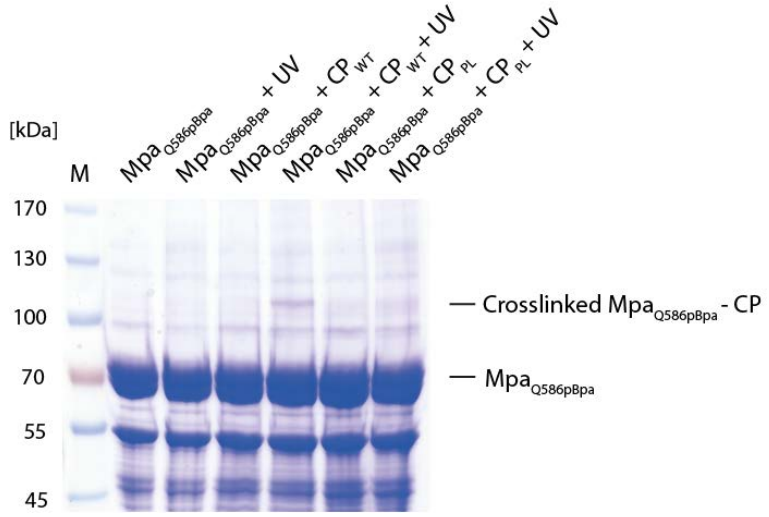

Fig. 3.4.3: Crosslinking of full-length $Mpa_{Q586pBpa}$ to CP_{WT} or CP_{PL} at a ratio of 2.5:1.

The CP pocket lysine mutant shows that the lysine at position 52 is essential for the binding of Mpa, with no crosslinking occurring when the K52A mutation is introduced. Thus, the specificity of the binding is confirmed. Again, the band consisting of crosslinked $Mpa_{Q586pBpa}$ and CP is located between 100 and 130 kDa, in contrast to the expected size of 94.6 kDa. Less than 10% of the $Mpa_{Q586pBpa}$ reacted with the CP despite an $Mpa_{Q586pBpa}$: CP ratio of 2.5 : 1.

It has been established with a high degree of confidence that $Mpa_{Q586pBpa}$ binds and can be photocrosslinked to the CP 28-mer, and that the binding is specific and dependent on the lysine 52 in the CPα-subunit's binding sites. However, the product of this reaction is larger than expected by about 20-25 kDa. Although some possibilities - such as $Mpa_{Q586pBpa}$ crosslinked to a CPα dimer - could be excluded, the reason for this disparity remain unknown. Further analysis of the crosslinked protein complex using mass spectrometry could be necessary to solve this problem. The efficiency is low and is neither improved by longer exposure to UV, nor by higher ratios of $Mpa_{Q586pBpa}$ to CP or the addition of AMPPNP. Despite purification by NiNTA-IMAC and SEC, the $Mpa_{Q586pBpa}$ samples were

highly impure, which might lower the efficiency further. Alternative protocols and conditions will likely have to be tested before purification of the crosslinked complex can be performed on a larger scale.

When comparing the crosslinks of the peptides and that of the full-length $Mpa_{Q586pBpa}$ (see section **3.2.**), it is evident that the efficiency of the former is significantly higher than that of the latter, although even with the peptides less than half of them were crosslinked. The hexamerisation of the full-length $Mpa_{Q586pBpa}$ could have a steric influence on the crosslinking process or perhaps shielded the *p*Bpa residue from the UV radiation. Similarly, the C-terminal *p*BpaYL sequences might be less accessible as a part of the hexamer because they are partially occluded by the neighboring units. If this is the case, there could be a need to extricate the tails before they can bind to the CP, which would require an additional, as yet unidentified protein to assist. Such a protein could be difficult to detect if it only interacts with Mpa immediately before the assembly of the holoproteasome.

3.5. Electron microscopy of the crosslinked proteasome complex

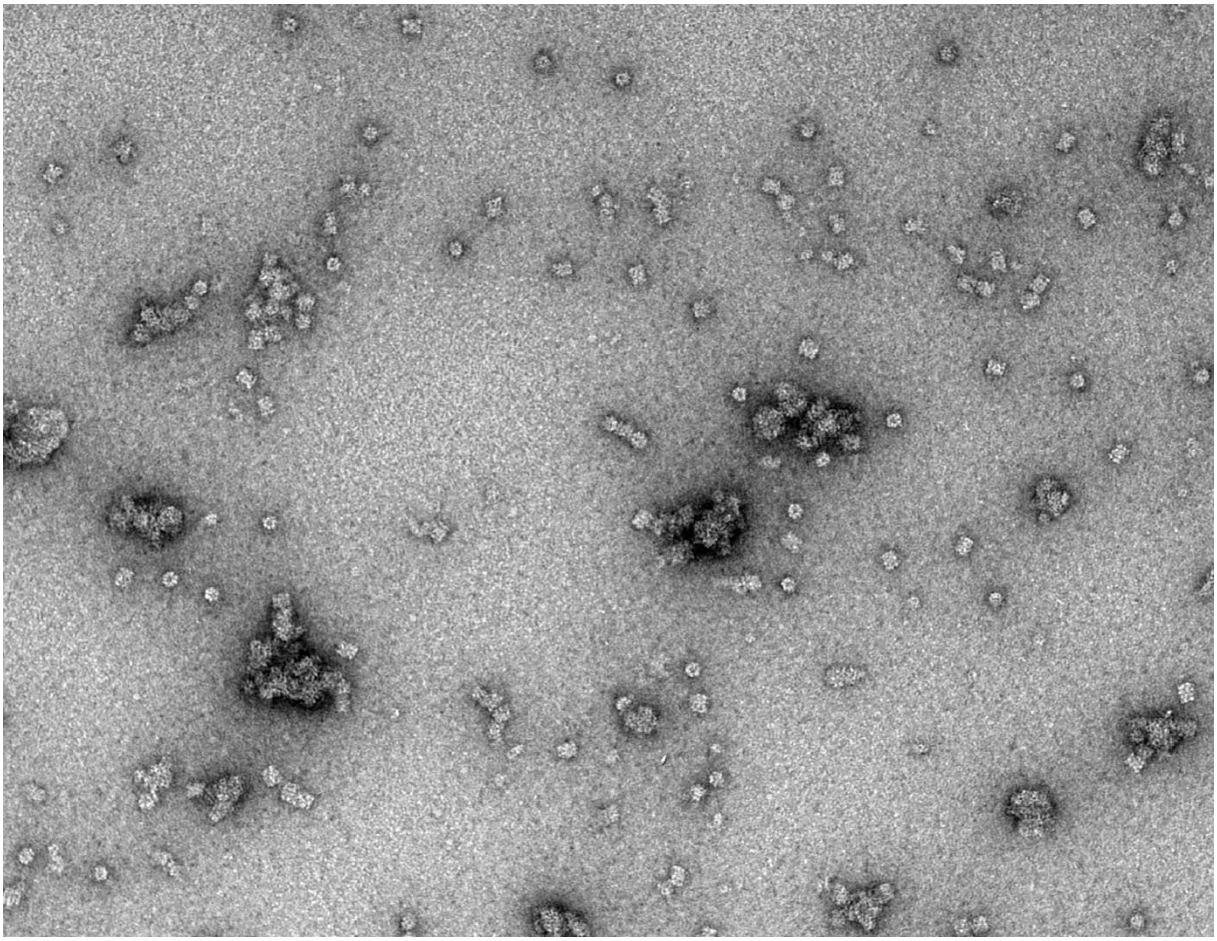

Fig. 3.7.1. Transmission electron micrograph of Mpa_{WT}. c = 0.25 mg/mL (diluted 1:10 from purified sample), stained with 2% uranyl acetate. Magnification: 89000 x at 80 kV.

Although the C-terminal coiled-coil domains of Mpa are not visible, the hexameric structure with the pore can be seen. Mpa resembles CP to some extent but does not exhibit the four-ring pattern when viewed laterally. Electron microscopy of Mpa in general was challenging due to a high degree of aggregation in other samples (not shown) compared to **Fig. 3.7.1**, even though the hexameric fractions of the SEC purification were used. Some aggregation is visible in **Fig. 3.7.1** near the center and the lower left as well. Previous experiences in our lab with the purification of Mpa had shown its significantly higher tendency to aggregate compared to CP. It is possible that in this case Mpa was caused to aggregate by the process of staining with 2% uranyl acetate, performed at room temperature.

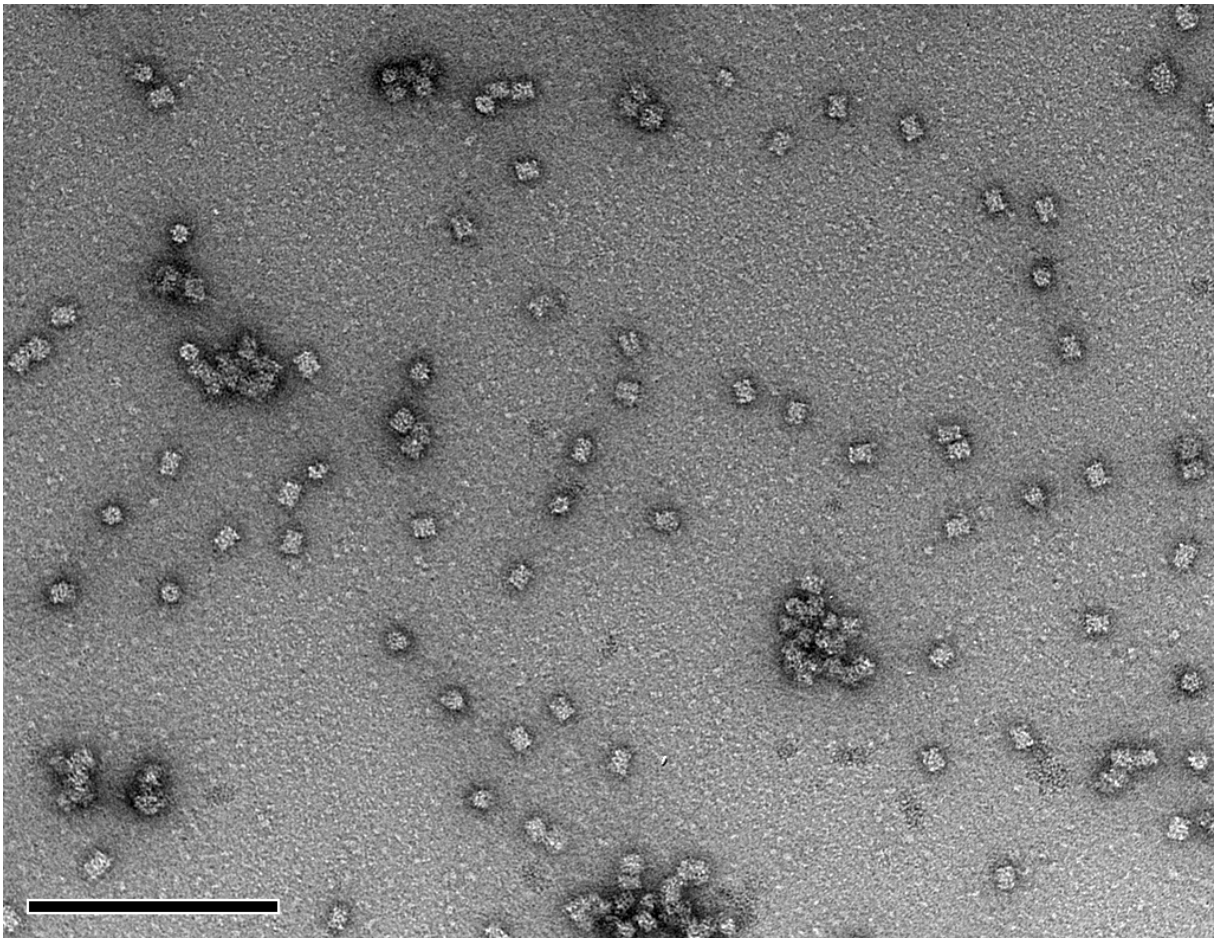

Fig. 3.7.2: Transmission electron micrograph of CP_{T54V} 28-mer. c = 0.7 mg/mL (diluted 1:10 from purified sample), stained with 2% uranyl acetate. Magnification: 110000 x at 80 kV. Scale bar: 200 nm.

The CP_{T54V} formed 28-mer barrel structures as expected, with four clearly identifiable heptameric rings and the central pore visible. Since the difference in circumference between 28-mers composed of processed and those of unprocessed CP is only approximately 1.5 nanometers, it is not possible to distinguish between them at this magnification and resolution. The N-terminal peptides occluding the gate are not visible for the same reason.

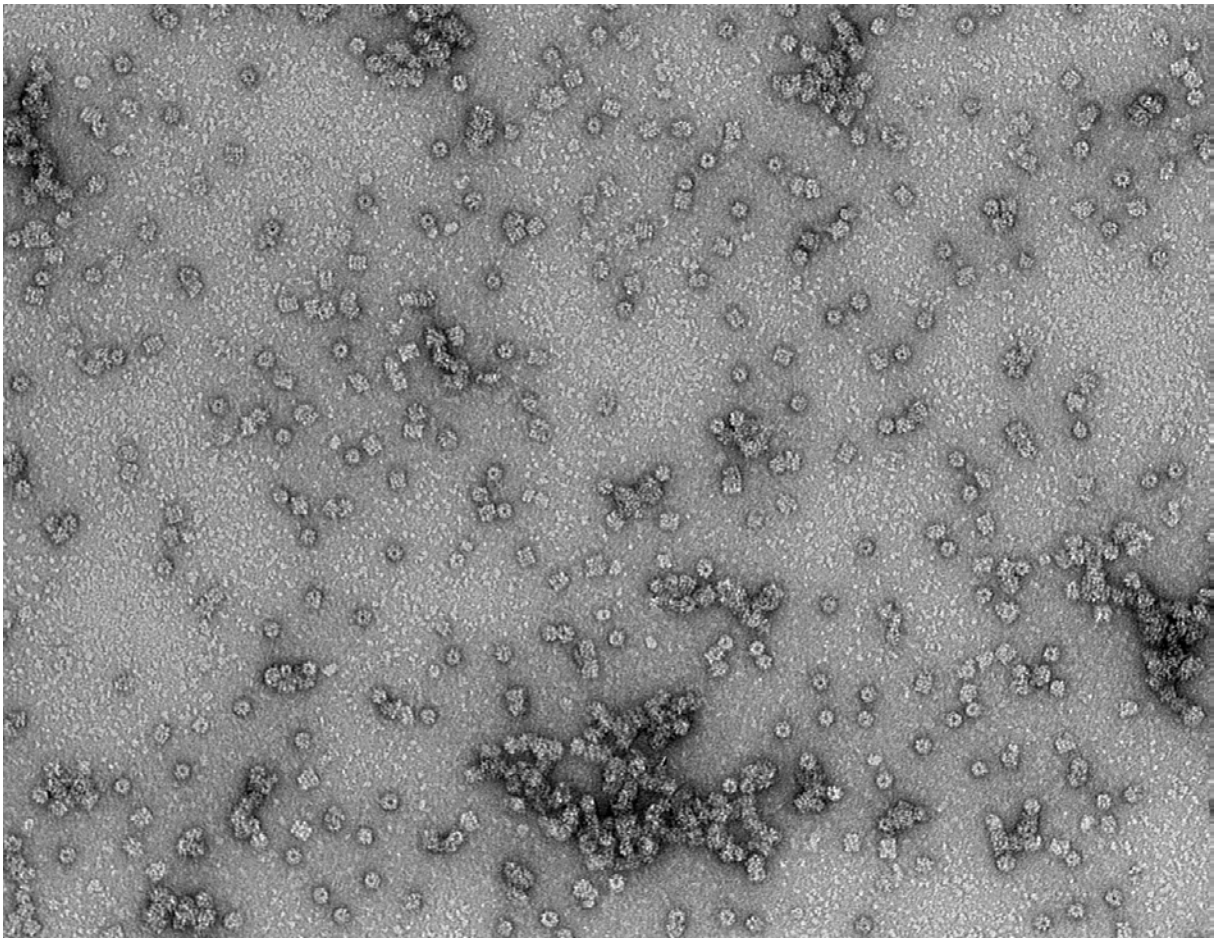

Fig. 3.7.3: Transmission electron micrograph of CP_{WT} 28-mer. c = 0.4 mg/mL, stained with 2% uranyl acetate. Magnification: 89000 x at 80 kV.

Compared to the CP_{T54V} 28-mer (see **Fig. 3.7.3**), no significant difference can be seen here with the wild type core particle, as expected since the β-propeptides fold into the cylinder and do not influence the structure except for an increase in circumference of about 1.5 nanometers. The central pore and the four rings can be clearly seen. It is interesting to compare the orientation of the core particles on the surface of the sample holder foil : while the CP_{T54V} complexes were overwhelmingly lying on their sides in all recorded photographs, the majority of the CP_{WT} 28-mers were standing upright. Although the overall structures of both are almost identical, the propeptide of the unprocessed $prcB_{T54V}$ (30.2 kDa compared to 24.6 kDa of the processed wild-type prcB) adds almost 10% to the total mass of the 20S core particle (758 kDa for the wild type core particle, 836 kDa for the T54V mutant core particle), which could increase a tendency to settle laterally.

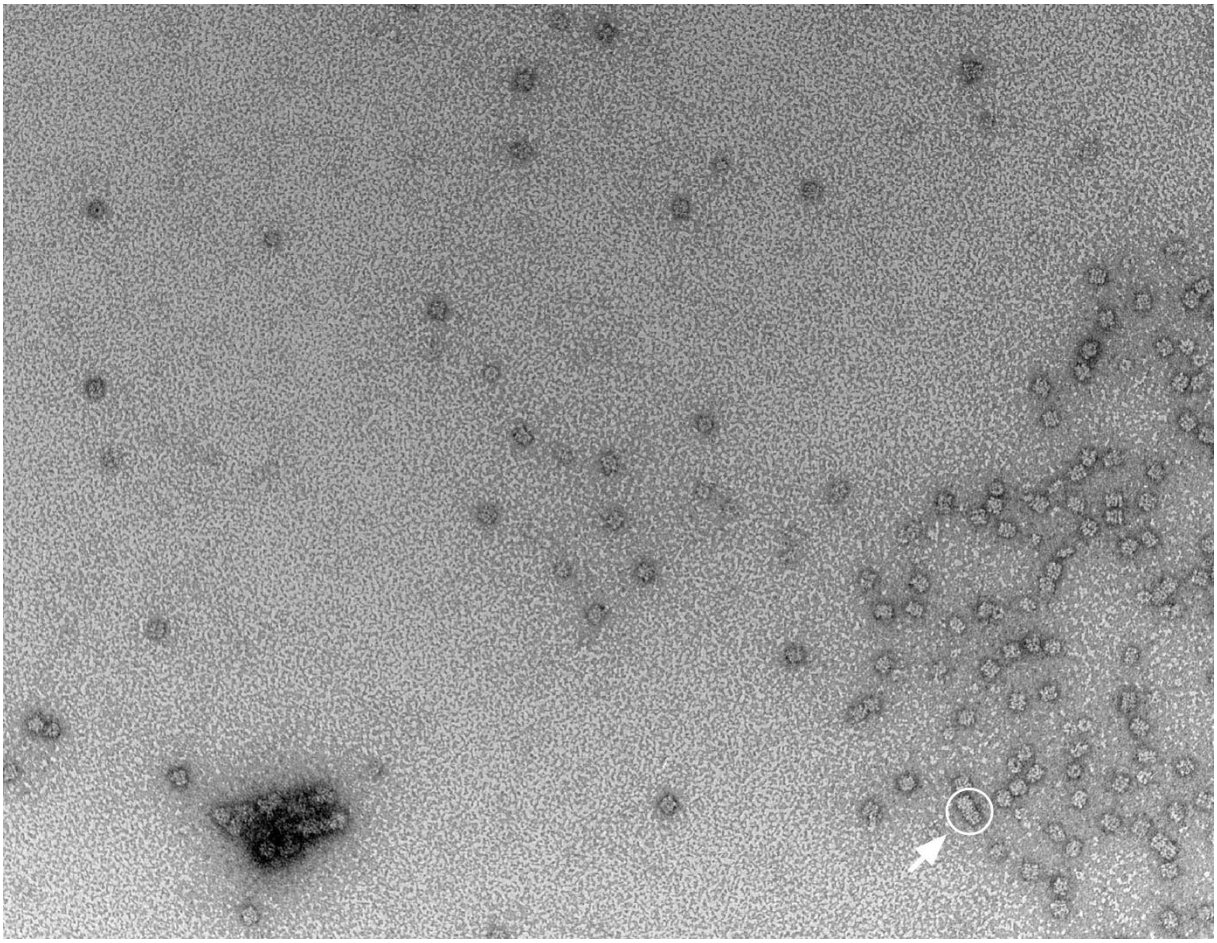

Fig. 3.7.4: Transmission electron micrograph of crosslinked $Mpa_{Q586pBpa}$ – $CP_{Strep\ II}$ proteasome complex. c = 0.2 mg/mL (diluted 1:100 from purified sample), stained with 2% uranyl acetate. Magnification: 71000 x at 80 kV. Scale bar: 500 nm. A potential single-crosslinked complex ($Mpa_{Q586pBpa}$-CP) is highlighted.

In EM of the crosslinked complex (**Fig. 3.7.4)**, no unambigious crosslinked holoproteasome complex - i.e. a CP-Strep II barrel connected to at least one $Mpa_{Q586pBpa}$ hexamer - was found. All the complexes seen were 28-mers without $Mpa_{Q586pBpa}$. The highlighted complex is a putative single-Mpa_{Q586F}-CP proteasome with Mpa_{Q586F} on the lower right, but considering the high amount of free CP in the vicinity it is difficult to distinguish between a true complex and free $Mpa_{Q586pBpa}$ and CP subcomplexes coincidentally alongside each other. Unbound $Mpa_{Q586pBpa}$ can be seen in the lower left, partially aggregated. As described in section **3.4.**, the efficiency of the crosslink is very low (see also **Fig. 2.22.3**)**,** note the ratio of $CP_{Strep\ II}$ to crosslinked $Mpa_{Q586pBpa}$), which results in a high amount of CP relative to a low concentration of $Mpa_{Q586pBpa}$ when using Strep II-tagged CP.

Conceivably, $Mpa_{Q586pBpa}$ might have separated from the core particle after the isolation of the complete proteasome by Strep-Tactin purification, but most likely the yield of the crosslink would have been too low to detect the complexes in any case. It is possible that the staining procedure, which was performed at room temperature, caused the aggregation of $Mpa_{Q586pBpa}$ as was the case with free wild type Mpa in other EM analyses (see **Fig. 3.7.1.**).

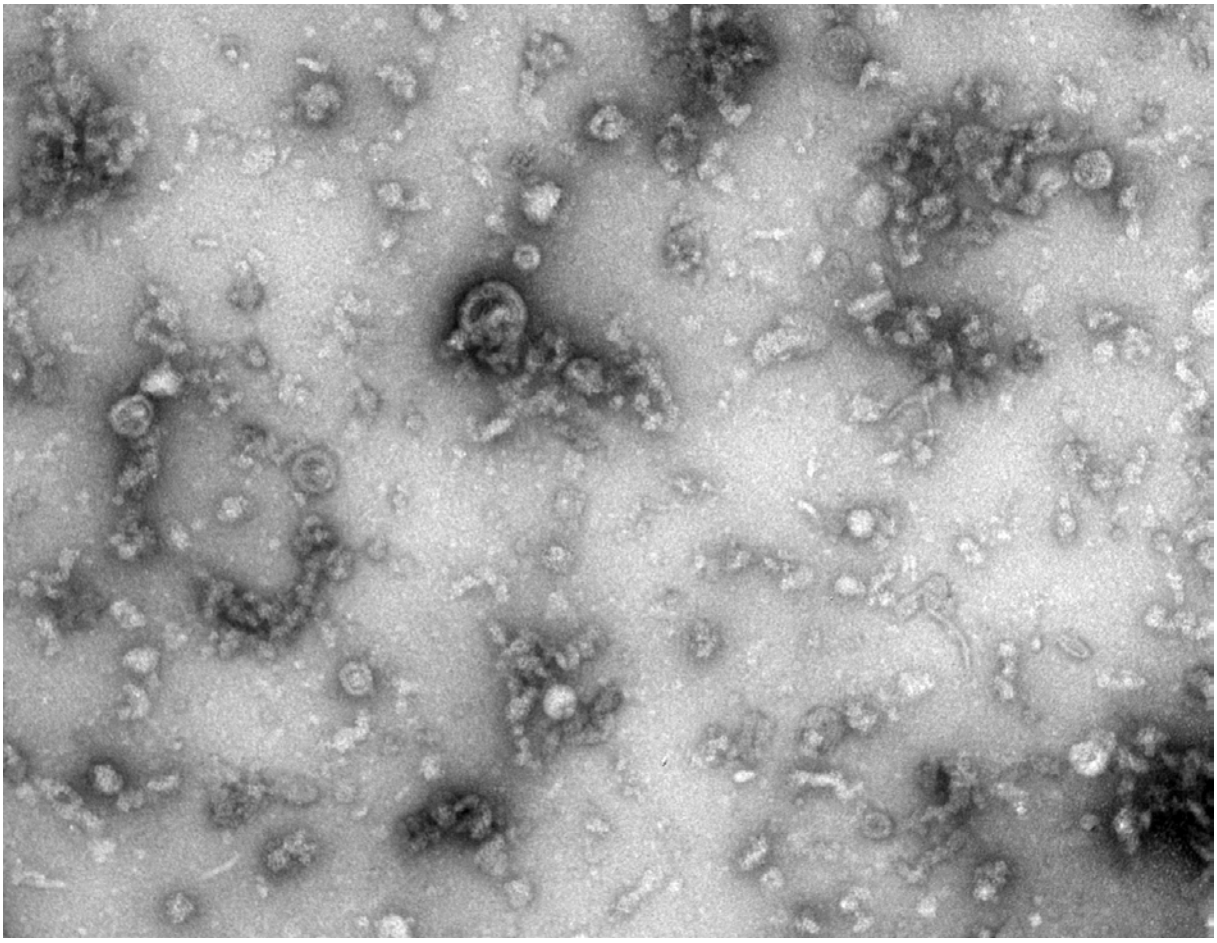

Fig. 3.7.5: Transmission electron micrograph of tricistronic Mpa_{Q586F} – CP proteasome complex. c = 0.49 mg/mL, stained with 2% uranyl acetate. Magnification: 71000 x at 80 kV. Scale bar: 500 nm.

Electron microscopy of the tricistronic Mpa_{Q586F} – CP complex after two consecutive SEC purification runs showed severe degradation of the proteins and no visible complex, confirming the disassembly of the proteasome seen in **Fig. 3.6.4.6.** The circular or spherical structures seen in **Fig. 3.7.5** are of unknown origin and could be caused by degraded proteins. The tricistronic complex therefore is not able to remain stable after repeated SEC, even in optimized buffer conditions that otherwise allow reliable purification.

3.6. Co-immunoprecipitation from Streptomyces griseus cell lysate

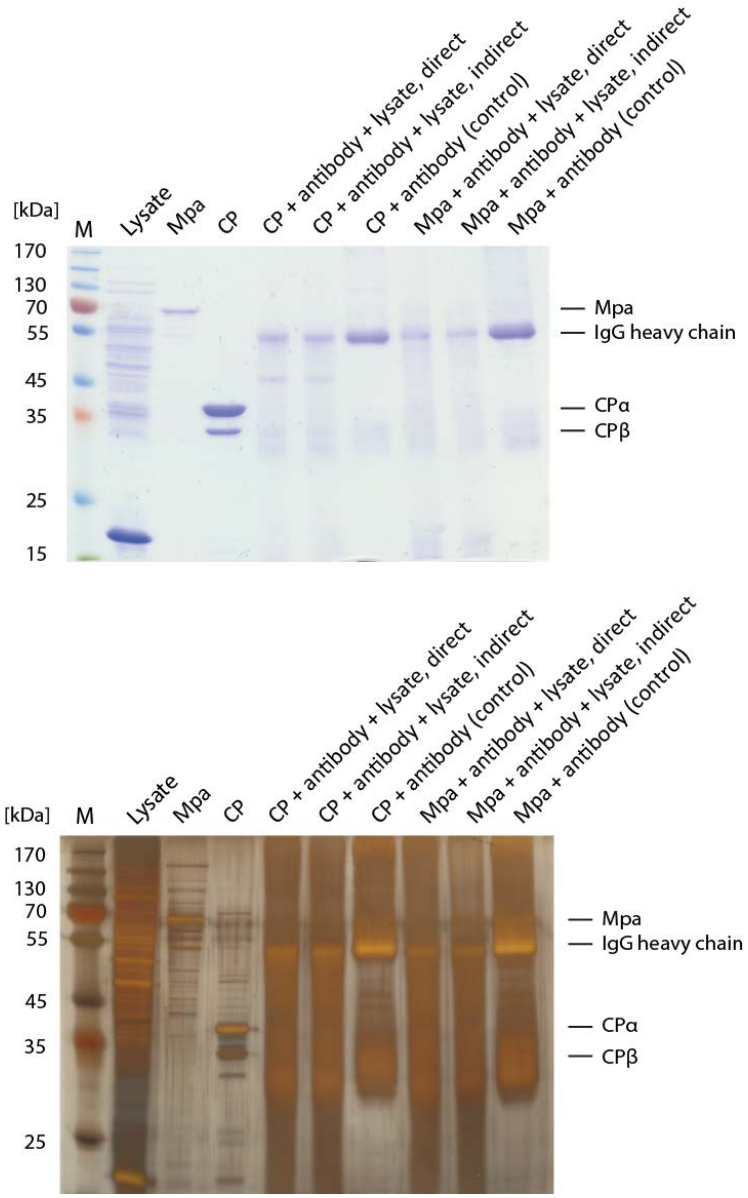

Fig. 3.12.1. Coomassie-stained (top) and silver-stained (bottom) gels of co-immunoprecipitation of Mpa and CP from S. griseus cell lysate.

In the immunoprecipitation (**Figure 3.12.1**) no precipitated Mpa (expected in lanes **4** and **5**) or CP (expected in lanes **7** and **8**) can be seen either in the Coomassie-stained or the silver-stained gel. Although some protein is visible in the approximate height of the CP bands when using Mpa as a bait, this is due to impurities in the antibody solution, since the same protein is visible in the control sample where only antibody is used (lane **9**). Although the amount of protein pulled down could be too low to detect, it is unlikely that nothing would be visible in the silver stain, which further reinforces the notion that in the cell, Mpa and CP do not interact directly. It must also be considered

that the conditions of the co-immunoprecipitation chosen here might have been detrimental to the binding.

3.7. Pull-down assays with Mpa and CP from *Streptomyces griseus* lysate and mass spectroscopy of elution fractions

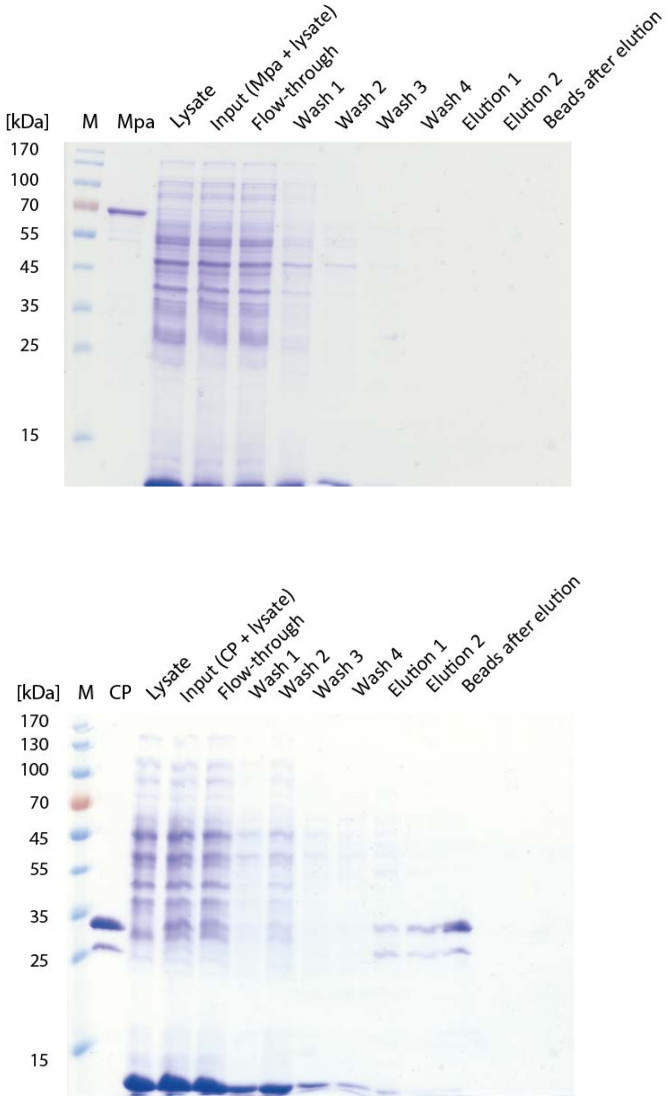

Fig. 3.11.1. Pull-downs from 15 mg *S. griseus* lysate using 45 µg Mpa (top) and 45 µg CP (bottom) as bait.

Neither of the two bait proteins were successful in pulling down the proteasome subunits from the cell lysate, at least not in a stoichiometric manner as visible from the gel. In the Mpa pulldown, the binding of the bait protein to the NiNTA agarose beads was less efficient than for CP, with no visible bands in the elution fractions, indicating that they separated during the washing steps or were not adequately bound to the beads to begin with. However, in a Western blot using anti-CP antibody, the

antibody unspecifically reacted with Mpa, showing its presence in the wash fractions (**Fig. 3.11.4**) and therefore its binding to the beads. In the CP pulldown, the elution of the bound bait protein from the beads was incomplete, with significant amounts present after eluting twice. Since isolated proteins could have been present in the elution fractions at concentrations too low to detect them by Coomassie staining, 3.75 µl of each elution were used for silver staining as described in section **2.13**.

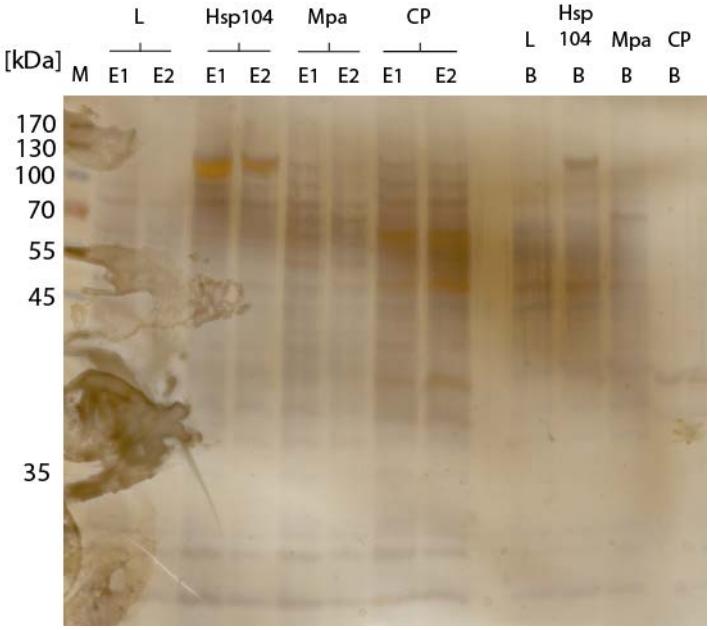

Fig. 3.11.3: Silver-stained SDS-PAGE gel of the pull-down elution fraction samples: elution fractions 1 and 2 (E1 and E2) of assays with lysate (L) and Hsp104 as a control bait. B: beads loaded into gel after elution (not submitted to mass spectrometry). 3.75 µL sample used per lane.

As seen in **Fig. 3.11.3**, no Mpa or CP was visible in the elution fractions when using silver staining, although the intensity of the background proteins was likely high enough to mask low amounts of both. In both of the CP-bait elutions a strong band is visible between 55 and 70 kDa that could represent isolated Mpa, but considering that bands of equivalent intensity appear throughout the fractions no definitive identification is possible.

Mass spectrometry analyis did not identify prcA/B in the Mpa-baited or Mpa in the CP-baited pulldown, indicating that the subcomplexes do not interact with each other *in vivo* under the conditions chosen here. The possibility that an additional third protein or post-translational modification of either Mpa or the core particle might be necessary for the interaction cannot be excluded.

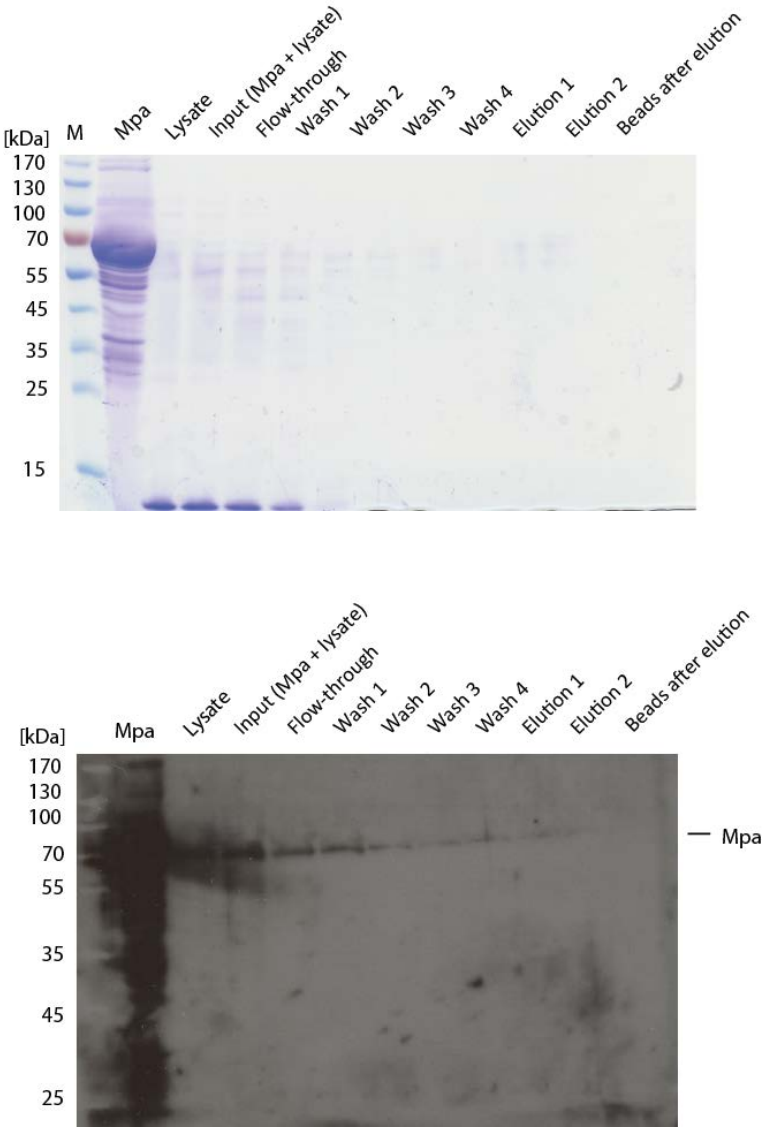

Fig. 3.11.4. Coomassie-stained gel (top) and Western blot (bottom) elution fraction samples from the repeat of the Mpa pull-down. The anti-CP-antibody used in the Western blot cross-reacted with Mpa (compare also to **Fig. 3.5.4**). No CP was detected in either the elution fractions or on the beads.

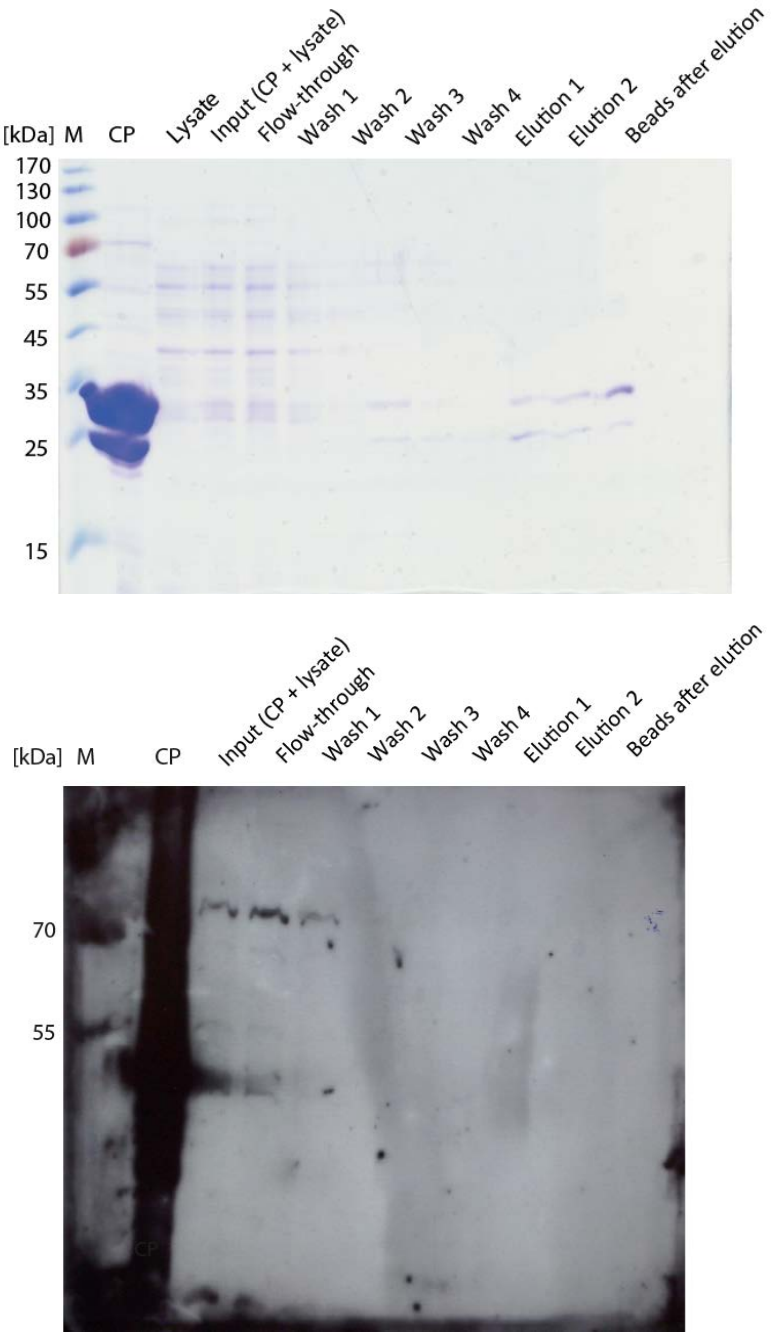

Fig. 3.11.5. Coomassie-stained gel (top) and Western blot with anti-Mpa antibody (bottom) elution fraction samples from the repeat of the CP pull-down. The antibody unspecifically reacted with high amounts of CP in the reference lane but not in the low amounts of elution 1 and 2.

The pull-downs did not show binding between CP and Mpa either in the Western blot or in the Coomassie stained gels even at high concentrations. Although the Western blot of the pull-down with CP using the anti-Mpa antibody showed a band in the vicinity of 70 kDa where Mpa would be expected in the lysate, flow-through and first wash fractions, none could be seen in the elution fractions or bound to the post-elution beads. (**Fig. 3.11.5**).

3.8. Pup-Luciferase unfolding assay

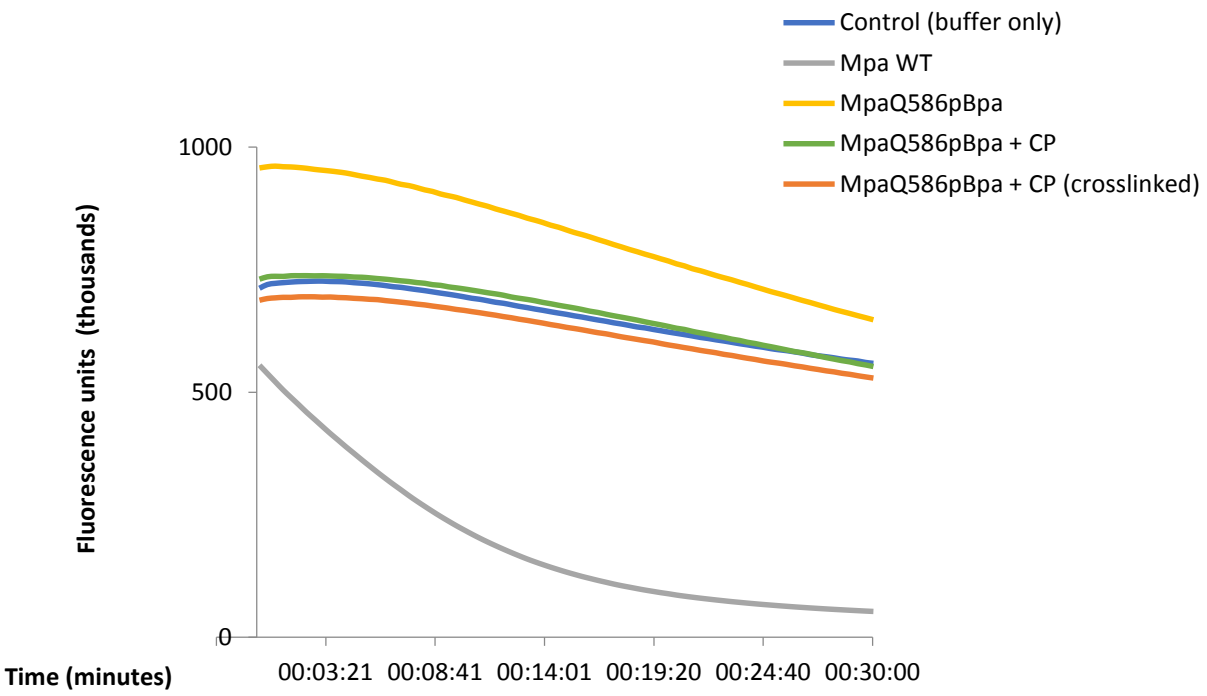

Fig. 3.8.1: Intensity of fluorescence during Luciferase unfolding by wild type Mpa, $Mpa_{Q586pBpa}$, $Mpa_{Q586pBpa}$ + CP and the crosslinked $Mpa_{Q586pBpa}$ + CP complex. Values are averaged from three parallel measurements for each curve.

Surprisingly, although Mpa_{WT} clearly showed unfolding of Pup-Luciferase, $Mpa_{Q586pBpa}$ was inactive either alone or crosslinked together with CP_{WT}. Considering the *p*Bpa mutation is located in the extreme C-terminal end tails of Mpa, on the opposite site of the Pup-binding coiled coil domains of the N-terminal end and away from the ATPase domain, any influence it might have either on Mpa's interaction with Pup or its unfolding activity could indicate that the tails and the coiled coil/ATPase domain are, while spatially separated, allosterically connected. It has been reported that the C-terminal pupylation of *M. tuberculosis*' Mpa at lysine 591 (outside the GQYL motif) results in the loss of Mpa's ATPase activity due to simultaneous binding of Pup to the N-terminal coiled-coil domain while it is linked to the C-terminal tail.[118] Considering $Mpa_{Q586pBpa}$ is also inactive when not crosslinked, the possibility that this deactivation is caused by the crosslinking of *p*Bpa to the coiled-coil domain can be excluded.

It is possible that only one of the two mechanisms required for unfolding a substrate – the binding of Pup and the unfoldase activity itself – was defective. $Mpa_{Q586pBpa}$ could have bound Pup-Luciferase but might have been unable to unfold it. Conversely, if the Pup-binding site on the N-terminal alpha helices of $Mpa_{Q586pBpa}$ were to be inactivated, $Mpa_{Q586pBpa}$ could not engage the substrate, even though its unfoldase ability would be undiminished.

3.9. Pup-PanB and Pup-GFP degradation assays

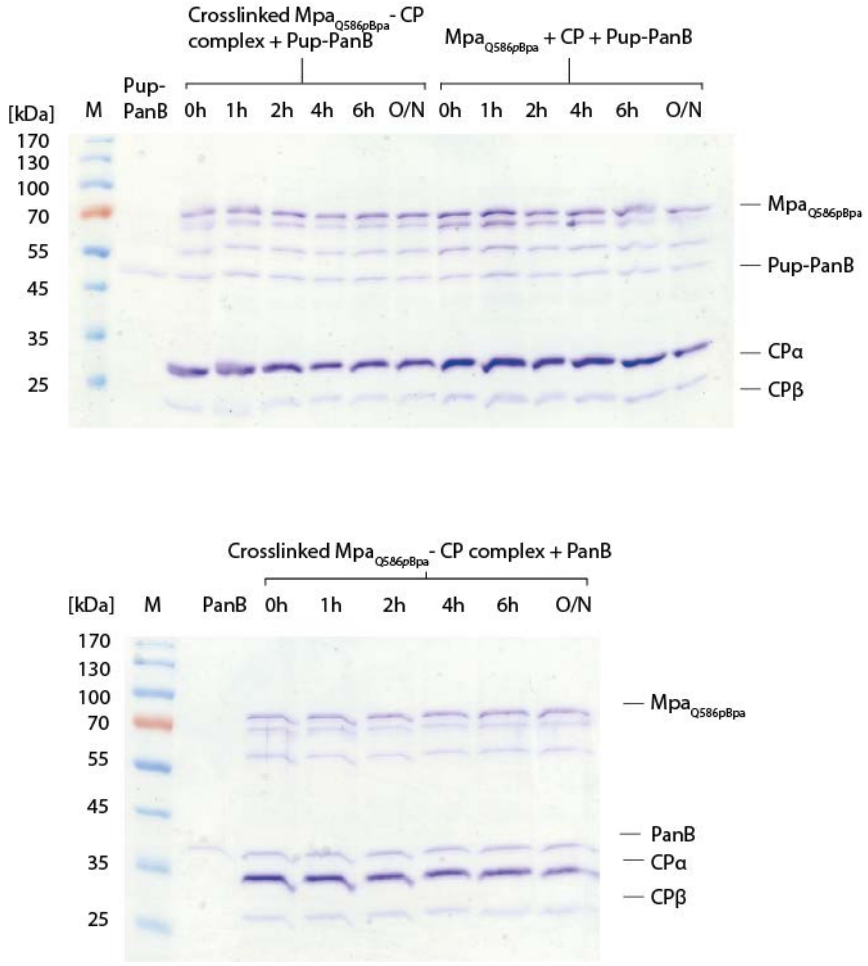

Fig. 3.9.1. Degradation assays of Pup-PanB fusion protein (top) and PanB alone (bottom) as a control.

No degradation of either the Pup-PanB fusion protein (**Fig. 3.9.1**, top) or PanB alone (**Fig. 3.9.1**, bottom) by the crosslinked complex could be seen after incubation at 26°C overnight. It should be noted that the crosslinked complex is not visible in the gels either, therefore it is questionable if the amount of complex would have been sufficient to degrade Pup-PanB/Pup even if the complex would have that ability in principle. Even without any crosslinked complex present in the Pup-PanB/Pup samples, Mpa$_{Q586pBpa}$ should have retained the ability to bind and unfold Pup. Similar to the luciferase unfolding assay (section **3.8**), it is possible that only either the substrate-binding ability or the unfoldase ability of Mpa$_{Q586pBpa}$ were deactivated, and that Mpa$_{Q586pBpa}$ would have been able to bind or degrade Pup-PanB, but not both.

3.10. Suc-LLVY-AMC fluorescent substrate degradation assay

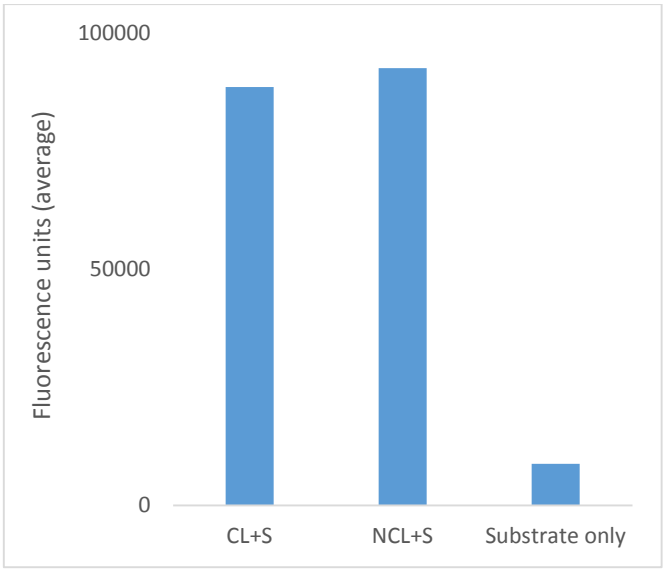

Fig. 3.9.1: Comparison of the peptidase activity between crosslinked $Mpa_{Q586pBPa}$ - CP proteasome complex together with substrate (CL + S), non-crosslinked proteasome components and substrate (NCL + S) and the negative control (substrate only). Each value was averaged from four measurements.

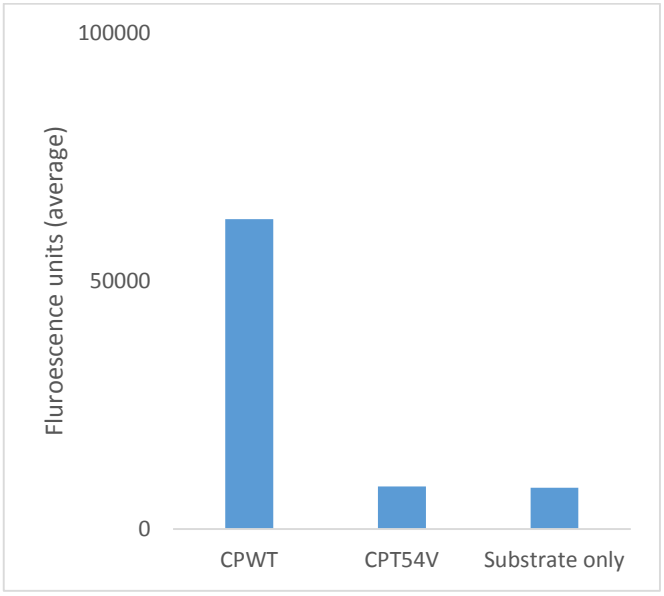

Fig. 3.9.2: Comparison of the peptidase activity between CP_{WT} and CP_{T54V}. Each value was averaged from four measurements.

There is no significant difference between the activity of CP when crosslinked to $Mpa_{Q586pBpa}$ and when free, indicating that the gate opening mechanism thought to be triggered by Mpa *in vivo* either does not occur by crosslinking, or that the gate is open constitutively. The most likely explanation, however, is that the amount of crosslinked complex was too low to detect any effect on the

fluorescence. In contrast to the eukaryotic proteasome, the actinobacterial proteasome gate is not entirely closed by the N-terminal peptides of the α-ring (see section **1.3.2** and **1.4.2**), which could be sufficient to allow the entry of small substrates like Suc-LLVY-AMC . It is interesting to note that the crosslinked $Mpa_{Q586pBpa}$ also does not significantly influence the proteolysis process negatively, suggesting that crosslinking is sterically at least a workable approximation to the actual binding and does not result in the blockage of the gate.

Another fluorogenic substrate degradation assay using the same protocol was set up to test the inactivity of the CP_{T54V} mutant (**Fig. 3.9.2**) The same concentrations as before (50 µM Suc-LLVY-AMC, 10 nM $CP_{WT/T54V}$ were used. Four measurements per sample were performed and the values were averaged. The inactivity of the CP_{T54V} mutant was thus conclusively demonstrated.

3.11. Influence of pH on the stability of the proteasome complex

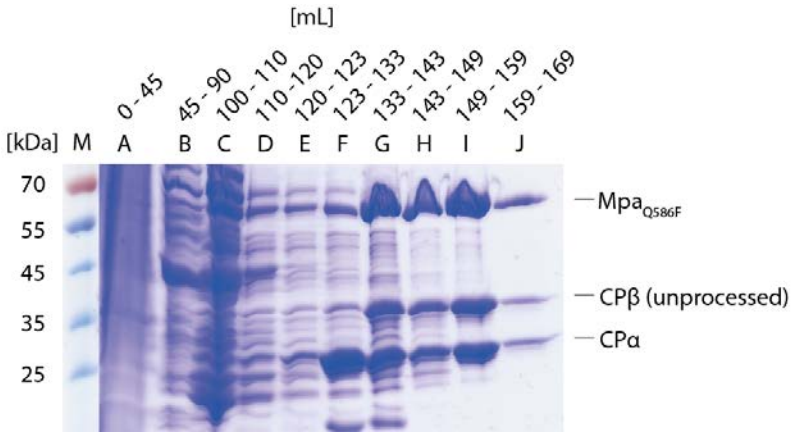

Fig. 3.6.1.1: SEC purification of the tricistronic Mpa_{Q586F}-CP (*mpa_{Q586F}-prcB-prcA)* proteasome complex, previously purified by NiNTA-IMAC. Note the unprocessed CP_{β} subunit (30.2 kDa). Fractions H-J were pooled and used for the stability tests.

The use of 50 mM MES buffer (pH = 6), resulted in the highest amount of Mpa_{Q586F} – CP complex relative to that of the aggregated Mpa_{Q586F} (Fig. **3.6.1.2**), especially when compared to the pH = 7 buffer (Fig. **3.6.1.3**). The absolute amount of Mpa_{Q586F} aggregate is also lower than under any other condition. There is no clear distinction between the three main peaks ($Mpa_{Q586F,}$ the holoproteasome and the free subcomplexes/subunits following the holoproteasome), with significant peak broadening and shouldering occurring. However, the Mpa_{Q586F} – CP complex peak itself can be easily and clearly distinguished from the Mpa_{Q586F} aggregate peak and the CP 28-mer peak. On the gel, all three subunits are visible and all three eluted over the entire length of the column, indicating that the complex partially dissociated into oligomers of varying size. Nonetheless, the majority of the proteins are concentrated in the fractions at around 1.05 mL, corresponding to a molecular weight of

significantly more than 669 kDa and therefore most likely containing the holoproteasome complex (1.54 MDa if both Mpa_{Q586F} hexamers bind to the CP, 1.15 MDa if only one binds).

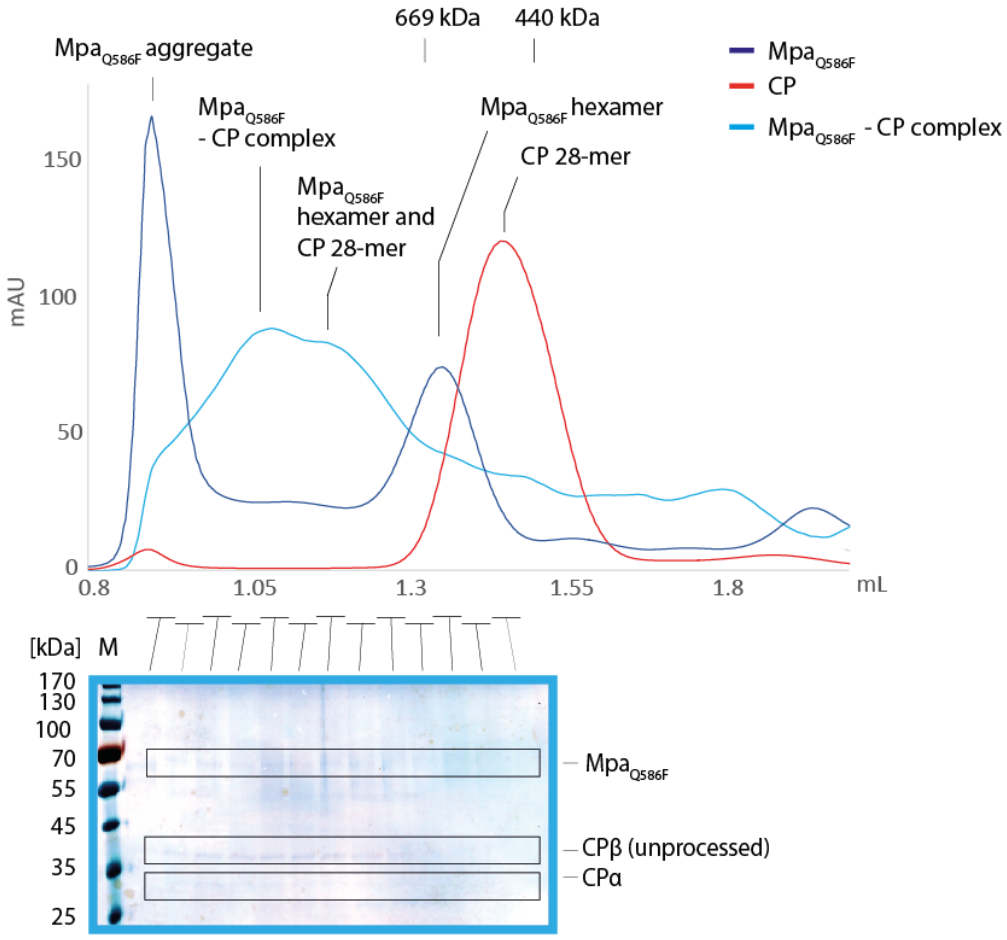

Fig. 3.6.1.2: SEC of the Mpa_{Q586F}-CP proteasome complex (c = 11 µM). Buffer: 50 mM MES, 75 mM NaCl, pH = 6.

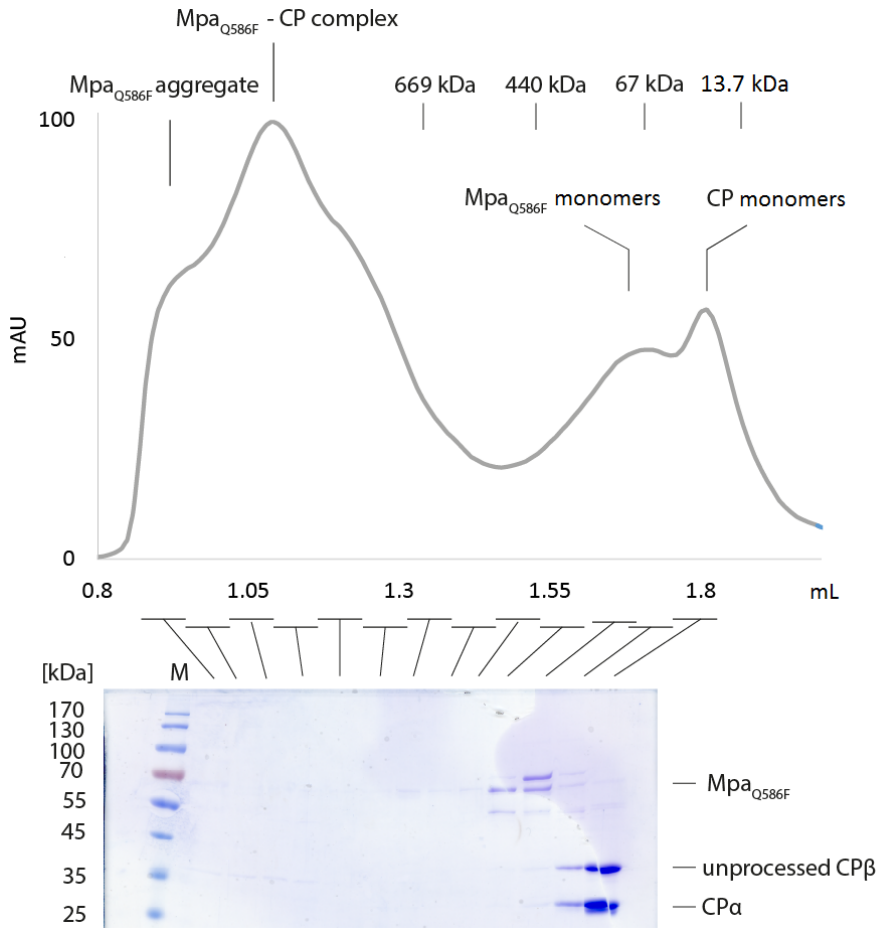

Fig. 3.6.1.3: SEC of the Mpa$_{Q586F}$-CP proteasome complex (c = 11.6 µM). Buffer: 50 mM $NaH_2PO_4 \cdot H_2O$, 75 mM NaCl, pH=7.

At 50 mM NaH_2PO_4 (pH = 7) (figure **3.6.1.3),** most of the complex seems to have dissociated into monomers, which is unexpected for a pH so close to the physiological value. In particular, the CP is concentrated in just two fractions at 1.8 mL, indicating that the prcA/B complexes fell apart almost entirely. Similarly, Mpa$_{Q586F}$ eluted as monomers as well, together with impurities of unknown composition both larger and smaller than Mpa (at approximately 70 kDa and 55 kDa, respectively). Surprisingly, despite the very low concentration of proteins in the fractions between 0.8 and 1.3 mL (the Mpa$_{Q586F}$-CP complex) as determined by SDS-PAGE, the peak corresponding to these fractions is of approximately the same height as those in figures **3.6.1.2.** and **3.6.1.4.** It is possible that the components of the CP disassembled into oligomers broadly comparable in size to that of the entire complex, which were individually too few to be visibly stained on the gel but together sufficient to cause the detected UV absorption. This phenomenon also occurred in subsequent tests, such as when using 50 mM Tris buffer (pH =7) (see below).

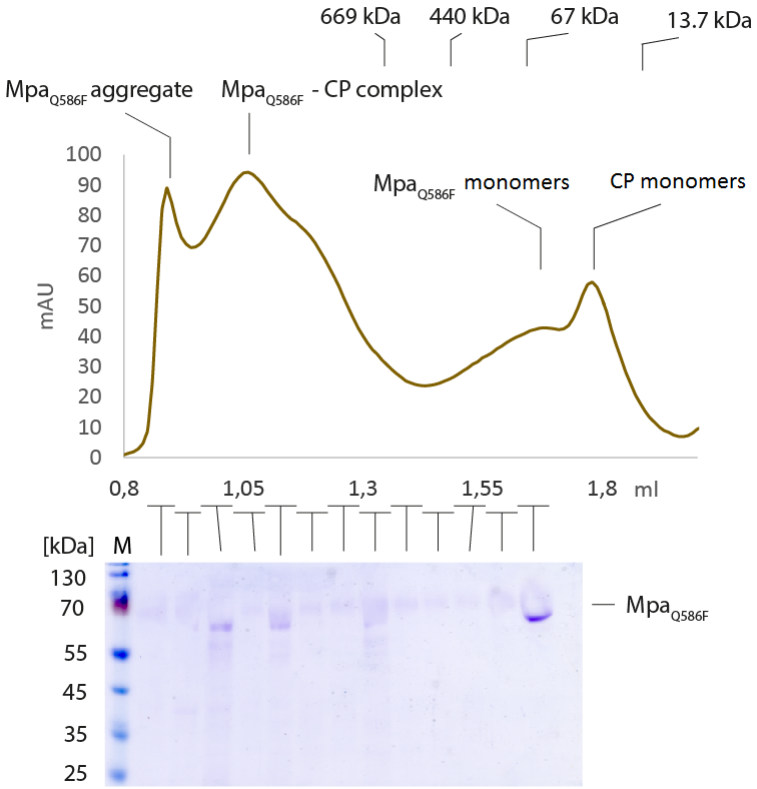

Fig. 3.6.1.4: SEC of the Mpa$_{Q586F}$-CP proteasome complex (c = 12.4 µM). Buffer: 50 mM Tris-HCl, 75 mM NaCl, pH = 8.

In 50 mM Tris-HCl (pH = 8), the proteasome complex dissociated completely, with CP almost undetectable in the complex peak at 1.1 mL and is most likely entirely contained in the monomeric peak around 1.5. As with pH = 7 (see figure **3.6.1.3**), it is notable that a pH so close to the physiological value would destabilize the proteasome. Here, not only were the complexes separated but the component subunits themselves were degraded and this buffer was therefore excluded from further tests.

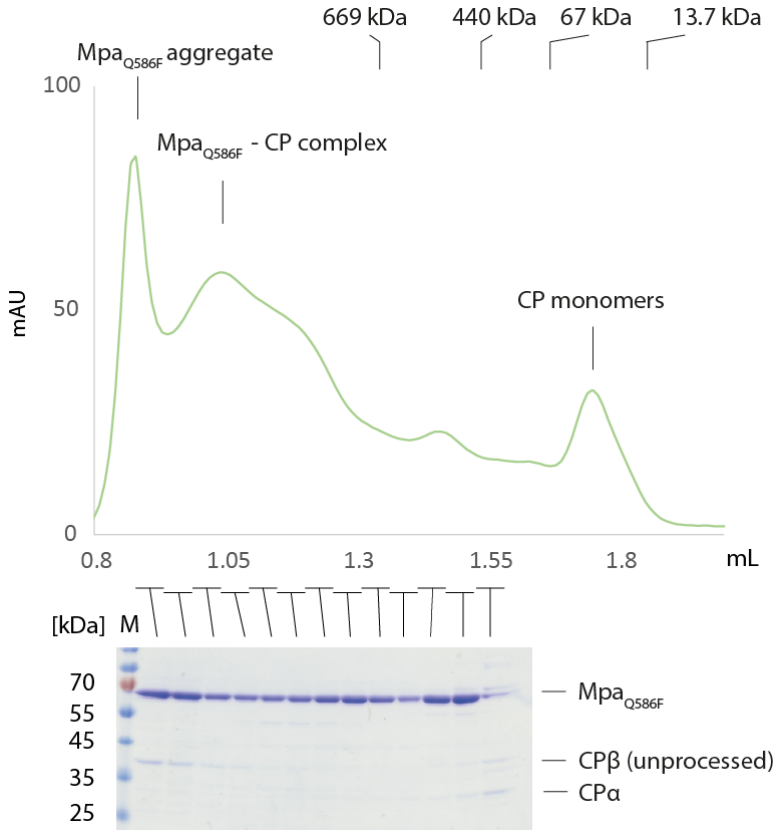

Fig. 3.6.1.5: SEC of the Mpa$_{Q586F}$-CP proteasome complex (c = 11.6 µM). Buffer: 50 mM CHES, 75 mM NaCl, pH = 9.

In 50 mM CHES (pH = 9) buffer, Mpa$_{Q586F}$ is present in a significantly higher concentration than the CP subunits in all fractions and elutes over the entire length of the column. Both prcA and prcB are barely visible in the fractions around 1.05 mL where the complex would be expected and there is a prominent CP subunit monomer peak at around 1.8 mL, indicating that the complex disassembled into Mpa oligomers and prcA/B monomers. Considering the size of the Mpa$_{Q586F}$ - CP complex peak, a certain percentage of the holoproteasome remained intact, but the amount is low, especially compared to the amount of Mpa$_{Q586F}$ aggregate. Therefore, the CHES (pH = 9) buffer was excluded from further testing as well.

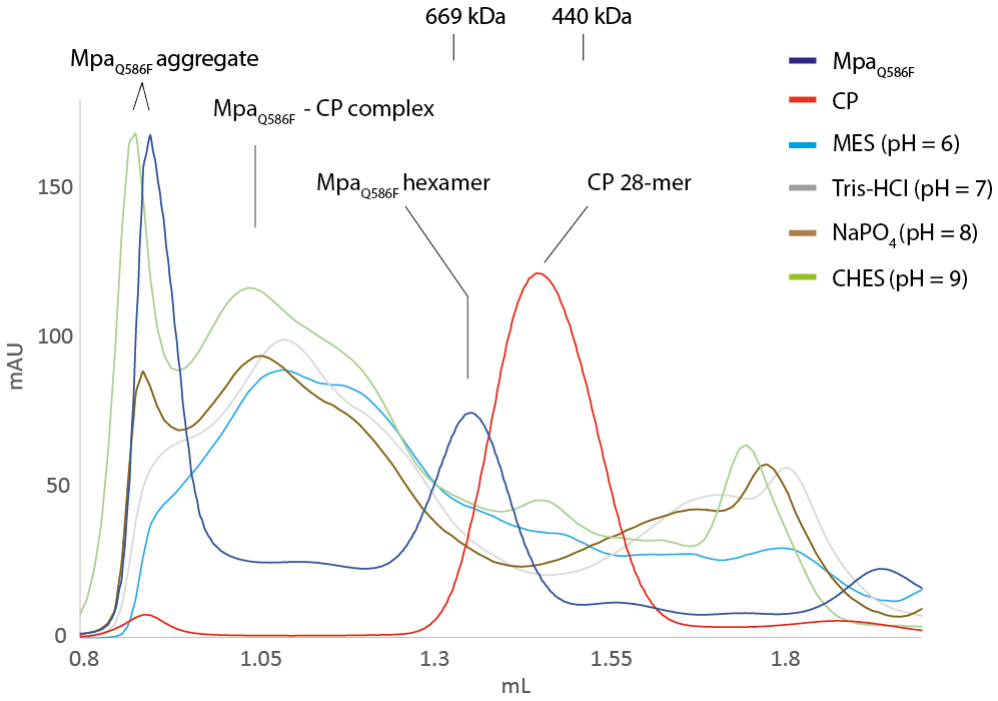

Fig. 3.6.1.2. Comparison of the Mpa$_{Q586F}$-CP proteasome complex stability under different buffer conditions.

In general, the pH of the buffer has a significant influence on the stability of the complex, as far as other factors can be ruled out. Specifically, pH 6 (see figure **3.6.1.2.**) and 9 (figure **3.6.1.5**) resulted in the highest amount of holoproteasomal complex compared to oligomeric or monomeric Mpa$_{Q586F}$ and CP, which were present under all conditions. Mpa$_{Q586F}$ aggregated in all buffers, but not to the same extent – at pH = 8 (figure **3.6.1.4**) the aggregate peak at 0.9 mL is much more prominent than at other pH values. The complex peak at approximately 1.1 mL lies between the Mpa hexamer and the CP 28-mer peak and is easily distinguishable from both. It is notable that the formation of Mpa$_{Q586F}$ aggregate seems to be directly correlated with an increase in pH, with the MES buffer (pH = 6) resulting in the least, Tris-HCl (pH = 7) in the third highest, NaPO$_4$ (pH = 8) in the second highest and CHES (pH = 9) in the highest amount of aggregate.

The pH tests indicated that Na-phosphate buffer (pH = 7), Tris buffer (pH = 8) and CHES buffer (pH = 9) were all detrimental to the stability of the complex and therefore, 50 mM MES (pH = 6) was chosen as the best condition to test the complex stability. As a next step, the influence of the salt concentration of the buffer was tested.

3.12. Influence of the salt concentration on the stability of the proteasome complex

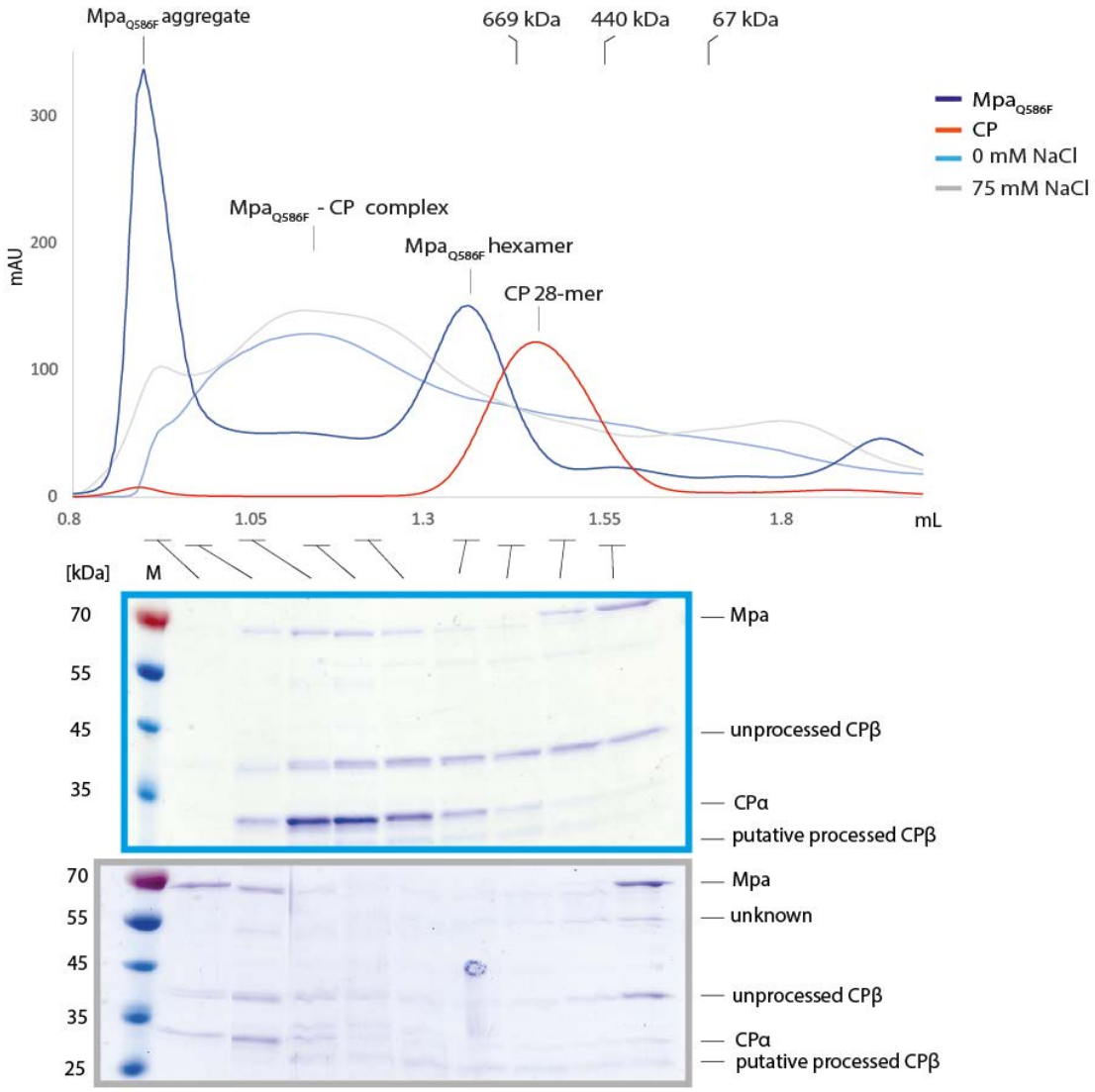

Fig. 3.6.2.1. SEC of the Mpa$_{Q586F}$-CP proteasome complex () in MES, pH = 6 with 0 mM (top, c = 11.1 µM) and 75 mM NaCl (bottom, c = 11.7 µM).

In the no-salt buffer (figure **3.6.2.1,** upper gel), the proteasome complex can be isolated to a high degree of purity and cohesion of the subcomplexes. However, the majority of both Mpa$_{Q586F}$ and prcA are concentrated in the first fractions - which contain the holoproteasome - but unprocessed prcB is present in every fraction in an equal amount. This indicates that the core particle at least partially dissociated into prcA and prcB oligomers of unequal size, while the majority of the Mpa$_{Q586F}$ remained stable and bound to the intact CP complexes.

In the 75 mM NaCl buffer, in comparison, the elution contains more impurities and appears to have significantly dissociated or been degraded in the fractions where the 0 mM NaCl buffer contains the highest concentrations of the complex. Although the first fraction consists of pure complex with an acceptable ratio of Mpa$_{Q586F}$ to CP, the subsequent fractions show high levels of impurities and degradation products but almost no Mpa$_{Q586F}$. It is only in the last fraction (1.65 mL) that the majority

of Mpa_{Q586F} is contained, where it elutes together with unprocessed CPβ and small amounts of CPα. Therefore, the 75 mM NaCl condition was excluded from further testing. The 75 mM NaCl buffer also shows a slightly higher tendency of free Mpa_{Q586F} to aggregate compared to the no-salt condition, although the amount of aggregate is low in both buffers.

In both the 0 mM and the 75 mM NaCl buffer, an unknown protein is visible below CP_{α} at approximately 25 kDa. It is possible that this band could consist of prcB that was autocatalytically processed during the purification (size of the processed form: 24.6 kDa). If so, this would constitute evidence that the co-expression of Mpa_{Q586F}, prcA and prcB does not irreversibly abolish the maturation of the β-subunit, although most of the prcB in the complex retained its propeptide. In the 0 mM NaCl condition, the putative processed prcB co-elutes with the holoproteasome complex between 1.05 and 1.3 mL, indicating that it was present not merely in the form of free subunits that were then post-processed during purification but was a part of the complex. This would signify that the tricistronic proteasome consists of a combination of unprocessed and processed CPβ subunits, with a clear majority of the former.

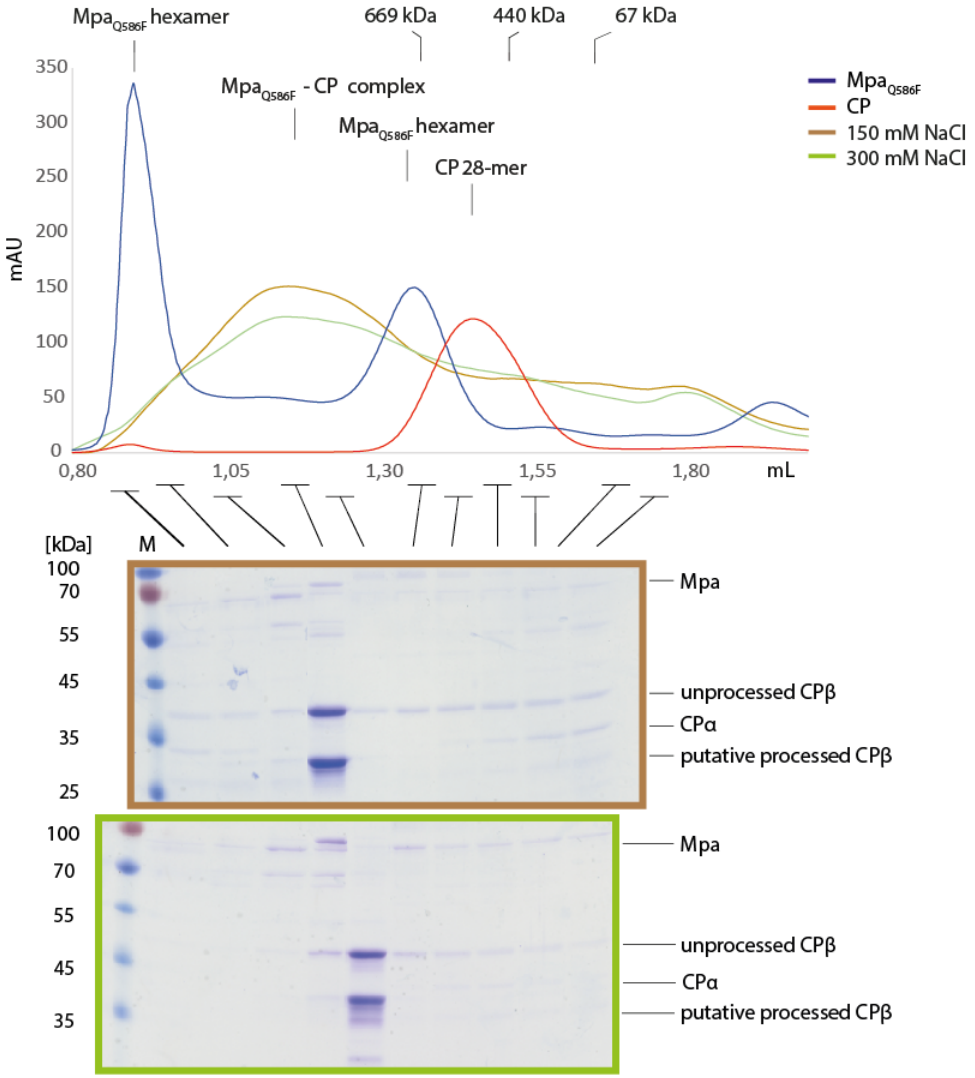

Fig. 3.6.2.2. SEC of the Mpa$_{Q586F}$-CP proteasome complex in MES, pH = 6 with 150 mM (top, c = 11.7 µM) and 300 mM NaCl (bottom, c = 10.4 µM).

The comparison between the 150 mM and 300 mM NaCl conditions (figure **3.6.2.2**) shows an unexpectedly high concentration of both CPβ and CPα (at 1.15 mL for 150 mM NaCl and 1.25 mL at 300 mM NaCl) with only a minuscule amount of Mpa present in the former and none at all in the latter fraction. Under these two conditions, almost no complex remained stable to be eluted, and they were therefore excluded as well. As in the 0 mM NaCl and 75 mM NaCl conditions (figure **3.6.2.1**), putative processed prcB was present.

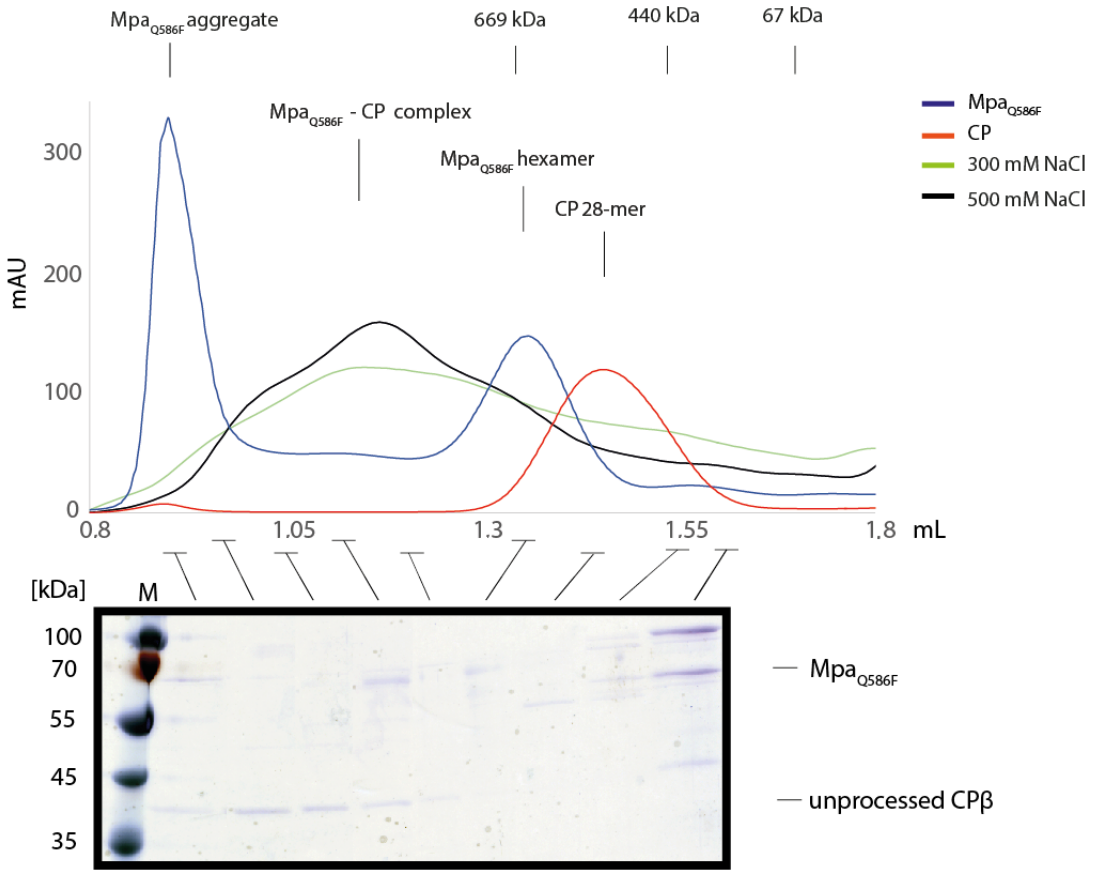

Fig. 3.6.2.3. SEC of the Mpa$_{Q586F}$-CP proteasome complex (c = 11 µM) in MES, pH = 6 with 500 mM NaCl. The curve of the 300 mM NaCl buffer was added for comparison.

In the 500 mM NaCl condition, the complex dissociated completely and almost the entire Mpa$_{Q586F}$ and both prcA and prcB were eluted as oligomers, therefore this buffer was excluded from further testing. The high salt concentration did however not result in the aggregation of the proteins as might be expected. Again, the height of the UV absorption peak did not correspond to the concentration of the proteins visible in the gel.

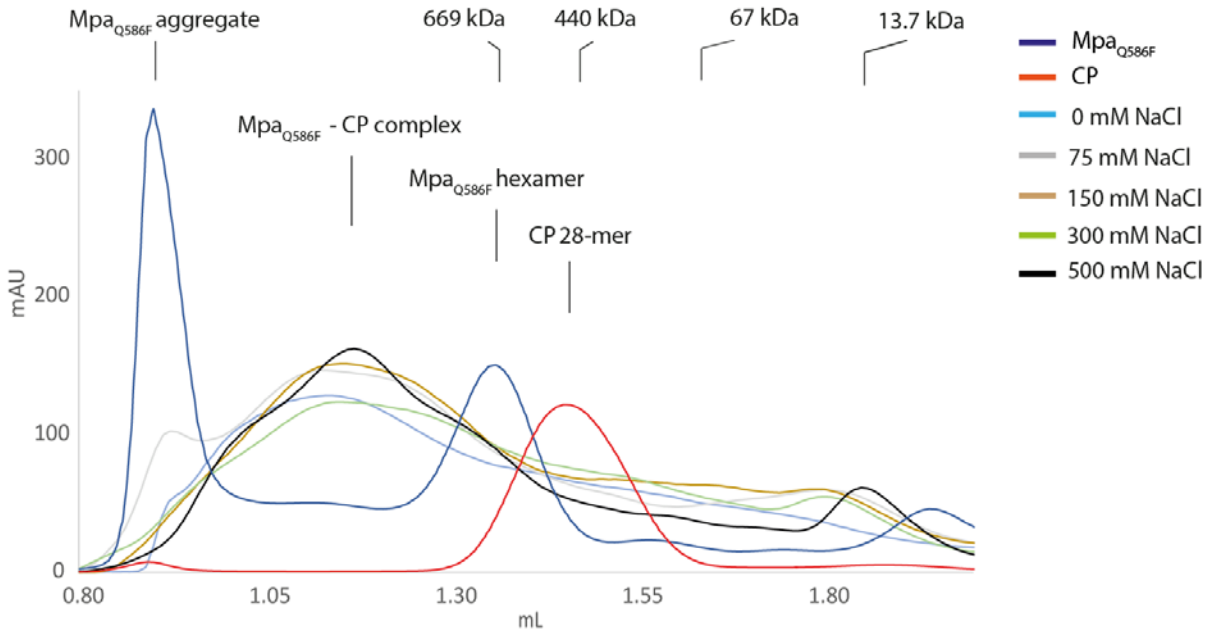

Fig. 3.6.2.4 Comparison of the Mpa$_{Q586F}$-CP proteasome complex stability in various salt concentrations. Buffer: 50 mM MES, pH = 6.

Judging by the comparison of the curves in figure **3.6.2.4** alone, there does not seem to be a significant influence of the salt concentration on the stability of the complex. The complex peaks are clearly distinguishable from both the Mpa peaks and the CP peak in all conditions, with very little aggregated Mpa$_{Q586F}$ present. However, subsequent analysis of the complex peak fractions by SDS-PAGE revealed clear differences between the buffer conditions in regards to the makeup of the complex.

Of the buffers tested, the 0 mM NaCl buffer (figure **3.6.2.1.**) gave the best result by far. All other conditions were inferior in one or both desired aspects (stability and purity of the complex), in particular the high salt buffer with 500 mM NaCl (figure **3.6.2.3**), in which the proteasome disassembled completely. A band that could represent processed prcB was visible in all conditions except 500 mM NaCl, indicating that the tricistronic complex could consist of both processed and unprocessed CPβ subunits. In the no-salt buffer, the complex fractions (1.05 – 1.25 mL) are of high purity and the fractions following the complex peak (1.35 -1.65 mL) contain only trace amounts of Mpa, indicating that the peak indeed consists of the complex and not merely unbound Mpa eluting over the entire length of the column together with CP. Thus, as the optimal buffer condition for future experiments on complex stability, 50 mM MES (pH = 6), 0 mM NaCl was determined.

3.13. Influence of nucleotides on the stability of the proteasome complex

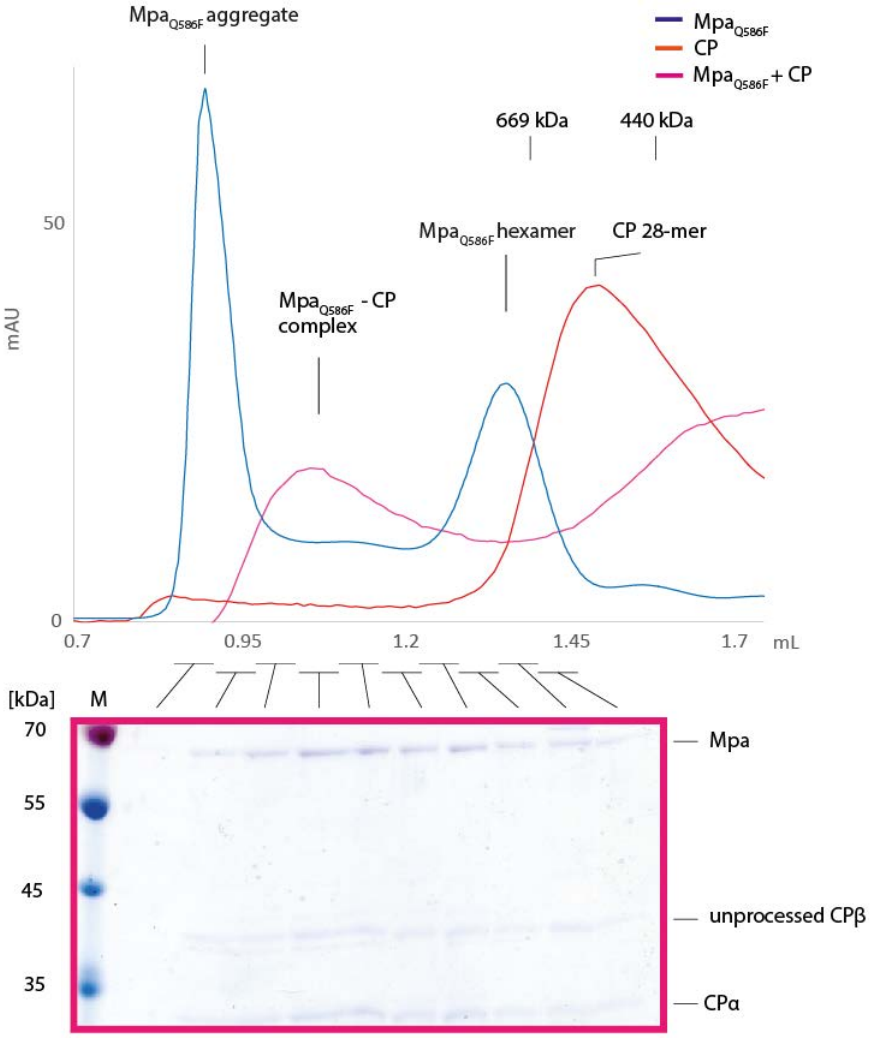

Fig. 3.6.3.1. SEC of the Mpa$_{Q586F}$-CP proteasome complex (c = 11.7 µM) without added nucleotide. CP$_{WT}$, and Mpa curves for comparison.

Although the proteasome could be isolated to a high degree of purity in the buffer containing no nucleotides (figure **3.6.3.1**), the concentration of the complex was low due to dissociation of the subunits, which were present in all fractions at the approximate same amount. Here, no putative processed CPβ subunits could be seen (compare figures **3.6.2.1** and **3.6.2.2**), although these, at usually only half of the concentration of the processed prcB, could have been indetectable due to the generally low amount of protein. Compared to the nucleotide-containing buffers (figures **3.6.3.2 - 3.6.3.4**), this condition was markedly inferior and was therefore not chosen for future experiments.

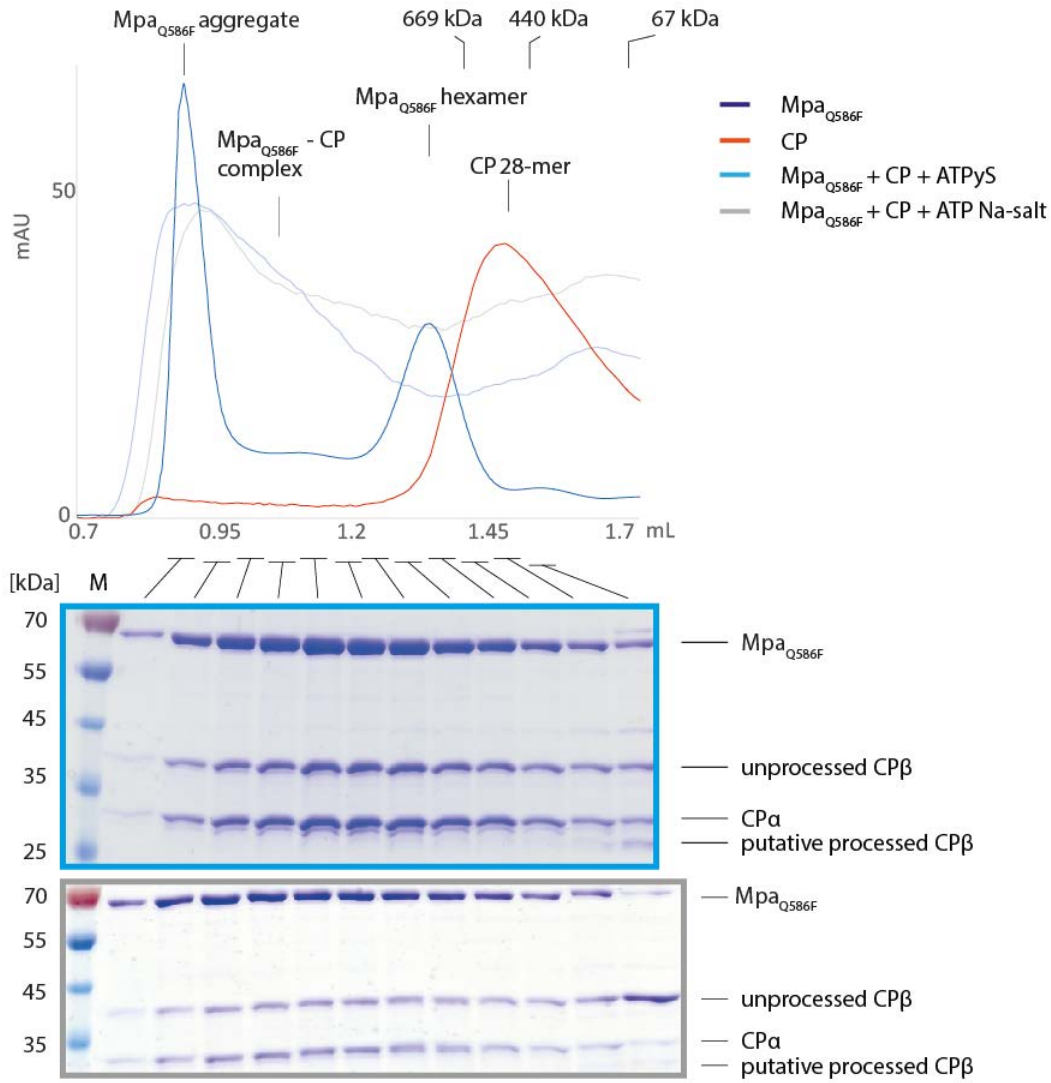

Fig. 3.6.3.2. SEC of the Mpa$_{Q586F}$-CP proteasome complex with 2 µM ATPγS and 2 mM ATP sodium salt in the sample and 2 mM of each nucleotide in the running buffer (50 mM MES, pH = 6, 0 M NaCl) respectively. $c_{Complex}$ = 11.7 µM. CP$_{WT}$ and Mpa curves for comparison.

In both buffers containing either ATPγS or ATP sodium salt (figure **3.6.3.2** top and bottom), the purification of the complex was significantly improved compared to that of buffer without nucleotides (figure **3.6.3.1**). In the 2 mM ATPγS buffer (figure **3.6.3.2,** top) most of the complex was concentrated in the fractions between 0.95 mL and 1.3 mL (although all three subunit proteins were present in the later fractions as well), indicating that its tendency to disassemble was decreased compared to the non-nucleotide buffer. In the buffer containing 2 mM ATP sodium salt (figure **3.6.3.2**, bottom), the stability was slightly lower but the differences between the nucleotides are negligible. Notably, the peak under both conditions was shifted towards the aggregate form of Mpa$_{Q586F}$ (see also figure **3.6.3.4** for a comparison of the curves). In the Mpa$_{Q586F}$ aggregate fraction (0.85 - 0.9 mL), prcA/B is present as well. These observations could be explained by the binding of the nucleotides causing a slight conformational shift in Mpa$_{Q586F}$ that reduces its ability to bind the CP and

increases the tendency of free Mpa_{Q586F} to aggregate. It is possible that this nucleotide-induced aggregation also occurs with the entire complex while Mpa_{Q586F} is still bound, which would be consistent with the presence of the CP subunits in the first fraction. In both buffers, a band that could represent processed CPβ is visible below CPα in the later fractions, although the presence of other bands between Mpa_{Q586F} and prcA/B suggests that this protein could also be an impurity. Comparison to the pure CP peak shows that if this band indeed consists of processed CPβ, it might have been part of core particles consisting of a mixture of processed and unprocessed prcB that separated from Mpa_{Q586F} (see also figure **3.6.2.1,** where the putative processed CPβ subunits eluted as part of the Mpa_{Q586F}-CP complex).

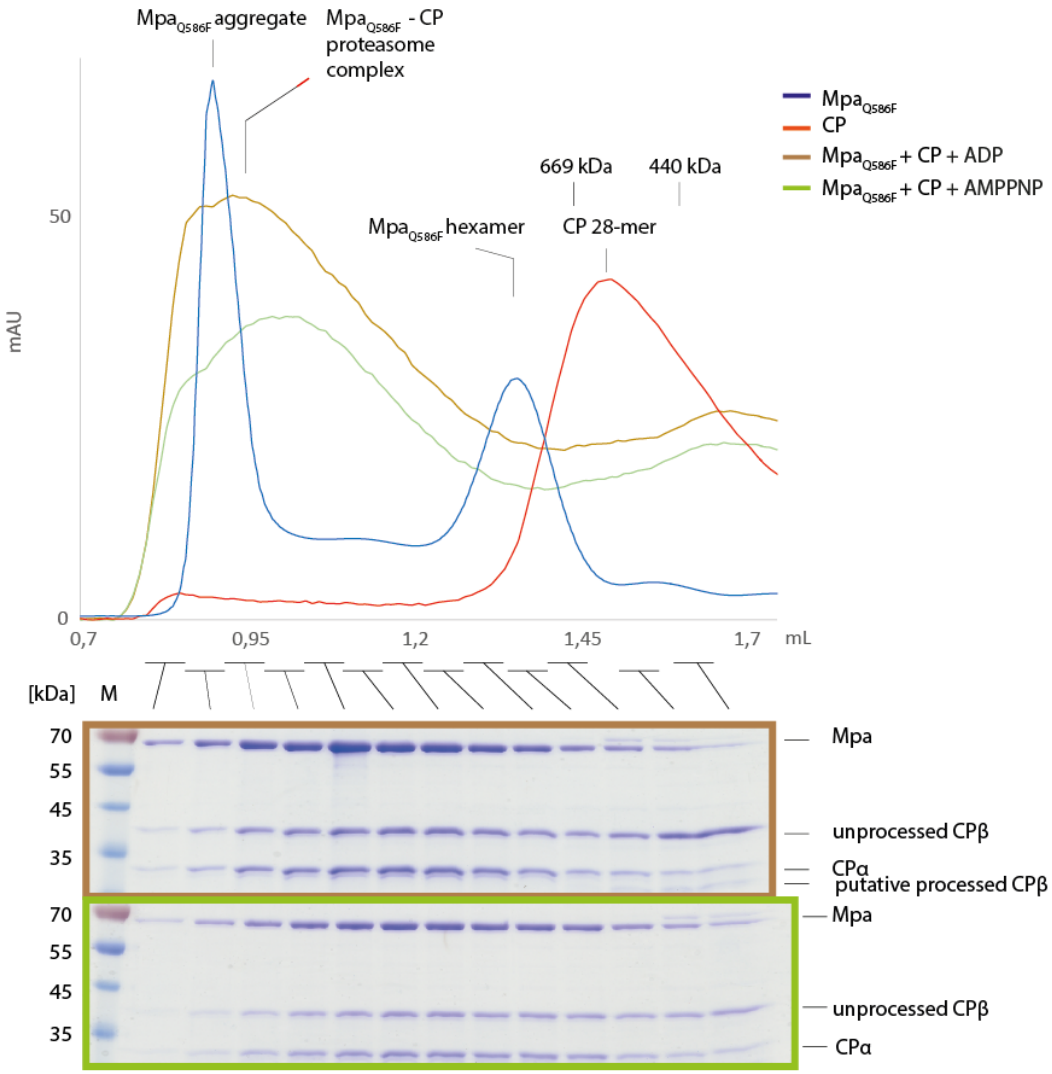

Fig. 3.6.3.3. Mpa_{Q586F}-CP proteasome complex gel filtration with 2 µM ADP (top) and 2 mM AMPPNP (bottom) in the sample and 2 µM of each nucleotide in the running buffer (50 mM MES, pH = 6, 0 M NaCl) respectively. $c_{Complex}$ = 11.7 µM. CP_{WT} and Mpa curves for comparison.

Like the buffers containing ATPγS or ATP sodium salt, those containing ADP and AMPPNP (figure **3.6.3.3**) showed significantly improved purification and stability of the holoproteasome compared to the non-nucleotide buffer, with most of the complex eluting intact. Even here, a small percentage of the proteasome dissociated into its subcomplexes. Some processed prcB might be present, but although contrary to the ATPγS/ADP condition (figure **3.6.3.2**) no impurities are visible near the prcA/B bands, it would be difficult to distinguish from other, contaminating proteins.

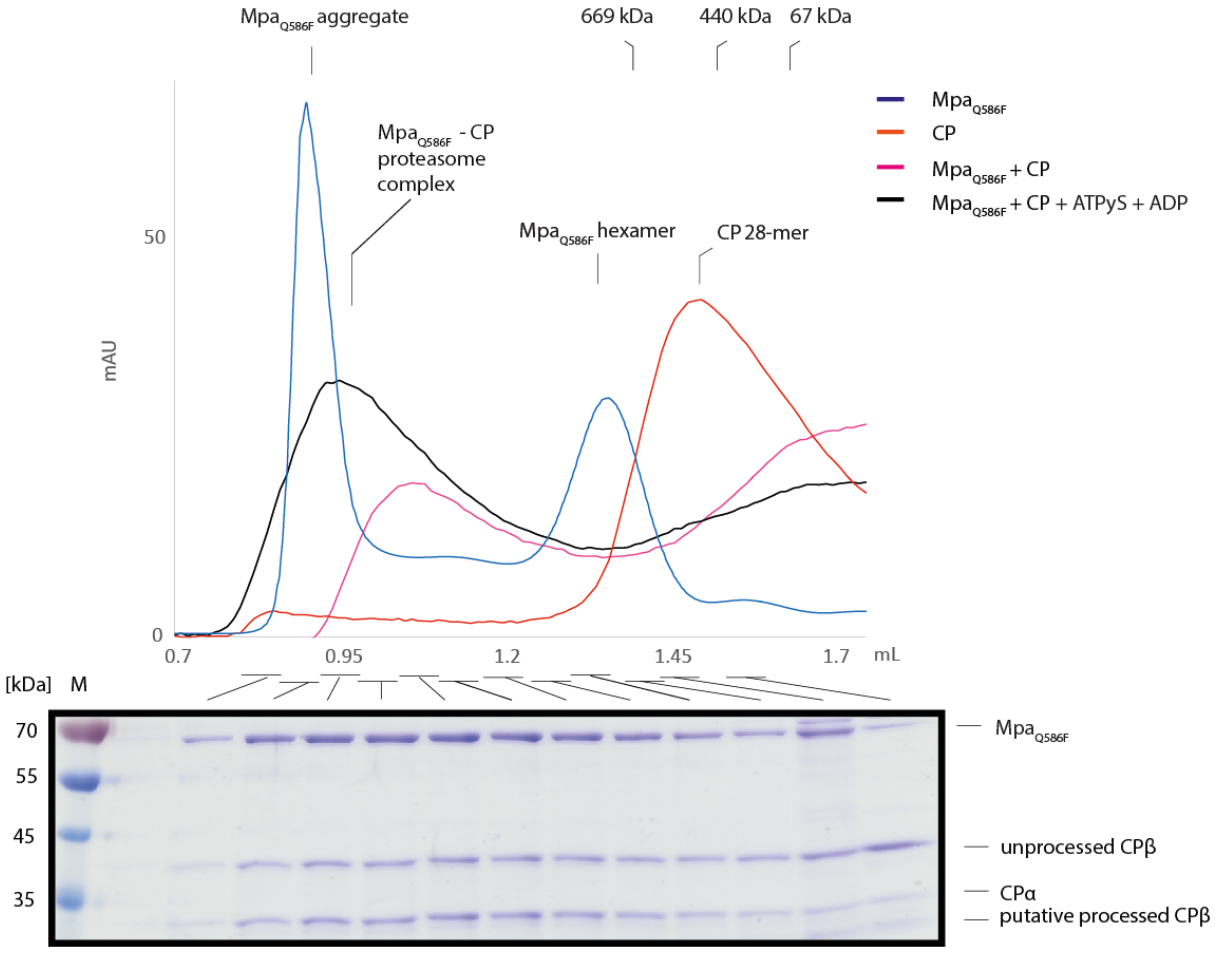

Fig. 3.6.3.4. Mpa$_{Q586F}$-CP proteasome complex gel filtration with 1 mM ATPγS and 1 mM ADP in the sample and 1 µM of both nucleotides in the running buffer (50 mM MES, pH = 6, 0 M NaCl). $c_{Complex}$ = 11.7 µM. CP_{WT} and Mpa curves for comparison.

Combining ATPγS and ADP (figure **3.6.3.4.**) resulted in a markedly cleaner and more stable purification compared to the buffer containing no nucleotides (figure **3.6.3.1.**) but did otherwise not show improvements compared to the previous buffers (figures **3.6.3.2** and **3.6.3.3**). Like in the previous buffers , putative processed prcB is visible in the fractions corresponding to the CP 28-mer .

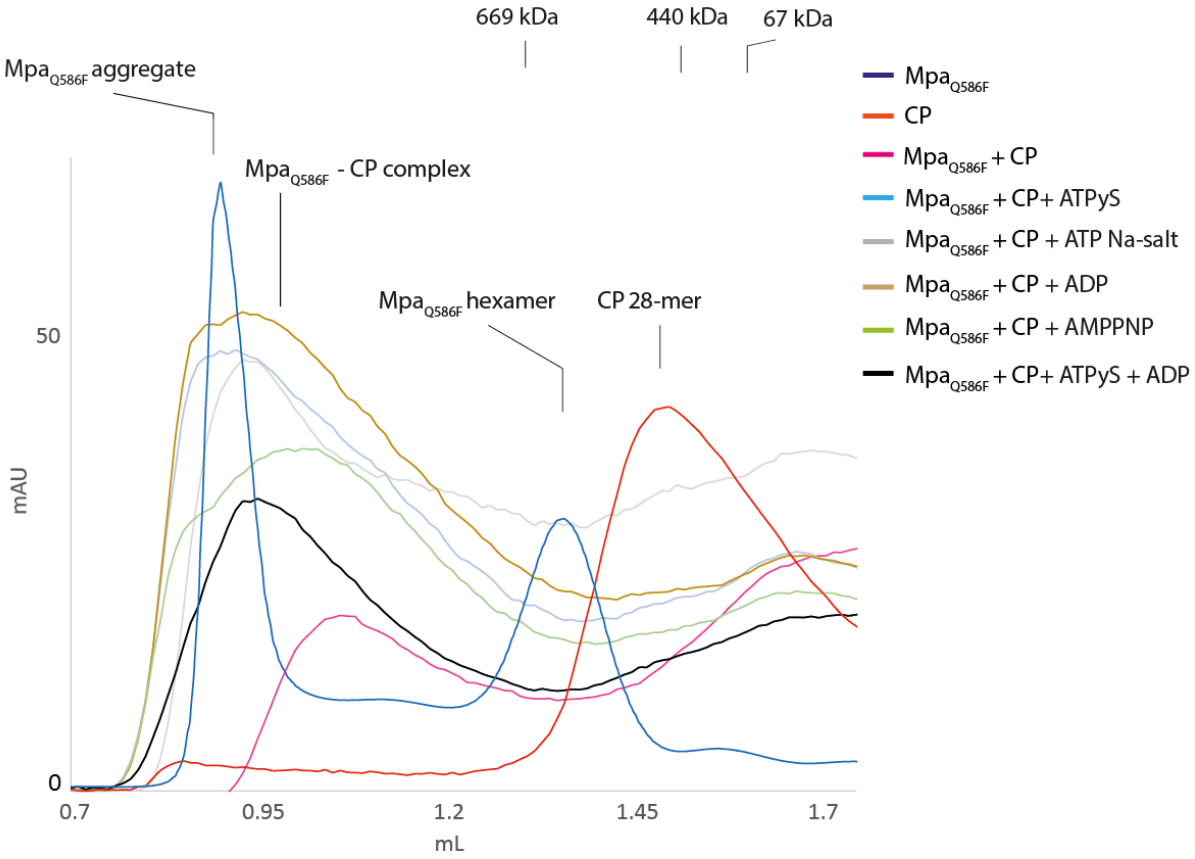

Fig. 3.6.3.5 Comparison of the Mpa$_{Q586F}$-CP proteasome complex stability in 50 mM MES (pH = 6) containing 2 µM ATPγS, ATP sodium salt, ADP, or AMPPNP.

The comparison only of the chromatograms of the complex SECs with added nucleotides, akin to the salt concentration tests, show very little difference between the different buffers. However, the presence of nucleotides has a clear effect on the stability of the complex: the tendency of Mpa$_{Q586F}$ – CP to separate and of the subcomplexes themselves to disassemble into monomers is markedly decreased, allowing the isolation of the entire complex to a high degree of purity.

Notably, the complex peaks are shifted towards the Mpa aggregate peak at 0.9 mL compared to that of the complex without them (between 1 and 1.1 mL). It is possible that the binding of the nucleotides to the bound Mpa$_{Q586F}$ causes a conformational change that decreases its ability to bind to CP, causes it to separate from it and to aggregate as a free subcomplex. Alternatively, the conformational change induced by the binding of the nucleotides to Mpa$_{Q586F}$ could induce aggregation while still part of the Mpa$_{Q586F}$ – CP complex. The presence of a band corresponding to the size of processed prcB (see figures **3.6.3.2** - **3.6.3.4**) could be indicative of autocatalytic cleavage occurring after the translation even though normally, the co-expression of the proteasomal genes prevents this.

With all the nucleotide-containing buffers showing superior results to the non-nucleotide buffers and only marginal differences visible between them, 50 mM MES (pH = 6) + 2 µM ATPγS was chosen as the optimal condition due to its slightly higher purity and stability compared to the other conditions.

3.14. Binding of Pup-GFP and Pup-PanB to the proteasome complex

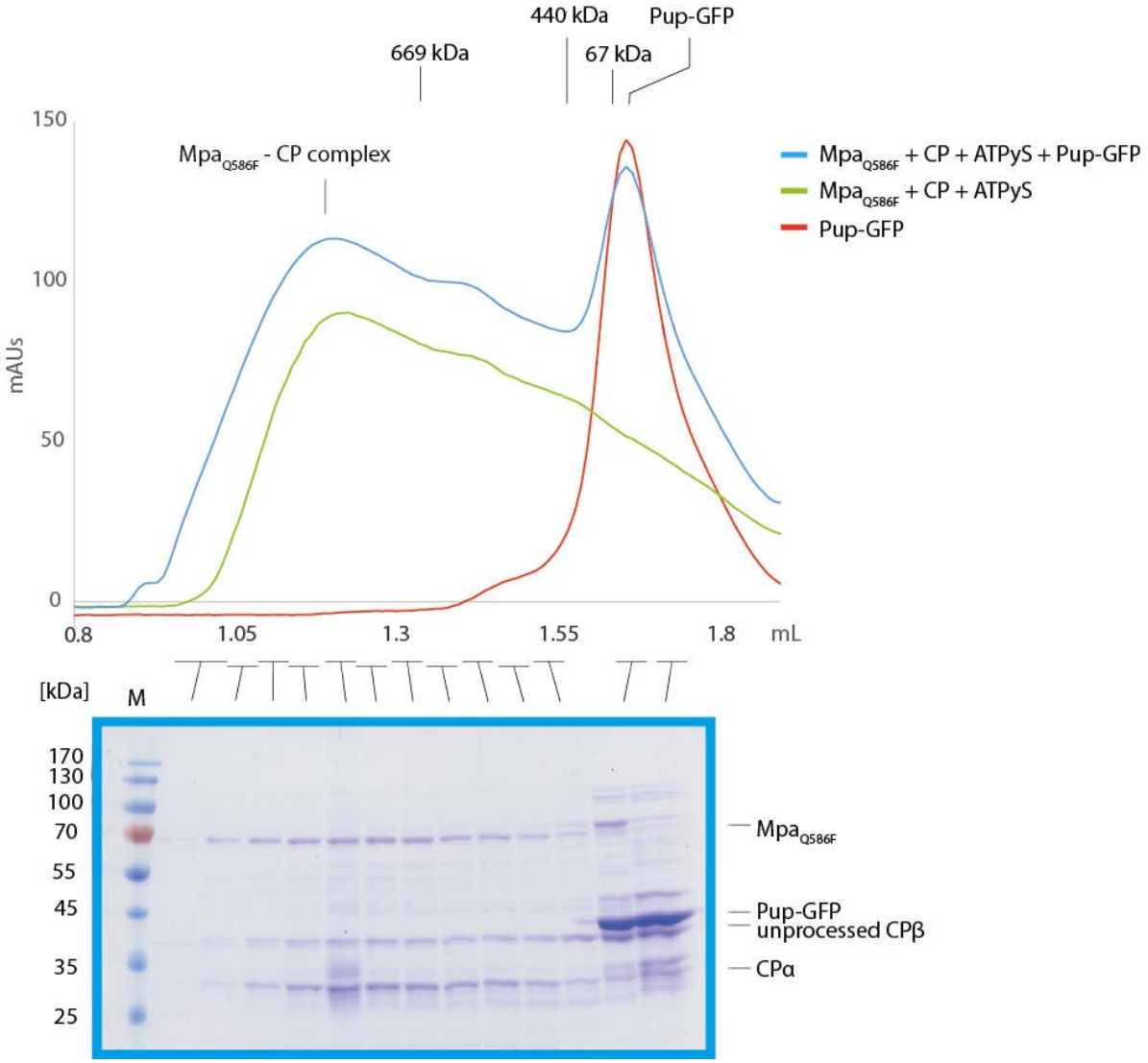

Fig. 3.6.4.1. Mpa$_{Q586F}$-CP proteasome complex in 50 mM MES (pH = 6), 0mM NaCl buffer + 5 µM/mM ATPγS + Pup-GFP $c_{MpaQ586F-CP}$ = 11 µM. $c_{Pup-GFP}$ = 29.6 µM.

Combining the proteasome complex with Pup-GFP does not result in binding. None of the Pup-GFP was bound to the Mpa$_{Q586F}$ – CP complex, although it co-eluted with some of its monomers. Considering that the interaction between Pup and Mpa is well established, and the Q586F mutation in the C-terminal tail should have no effect on the N-terminal coiled-coil domains with which Mpa binds to Pup, this result is unexpected. However, subsequent unfolding experiments with the crosslinked complex and Pup-Luciferase as a substrate showed a similar result, namely that neither free nor crosslinked MpaQ586$_{pBpa}$ was able to unfold Pup-Luciferase while wild type Mpa did show unfoldase activity (see figures **3.7.2** and **3.7.3** for curves and additional discussion).

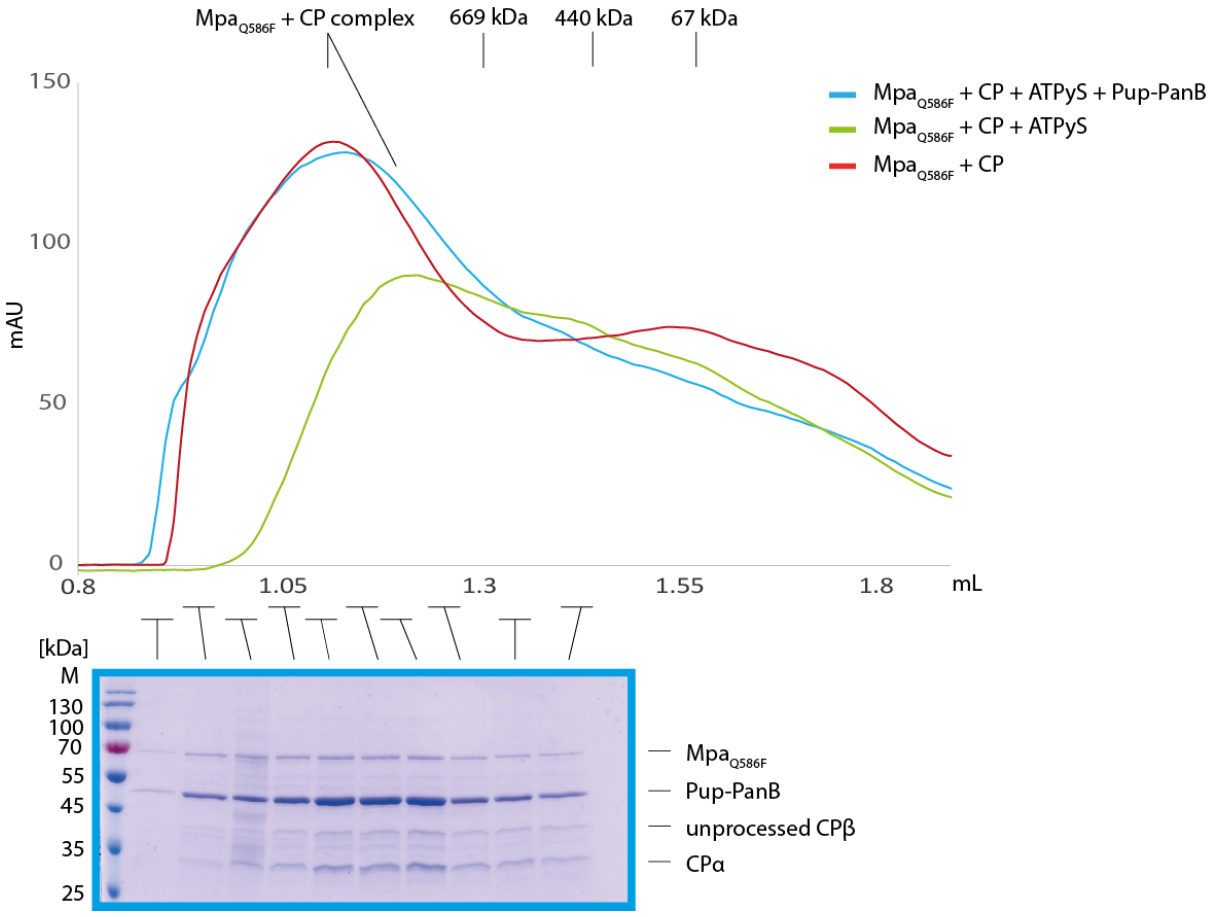

Fig. 3.6.4.2 Mpa$_{Q586F}$-CP proteasome complex in MES pH = 6, 0mM NaCl buffer + 5 µM/mM ATPγS + 5 µM/mM ATPγS + Pup-PanB. $c_{MpaQ586F-CP}$ = 11 µM. $c_{Pup-PanB}$ = 27.6 µM.

Although the Pup-PanB fusion protein eluted concurrently with the proteasome, its characteristic of forming oligomers of comparable size to the Mpa$_{Q586F}$-CP complex (700 - 800 kDa for the Pup-PanB oligomer compared to 1150 kDa for a Mpa$_{Q586F}$ hexamer bound to the CP) makes a distinction between binding and mere co-elution difficult. The concentration per fraction of Pup-PanB visible in the gel corresponds broadly with that of the proteasome subunits, but while this would be expected if the substrate had interacted with Mpa$_{Q586F}$ it does not constitute evidence for interaction. Thus, the binding of the recombinant proteasome by Pup-PanB, especially when compared to the lack of interaction with Pup-GFP (see figure **3.6.4.1**), cannot be confirmed under these conditions.

In this experiment, Pup-PanB could not have been degraded due to the use of the non-hydrolyzable ATP analogue ATPγS. Even if ATP had been used and the interaction had taken place, the timespan between the interaction and the SEC (less than 30 minutes) would very likely have been too short to detect substrate degradation. The question whether the recombinant proteasome is capable of unfolding and degrading its substrates was adressed in three subsequent experiments (see sections **3.8** – **3.10**).

3.15. Assembly of the proteasome complex and stability after repeated SEC

In previous experiments in our lab, the proteasome complex had been shown to disassociate after repeated SEC, most likely due to the decreasing concentration. After determining the optimal buffer parameters (50 mM MES (pH = 6), 2 µM ATPγS) to stabilize the complex during SEC (see sections **2.12-2.15**), it was attempted to perform multiple SEC runs under these conditions to test whether they would allow the complex to remain stable. The tricistronic *mpa$_{Q586F}$-prcB-His$_6$-prcA* complex was expressed and purified by NiNTA as described in sections **2.5** and **2.7.** The five purest elution fractions were pooled, concentrated to 2 mL (c = 19.4 µM) in a Vivaspin concentrator (MWCO = 10.000 Da) and SEC-purified on a GE Healthcare Superose 6 XK16/70 column at 4°C with a flow rate of 0.5 mL/min (see figure **3.6.4.5**). In all purifications, the 50 mM MES (pH = 6) + 2 µM ATPγS buffer was used.

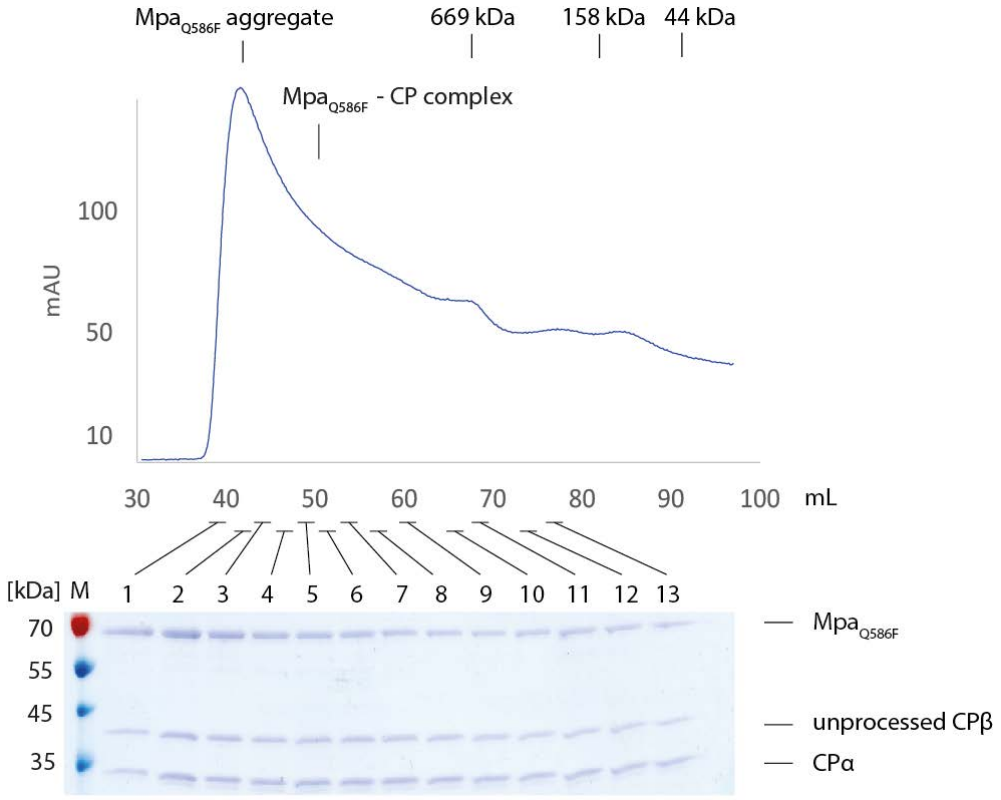

Fig. 3.6.5.1. SEC purification of the proteasomal complex on a GE Healthcare Superose 6 XK16/70 column. Fractions 5-9 (batch 1) and the rest of the fractions (batch 2) were pooled and used for the next SEC (see **Fig. 3.6.4.6**)

Although a sizable percentage of the Mpa$_{Q586F}$ had aggregated (presumably together with parts of the holoproteasome), the gel showed that the complex in general had eluted as previously demonstrated in section **3.6.3**. Fractions 5-9 of the SEC were pooled as batch 1 (c = 6.8 µM), loaded into a GE Healthcare Superose 6 3.2/300 column and purified again as described in section **3.6.3.** (figure

3.6.4.5). The remaining fractions (1-4, 6-13) were pooled as batch 2 (c = 3.9 µM) and reloaded as well (figure **3.6.4.6**.)

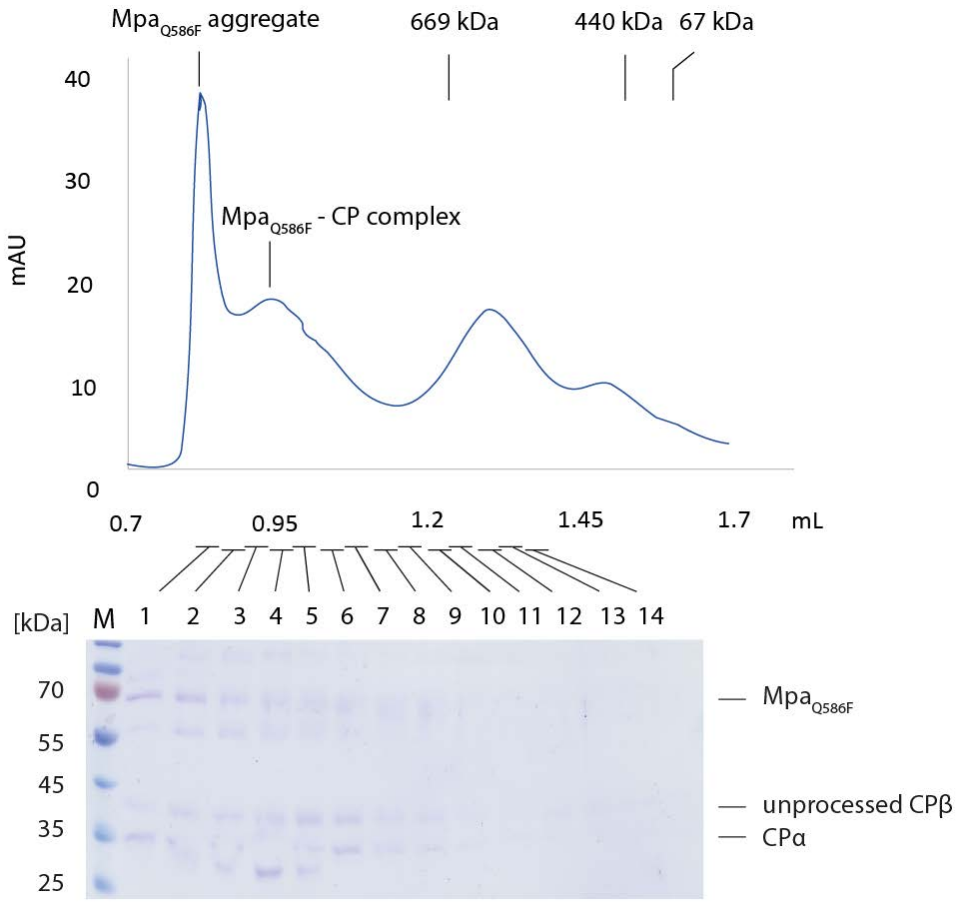

Fig. 3.6.5.2. Second SEC purification of the fractions 5-9 (batch 1) of the previous SEC purification (see Fig. **3.6.5.1**) on a GE Healthcare Superose 6 3.2/300 column. Fractions 3 - 5 were used for EM (see section **3.7**).

Although the components of the complex can still be seen clearly, there are degradation products visible below Mpa and possibly below CPα (fractions 4 and 5). The peak at 0.95 mL corresponds to the proteasome peak in previous runs (compare to that of the buffer test in Fig. **3.6.1.2**). For further analysis, fractions 3 -5 were used for negative stain electron microscopy (see section **3.7**).No third purification was attempted since the complex had already started to dissociate.

In the SEC of batch 2 (not shown), the entirety of the complex aggregated. No proteasome peak was observed and none of the fractions could be used for EM analysis. This hints at a difference in the behaviour of the complex regarding stability between the peak elution fractions of batch 1 and the rest of the fractions. Considering that batch 2 included the Mpa$_{Q586F}$ aggregate fractions, it is likely that these induced the rest of the Mpa$_{Q586F}$ bound to the CP and terefore the entire complex to aggregate as well. It must be concluded that the aggregation of Mpa$_{Q586F}$ during SEC is not reversible

by further purification and that buffer conditions otherwise favorable to the stability of the complex cannot prevent its disassembly due to the decrease in concentration during repeated SEC.

3.16. Crystallization studies of wild type and selenomethionine-Mpa

An initial hit was found after 7 days in the JBS Classic 2 B1 condition (100 mM Tris-HCl (pH = 8.5), 16% PEG 4000, 200 mM $LiSO_4$) at 4°C. To fine-screen the condition, a 96-well plate was prepared with the following parameters and stored at 4°C:

0.1 M Tris-HCl (pH = 8.2 – 8.8)
10-24% PEG
0.1/0.2/0.3 M $LiSO_4$

No further crystal growth could be observed under any of these conditions.

Four cryoprotectant solutions were prepared and tested:

- 0.1 M Tris-HCl (pH = 8.5), 20% PEG 4000, 0.2 M $LiSO_4$
- 0.1 M Tris-HCl (pH = 8.5), 25% PEG 4000, 0.2 M $LiSO_4$
- 0.1 M Tris-HCl (pH = 8.5), 30% PEG 4000, 0.2 M $LiSO_4$
- 0.1 M Tris-HCl (pH = 8.5), 15% PEG 4000, 0.2 M $LiSO_4$, 15% MPD

Solution 4 was chosen for the diffraction tests. The crystal (not shown) was tested in-house, but did not diffract.

A second hit was found in the JBS Classic 2 D5 condition (100 mM Tris-HCl (pH = 8.5), 30% PEG 4000, 200 mM $MgCl_2$ (not shown). The crystal did not show polarization but diffracted to only 20 Å during in-house testing and was therefore discarded. A third hit was found in the Morpheus HT-96 Green Screen at condition F10 (0.1 M bicine/Tris (pH = 8.5), 30% ethylene glycol / PEG 8000 mix, 0.12 M monosaccharide mix[5] at 4°C (**Fig. 3.11.1.**). The diffraction of the crystals were tested in-house. Only one of them diffracted, at a resolution of 10-15 Å. The crystal was then tested at ESRF Grenoble in beamline ID23-1 and diffracted there to 9 Å.

[5] (0.2M D-glucose, 0.2 M D-mannose, 0.2 M D-galactose, 0.2 M L-fucose, 0.2 M D-xylose, 0.2 M N-acetyl-D-glucosamine),

To fine-screen the Morpheus condition, three new plates were prepared. Since the amount of available purified Mpa was too low, previously purified selenomethionine-labeled Mpa (SeMet-Mpa) + 10 mM $MgCl_2$ + 10 mM AMPPNP was used for the plates at a concentration of 21.5 mg/mL :

1. bicine/Trizma base, pH = 8.3/8.7 (48 wells each)
   PEG 8000: 6/8/10/12/14/16% (2 x 48 wells)
   Ethylene glycol: 17-24%
   20 mM monosaccharide mix[2]

2. bicine/Trizma base, pH = 8.5
   PEG 8000: 8/10/12/14% (3 x 32 wells)
   Ethylene glycol: 17-24%
   10/20/50 mM monosaccharide mix[2] (3 x 32 wells)

3. Morpheus Green Screen condition F10 (see above) for all wells
   Hampton 96 Additive Screen

No crystals formed in the two gradient screens but two were found in the Morpheus F10 + additive screen (**Fig. 3.11.2**), one in a condition containing 40% acetone, the other containing 0.1 M spermidine. The reservoir solution was found to act as a cryoprotectant on its own. The crystal in the acetone-containing condition diffracted to 8 Å, was subsequently tested at ESRF Grenoble in beamline ID23-1 and diffracted there to 6-7 Å. Of the spermidine-containing fine screen condition, three crystals diffracted in-house to 10, 14 and 18 Å, respectively. At ESRF Grenoble, the second one diffracted to 7.7 - 8 Å, the other ones did not diffract at all.

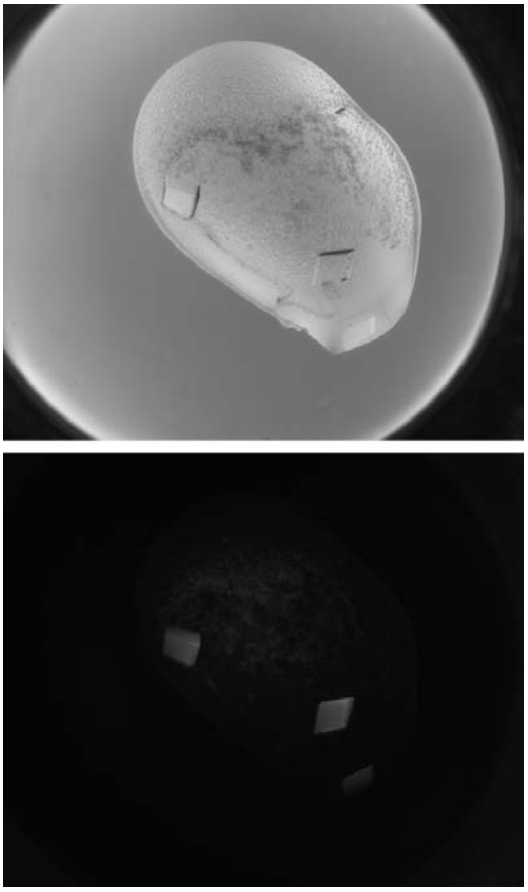

Fig. 3.13.1. Mpa (18.14 mg/mL) crystals in Morpheus HT-96 Green Screen F10.2 grown at 4°C. Top: visible light, bottom: UV.

Conditions:	0.1 M bicine/Tris (pH = 8.5)
	10 mM $MgCl_2$
	10 mM AMPPNP
	0.12 M monosaccharide mix
	30% ethylene glycol / PEG 8000 mix

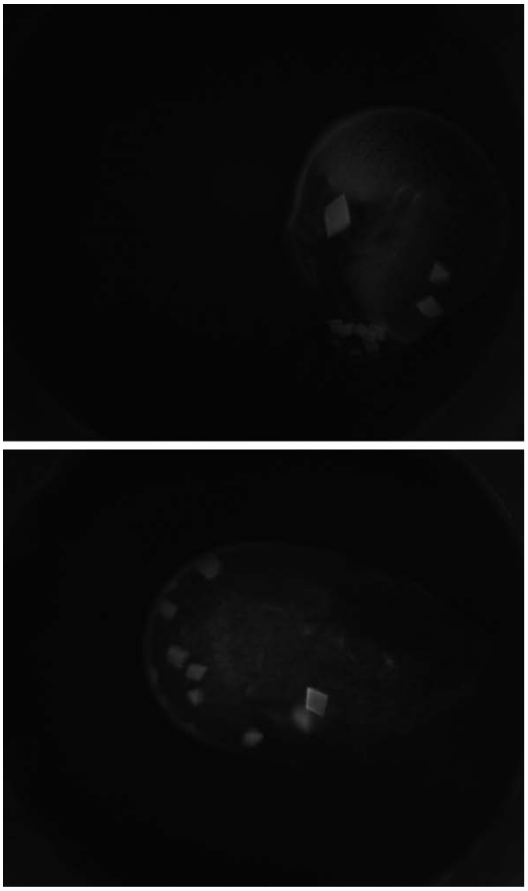

Fig. 3.13.2. Selenomethionine-Mpa (21.5 mg/mL) crystals grown in Morpheus F10.2-based fine screen + Hampton 96x additive screen under UV light.

Conditions: 0.1 M bicine/Tris (pH = 8.5)
10 mM $MgCl_2$
10 mM AMPPNP
10% PEG8000
20% ethylene glycol
0.02 M monosaccharide mix
40 % acetone (top) / 0.1 M spermidine (bottom)

4. SUMMARY AND CONCLUSIONS

In this study, the binding of the Mpa hexamer and the core particle of the mycobacterial proteasome was investigated in regards to the affinity of the subcomplexes to each other *in vitro,* the influence of the C-terminal QYL motif of Mpa on the interaction and the effect of mutations therein, the presence of additional factors that might be required for the binding, the feasibility of creating artificial holoproteasomes both through the introduction of a photoreactive, photocrosslinkable amino acid into Mpa and the introduction of the HbYX motif, the stability of the proteasome during purification and the effects of forming the proteasomal complex on the ability of Mpa to unfold substrates.

It has been previously established with a high degree of confidence that Mpa and CP interact only at an extremely low level *in vitro* and that the formation of the complex therefore must be dependent on a more complicated mechanism than simple binding of the C-terminal tails of Mpa to the pockets on CP's α-ring surfaces. The results of this study have confirmed that the process must be decidedly less trivial than what could be assumed from the existing knowledge of proteasome complexes.

The crosslinking experiments showed that both the permanent linking of the C-terminal Mpa peptide and that of the full-length protein to the CP can be relatively easily accomplished, although the process is inefficient and the yield of crosslinked complex is very low. The fluorogenic substrate degradation assays showed that the linking of $Mpa_{Q586pBpa}$ to CP does not increase the peptidase activity of the latter, indicating that the gate opening mechanism of CP either cannot be triggered by simply crosslinking Mpa, that the default semi-open state of the CP is sufficient to allow the entry of small substrates or that the amount of crosslinked complex was too low to have a measurable effect. Similarly, the degradation of the tagging protein Pup - either alone or fused to the Mpa substrate PanB – by the crosslinked $Mpa_{Q586pBpa}$-CP complex has not been observed, most likely due to the low amount of crosslinked complex present. The lack of unfolding activity by the crosslinked complex as well as $Mpa_{Q586pBpa}$ as seen in the luciferase test is notable, given that the wild type Mpa did retain its activity under the same conditions and a mutation in the extreme C-terminal end of Mpa would have to influence the binding or unfoldase activity in the central AAA-ATPase domain.

The failure to detect the photocrosslinked Mpa-CP complex in electron micrographs was not entirely surprising, given that the percentage of successfully crosslinks is low and the probability to detect them among the free proteins is even lower. Future studies using this approach will likely have to improve the yield of the crosslink, or use an alternative protocol in order to produce more material before the complex can be confirmed by EM. Although the size exclusion chromatography tests in this study using the Mpa_{Q586F} mutant have shown that the separation between the complex, Mpa in its aggregated and free forms and the free CP is possible in principle, the resolution is low and must be improved as well. The establishment of a SEC buffer condition where the complex can be relatively stably purified (50 mM MES, 0 mM NaCl, pH = 6) should prove to be useful for future experiments.

In the pull-down assays using Mpa or the core particle as bait, mass spectrometry did not detect either prcA or Mpa/ARC in the elution, providing evidence that the interaction with Mpa and CP *in vivo*, under the conditions used here, does not occur. Active assembly of the proteasome might be triggered only by cellular stress signals or the presence of damaged proteins, with the baseline

interaction between its components remaining on a low level when not needed. Alternatively, an unidentified additional factor could be required for the binding. The nature of this hypothetical assisting factor could be based on a clamping function that engages both Mpa and CP, alternatively, posttranslational modifications such as glutamine acetylation, O-linked glycosylation, S-glutathiolation, N-myristoylation methylation or phoshphorylation (comparable to the phosphorylation of the prcA residues T84, T202 and T178 by PknB, which enhances the degradation of the substrate Ino1, or the phosphorylation of unprocessed prcB and prcA by PknA, which decreases the tendency of the core particle to assemble) might play a role as well.

It is notable that in the structurally similar eukaryotic Rpt1-6 ATPase hexamer ring, only three of the six C-terminal tails (Rpt2, Rpt3 and Rpt5) end in the HbYX motif and only two of those are essential for the binding of the ring to the core particle. The tails of Rpt1, Rpt4 and Rpt6 do not contain the HbYX motif and are non-essential for RP-CP interaction, although Rpt6 increases the stability of the complex. With the Mpa hexamer, the QYL motif could be modified by the unknown factor or factors in a similar way, enabling some of its C-terminal tails to bind to the CP while leaving others unaltered and not involved in binding. The tails of Mpa were not among the peptides identified in mass spectrometry, but even if they were, the modification itself might be triggered only by cellular stress signals.

It is also possible that proteins with known functions in the proteasomal pathway play an additional role in the creation of the proteasome complex. The Pup ligase PafA, for example, might serve as a trigger in a “dynamic assembly” of the Mpa-CP complex, where a transient form of the proteasome is only completed when there is an actual substrate to be degraded. The possibility that the lack of assembly factors alters the conformation of the N-terminal domain of recombinant Mpa/prcAB has also been suggested, considering that N-terminal deletion mutants of both proteins have been shown to interact *in vitro.*

The recent discovery of the novel protein complex Bpa (bacterial proteasome activator) in *Mycobacterium tuberculosis*, which competes with Mpa for the proteasome and can stimulate the degradation of substrates, is a strong indication that there could exist more, unidentified factors involved in both the assembly and the function of the proteasome.[119] Although Bpa was found by scanning the genome for the HbYX motif, other proteins that interact with Mpa, CP or both might not terminate in this sequence and it will likely not be sufficient to restrain the search to potential binding partners that contain it.

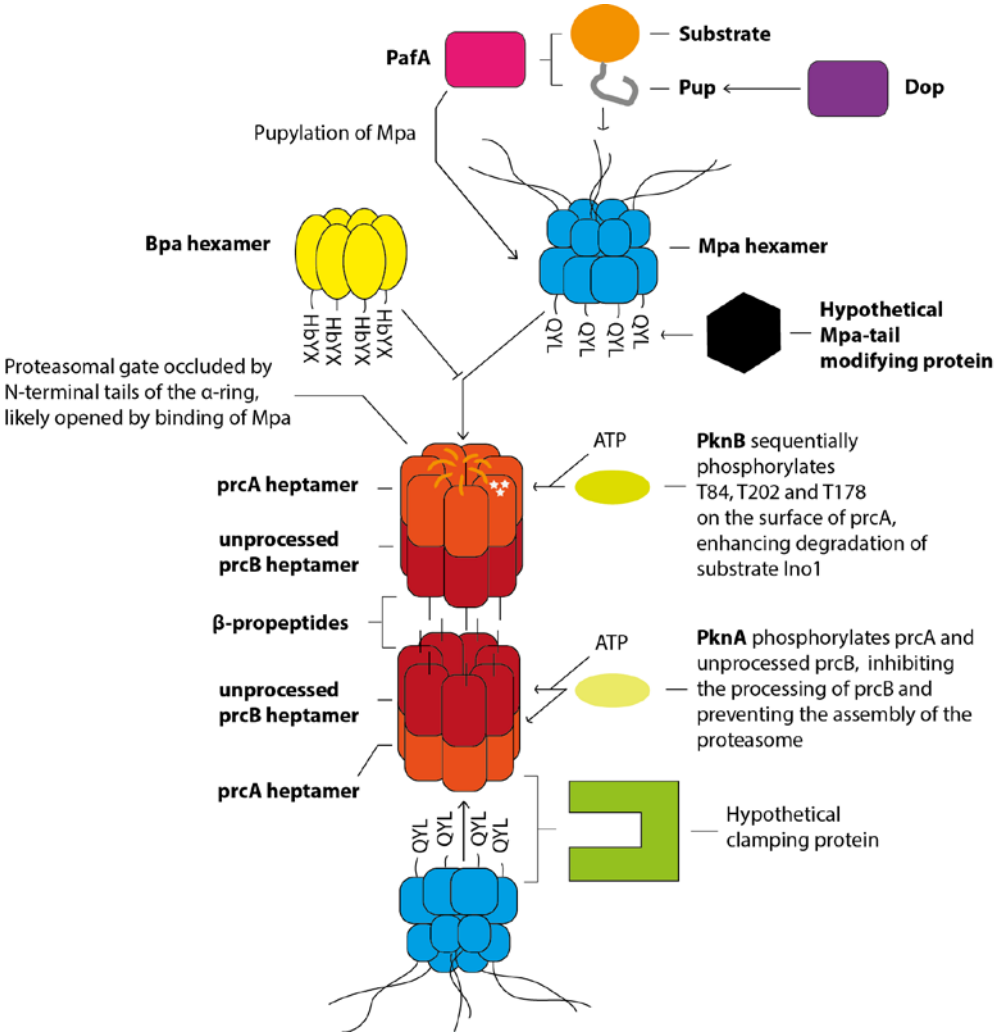

Fig. 4.1: Proposed model of the *Mycobacterium tuberculosis* proteasome. Bpa competes with Mpa for the binding to the CP and inhibits the degradation of the substrate. Post-translational modification of Mpa's C-terminal tails, specifically the QYL glutamine, could increase hydrophobicity and allow the non-HbYX QYL motif to bind to the CP. The symmetry mismatch between Mpa hexamer and CP heptamer could be solved by selective modification of alternating tails akin to the eukaryotic Rpt1-6 ring. A clamping protein could hold Mpa and the CP together, similar to the eukaryotic Rpn7.

5. REFERENCES

1 WHO. Global Tuberculosis Report 2014. (2014).

2 Getahun, H., Gunneberg, C., Granich, R. & Nunn, P. HIV Infection—Associated Tuberculosis: The Epidemiology and the Response. *Clinical Infectious Diseases* **50**, S201-S207, doi:10.1086/651492 (2010).

3 WHO. Global Tuberculosis Report 2013. (2013).

4 Hirnschall, G. in *Eliminating TB Deaths: Time to Step Up the HIV Response.* (WHO).

5 de Noronha, A. L. L., Báfica, A., Nogueira, L., Barral, A. & Barral-Netto, M. Lung granulomas from Mycobacterium tuberculosis/HIV-1 co-infected patients display decreased in situ TNF production. *Pathology - Research and Practice* **204**, 155-161 (2008).

6 Saini, D. *et al.* Ultra-low Dose of Mycobacterium tuberculosis Aerosol Creates Partial Infection in Mice. *Tuberculosis (Edinburgh, Scotland)* **92**, 160-165, doi:10.1016/j.tube.2011.11.007 (2012).

7 WHO. Treatment of Tuberculosis: Guidelines for National Programmes. (2003).

8 Todar, K. *Todar's Online Textbook of Bacteriology*. (University of Wisconsin-Madison Department of Bacteriology, 2006).

9 Pieters, J. & Ploegh, H. Chemical Warfare and Mycobacterial Defense. *Science* **302**, 1900-1902, doi:10.1126/science.1092873 (2003).

10 Daniel, J., Maamar, H., Deb, C., Sirakova, T. D. & Kolattukudy, P. E. *Mycobacterium tuberculosis* Uses Host Triacylglycerol to Accumulate Lipid Droplets and Acquires a Dormancy-Like Phenotype in Lipid-Loaded Macrophages. *PLoS Pathog* **7**, e1002093, doi:10.1371/journal.ppat.1002093 (2011).

11 Mehrotra, P. *et al.* Pathogenicity of *Mycobacterium tuberculosis* Is Expressed by Regulating Metabolic Thresholds of the Host Macrophage. *PLoS Pathog* **10**, e1004265, doi:10.1371/journal.ppat.1004265 (2014).

12 Zhang, Y. Persistent and dormant tubercle bacilli and latent tuberculosis. *Frontiers in bioscience : a journal and virtual library* **9**, 1136-1156 (2004).

13 Cole, S. T. *et al.* Deciphering the biology of Mycobacterium tuberculosis from the complete genome sequence. *Nature* **393**, 537-544 (1998).

14 Darwin, H. http://microbiology-parasitology.med.nyu.edu/heran-darwin

15 Ginsberg, A. M. & Spigelman, M. Challenges in tuberculosis drug research and development. *Nat Med* **13**, 290-294 (2007).

16 Darwin, K. H., Ehrt, S., Gutierrez-Ramos, J. C., Weich, N. & Nathan, C. F. The proteasome of Mycobacterium tuberculosis is required for resistance to nitric oxide. *Science* **302**, 1963-1966, doi:10.1126/science.1091176 (2003).

17 Wagner, J. M. *et al.* Understanding specificity of the mycosin proteases in ESX/type VII secretion by structural and functional analysis. *Journal of structural biology* **184**, 115-128, doi:10.1016/j.jsb.2013.09.022 (2013).

18 Roberts, D. M., Personne, Y., Ollinger, J. & Parish, T. Proteases in Mycobacterium tuberculosis pathogenesis: potential as drug targets. *Future microbiology* **8**, 621-631, doi:10.2217/fmb.13.25 (2013).

19 Lin, G. *et al.* Inhibitors selective for mycobacterial versus human proteasomes. *Nature* **461**, 621-626 (2009).

20 Cheng, Y. & Pieters, J. Novel Proteasome Inhibitors as Potential Drugs to Combat Tuberculosis. *Journal of Molecular Cell Biology* **2**, 173-175, doi:10.1093/jmcb/mjp053 (2010).

21 Lecker, S. H., Goldberg, A. L. & Mitch, W. E. Protein Degradation by the Ubiquitin–Proteasome Pathway in Normal and Disease States. *Journal of the American Society of Nephrology* **17**, 1807-1819, doi:10.1681/asn.2006010083 (2006).

22 Tyedmers, J., Mogk, A. & Bukau, B. Cellular strategies for controlling protein aggregation. *Nat Rev Mol Cell Biol* **11**, 777-788 (2010).

23 Komander, D. & Rape, M. The Ubiquitin Code. *Annual Review of Biochemistry* **81**, 203-229, doi:doi:10.1146/annurev-biochem-060310-170328 (2012).
24 Tomko, R. J. & Hochstrasser, M. Molecular Architecture and Assembly of the Eukaryotic Proteasome. *Annual review of biochemistry* **82**, 10.1146/annurev-biochem-060410-150257, doi:10.1146/annurev-biochem-060410-150257 (2013).
25 Nussbaum, A. K. *et al.* Cleavage motifs of the yeast 20S proteasome β subunits deduced from digests of enolase 1. *Proceedings of the National Academy of Sciences of the United States of America* **95**, 12504-12509 (1998).
26 Orlowski, M. & Wilk, S. Ubiquitin-independent proteolytic functions of the proteasome. *Archives of Biochemistry and Biophysics* **415**, 1-5 (2003).
27 Sauer, R. T. & Baker, T. A. AAA+ Proteases: ATP-Fueled Machines of Protein Destruction. *Annual Review of Biochemistry* **80**, 587-612, doi:doi:10.1146/annurev-biochem-060408-172623 (2011).
28 Chen, L. & Madura, K. Rad23 promotes the targeting of proteolytic substrates to the proteasome. *Molecular and cellular biology* **22**, 4902-4913 (2002).
29 Striebel, F., Imkamp, F., Özcelik, D. & Weber-Ban, E. Pupylation as a signal for proteasomal degradation in bacteria. *Biochimica et Biophysica Acta (BBA) - Molecular Cell Research* **1843**, 103-113 (2014).
30 Kleiger, G. & Mayor, T. Perilous journey: a tour of the ubiquitin–proteasome system. *Trends in Cell Biology* **24**, 352-359 (2014).
31 Ravid, T. & Hochstrasser, M. Degradation signal diversity in the ubiquitin-proteasome system. *Nature reviews. Molecular cell biology* **9**, 679-690, doi:10.1038/nrm2468 (2008).
32 Pickart, C. M. & Fushman, D. Polyubiquitin chains: polymeric protein signals. *Current Opinion in Chemical Biology* **8**, 610-616 (2004).
33 Fushman, D. & Wilkinson, K. D. Structure and recognition of polyubiquitin chains of different lengths and linkage. *F1000 biology reports* **3**, 26, doi:10.3410/b3-26 (2011).
34 Groll, M. *et al.* Structure of 20S proteasome from yeast at 2.4 A resolution. *Nature* **386**, 463-471, doi:10.1038/386463a0 (1997).
35 Voges, D., Zwickl, P. & Baumeister, W. The 26S proteasome: a molecular machine designed for controlled proteolysis. *Annu Rev Biochem* **68**, 1015-1068, doi:10.1146/annurev.biochem.68.1.1015 (1999).
36 Nandi, D., Tahiliani, P., Kumar, A. & Chandu, D. The ubiquitin-proteasome system. *J Biosci* **31**, 137-155, doi:10.1007/BF02705243 (2006).
37 Hu, G. *et al.* Structure of the Mycobacterium tuberculosis proteasome and mechanism of inhibition by a peptidyl boronate. *Molecular Microbiology* **59**, 1417-1428, doi:10.1111/j.1365-2958.2005.05036.x (2006).
38 Groll, M. *et al.* A gated channel into the proteasome core particle. *Nature structural biology* **7**, 1062-1067, doi:10.1038/80992 (2000).
39 Kunjappu, M. J. & Hochstrasser, M. Assembly of the 20S proteasome. *Biochimica et Biophysica Acta (BBA) - Molecular Cell Research* **1843**, 2-12 (2014).
40 Osmulski, P. A., Hochstrasser, M. & Gaczynska, M. A Tetrahedral Transition State at the Active Sites of the 20S Proteasome Is Coupled to Opening of the α-Ring Channel. *Structure* **17**, 1137-1147, doi:10.1016/j.str.2009.06.011.
41 Groll, M. *et al.* A gated channel into the proteasome core particle. *Nat Struct Mol Biol* **7**, 1062-1067 (2000).
42 Whitby, F. G. *et al.* Structural basis for the activation of 20S proteasomes by 11S regulators. *Nature* **408**, 115-120, doi:10.1038/35040607 (2000).
43 Forster, A., Masters, E. I., Whitby, F. G., Robinson, H. & Hill, C. P. The 1.9 A structure of a proteasome-11S activator complex and implications for proteasome-PAN/PA700 interactions. *Mol Cell* **18**, 589-599, doi:10.1016/j.molcel.2005.04.016 (2005).
44 Ortega, J. *et al.* The axial channel of the 20S proteasome opens upon binding of the PA200 activator. *J Mol Biol* **346**, 1221-1227, doi:10.1016/j.jmb.2004.12.049 (2005).

45 Schmidt, M. *et al.* The HEAT repeat protein Blm10 regulates the yeast proteasome by capping the core particle. *Nat Struct Mol Biol* **12**, 294-303, doi:10.1038/nsmb914 (2005).
46 Kohler, A. *et al.* The axial channel of the proteasome core particle is gated by the Rpt2 ATPase and controls both substrate entry and product release. *Mol Cell* **7**, 1143-1152 (2001).
47 Marques, A. J., Palanimurugan, R., Matias, A. C., Ramos, P. C. & Dohmen, R. J. Catalytic Mechanism and Assembly of the Proteasome. *Chemical Reviews* **109**, 1509-1536, doi:10.1021/cr8004857 (2009).
48 Heinemeyer, W., Fischer, M., Krimmer, T., Stachon, U. & Wolf, D. H. The active sites of the eukaryotic 20 S proteasome and their involvement in subunit precursor processing. *J Biol Chem* **272**, 25200-25209 (1997).
49 Kisselev, A. F., Akopian, T. N., Woo, K. M. & Goldberg, A. L. The sizes of peptides generated from protein by mammalian 26 and 20 S proteasomes. Implications for understanding the degradative mechanism and antigen presentation. *J Biol Chem* **274**, 3363-3371 (1999).
50 Bode, N. J. & Darwin, K. H. The Pup-Proteasome System of Mycobacteria. *Microbiology spectrum* **2**, doi:10.1128/microbiolspec.MGM2-0008-2013 (2014).
51 Arendt, C. S. & Hochstrasser, M. Eukaryotic 20S proteasome catalytic subunit propeptides prevent active site inactivation by N-terminal acetylation and promote particle assembly. *The EMBO journal* **18**, 3575-3585, doi:10.1093/emboj/18.13.3575 (1999).
52 Witt, S. *et al.* Proteasome Assembly Triggers a Switch Required for Active-Site Maturation. *Structure* **14**, 1179-1188 (2006).
53 Chen, P. & Hochstrasser, M. Autocatalytic subunit processing couples active site formation in the 20S proteasome to completion of assembly. *Cell* **86**, 961-972 (1996).
54 Ramos, P. C., Hockendorff, J., Johnson, E. S., Varshavsky, A. & Dohmen, R. J. Ump1p is required for proper maturation of the 20S proteasome and becomes its substrate upon completion of the assembly. *Cell* **92**, 489-499, doi:10.1016/s0092-8674(00)80942-3 (1998).
55 Groll, M. *et al.* The catalytic sites of 20S proteasomes and their role in subunit maturation: a mutational and crystallographic study. *Proc Natl Acad Sci U S A* **96**, 10976-10983 (1999).
56 Li, X., Kusmierczyk, A. R., Wong, P., Emili, A. & Hochstrasser, M. beta-Subunit appendages promote 20S proteasome assembly by overcoming an Ump1-dependent checkpoint. *The EMBO journal* **26**, 2339-2349, doi:10.1038/sj.emboj.7601681 (2007).
57 Takagi, K. *et al.* Pba3-Pba4 heterodimer acts as a molecular matchmaker in proteasome alpha-ring formation. *Biochemical and biophysical research communications* **450**, 1110-1114, doi:10.1016/j.bbrc.2014.06.119 (2014).
58 Kusmierczyk, A. R., Kunjappu, M. J., Kim, R. Y. & Hochstrasser, M. A conserved 20S proteasome assembly factor requires a C-terminal HbYX motif for proteasomal precursor binding. *Nat Struct Mol Biol* **18**, 622-629 (2011).
59 Fehlker, M., Wendler, P., Lehmann, A. & Enenkel, C. *Blm3 is part of nascent proteasomes and is involved in a late stage of nuclear proteasome assembly*. Vol. 4 (2003).
60 Dange, T. *et al.* Blm10 protein promotes proteasomal substrate turnover by an active gating mechanism. *J Biol Chem* **286**, 42830-42839, doi:10.1074/jbc.M111.300178 (2011).
61 Smith, D. M., Benaroudj, N. & Goldberg, A. Proteasomes and their associated ATPases: a destructive combination. *Journal of structural biology* **156**, 72-83, doi:10.1016/j.jsb.2006.04.012 (2006).
62 Riedinger, C. *et al.* Structure of Rpn10 and its interactions with polyubiquitin chains and the proteasome subunit Rpn12. *J Biol Chem* **285**, 33992-34003, doi:10.1074/jbc.M110.134510 (2010).
63 Zhang, F. *et al.* Structural Insights Into The Regulatory Particle Of The Proteasome From Methanocaldococcus jannaschii. *Molecular Cell* **34**, 473-484, doi:10.1016/j.molcel.2009.04.021 (2009).
64 Saeki, Y. & Tanaka, K. Unlocking the Proteasome Door. *Molecular Cell* **27**, 865-867 (2007).
65 Rabl, J. *et al.* Mechanism of Gate Opening in the 20S Proteasome by the Proteasomal ATPases. *Molecular Cell* **30**, 360-368, doi:10.1016/j.molcel.2008.03.004 (2008).

66 Yu, Y. *et al. Interactions of PAN's C-termini with archaeal 20S proteasome and implications for the eukaryotic proteasome–ATPase interactions*. Vol. 29 (2010).
67 Kim, Y.-C. & DeMartino, G. N. C Termini of Proteasomal ATPases Play Nonequivalent Roles in Cellular Assembly of Mammalian 26 S Proteasome. *J Biol Chem* **286**, 26652-26666, doi:10.1074/jbc.M111.246793 (2011).
68 Kumar, B., Kim, Y. C. & DeMartino, G. N. The C terminus of Rpt3, an ATPase subunit of PA700 (19 S) regulatory complex, is essential for 26 S proteasome assembly but not for activation. *J Biol Chem* **285**, 39523-39535, doi:10.1074/jbc.M110.153627 (2010).
69 Kusmierczyk, A. R., Kunjappu, M. J., Funakoshi, M. & Hochstrasser, M. A multimeric assembly factor controls the formation of alternative 20S proteasomes. *Nature Structural & Molecular Biology* **15**, 237-244, doi:10.1038/nsmb.1389 (2008).
70 Yu, Z. *et al.* Base-CP proteasome can serve as a platform for stepwise lid formation. *Bioscience reports*, doi:10.1042/bsr20140173 (2015).
71 Isono, E., Saeki, Y., Yokosawa, H. & Toh-e, A. Rpn7 Is Required for the Structural Integrity of the 26 S Proteasome of Saccharomyces cerevisiae. *Journal of Biological Chemistry* **279**, 27168-27176, doi:10.1074/jbc.M314231200 (2004).
72 De Mot, R. Actinomycete-like proteasomes in a Gram-negative bacterium. *Trends in Microbiology* **15**, 335-338 (2007).
73 Valas, R. E. & Bourne, P. E. Rethinking proteasome evolution: two novel bacterial proteasomes. *Journal of molecular evolution* **66**, 494-504, doi:10.1007/s00239-008-9075-7 (2008).
74 Rohrwild, M. *et al.* HslV-HslU: A novel ATP-dependent protease complex in Escherichia coli related to the eukaryotic proteasome. *Proceedings of the National Academy of Sciences* **93**, 5808-5813 (1996).
75 Gandotra, S., Lebron, M. B. & Ehrt, S. The *Mycobacterium tuberculosis* Proteasome Active Site Threonine Is Essential for Persistence Yet Dispensable for Replication and Resistance to Nitric Oxide. *PLoS Pathog* **6**, e1001040, doi:10.1371/journal.ppat.1001040 (2010).
76 Valas, R. & Bourne, P. The origin of a derived superkingdom: how a gram-positive bacterium crossed the desert to become an archaeon. *Biology Direct* **6**, 16 (2011).
77 Guth, E., Thommen, M. & Weber-Ban, E. Mycobacterial Ubiquitin-like Protein Ligase PafA Follows a Two-step Reaction Pathway with a Phosphorylated Pup Intermediate. *Journal of Biological Chemistry* **286**, 4412-4419, doi:10.1074/jbc.M110.189282 (2011).
78 Festa, R. A. *et al.* Prokaryotic ubiquitin-like protein (Pup) proteome of Mycobacterium tuberculosis [corrected]. *PLoS One* **5**, e8589, doi:10.1371/journal.pone.0008589 (2010).
79 Watrous, J. *et al.* Expansion of the mycobacterial "PUPylome". *Molecular bioSystems* **6**, 376-385, doi:10.1039/b916104j (2010).
80 Gottesman, S., Roche, E., Zhou, Y. & Sauer, R. T. The ClpXP and ClpAP proteases degrade proteins with carboxy-terminal peptide tails added by the SsrA-tagging system. *Genes & development* **12**, 1338-1347 (1998).
81 Karzai, A. W., Roche, E. D. & Sauer, R. T. The SsrA-SmpB system for protein tagging, directed degradation and ribosome rescue. *Nat Struct Mol Biol* **7**, 449-455 (2000).
82 Consortium, U. (2015).
83 Pearce, M. J., Mintseris, J., Ferreyra, J., Gygi, S. P. & Darwin, K. H. Ubiquitin-Like Protein Involved in the Proteasome Pathway of Mycobacterium tuberculosis. *Science* **322**, 1104-1107, doi:10.1126/science.1163885 (2008).
84 Cerda-Maira, F. A. *et al.* Molecular Analysis of the Prokaryotic Ubiquitin-Like Protein (Pup) Conjugation Pathway in Mycobacterium tuberculosis. *Molecular microbiology* **77**, 1123-1135, doi:10.1111/j.1365-2958.2010.07276.x (2010).
85 Chen, X. *et al.* Prokaryotic Ubiquitin-Like Protein Pup Is Intrinsically Disordered. *Journal of Molecular Biology* **392**, 208-217 (2009).

86 Sutter, M., Damberger, F. F., Imkamp, F., Allain, F. H. T. & Weber-Ban, E. Prokaryotic Ubiquitin-like Protein (Pup) Is Coupled to Substrates via the Side Chain of Its C-Terminal Glutamate. *Journal of the American Chemical Society* **132**, 5610-5612, doi:10.1021/ja910546x (2010).
87 Ozcelik, D. *et al.* Structures of Pup ligase PafA and depupylase Dop from the prokaryotic ubiquitin-like modification pathway. *Nature communications* **3**, 1014, doi:10.1038/ncomms2009 (2012).
88 Striebel, F. *et al.* Bacterial ubiquitin-like modifier Pup is deamidated and conjugated to substrates by distinct but homologous enzymes. *Nat Struct Mol Biol* **16**, 647-651, doi:10.1038/nsmb.1597 (2009).
89 Elharar, Y. *et al. Survival of mycobacteria depends on proteasome-mediated amino acid recycling under nutrient limitation*. Vol. 33 (2014).
90 Maldonado, A. Y., Burz, D. S., Reverdatto, S. & Shekhtman, A. Fate of pup inside the Mycobacterium proteasome studied by in-cell NMR. *PLoS One* **8**, e74576, doi:10.1371/journal.pone.0074576 (2013).
91 Forer, N., Korman, M., Elharar, Y., Vishkautzan, M. & Gur, E. Bacterial Proteasome and PafA, the Pup Ligase, Interact to Form a Modular Protein Tagging and Degradation Machine. *Biochemistry* **52**, 9029-9035, doi:10.1021/bi401017b (2013).
92 Burns, K. E., Pearce, M. J. & Darwin, K. H. Prokaryotic ubiquitin-like protein provides a two-part degron to Mycobacterium proteasome substrates. *Journal of bacteriology* **192**, 2933-2935, doi:10.1128/jb.01639-09 (2010).
93 Festa, R. A., Pearce, M. J. & Darwin, K. H. Characterization of the proteasome accessory factor (paf) operon in Mycobacterium tuberculosis. *Journal of bacteriology* **189**, 3044-3050, doi:10.1128/jb.01597-06 (2007).
94 Striebel, F., Kress, W. & Weber-Ban, E. Controlled destruction: AAA+ ATPases in protein degradation from bacteria to eukaryotes. *Current opinion in structural biology* **19**, 209-217, doi:10.1016/j.sbi.2009.02.006 (2009).
95 Cerda-Maira, F. & Darwin, K. H. The Mycobacterium tuberculosis proteasome: more than just a barrel-shaped protease. *Microbes Infect* **11**, 1150-1155, doi:10.1016/j.micinf.2009.08.003 (2009).
96 Lin, G. *et al.* Mycobacterium tuberculosis prcBA genes encode a gated proteasome with broad oligopeptide specificity. *Molecular microbiology* **59**, 1405-1416, doi:10.1111/j.1365-2958.2005.05035.x (2006).
97 Kwon, Y. D., Nagy, I., Adams, P. D., Baumeister, W. & Jap, B. K. Crystal structures of the Rhodococcus proteasome with and without its pro-peptides: implications for the role of the pro-peptide in proteasome assembly. *J Mol Biol* **335**, 233-245 (2004).
98 Li, D. *et al. Structural basis for the assembly and gate closure mechanisms of the Mycobacterium tuberculosis 20S proteasome*. Vol. 29 (2010).
99 Zühl, F., Seemüller, E., Golbik, R. & Baumeister, W. Dissecting the assembly pathway of the 20S proteasome. *FEBS Letters* **418**, 189-194 (1997).
100 Zwickl, P., Kleinz, J. & Baumeister, W. Critical elements in proteasome assembly. *Nature structural biology* **1**, 765-770 (1994).
101 Anandan, T. *et al.* Phosphorylation regulates mycobacterial proteasome. *J Microbiol.* **52**, 743-754, doi:10.1007/s12275-014-4416-2 (2014).
102 Darwin, K. H., Lin, G., Chen, Z., Li, H. & Nathan, C. F. Characterization of a Mycobacterium tuberculosis proteasomal ATPase homologue. *Molecular Microbiology* **55**, 561-571, doi:10.1111/j.1365-2958.2004.04403.x (2005).
103 Pearce, M. J. *et al.* Identification of substrates of the Mycobacterium tuberculosis proteasome. *The EMBO Journal* **25**, 5423-5432, doi:10.1038/sj.emboj.7601405 (2006).
104 Vishwanath, V., Meera, R., Narayanan, P. & Puvanakrishnan, R. Fate of Mycobacterium tuberculosis inside rate peritoneal macrophages in vitro. *Mol Cell Biochem* **175**, 169-175, doi:10.1023/A:1006848900722 (1997).

105 Striebel, F., Hunkeler, M., Summer, H. & Weber-Ban, E. The mycobacterial Mpa–proteasome unfolds and degrades pupylated substrates by engaging Pup's N-terminus. *EMBO Journal* **29**, 1262-1271, doi:10.1038/emboj.2010.23 (2010).
106 Finley, D., Ulrich, H. D., Sommer, T. & Kaiser, P. The Ubiquitin–Proteasome System of Saccharomyces cerevisiae. *Genetics* **192**, 319-360, doi:10.1534/genetics.112.140467 (2012).
107 Wolf, S. *et al.* Characterization of ARC, a divergent member of the AAA ATPase family from Rhodococcus erythropolis. *J Mol Biol* **277**, 13-25, doi:10.1006/jmbi.1997.1589 (1998).
108 Zhang, X. *et al.* The N-terminal coiled coil of the Rhodococcus erythropolis ARC AAA ATPase is neither necessary for oligomerization nor nucleotide hydrolysis. *Journal of structural biology* **146**, 155-165, doi:10.1016/j.jsb.2003.10.020 (2004).
109 Wang, T. *et al.* Structural Insights on the Mycobacterium tuberculosis Proteasomal ATPase Mpa. *Structure* **17**, 1377-1385, doi:10.1016/j.str.2009.08.010 (2009).
110 Wang, T., Darwin, K. H. & Li, H. Binding-induced folding of prokaryotic ubiquitin-like protein on the Mycobacterium proteasomal ATPase targets substrates for degradation. *Nat Struct Mol Biol* **17**, 1352-1357 (2010).
111 Sutter, M., Striebel, F., Damberger, F. F., Allain, F. H. T. & Weber-Ban, E. A distinct structural region of the prokaryotic ubiquitin-like protein (Pup) is recognized by the N-terminal domain of the proteasomal ATPase Mpa. *FEBS Letters* **583**, 3151-3157 (2009).
112 Djuranovic, S. *et al.* Structure and Activity of the N-Terminal Substrate Recognition Domains in Proteasomal ATPases. *Molecular Cell* **34**, 580-590, doi:10.1016/j.molcel.2009.04.030 (2009).
113 Matyskiela, M. E. & Martin, A. Design Principles of a Universal Protein Degradation Machine. *Journal of Molecular Biology* **425**, 199-213 (2013).
114 Smith, D. M. *et al.* Docking of the Proteasomal ATPases' Carboxyl Termini in the 20S Proteasome's α Ring Opens the Gate for Substrate Entry. *Molecular Cell* **27**, 731-744, doi:10.1016/j.molcel.2007.06.033 (2007).
115 Cerda-Maira, F. & Darwin, K. H. The Mycobacterium tuberculosis proteasome: more than just a barrel-shaped protease. *Microbes and infection / Institut Pasteur* **11**, 1150-1155, doi:10.1016/j.micinf.2009.08.003 (2009).
116 Burns, K. E. *et al.* "Depupylation" of Prokaryotic Ubiquitin-like Protein from Mycobacterial Proteasome Substrates. *Molecular Cell* **39**, 821-827 (2010).
117 Imkamp, F. *et al.* Dop functions as a depupylase in the prokaryotic ubiquitin-like modification pathway. *EMBO Reports* **11**, 791-797, doi:10.1038/embor.2010.119 (2010).
118 Delley, C. L., Striebel, F., Heydenreich, F. M., Özcelik, D. & Weber-Ban, E. Activity of the mycobacterial proteasomal ATPase Mpa is reversibly regulated by pupylation. *J Biol Chem* **287**, 7907-7914, doi:10.1074/jbc.m111.331124 (2012).
119 Delley, C. L. *et al.* Bacterial Proteasome Activator Bpa (Rv3780) Is a Novel Ring-Shaped Interactor of the Mycobacterial Proteasome. *PLoS ONE* **9**, e114348, doi:10.1371/journal.pone.0114348 (2014).
120 Tomko, R. J., Jr., Funakoshi, M., Schneider, K., Wang, J. & Hochstrasser, M. Heterohexameric ring arrangement of the eukaryotic proteasomal ATPases: implications for proteasome structure and assembly. *Mol Cell* **38**, 393-403, doi:10.1016/j.molcel.2010.02.035 (2010).
121 Egerton, M. *et al.* VCP, the mammalian homolog of cdc48, is tyrosine phosphorylated in response to T cell antigen receptor activation. *The EMBO journal* **11**, 3533-3540 (1992).
122 Madeo, F., Schlauer, J., Zischka, H., Mecke, D. & Fröhlich, K.-U. Tyrosine Phosphorylation Regulates Cell Cycle-dependent Nuclear Localization of Cdc48p. *Molecular Biology of the Cell* **9**, 131-141, doi:10.1091/mbc.9.1.131 (1998).
123 Pearce, M. J. *et al. Identification of substrates of the Mycobacterium tuberculosis proteasome*. Vol. 25 (2006).
124 Benaroudj, N., Zwickl, P., Seemüller, E., Baumeister, W. & Goldberg, A. L. ATP Hydrolysis by the Proteasome Regulatory Complex PAN Serves Multiple Functions in Protein Degradation. *Molecular Cell* **11**, 69-78 (2003).

125 Lowe, J. *et al.* Crystal structure of the 20S proteasome from the archaeon T. acidophilum at 3.4 A resolution. *Science* **268**, 533-539, doi:10.1126/science.7725097 (1995).
126 Maupin-Furlow, J. A. Archaeal proteasomes and sampylation. *Sub-cellular biochemistry* **66**, 297-327, doi:10.1007/978-94-007-5940-4_11 (2013).
127 Djuranovic, S. *et al.* Structure and activity of the N-terminal substrate recognition domains in proteasomal ATPases. *Mol Cell* **34**, 580-590, doi:10.1016/j.molcel.2009.04.030 (2009).
128 Smith, D. M. *et al.* ATP binding to PAN or the 26S ATPases causes association with the 20S proteasome, gate opening, and translocation of unfolded proteins. *Mol Cell* **20**, 687-698, doi:10.1016/j.molcel.2005.10.019 (2005).
129 Sassetti, C. M., Boyd, D. H. & Rubin, E. J. Genes required for mycobacterial growth defined by high density mutagenesis. *Mol Microbiol* **48**, 77-84 (2003).
130 Gandotra, S., Schnappinger, D., Monteleone, M., Hillen, W. & Ehrt, S. In vivo gene silencing identifies the Mycobacterium tuberculosis proteasome as essential for the bacteria to persist in mice. *Nat Med* **13**, 1515-1520, doi:10.1038/nm1683 (2007).
131 Raju, R. M. *et al.* Post-Translational Regulation via Clp Protease Is Critical for Survival of *Mycobacterium tuberculosis*. *PLoS Pathog* **10**, e1003994, doi:10.1371/journal.ppat.1003994 (2014).
132 Wilkins, M. R. *et al.* Protein identification and analysis tools in the ExPASy server. *Methods in molecular biology (Clifton, N.J.)* **112**, 531-552 (1999).
133 Chin, J. W., Martin, A. B., King, D. S., Wang, L. & Schultz, P. G. Addition of a photocrosslinking amino acid to the genetic code of Escherichia coli. *Proceedings of the National Academy of Sciences* **99**, 11020-11024, doi:10.1073/pnas.172226299 (2002).
134 Hindi, S. *Photoactive molecular probes for protein kinases: Development of selective photoligands for lympocyte specific kinase (Lck)* 3284487 thesis, City University of New York, (2007).
135 Ai, H. W., Shen, W., Sagi, A., Chen, P. R. & Schultz, P. G. Probing protein-protein interactions with a genetically encoded photo-crosslinking amino acid. *Chembiochem : a European journal of chemical biology* **12**, 1854-1857, doi:10.1002/cbic.201100194 (2011).
136 Laemmli, U. K. Cleavage of structural proteins during the assembly of the head of bacteriophage T4. *Nature* **227**, 680-685 (1970).
137 *ExPASy ProtParam*.
138 Chin, J. W., Martin, A. B., King, D. S., Wang, L. & Schultz, P. G. Addition of a photocrosslinking amino acid to the genetic code of Escherichia coli. *Proceedings of the National Academy of Sciences of the United States of America* **99**, 11020-11024, doi:10.1073/pnas.172226299 (2002).
139 Park, S., Kim, W., Tian, G., Gygi, S. P. & Finley, D. Structural defects in the regulatory particle-core particle interface of the proteasome induce a novel proteasome stress response. *J Biol Chem* **286**, 36652-36666, doi:10.1074/jbc.M111.285924 (2011).
140 Green, N. M. Avidin. *Advances in protein chemistry* **29**, 85-133 (1975).
141 Schmidt, T. G. M. & Skerra, A. The Strep-tag system for one-step purification and high-affinity detection or capturing of proteins. *Nat. Protocols* **2**, 1528-1535 (2007).
142 *Strep-tag-Strep Tactin system for purification of recombinant proteins*.
143 Pearce, M. J. *et al.* Identification of substrates of the Mycobacterium tuberculosis proteasome. *EMBO Journal* **25**, 5423-5432, doi:10.1038/sj.emboj.7601405 (2006).
144 Zheng, Y. *et al.* Identification of plant-derived natural products as potential inhibitors of the Mycobacterium tuberculosis proteasome. *BMC Complementary and Alternative Medicine* **14**, 400, doi:10.1186/1472-6882-14-400 (2014).
145 Dang, L. C., Melandri, F. D. & Stein, R. L. Kinetic and mechanistic studies on the hydrolysis of ubiquitin C-terminal 7-amido-4-methylcoumarin by deubiquitinating enzymes. *Biochemistry* **37**, 1868-1879, doi:10.1021/bi9723360 (1998).

146 von Delft, F. *et al.* Structure of E. coli Ketopantoate Hydroxymethyl Transferase Complexed with Ketopantoate and Mg2+, Solved by Locating 160 Selenomethionine Sites. *Structure* **11**, 985-996 (2003).
147 Kurtov, D., Kinghorn, J. R. & Unkles, S. E. The Aspergillus nidulans panB gene encodes ketopantoate hydroxymethyltransferase, required for biosynthesis of pantothenate and Coenzyme A. *Molecular & general genetics : MGG* **262**, 115-120 (1999).
148 Tanaka, Y., Bond, M. R. & Kohler, J. J. Photocrosslinkers illuminate interactions in living cells. *Molecular bioSystems* **4**, 473-480, doi:10.1039/B803218A (2008).

6. SUPPLEMENTARY INFORMATION

6.1. ITC curves

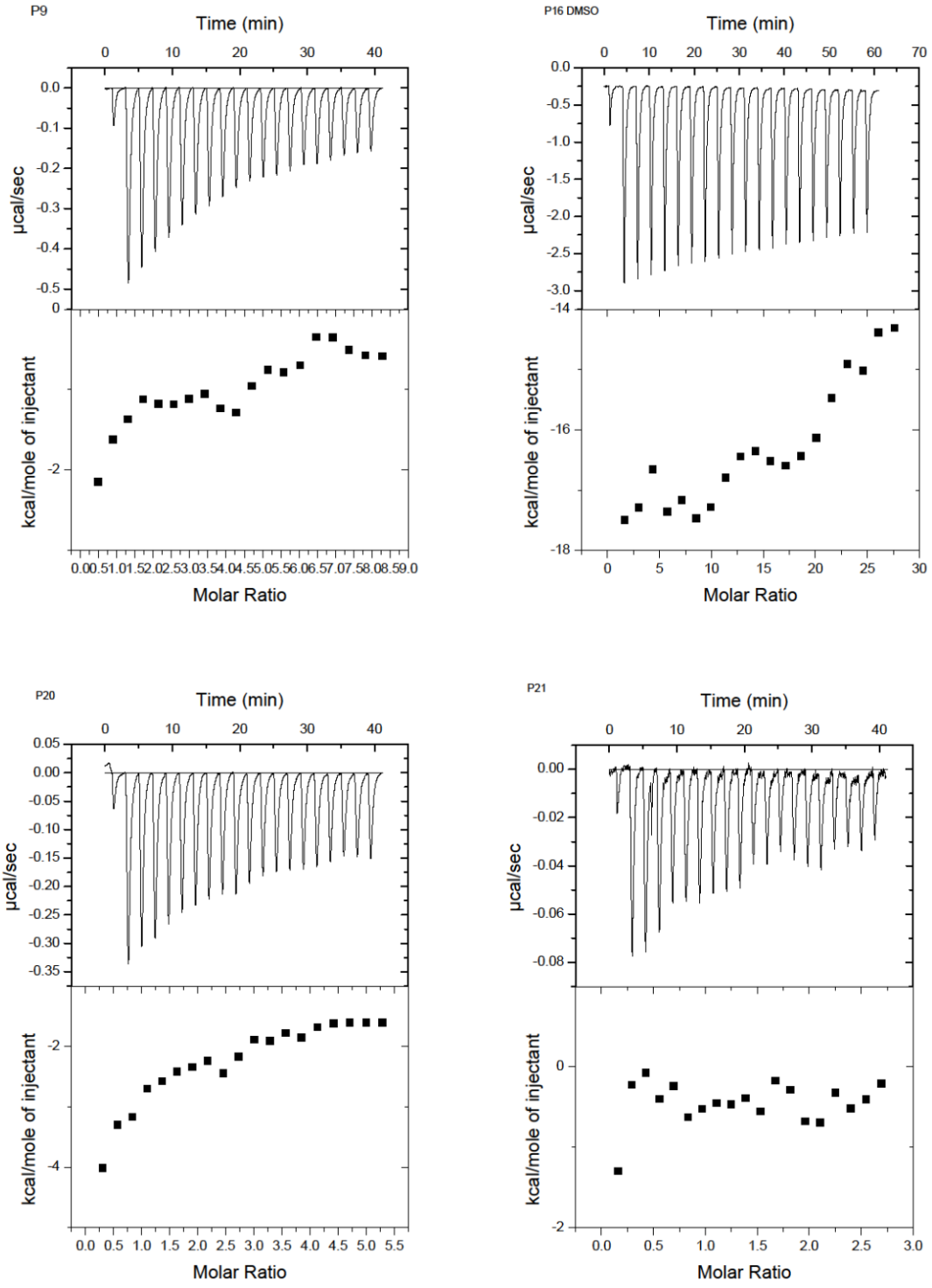

Fig. S1: Top left: ITC of peptide 9 and CP_{WT}. Concentrations: P9: 166.2 µM, CP_{WT}-28-mer: 8 µM. **Top right:** ITC of peptide 16 (dissolved in DMSO) and CP_{WT}. Concentrations: P16: 249 µM, CP_{WT}-28-mer: 1.3 µM.

Bottom left: ITC of peptide 20 and CP_{WT}. Concentrations: P20: 290 µM, CP_{WT}-28-mer: 7.9 µM. **Bottom right**: ITC of peptide 21 and CP_{WT}. Concentrations: P21: 146.9 µM, CP_{WT}- 28-mer: 7.8 µM

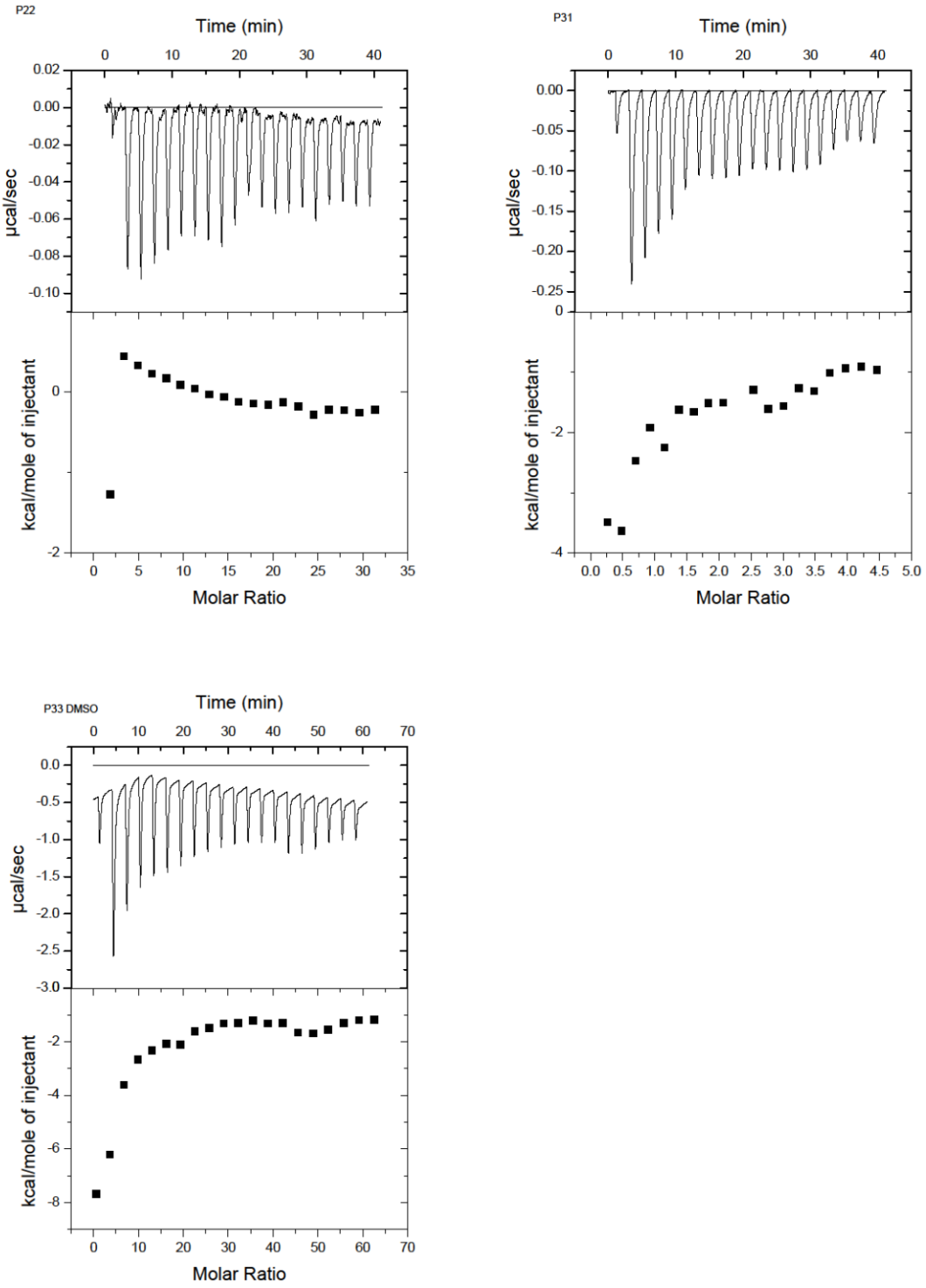

Fig. S2. Top left: ITC of peptide 22 and CP_{WT}. Concentrations: P22: 457 µM, CP_{WT}-28-mer: 2.1 µM.

Top right: ITC of peptide 31 and CP_{WT}. Concentrations: P31: 213.5 µM, CP_{WT}-28-mer: 6.9 µM.

Bottom left: ITC of peptide 33 (dissolved in DMSO) and CP_{WT}. Concentrations: P31: 1.06 mM, CP_{WT}-28-mer: 2.4 µM.

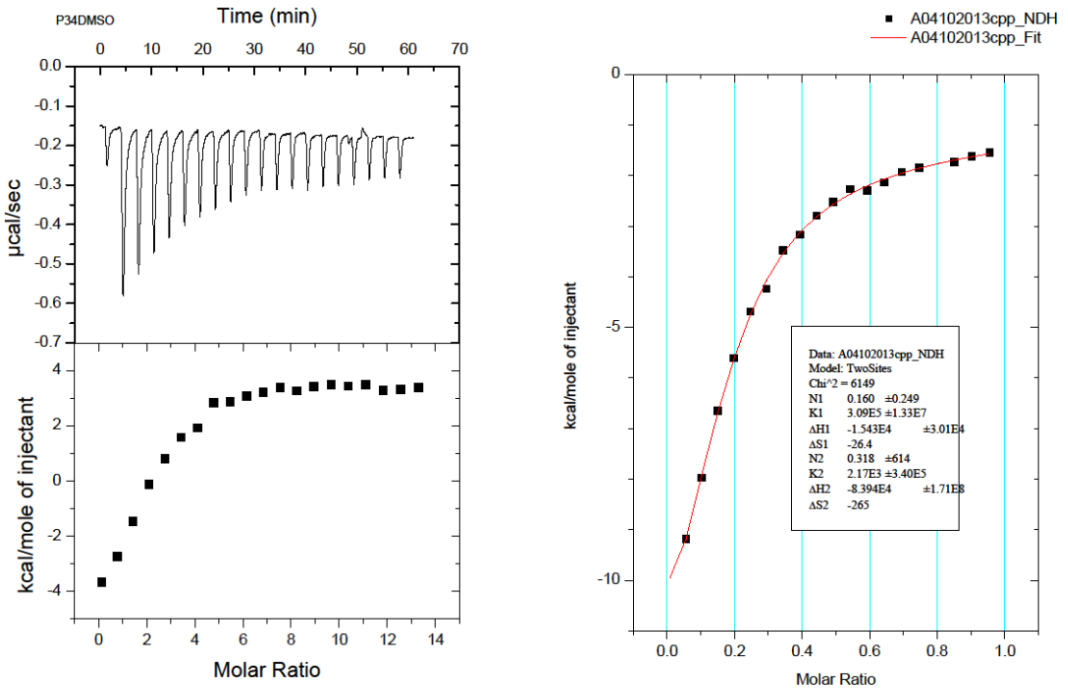

Fig. S3. Left: ITC of peptide 34 (dissolved in DMSO) and CP_{WT}. Concentrations: P34: 212 µM, CP_{WT} -28-mer: 2.2 µM.

Right: Curve fitting of ITC of peptide 34 and CP_{WT} -28-mer.

6.2. Mass spectrometry analysis of Mpa-baited and CP-baited pulldown (next page)

Gene Name	Description	MW[kDa]	sample_Mpa_50per							sample_Cp_50per						
			Coverage	# Peptides	# PSMs	Area	Rel. Area (%)	Norm. Area	ControlQ	Coverage	# Peptides	# PSMs	Area	Rel. Area (%)	Norm. Area	ControlQ
	RecName: Full=60 kDa chaperonin 1; AltName: Full=Protein Cpn60 1; AltName: Full=groEL1 protein	57,3	16,82	6	30	1,52E+10	5,85	2,82E+07	2,56	15,90	7	40	5,45E+10	2,92	1,01E+08	0,00
	RecName: Full=60 kDa chaperonin 1; AltName: Full=GroEL protein 1; AltName: Full=HSP58; AltName: Full=Protein Cpn60 1	56,7	26,85	13	52	1,52E+10	5,85	2,82E+07	2,56	30,19	14	68	5,45E+10	2,92	1,01E+08	0,00
groEL	RecName: Full=60 kDa chaperonin 1; AltName: Full=Protein Cpn60 1; AltName: Full=groEL1 protein	57,0	22,88	9	35	1,52E+10	5,85	2,81E+07	2,56	27,49	11	73	5,45E+10	2,92	1,01E+08	0,00
infA	RecName: Full=Translation initiation factor IF-1	8,4	27,40	2	8	4,86E+09	1,86	6,65E+07	0,00	35,62	3	14	1,83E+10	0,98	2,51E+08	0,00
ndk	RecName: Full=Nucleoside diphosphate kinase; Short=NDK; Short=NDP kinase; AltName: Full=Nucleoside-2-P kinase	15,0	18,98	2	12	6,28E+09	2,41	4,59E+07	0,00	21,90	4	15	9,20E+09	0,49	6,72E+07	0,00
tuf	RecName: Full=Elongation factor Tu 1; Short=EF-Tu 1	43,8	28,46	10	53	6,00E+09	2,30	1,51E+07	0,00	49,62	18	148	3,47E+10	1,86	8,75E+07	0,00
groEL	RecName: Full=60 kDa chaperonin 1; AltName: Full=GroEL protein 1; AltName: Full=Heat shock protein 60 1; AltName: Full=Protein Cpn60 1	56,8	1,84	1	2	6,29E+09	2,41	1,16E+07	0,42	1,84	1	4	1,20E+10	0,64	2,21E+07	271,39
groEL	RecName: Full=60 kDa chaperonin 2; AltName: Full=GroEL protein 2; AltName: Full=Protein Cpn60 2	56,5	5,03	2	3	3,15E+09	1,21	5,87E+06	0,53	12,10	5	9	4,06E+09	0,22	7,56E+06	0,00
Mfl621	RecName: Full=Elongation factor Tu; Short=EF-Tu	42,9	2,28	1	2	2,83E+09	1,08	7,17E+06	0,88	2,28	1	3	1,44E+10	0,77	3,66E+07	128,17
SCO1640	RecName: Full=Pup--protein ligase; AltName: Full=Proteasome accessory factor A; AltName: Full=Pup-conjugating enzyme	52,1	31,57	14	41	3,87E+09	1,49	8,55E+06	0,00	44,37	18	52	6,67E+09	0,36	1,47E+07	0,00
tuf	RecName: Full=Elongation factor Tu-1; Short=EF-Tu-1	43,8	36,27	12	65	2,74E+09	1,05	6,89E+06	28,73	59,95	20	159	4,96E+10	2,66	1,25E+08	2.462,50
Noca_3922	RecName: Full=Elongation factor Tu; Short=EF-Tu	43,8	18,39	6	47	1,77E+09	0,68	4,45E+06	0,00	22,17	8	116	1,86E+10	1,00	4,70E+07	0,00
Francci3_0580	RecName: Full=Elongation factor Tu; Short=EF-Tu	43,9	15,87	6	44	2,19E+09	0,84	5,52E+06	0,00	26,70	10	64	8,88E+09	0,48	2,24E+07	0,00
Dde_2989	RecName: Full=Elongation factor Tu; Short=EF-Tu	43,4	10,33	4	40	1,55E+09	0,59	3,89E+06	2,90	10,33	5	50	8,88E+09	0,48	2,24E+07	0,00
tuf	RecName: Full=Elongation factor Tu; Short=EF-Tu	44,0	12,85	5	38	2,29E+09	0,88	5,78E+06	0,30	27,20	10	68	9,80E+09	0,52	2,47E+07	38,44
groEL	RecName: Full=60 kDa chaperonin 2; AltName: Full=GroEL protein 2; AltName: Full=Protein Cpn60 2	57,0	5,59	3	4	2,28E+09	0,87	4,24E+06	0,00	4,28	2	7	6,68E+09	0,36	1,24E+07	0,00

Gene Name	Description	MW[kDa]	sample_Mpa_50per							sample_Cp_50per						
			Coverage	# Peptides	# PSMs	Area	Rel. Area (%)	Norm. Area	ControlQ	Coverage	# Peptides	# PSMs	Area	Rel. Area (%)	Norm. Area	ControlQ
groEL	RecName: Full=60 kDa chaperonin; AltName: Full=GroEL protein; AltName: Full=Protein Cpn60	58,0	2,04	2	4	2,36E+09	0,91	4,39E+06	0,10	2,04	2	10	1,13E+10	0,61	2,10E+07	255,73
Pden_0756	RecName: Full=Elongation factor Tu; Short=EF-Tu	42,9	2,30	1	2	2,83E+09	1,08	7,23E+06	0,37	2,30	1	3	1,44E+10	0,77	3,69E+07	56,55
tuf	RecName: Full=Elongation factor Tu; Short=EF-Tu	43,0	2,28	1	2	2,83E+09	1,08	7,15E+06	0,37	2,28	1	3	1,44E+10	0,77	3,65E+07	56,55
	RecName: Full=Glutamine synthetase 1; AltName: Full=Glutamate--ammonia ligase I; AltName: Full=Glutamine synthetase I; Short=GSI	52,5	31,98	14	48	1,75E+09	0,67	3,74E+06	0,00	40,94	18	72	1,18E+10	0,63	2,52E+07	0,00
groEL	RecName: Full=60 kDa chaperonin 4; AltName: Full=GroEL protein 4; AltName: Full=Protein Cpn60 4	56,7	7,04	4	8	2,74E+09	1,05	5,07E+06	0,18	5,56	4	8	4,95E+09	0,27	9,17E+06	111,99
	RecName: Full=Ectoine hydroxylase	32,7	24,58	6	25	1,91E+09	0,73	6,41E+06	0,00	20,88	5	14	3,10E+09	0,17	1,04E+07	0,00
	RecName: Full=Elongation factor Tu; Short=EF-Tu	43,8	5,54	2	4	2,83E+09	1,08	7,12E+06	0,00	5,54	2	12	1,00E+10	0,54	2,52E+07	0,00
Tfu_1788	RecName: Full=Pup--protein ligase; AltName: Full=Proteasome accessory factor A; AltName: Full=Pup-conjugating enzyme	51,8	17,04	8	16	2,17E+09	0,83	4,81E+06	0,00	15,49	8	19	4,62E+09	0,25	1,02E+07	0,00
aroC	RecName: Full=Chorismate synthase; AltName: Full=5-enolpyruvylshikimate-3-phosphate phospholyase	41,6	22,08	8	20	1,63E+09	0,63	4,13E+06	0,00	27,66	11	40	6,63E+09	0,36	1,68E+07	0,00
SCO5426	RecName: Full=6-phosphofructokinase 2; AltName: Full=Phosphofructokinase 2; AltName: Full=Phosphohexokinase 2	36,4	11,73	4	8	1,05E+09	0,40	3,07E+06	0,00	16,72	5	10	4,25E+09	0,23	1,25E+07	0,00
tufA	RecName: Full=Elongation factor Tu; Short=EF-Tu	43,5	7,32	2	3	1,44E+09	0,55	3,65E+06	0,00	14,90	5	12	6,96E+09	0,37	1,76E+07	0,00
	RecName: Full=Probable phosphoketolase	88,1	4,77	5	12	1,29E+09	0,50	1,62E+06	0,00	6,28	5	10	2,08E+09	0,11	2,61E+06	0,00
SCO1947	RecName: Full=Glyceraldehyde-3-phosphate dehydrogenase; Short=GAPDH	36,2	17,56	6	11	1,24E+09	0,48	3,68E+06	8,73	38,10	11	26	7,11E+09	0,38	2,12E+07	0,00
pyrG	RecName: Full=CTP synthase; AltName: Full=CTP synthetase; AltName: Full=UTP--ammonia ligase	60,1	9,84	5	13	1,14E+09	0,44	2,08E+06	0,00	27,14	12	27	3,94E+09	0,21	7,18E+06	0,00
Tfu_2353	RecName: Full=Serine hydroxymethyltransferase; Short=SHMT; Short=Serine methylase	45,1	6,38	3	4	9,20E+08	0,35	2,17E+06	0,00	6,38	3	5	2,39E+09	0,13	5,65E+06	0,00
xfp	RecName: Full=Probable phosphoketolase	89,3	1,12	1	2	1,12E+09	0,43	1,39E+06	0,00	3,23	2	5	1,98E+09	0,11	2,47E+06	0,00

Gene Name	Description	MW[kDa]	sample_Mpa_50per							sample_Cp_50per						
			Coverage	# Peptides	# PSMs	Area	Rel. Area (%)	Norm. Area	ControlQ	Coverage	# Peptides	# PSMs	Area	Rel. Area (%)	Norm. Area	ControlQ
glyA	RecName: Full=Serine hydroxymethyltransferase; Short=SHMT; Short=Serine methylase	45,0	17,86	6	12	9,47E+08	0,36	2,26E+06	0,00	24,76	8	15	3,12E+09	0,17	7,44E+06	0,00
SCO1496	RecName: Full=Chorismate synthase; AltName: Full=5-enolpyruvylshikimate-3-phosphate phospholyase	41,6	14,47	6	16	1,18E+09	0,45	3,00E+06	0,00	24,11	9	27	4,91E+09	0,26	1,25E+07	0,00
tuf	RecName: Full=Elongation factor Tu; Short=EF-Tu	43,3	5,58	2	15	7,11E+08	0,27	1,80E+06	0,92	3,81	1	18	6,11E+09	0,33	1,55E+07	111,90
Mmc1_0860	RecName: Full=30S ribosomal protein S14 type Z	7,0		0	0	0,00E+00			0,00		0	0	0,00E+00			0,00
	RecName: Full=10 kDa chaperonin; AltName: Full=GroES protein; AltName: Full=Protein Cpn10	11,0	66,67	5	13	8,81E+08	0,34	8,64E+06	0,00	57,84	4	12	2,20E+09	0,12	2,16E+07	0,00
	RecName: Full=Chaperone protein DnaK; AltName: Full=HSP70; AltName: Full=Heat shock 70 kDa protein; AltName: Full=Heat shock protein 70	66,6	32,69	19	25	1,42E+09	0,55	2,31E+06	0,00	38,83	21	36	3,45E+09	0,18	5,58E+06	5,96
	RecName: Full=Glutamine synthetase 1; AltName: Full=Glutamate--ammonia ligase I; AltName: Full=Glutamine synthetase I; Short=GSI	52,2	10,23	4	8	6,32E+08	0,24	1,35E+06	0,00	10,66	5	13	3,43E+09	0,18	7,31E+06	0,00
	RecName: Full=2-methylisoborneol synthase; Short=2-MIB synthase	47,5	25,40	9	13	7,68E+08	0,30	1,76E+06	0,00	40,27	12	19	1,64E+09	0,09	3,75E+06	0,00
	RecName: Full=50S ribosomal protein L27	8,9	30,59	2	7	5,97E+08	0,23	7,03E+06	0,00	54,12	3	9	2,60E+09	0,14	3,06E+07	0,00
	RecName: Full=Diaminopimelate decarboxylase; Short=DAP decarboxylase; Short=DAPDC	46,6	1,83	1	2	1,03E+09	0,39	2,35E+06	0,00	2,06	2	5	1,74E+09	0,09	3,98E+06	0,00
glgX	RecName: Full=Glycogen debranching enzyme; AltName: Full=Glycogen operon protein GlgX	74,2	1,21	1	1	6,32E+08	0,24	9,55E+05	0,00	1,21	1	1	7,49E+08	0,04	1,13E+06	0,00
glyA	RecName: Full=Serine hydroxymethyltransferase; Short=SHMT; Short=Serine methylase	45,2	4,38	2	2	7,29E+08	0,28	1,77E+06	0,00	4,38	2	3	1,19E+09	0,06	2,88E+06	0,00
guaA	RecName: Full=GMP synthase [glutamine-hydrolyzing]; AltName: Full=GMP synthetase; AltName: Full=Glutamine amidotransferase	56,7	3,59	2	2	4,80E+08	0,18	9,08E+05	0,00	3,59	2	3	1,83E+09	0,10	3,46E+06	0,00
SCO1214	RecName: Full=6-phosphofructokinase 3; AltName: Full=Phosphofructokinase 3; AltName: Full=Phosphohexokinase 3	36,4	10,26	4	4	2,50E+08	0,10	7,34E+05	0,00	10,26	4	6	1,03E+09	0,05	3,01E+06	0,00

Gene Name	Description	MW[kDa]	sample_Mpa_50per							sample_Cp_50per						
			Coverage	# Peptides	# PSMs	Area	Rel. Area (%)	Norm. Area	ControlQ	Coverage	# Peptides	# PSMs	Area	Rel. Area (%)	Norm. Area	ControlQ
miaA	RecName: Full=tRNA dimethylallyltransferase; AltName: Full=Dimethylallyl diphosphate:tRNA dimethylallyltransferase; Short=DMAPP:tRNA dimethylallyltransferase; Short=DMATase; AltName: Full=Isopentenyl-diphosphate:tRNA isopentenyltransferase; Short=IPP transferase; Short=IPPT; Short=IPTase	33,5	2,33	1	1	9,08E+08	0,35	3,02E+06	0,00		0	0	0,00E+00			0,00
guaA	RecName: Full=GMP synthase [glutamine-hydrolyzing]; AltName: Full=GMP synthetase; AltName: Full=Glutamine amidotransferase	56,6	9,70	4	7	3,67E+08	0,14	6,98E+05	0,00	20,53	7	13	1,92E+09	0,10	3,66E+06	0,00
guaA	RecName: Full=GMP synthase [glutamine-hydrolyzing]; AltName: Full=GMP synthetase; AltName: Full=Glutamine amidotransferase	56,7	11,43	4	8	3,49E+08	0,13	6,65E+05	0,00	20,00	7	17	1,64E+09	0,09	3,12E+06	0,00
	RecName: Full=50S ribosomal protein L7/L12; Short=SA1	13,3	17,32	2	4	8,55E+08	0,33	6,73E+06	0,00	10,24	1	4	2,51E+09	0,13	1,98E+07	0,00
glyA	RecName: Full=Serine hydroxymethyltransferase; Short=SHMT; Short=Serine methylase	45,1	5,10	2	2	6,45E+08	0,25	1,57E+06	0,00	5,10	2	4	1,11E+09	0,06	2,70E+06	0,00
rpsJ	RecName: Full=30S ribosomal protein S10	11,5	26,47	2	4	8,09E+08	0,31	7,93E+06	0,00	27,45	3	8	2,55E+09	0,14	2,50E+07	0,00
hslO	RecName: Full=33 kDa chaperonin; AltName: Full=Heat shock protein 33 homolog; Short=HSP33	34,3		0	0	0,00E+00			0,00		0	0	0,00E+00			0,00
VV0715	RecName: Full=Chaperone protein ClpB	96,0	1,52	1	2	8,36E+08	0,32	9,76E+05	0,00	1,75	2	3	1,20E+09	0,06	1,40E+06	45,97
	RecName: Full=Acetylglutamate kinase; AltName: Full=N-acetyl-L-glutamate 5-phosphotransferase; AltName: Full=NAG kinase; Short=AGK	32,4	3,61	1	3	8,46E+08	0,32	2,77E+06	0,00	3,61	1	4	3,36E+09	0,18	1,10E+07	0,00
	RecName: Full=60 kDa chaperonin 2; AltName: Full=GroEL protein 2; AltName: Full=HSP56; AltName: Full=Protein Cpn60 2	56,7	22,59	10	20	1,08E+09	0,41	2,00E+06	0,18	21,85	11	20	2,72E+09	0,15	5,03E+06	0,00
purA	RecName: Full=Adenylosuccinate synthetase; Short=AMPSase; Short=AdSS; AltName: Full=IMP--aspartate ligase	46,1	10,77	3	5	2,68E+08	0,10	6,27E+05	0,00	10,77	3	7	8,60E+08	0,05	2,01E+06	0,00
SCO1921	RecName: Full=Probable cysteine desulfurase	45,9	5,98	3	6	8,20E+08	0,31	1,96E+06	0,00	5,74	3	4	8,37E+08	0,04	2,00E+06	0,00
valS	RecName: Full=Valine--tRNA ligase; AltName: Full=Valyl-tRNA synthetase; Short=ValRS	101,2	1,67	2	6	3,60E+08	0,14	4,02E+05	0,00	1,67	2	5	1,39E+09	0,07	1,55E+06	0,00
tuf	RecName: Full=Elongation factor Tu; Short=EF-Tu	43,5	9,14	3	17	7,20E+08	0,28	1,83E+06	0,06	6,35	2	19	3,12E+09	0,17	7,93E+06	6,47

Gene Name	Description	MW[kDa]	sample_Mpa_50per							sample_Cp_50per						
			Coverage	# Peptides	# PSMs	Area	Rel. Area (%)	Norm. Area	ControlQ	Coverage	# Peptides	# PSMs	Area	Rel. Area (%)	Norm. Area	ControlQ
	RecName: Full=Streptomycin 6-kinase; AltName: Full=APH(6); AltName: Full=Streptidine kinase; AltName: Full=Streptomycin 6-phosphotransferase	33,2	21,82	5	10	4,29E+08	0,16	1,40E+06	0,00	39,09	8	24	3,14E+09	0,17	1,02E+07	0,00
PMN2A_0187	RecName: Full=Phosphoribosylformylglycinamidine synthase 1; AltName: Full=Phosphoribosylformylglycinamidine synthase I; Short=FGAM synthase I	23,5	5,53	1	1	4,44E+08	0,17	2,04E+06	0,00		0	0	0,00E+00			0,00
SCO1916	RecName: Full=2,3,4,5-tetrahydropyridine-2,6-dicarboxylate N-succinyltransferase; AltName: Full=Tetrahydrodipicolinate N-succinyltransferase; Short=THDP succinyltransferase; Short=THP succinyltransferase; AltName: Full=Tetrahydropicolinate succinylase	33,9	8,81	3	7	5,87E+08	0,23	1,79E+06	0,00	8,81	3	6	2,16E+09	0,12	6,56E+06	0,00
Sde_3968	RecName: Full=ATP synthase subunit alpha; AltName: Full=ATP synthase F1 sector subunit alpha; AltName: Full=F-ATPase subunit alpha	55,0		0	0	0,00E+00			0,00		0	0	0,00E+00			0,00
SCO3409	RecName: Full=Inorganic pyrophosphatase; AltName: Full=Pyrophosphate phospho-hydrolase; Short=PPase	18,7	19,02	4	8	8,93E+08	0,34	5,48E+06	0,00	32,52	7	17	3,73E+09	0,20	2,29E+07	0,00
rpsB	RecName: Full=30S ribosomal protein S2	33,4	25,32	7	17	4,63E+08	0,18	1,50E+06	0,00	18,83	5	11	1,70E+09	0,09	5,53E+06	0,00
	RecName: Full=Chaperone protein ClpB	97,4	0,91	1	1	8,33E+07	0,03	9,45E+04	0,00	0,91	1	1	2,08E+08	0,01	2,36E+05	0,00
	RecName: Full=50S ribosomal protein L21	11,6	28,30	3	5	6,67E+08	0,26	6,29E+06	0,00	19,81	2	5	1,73E+09	0,09	1,63E+07	0,00
hisG	RecName: Full=ATP phosphoribosyltransferase; Short=ATP-PRT; Short=ATP-PRTase	30,9	6,67	2	5	2,88E+08	0,11	1,01E+06	0,00	6,67	2	2	7,26E+08	0,04	2,55E+06	0,00
groEL	RecName: Full=60 kDa chaperonin 2; AltName: Full=GroEL protein 2; AltName: Full=Protein Cpn60 2	56,8	12,94	7	13	8,98E+08	0,34	1,66E+06	0,06	11,09	6	9	2,00E+09	0,11	3,70E+06	45,24
	RecName: Full=30S ribosomal protein S19	2,9	33,33	1	1	4,27E+08	0,16	1,78E+07	0,00	33,33	1	1	1,63E+09	0,09	6,81E+07	0,00
	RecName: Full=30S ribosomal protein S10	11,5	22,55	3	9	1,57E+09	0,60	1,54E+07	0,00	34,31	5	13	6,64E+09	0,36	6,51E+07	0,00
SCO1484	RecName: Full=Carbamoyl-phosphate synthase small chain; AltName: Full=Carbamoyl-phosphate synthetase glutamine chain	40,9	2,37	1	1	4,47E+08	0,17	1,18E+06	0,00	8,68	2	3	7,22E+08	0,04	1,90E+06	0,00
rpsJ	RecName: Full=30S ribosomal protein S10	11,5	22,55	3	9	1,52E+09	0,58	1,49E+07	0,00	22,55	3	10	7,46E+09	0,40	7,31E+07	0,00

Gene Name	Description	MW[kDa]	sample_Mpa_50per							sample_Cp_50per						
			Coverage	# Peptides	# PSMs	Area	Rel. Area (%)	Norm. Area	ControlQ	Coverage	# Peptides	# PSMs	Area	Rel. Area (%)	Norm. Area	ControlQ
carB	RecName: Full=Carbamoyl-phosphate synthase large chain; AltName: Full=Carbamoyl-phosphate synthetase ammonia chain	118,9	1,35	2	3	3,01E+08	0,12	2,70E+05	0,00	1,35	2	2	3,97E+08	0,02	3,57E+05	0,00
glpK	RecName: Full=Glycerol kinase 2; AltName: Full=ATP:glycerol 3-phosphotransferase 2; AltName: Full=Glycerokinase 2; Short=GK 2	55,5	10,06	5	7	3,34E+08	0,13	6,60E+05	0,00	19,53	8	15	7,81E+08	0,04	1,54E+06	0,00
aroC	RecName: Full=Chorismate synthase; AltName: Full=5-enolpyruvylshikimate-3-phosphate phospholyase	41,9	6,22	3	6	2,55E+08	0,10	6,33E+05	0,00	6,22	4	12	2,68E+09	0,14	6,67E+06	0,00
valS	RecName: Full=Valine--tRNA ligase; AltName: Full=Valyl-tRNA synthetase; Short=ValRS	97,5		0	0	0,00E+00			0,00	1,60	1	2	8,19E+08	0,04	9,37E+05	0,00
clpP2	RecName: Full=ATP-dependent Clp protease proteolytic subunit 4; AltName: Full=Endopeptidase Clp 4	24,9	3,54	1	1	5,74E+08	0,22	2,54E+06	0,00	3,54	1	1	1,69E+09	0,09	7,49E+06	0,00
valS	RecName: Full=Valine--tRNA ligase; AltName: Full=Valyl-tRNA synthetase; Short=ValRS	97,5	2,06	1	3	4,31E+08	0,17	4,94E+05	0,00	2,06	1	6	1,79E+09	0,10	2,04E+06	0,00
SCO5368	RecName: Full=ATP synthase subunit c; AltName: Full=ATP synthase F(0) sector subunit c; AltName: Full=F-type ATPase subunit c; Short=F-ATPase subunit c; AltName: Full=Lipid-binding protein	7,6	11,84	1	1	3,60E+08	0,14	4,74E+06	0,00	11,84	1	1	1,06E+09	0,06	1,39E+07	0,00
guaA	RecName: Full=GMP synthase [glutamine-hydrolyzing]; AltName: Full=GMP synthetase; AltName: Full=Glutamine amidotransferase	58,0	2,15	1	3	3,96E+08	0,15	7,75E+05	0,00	2,15	1	2	1,52E+09	0,08	2,98E+06	0,00
	RecName: Full=Tripeptidyl aminopeptidase; Short=Tap; Flags: Precursor	58,2	8,38	3	6	2,39E+08	0,09	4,45E+05	0,00	8,01	3	3	3,91E+08	0,02	7,27E+05	0,00
PPA1182	RecName: Full=Chorismate synthase; AltName: Full=5-enolpyruvylshikimate-3-phosphate phospholyase	41,9	3,27	2	4	5,73E+07	0,02	1,44E+05	0,00	7,79	4	12	1,69E+09	0,09	4,24E+06	0,00
purA	RecName: Full=Adenylosuccinate synthetase; Short=AMPSase; Short=AdSS; AltName: Full=IMP--aspartate ligase	47,8		0	0	0,00E+00			0,00	3,42	1	2	4,23E+08	0,02	9,66E+05	0,00
SP_0820	RecName: Full=ATP-dependent Clp protease ATP-binding subunit ClpE; AltName: Full=Exported protein 4	83,8	2,66	1	5	2,44E+08	0,09	3,24E+05	0,00	2,66	1	7	9,30E+08	0,05	1,24E+06	0,00
ppc	RecName: Full=Phosphoenolpyruvate carboxylase; Short=PEPC; Short=PEPCase	101,1	8,68	7	11	2,17E+08	0,08	2,39E+05	0,00	15,16	11	15	1,49E+09	0,08	1,63E+06	0,00
SCO3127	RecName: Full=Phosphoenolpyruvate carboxylase; Short=PEPC; Short=PEPCase	101,2	10,21	8	13	2,17E+08	0,08	2,39E+05	0,00	17,34	13	22	1,48E+09	0,08	1,62E+06	0,00

Gene Name	Description	MW[kDa]	sample_Mpa_50per							sample_Cp_50per						
			Coverage	# Peptides	# PSMs	Area	Rel. Area (%)	Norm. Area	ControlQ	Coverage	# Peptides	# PSMs	Area	Rel. Area (%)	Norm. Area	ControlQ
SCO2504	RecName: Full=Glycine--tRNA ligase; AltName: Full=Glycyl-tRNA synthetase; Short=GlyRS	52,4	12,17	6	9	2,62E+08	0,10	5,69E+05	0,00	10,65	5	9	1,29E+09	0,07	2,81E+06	0,00
SCO4729	RecName: Full=DNA-directed RNA polymerase subunit alpha; Short=RNAP subunit alpha; AltName: Full=RNA polymerase subunit alpha; AltName: Full=Transcriptase subunit alpha	36,7	21,47	6	10	2,71E+08	0,10	7,96E+05	0,00	36,76	9	13	8,31E+08	0,04	2,44E+06	0,00
Noca_2639	RecName: Full=Proteasome-associated ATPase; AltName: Full=AAA ATPase forming ring-shaped complexes; Short=ARC; AltName: Full=Proteasomal ATPase	64,5	14,04	8	22	1,91E+09	0,73	3,28E+06	0,01	7,02	3	4	1,69E+08	0,01	2,89E+05	0,48
	RecName: Full=Glycogen debranching enzyme; AltName: Full=Glycogen operon protein GlgX	73,6	1,37	1	2	2,41E+08	0,09	3,67E+05	0,00	1,37	1	2	4,06E+08	0,02	6,16E+05	0,00
SCO4078	RecName: Full=Phosphoribosylformylglycinamidine synthase 1; AltName: Full=Phosphoribosylformylglycinamidine synthase I; Short=FGAM synthase I	24,5	4,42	1	1	3,37E+08	0,13	1,49E+06	0,00		0	0	0,00E+00			0,00
SCO1648	RecName: Full=Proteasome-associated ATPase; AltName: Full=AAA ATPase forming ring-shaped complexes; Short=ARC; AltName: Full=Proteasomal ATPase	65,1	29,25	17	55	1,47E+10	5,65	2,50E+07	0,04	18,20	9	17	1,85E+09	0,10	3,15E+06	4,77
groEL	RecName: Full=60 kDa chaperonin; AltName: Full=GroEL protein; AltName: Full=Heat shock protein 60; AltName: Full=Protein Cpn60	57,9	3,87	1	2	1,17E+08	0,05	2,16E+05	0,02	3,87	1	5	4,31E+09	0,23	7,93E+06	0,00
dtxR	RecName: Full=Diphtheria toxin repressor; AltName: Full=Iron-dependent diphtheria tox regulatory element; AltName: Full=Tox regulatory factor	26,9	5,83	1	1	2,90E+08	0,11	1,21E+06	0,00	5,83	1	2	1,27E+09	0,07	5,28E+06	0,00
	RecName: Full=Polyphosphate kinase; AltName: Full=ATP-polyphosphate phosphotransferase; AltName: Full=Polyphosphoric acid kinase	79,2	7,97	6	8	3,00E+08	0,12	4,27E+05	0,00	16,64	10	17	1,09E+09	0,06	1,55E+06	0,00
SCO4710	RecName: Full=50S ribosomal protein L29	8,4	27,03	2	4	6,40E+08	0,25	8,65E+06	0,00	17,57	1	1	3,97E+08	0,02	5,37E+06	0,00
gatB	RecName: Full=Aspartyl/glutamyl-tRNA(Asn/Gln) amidotransferase subunit B; Short=Asp/Glu-ADT subunit B	56,6		0	0	0,00E+00			0,00		0	0	0,00E+00			0,00
SCO3549	RecName: Full=Anti-sigma-B factor antagonist; AltName: Full=Anti-anti-sigma-B factor	12,3	21,24	2	2	2,29E+08	0,09	2,02E+06	0,00	14,16	1	3	2,80E+09	0,15	2,47E+07	0,00
guaB2	RecName: Full=Inosine-5'-monophosphate dehydrogenase; Short=IMP dehydrogenase; Short=IMPD; Short=IMPDH	54,8	2,27	1	1	4,14E+08	0,16	7,83E+05	0,73	2,27	1	1	8,29E+08	0,04	1,57E+06	106,68

Gene Name	Description	MW[kDa]	sample_Mpa_50per							sample_Cp_50per						
			Coverage	# Peptides	# PSMs	Area	Rel. Area (%)	Norm. Area	ControlQ	Coverage	# Peptides	# PSMs	Area	Rel. Area (%)	Norm. Area	ControlQ
purA	RecName: Full=Adenylosuccinate synthetase; Short=AMPSase; Short=AdSS; AltName: Full=IMP--aspartate ligase	46,8	2,55	1	2	2,40E+08	0,09	5,56E+05	0,00	2,55	1	2	6,51E+08	0,03	1,51E+06	0,00
Noca_3923	RecName: Full=Elongation factor G; Short=EF-G	77,5	1,00	1	2	3,47E+08	0,13	4,94E+05	0,00	1,71	1	1	4,46E+08	0,02	6,34E+05	0,00
carA	RecName: Full=Carbamoyl-phosphate synthase small chain; AltName: Full=Carbamoyl-phosphate synthetase glutamine chain	40,8	4,74	2	2	2,78E+08	0,11	7,32E+05	0,00	6,58	2	3	5,62E+08	0,03	1,48E+06	0,00
Tfu_3012	RecName: Full=Adenylosuccinate synthetase; Short=AMPSase; Short=AdSS; AltName: Full=IMP--aspartate ligase	46,7	4,45	1	7	3,18E+08	0,12	7,44E+05	0,00	4,45	1	6	9,18E+08	0,05	2,15E+06	0,00
valS	RecName: Full=Valine--tRNA ligase; AltName: Full=Valyl-tRNA synthetase; Short=ValRS	99,8	1,02	1	1	3,40E+08	0,13	3,84E+05	0,00	1,24	2	3	3,16E+08	0,02	3,57E+05	0,00
rpsL	RecName: Full=30S ribosomal protein S12	13,8	14,63	2	2	3,34E+08	0,13	2,72E+06	0,00	9,76	2	2	1,17E+09	0,06	9,49E+06	0,00
katA	RecName: Full=Catalase	54,5	1,66	1	1	1,07E+09	0,41	2,23E+06	0,00		0	0	0,00E+00			0,00
SCO1391	RecName: Full=Phosphoenolpyruvate-protein phosphotransferase; AltName: Full=Phosphotransferase system, enzyme I	57,2	5,76	3	4	2,02E+08	0,08	3,64E+05	0,00	4,32	2	3	5,12E+08	0,03	9,20E+05	0,00
	RecName: Full=Adenosylhomocysteinase; AltName: Full=S-adenosyl-L-homocysteine hydrolase; Short=AdoHcyase	52,5	10,58	5	5	1,99E+08	0,08	4,12E+05	0,00	12,24	4	6	5,51E+08	0,03	1,14E+06	0,00
guaA	RecName: Full=GMP synthase [glutamine-hydrolyzing]; AltName: Full=GMP synthetase; AltName: Full=Glutamine amidotransferase	56,7	3,59	2	2	1,49E+08	0,06	2,81E+05	0,00	8,32	4	5	5,30E+08	0,03	1,00E+06	0,00
dnaK	RecName: Full=Chaperone protein DnaK; AltName: Full=HSP70; AltName: Full=Heat shock 70 kDa protein; AltName: Full=Heat shock protein 70	65,7	2,28	2	3	3,17E+08	0,12	5,16E+05	0,00	2,28	2	4	7,70E+08	0,04	1,25E+06	1,33
pnp	RecName: Full=Polyribonucleotide nucleotidyltransferase; AltName: Full=Polynucleotide phosphorylase; Short=PNPase	79,2	10,98	8	11	3,05E+08	0,12	4,13E+05	0,28	12,60	9	13	7,64E+08	0,04	1,04E+06	0,00
	RecName: Full=Polyribonucleotide nucleotidyltransferase; AltName: Full=Polynucleotide phosphorylase; Short=PNPase	79,1	9,05	6	8	2,66E+08	0,10	3,60E+05	0,24	13,24	8	11	7,64E+08	0,04	1,03E+06	0,00

Gene Name	Description	MW[kDa]	sample_Mpa_50per							sample_Cp_50per						
			Coverage	# Peptides	# PSMs	Area	Rel. Area (%)	Norm. Area	ControlQ	Coverage	# Peptides	# PSMs	Area	Rel. Area (%)	Norm. Area	ControlQ
rpoB	RecName: Full=DNA-directed RNA polymerase subunit beta; Short=RNAP subunit beta; AltName: Full=RNA polymerase subunit beta; AltName: Full=Transcriptase subunit beta	128,4	14,81	14	17	2,55E+08	0,10	2,20E+05	0,00	17,23	15	19	7,18E+08	0,04	6,19E+05	0,00
	RecName: Full=DNA-directed RNA polymerase subunit beta; Short=RNAP subunit beta; AltName: Full=RNA polymerase subunit beta; AltName: Full=Transcriptase subunit beta	128,2	14,73	14	17	2,55E+08	0,10	2,20E+05	0,00	17,66	16	21	7,18E+08	0,04	6,19E+05	0,00
rplP	RecName: Full=50S ribosomal protein L16	15,8	7,91	1	3	1,94E+08	0,07	1,40E+06	0,00	24,46	2	2	3,31E+08	0,02	2,38E+06	0,00
	RecName: Full=Urease subunit gamma; AltName: Full=Urea amidohydrolase subunit gamma	11,1		0	0	0,00E+00			0,00		0	0	0,00E+00			0,00
SCO5556	RecName: Full=DNA-binding protein HU 2	22,3	4,59	1	1	3,69E+08	0,14	1,69E+06	0,00	4,59	1	1	3,29E+08	0,02	1,51E+06	0,00
pyrG	RecName: Full=CTP synthase; AltName: Full=CTP synthetase; AltName: Full=UTP--ammonia ligase	59,6	2,26	1	2	1,12E+08	0,04	2,10E+05	0,00	2,26	1	1	4,14E+08	0,02	7,78E+05	0,00
ZMO0177	RecName: Full=Glyceraldehyde-3-phosphate dehydrogenase; Short=GAPDH	36,1	4,15	1	1	1,45E+07	0,01	4,31E+04	0,00		0	0	0,00E+00			0,00
SAV_6677	RecName: Full=Proteasome-associated ATPase; AltName: Full=AAA ATPase forming ring-shaped complexes; Short=ARC; AltName: Full=Proteasomal ATPase	65,1	28,74	16	48	1,40E+10	5,39	2,39E+07	0,04	17,69	8	12	1,05E+09	0,06	1,79E+06	2,85
	RecName: Full=50S ribosomal protein L2	30,5	21,22	4	5	1,46E+08	0,06	5,25E+05	0,00	20,86	4	10	6,05E+08	0,03	2,18E+06	0,00
rpsA	RecName: Full=30S ribosomal protein S1	53,2	8,94	4	7	4,26E+08	0,16	8,86E+05	0,00	8,52	4	10	8,86E+08	0,05	1,84E+06	0,00
	RecName: Full=Phosphate-binding protein; Short=HPBP	38,5		0	0	0,00E+00			0,00		0	0	0,00E+00			0,00
	RecName: Full=Hemolysin B	93,3	1,33	1	1	2,82E+08	0,11	3,41E+05	0,00	0,85	1	1	1,31E+08	0,01	1,58E+05	0,00
Tfu_0092	RecName: Full=Malate dehydrogenase	35,1		0	0	0,00E+00			0,00	2,73	1	1	2,39E+08	0,01	7,23E+05	0,00
DR_0325	RecName: Full=Malate dehydrogenase	35,1		0	0	0,00E+00			0,00	2,73	1	1	1,51E+08	0,01	4,56E+05	0,00
mdh	RecName: Full=Malate dehydrogenase	35,4	2,74	1	1	3,01E+07	0,01	9,18E+04	0,00		0	0	0,00E+00			0,00
argB	RecName: Full=Acetylglutamate kinase; AltName: Full=N-acetyl-L-glutamate 5-phosphotransferase; AltName: Full=NAG kinase; Short=AGK	32,3	3,95	1	3	4,08E+08	0,16	1,34E+06	0,00	6,91	2	3	2,89E+08	0,02	9,50E+05	0,00
	RecName: Full=Glutamine synthetase; AltName: Full=Glutamate--ammonia ligase	51,9		0	0	0,00E+00			0,00		0	0	0,00E+00			0,00
rplB	RecName: Full=50S ribosomal protein L2	30,7	7,91	2	3	1,23E+08	0,05	4,44E+05	0,00	3,60	1	1	1,41E+08	0,01	5,07E+05	0,17

Gene Name	Description	MW[kDa]	sample_Mpa_50per							sample_Cp_50per						
			Coverage	# Peptides	# PSMs	Area	Rel. Area (%)	Norm. Area	ControlQ	Coverage	# Peptides	# PSMs	Area	Rel. Area (%)	Norm. Area	ControlQ
infB	RecName: Full=Translation initiation factor IF-2	105,6	5,52	5	5	2,42E+08	0,09	2,34E+05	0,00	4,55	4	5	5,45E+08	0,03	5,28E+05	0,00
	RecName: Full=Putative phosphoribosylformylglycinamidine cyclo-ligase; Short=AIRS; AltName: Full=AIR synthase; AltName: Full=Phosphoribosyl-aminoimidazole synthetase	19,0	6,04	1	1	2,37E+08	0,09	1,30E+06	0,00	6,04	1	2	9,09E+08	0,05	5,00E+06	0,00
SCO4661	RecName: Full=Elongation factor G 1; Short=EF-G 1	77,6	12,99	6	10	2,21E+08	0,08	3,12E+05	0,00	15,96	8	11	1,46E+09	0,08	2,06E+06	0,00
ligA	RecName: Full=DNA ligase; AltName: Full=Polydeoxyribonucleotide synthase [NAD(+)]	80,4	6,16	4	5	1,63E+08	0,06	2,24E+05	0,00	7,40	5	5	7,45E+08	0,04	1,02E+06	0,00
	RecName: Full=Fructose-bisphosphate aldolase; Short=FBP aldolase; Short=FBPA; AltName: Full=Fructose-1,6-bisphosphate aldolase	36,5		0	0	0,00E+00			0,00	2,94	1	1	5,41E+08	0,03	1,59E+06	0,00
Tfu_1809	RecName: Full=Proteasome-associated ATPase; AltName: Full=AAA ATPase forming ring-shaped complexes; Short=ARC; AltName: Full=Proteasomal ATPase	65,3	11,64	7	23	3,13E+09	1,20	5,36E+06	0,01	6,34	3	5	4,93E+08	0,03	8,45E+05	1,61
rpsE	RecName: Full=30S ribosomal protein S5	20,3	20,40	3	4	1,59E+08	0,06	7,91E+05	0,00	37,31	5	8	7,07E+08	0,04	3,52E+06	0,00
rpoB	RecName: Full=DNA-directed RNA polymerase subunit beta; Short=RNAP subunit beta; AltName: Full=RNA polymerase subunit beta; AltName: Full=Transcriptase subunit beta	128,4	3,54	4	5	1,70E+08	0,07	1,47E+05	0,48	4,83	5	5	5,07E+08	0,03	4,38E+05	0,00
rpoH	RecName: Full=RNA polymerase sigma factor RpoH; AltName: Full=RNA polymerase sigma-32 factor	32,6	3,52	1	3	4,99E+09	1,92	1,76E+07	0,03	3,52	1	1	5,82E+08	0,03	2,05E+06	0,00
ahcY	RecName: Full=Adenosylhomocysteinase; AltName: Full=S-adenosyl-L-homocysteine hydrolase; Short=AdoHcyase	51,1	2,58	1	1	1,70E+08	0,07	3,65E+05	0,00	2,58	1	1	6,07E+08	0,03	1,30E+06	0,00
	RecName: Full=Glucose-6-phosphate 1-dehydrogenase 2; Short=G6PD 2	57,3	3,50	2	2	1,94E+08	0,07	3,77E+05	0,00	2,14	1	1	5,28E+08	0,03	1,03E+06	0,00
infC	RecName: Full=Translation initiation factor IF-3	24,2	7,37	1	2	1,25E+08	0,05	5,76E+05	0,00	11,52	2	2	5,09E+08	0,03	2,34E+06	0,00
	RecName: Full=ATP synthase subunit beta; AltName: Full=ATP synthase F1 sector subunit beta; AltName: Full=F-ATPase subunit beta	51,1	4,94	2	2	1,81E+08	0,07	3,89E+05	0,14	4,94	2	4	8,26E+08	0,04	1,77E+06	5,11
SCO7154	RecName: Full=Ketol-acid reductoisomerase 2; AltName: Full=Acetohydroxy-acid isomeroreductase 2; AltName: Full=Alpha-keto-beta-hydroxylacyl reductoisomerase 2	36,3	10,24	3	3	1,65E+08	0,06	4,96E+05	0,00	10,24	3	5	4,58E+08	0,02	1,38E+06	0,00

Gene Name	Description	MW[kDa]	sample_Mpa_50per							sample_Cp_50per						
			Coverage	# Peptides	# PSMs	Area	Rel. Area (%)	Norm. Area	ControlQ	Coverage	# Peptides	# PSMs	Area	Rel. Area (%)	Norm. Area	ControlQ
hisB	RecName: Full=Imidazoleglycerol-phosphate dehydratase; Short=IGPD	21,6	4,57	1	2	2,59E+08	0,10	1,32E+06	0,00	5,58	1	2	6,09E+08	0,03	3,09E+06	0,00
rplB	RecName: Full=50S ribosomal protein L2	31,2	6,79	2	3	1,04E+08	0,04	3,71E+05	0,00	8,57	2	2	9,89E+07	0,01	3,53E+05	0,12
hpd	RecName: Full=4-hydroxyphenylpyruvate dioxygenase; Short=4HPPD; Short=HPD; Short=HPPDase	41,8	4,46	1	1	0,00E+00			0,00	12,07	3	4	2,62E+08	0,01	6,88E+05	0,00
gdhA	RecName: Full=NADP-specific glutamate dehydrogenase; Short=NADP-GDH	49,5		0	0	0,00E+00			0,00	2,23	1	1	3,32E+08	0,02	7,42E+05	0,00
SCO3619	RecName: Full=Nucleoid-associated protein SCO3619	11,7	20,00	2	2	1,55E+08	0,06	1,35E+06	0,00	11,30	1	1	2,31E+08	0,01	2,01E+06	0,00
rpsB	RecName: Full=30S ribosomal protein S2	29,9	8,79	2	3	2,23E+08	0,09	8,18E+05	0,00	8,79	2	6	7,61E+08	0,04	2,79E+06	0,00
SCO4159	RecName: Full=Transcriptional regulatory protein GlnR	28,9	13,48	2	3	1,59E+08	0,06	5,95E+05	0,00	13,48	2	4	6,14E+08	0,03	2,30E+06	0,00
	RecName: Full=Superoxide dismutase [Mn]	15,0	5,07	1	1	6,35E+07	0,02	4,60E+05	0,00	5,07	1	1	1,29E+08	0,01	9,33E+05	0,00
SCO1578	RecName: Full=Acetylglutamate kinase; AltName: Full=N-acetyl-L-glutamate 5-phosphotransferase; AltName: Full=NAG kinase; Short=AGK	32,4	3,59	1	3	0,00E+00			0,00	6,54	2	2	1,00E+08	0,01	3,27E+05	0,00
SCO5373	RecName: Full=ATP synthase subunit beta; AltName: Full=ATP synthase F1 sector subunit beta; AltName: Full=F-ATPase subunit beta	52,1	6,07	2	2	1,42E+08	0,05	2,98E+05	0,00	6,07	2	3	1,30E+09	0,07	2,72E+06	0,00
	RecName: Full=Acetolactate synthase large subunit IlvB1; Short=ALS; AltName: Full=Acetohydroxy-acid synthase large subunit; Short=AHAS	66,1	2,10	1	2	1,50E+08	0,06	2,43E+05	0,00	2,10	1	1	2,54E+08	0,01	4,11E+05	0,00
prsA1	RecName: Full=Ribose-phosphate pyrophosphokinase; Short=RPPK; AltName: Full=Phosphoribosyl pyrophosphate synthase; Short=P-Rib-PP synthase; Short=PRPP synthase	35,3	10,80	3	4	1,41E+08	0,05	4,36E+05	0,00	21,91	5	7	5,00E+08	0,03	1,54E+06	0,00
	RecName: Full=Glutamine synthetase 2; AltName: Full=Glutamate--ammonia ligase II; AltName: Full=Glutamine synthetase II; Short=GSII	37,2	6,71	2	3	1,90E+08	0,07	5,53E+05	0,00	4,08	1	2	1,20E+09	0,06	3,50E+06	0,00
rpsS	RecName: Full=30S ribosomal protein S19	10,7	11,83	2	2	1,33E+08	0,05	1,43E+06	0,00	11,83	2	2	4,39E+08	0,02	4,72E+06	0,05
rpoB	RecName: Full=DNA-directed RNA polymerase subunit beta; Short=RNAP subunit beta; AltName: Full=RNA polymerase subunit beta; AltName: Full=Transcriptase subunit beta	153,2	1,16	2	3	1,65E+08	0,06	1,19E+05	0,31	0,58	1	1	4,83E+08	0,03	3,51E+05	91,77

Gene Name	Description	MW[kDa]	sample_Mpa_50per							sample_Cp_50per						
			Coverage	# Peptides	# PSMs	Area	Rel. Area (%)	Norm. Area	ControlQ	Coverage	# Peptides	# PSMs	Area	Rel. Area (%)	Norm. Area	ControlQ
ECP_2501	RecName: Full=Phosphoribosylformylglycinamidine cyclo-ligase; AltName: Full=AIR synthase; AltName: Full=AIRS; AltName: Full=Phosphoribosyl-aminoimidazole synthetase	36,8	4,64	1	1	2,04E+07	0,01	5,91E+04	0,00	4,64	1	1	2,42E+08	0,01	7,01E+05	0,00
engA	RecName: Full=GTPase Der; AltName: Full=GTP-binding protein EngA	53,3	2,24	1	1	9,24E+07	0,04	1,88E+05	0,00	1,63	1	1	1,02E+08	0,01	2,08E+05	0,00
rpsC	RecName: Full=30S ribosomal protein S3	30,0	10,55	3	5	2,98E+08	0,11	1,08E+06	0,00	11,27	3	4	5,27E+08	0,03	1,92E+06	0,00
	RecName: Full=Histidine ammonia-lyase; Short=Histidase	53,1	10,51	4	5	8,42E+07	0,03	1,64E+05	0,00	23,93	7	8	4,72E+08	0,03	9,19E+05	0,00
ML1316	RecName: Full=Proteasome-associated ATPase; AltName: Full=AAA ATPase forming ring-shaped complexes; Short=ARC; AltName: Full=Mycobacterial proteasome ATPase	67,4	3,94	3	9	1,12E+09	0,43	1,83E+06	0,01	1,81	1	2	2,45E+08	0,01	4,02E+05	0,00
	RecName: Full=Proteasome-associated ATPase; AltName: Full=AAA ATPase forming ring-shaped complexes; Short=ARC; AltName: Full=Proteasomal ATPase	66,4	7,65	5	14	1,57E+09	0,60	2,62E+06	0,01	4,49	2	3	2,10E+08	0,01	3,50E+05	0,34
RHA1_ro00849	RecName: Full=Proteasome-associated ATPase; AltName: Full=AAA ATPase forming ring-shaped complexes; Short=ARC; AltName: Full=Proteasomal ATPase	65,8	7,45	5	16	1,30E+09	0,50	2,20E+06	0,01	4,23	2	3	1,65E+08	0,01	2,80E+05	0,47
ribH	RecName: Full=6,7-dimethyl-8-ribityllumazine synthase; Short=DMRL synthase; Short=LS; Short=Lumazine synthase	16,8	15,53	2	4	1,13E+08	0,04	7,03E+05	0,00	6,83	1	1	3,22E+08	0,02	2,00E+06	0,00
	RecName: Full=Ferredoxin-dependent glutamate synthase 1; AltName: Full=Fd-GOGAT	169,0	0,77	1	2	8,11E+07	0,03	5,23E+04	0,00	0,77	1	1	3,59E+08	0,02	2,31E+05	0,00
secA	RecName: Full=Protein translocase subunit SecA	101,4	1,43	1	1	1,27E+08	0,05	1,40E+05	2,75	1,43	1	1	3,75E+08	0,02	4,13E+05	0,00
rpsP	RecName: Full=30S ribosomal protein S16	15,4	11,27	1	1	2,88E+08	0,11	2,03E+06	0,00	11,27	1	2	1,35E+09	0,07	9,50E+06	0,00
rpsK	RecName: Full=30S ribosomal protein S11	14,4	23,88	3	6	9,91E+07	0,04	7,40E+05	0,00	41,04	4	14	9,64E+08	0,05	7,19E+06	0,00
eno	RecName: Full=Enolase; AltName: Full=2-phospho-D-glycerate hydro-lyase; AltName: Full=2-phosphoglycerate dehydratase	45,8	15,42	4	6	1,32E+08	0,05	3,08E+05	0,00	18,46	5	8	4,55E+08	0,02	1,06E+06	0,00
sucC	RecName: Full=Succinyl-CoA ligase [ADP-forming] subunit beta; AltName: Full=Succinyl-CoA synthetase subunit beta; Short=SCS-beta	40,6	2,31	1	1	8,35E+07	0,03	2,15E+05	0,00	2,31	1	1	1,55E+08	0,01	3,99E+05	0,00
GOX1171	RecName: Full=Histidinol-phosphate aminotransferase 1; AltName: Full=Imidazole acetol-phosphate transaminase 1	44,1		0	0	0,00E+00			0,00		0	0	0,00E+00			0,00

Gene Name	Description	MW[kDa]	sample_Mpa_50per							sample_Cp_50per						
			Coverage	# Peptides	# PSMs	Area	Rel. Area (%)	Norm. Area	ControlQ	Coverage	# Peptides	# PSMs	Area	Rel. Area (%)	Norm. Area	ControlQ
SCO2927	RecName: Full=4-hydroxyphenylpyruvate dioxygenase; Short=4HPPD; Short=HPD; Short=HPPDase	41,8	7,61	2	2	7,65E+07	0,03	2,01E+05	0,00	11,02	4	5	2,84E+08	0,02	7,44E+05	0,00
	RecName: Full=NADP-specific glutamate dehydrogenase; Short=NADP-GDH	48,6		0	0	0,00E+00			0,00		0	0	0,00E+00			0,00
infB	RecName: Full=Translation initiation factor IF-2	106,8	5,35	5	5	1,97E+08	0,08	1,89E+05	0,00	6,02	5	8	5,97E+08	0,03	5,71E+05	0,00
SCO4827	RecName: Full=Malate dehydrogenase	34,6		0	0	0,00E+00			0,00	3,34	1	1	4,93E+08	0,03	1,50E+06	0,00
SCO2771	RecName: Full=Uncharacterized phosphatase SCO2771	28,4	3,44	1	1	1,20E+08	0,05	4,58E+05	0,00	9,54	2	2	3,80E+08	0,02	1,45E+06	0,00
SCO2301	RecName: Full=Putative GTP cyclohydrolase 1 type 2; AltName: Full=GTP cyclohydrolase I	30,2		0	0	0,00E+00			0,00	5,61	2	2	1,84E+08	0,01	6,46E+05	0,00
gdh	RecName: Full=NADP-specific glutamate dehydrogenase; Short=NADP-GDH	49,0	8,95	3	6	1,15E+08	0,04	2,58E+05	2,31	8,95	3	6	3,36E+08	0,02	7,51E+05	0,00
	RecName: Full=Exodeoxyribonuclease 7 small subunit; AltName: Full=Exodeoxyribonuclease VII small subunit; Short=Exonuclease VII small subunit	8,9	10,26	1	1	1,67E+08	0,06	2,14E+06	0,00	10,26	1	1	4,62E+08	0,02	5,93E+06	0,00
SCO2547	RecName: Full=Ribonuclease Z; Short=RNase Z; AltName: Full=tRNA 3 endonuclease; AltName: Full=tRNase Z	33,4	9,97	2	5	2,02E+08	0,08	6,71E+05	0,00	13,62	3	6	5,57E+08	0,03	1,85E+06	0,00
	RecName: Full=Depupylase	56,5	5,77	2	4	1,81E+08	0,07	3,60E+05	0,00	5,77	2	3	9,06E+08	0,05	1,80E+06	0,00
	RecName: Full=Enolase; AltName: Full=2-phospho-D-glycerate hydro-lyase; AltName: Full=2-phosphoglycerate dehydratase	44,9	3,50	1	2	1,56E+08	0,06	3,64E+05	0,00		0	0	0,00E+00			0,00
clpC	RecName: Full=Probable ATP-dependent Clp protease ATP-binding subunit	93,9	1,30	2	2	1,45E+08	0,06	1,72E+05	0,00	5,78	4	6	4,64E+08	0,02	5,47E+05	0,00
ureA	RecName: Full=Urease subunit gamma; AltName: Full=Urea amidohydrolase subunit gamma	11,0		0	0	0,00E+00			0,00	18,00	2	3	2,48E+08	0,01	2,48E+06	0,00
gatB	RecName: Full=Aspartyl/glutamyl-tRNA(Asn/Gln) amidotransferase subunit B; Short=Asp/Glu-ADT subunit B	54,5	3,56	2	2	6,08E+07	0,02	1,20E+05	0,00	2,57	1	2	6,69E+08	0,04	1,33E+06	0,00
	RecName: Full=30S ribosomal protein S7	17,4	17,95	2	2	9,22E+07	0,04	5,91E+05	0,73	14,10	2	2	3,06E+08	0,02	1,96E+06	0,00
SCO3878	RecName: Full=DNA polymerase III subunit beta	39,9	2,93	1	1	6,85E+07	0,03	1,82E+05	0,00	8,51	2	2	3,38E+08	0,02	8,99E+05	0,00
dapE	RecName: Full=Succinyl-diaminopimelate desuccinylase; Short=SDAP desuccinylase	39,9	2,17	1	1	1,98E+08	0,08	5,37E+05	0,00	2,17	1	1	4,38E+08	0,02	1,19E+06	0,00

Gene Name	Description	MW[kDa]	sample_Mpa_50per							sample_Cp_50per						
			Coverage	# Peptides	# PSMs	Area	Rel. Area (%)	Norm. Area	ControlQ	Coverage	# Peptides	# PSMs	Area	Rel. Area (%)	Norm. Area	ControlQ
	RecName: Full=Aminoglycoside 3'-phosphotransferase; AltName: Full=APH(3')-II; Short=APH(3')II; AltName: Full=Kanamycin kinase, type II; AltName: Full=Neomycin-kanamycin phosphotransferase type II	29,0		0	0	0,00E+00			0,00		0	0	0,00E+00			0,00
MSMEI_6720	RecName: Full=Inositol-3-phosphate synthase; Short=IPS; AltName: Full=Myo-inositol 1-phosphate synthase; Short=MI-1-P synthase; Short=MIP synthase	39,3	3,31	1	1	1,96E+08	0,08	5,40E+05	0,00	8,26	2	5	3,67E+08	0,02	1,01E+06	0,00
rpoC	RecName: Full=DNA-directed RNA polymerase subunit beta'; Short=RNAP subunit beta'; AltName: Full=RNA polymerase subunit beta'; AltName: Full=Transcriptase subunit beta'	145,0	10,39	12	15	1,17E+08	0,05	9,03E+04	0,06	10,55	11	13	3,16E+08	0,02	2,43E+05	0,00
frr	RecName: Full=Ribosome-recycling factor; Short=RRF; AltName: Full=Ribosome-releasing factor	20,7	8,65	1	1	1,78E+08	0,07	9,63E+05	0,00		0	0	0,00E+00			0,00
groEL	RecName: Full=60 kDa chaperonin 2; AltName: Full=GroEL protein 2; AltName: Full=Protein Cpn60 2	56,4	6,21	3	4	1,66E+08	0,06	3,13E+05	0,00	4,52	2	3	9,34E+08	0,05	1,76E+06	0,00
	RecName: Full=Glyceraldehyde-3-phosphate dehydrogenase A; Short=GAPDH-A	35,5	2,42	1	1	1,15E+08	0,04	3,48E+05	0,69	2,42	1	2	2,08E+08	0,01	6,27E+05	0,00
SCO1644	RecName: Full=Proteasome subunit beta; AltName: Full=20S proteasome beta subunit; AltName: Full=Proteasome core protein PrcB; Flags: Precursor	30,1	19,22	5	38	3,54E+08	0,14	1,26E+06	0,00	34,16	10	247	3,20E+11	17,14	1,14E+09	0,64
pepA	RecName: Full=Probable cytosol aminopeptidase; AltName: Full=Leucine aminopeptidase; Short=LAP; AltName: Full=Leucyl aminopeptidase	56,6	2,40	1	1	1,44E+08	0,06	2,87E+05	0,00	2,40	1	1	3,54E+08	0,02	7,06E+05	0,00
Arth_2173	RecName: Full=Proteasome-associated ATPase; AltName: Full=AAA ATPase forming ring-shaped complexes; Short=ARC; AltName: Full=Proteasomal ATPase	65,5	4,21	3	12	7,37E+08	0,28	1,24E+06	0,00		0	0	0,00E+00			0,00
carB	RecName: Full=Carbamoyl-phosphate synthase large chain; AltName: Full=Carbamoyl-phosphate synthetase ammonia chain	113,5		0	0	0,00E+00			0,00	1,46	1	1	3,48E+08	0,02	3,38E+05	0,00
clpB	RecName: Full=Chaperone protein ClpB	92,8		0	0	0,00E+00			0,00		0	0	0,00E+00			0,00
SCO3005	RecName: Full=Protein translocase subunit SecA	106,4	6,23	5	6	1,35E+08	0,05	1,42E+05	2,92	3,59	3	3	1,39E+08	0,01	1,47E+05	0,00

Gene Name	Description	MW[kDa]	sample_Mpa_50per							sample_Cp_50per						
			Coverage	# Peptides	# PSMs	Area	Rel. Area (%)	Norm. Area	ControlQ	Coverage	# Peptides	# PSMs	Area	Rel. Area (%)	Norm. Area	ControlQ
PPA1883	RecName: Full=DNA-directed RNA polymerase subunit beta'; Short=RNAP subunit beta'; AltName: Full=RNA polymerase subunit beta'; AltName: Full=Transcriptase subunit beta'	143,4	2,86	4	4	1,28E+08	0,05	9,92E+04	0,05	3,33	4	5	2,06E+08	0,01	1,60E+05	0,00
trpB	RecName: Full=Tryptophan synthase beta chain	45,5	7,71	3	4	1,11E+08	0,04	2,60E+05	0,00	2,80	1	2	6,64E+08	0,04	1,55E+06	0,00
SCO2037	RecName: Full=Tryptophan synthase beta chain	45,4	7,73	3	4	1,11E+08	0,04	2,61E+05	0,00	4,92	2	3	6,40E+08	0,03	1,50E+06	0,00
	RecName: Full=Probable aspartate aminotransferase; Short=AspAT; AltName: Full=Transaminase A	22,7	8,45	1	1	6,67E+07	0,03	3,13E+05	0,00	8,45	1	1	2,28E+08	0,01	1,07E+06	0,00
ppnK	RecName: Full=Probable inorganic polyphosphate/ATP-NAD kinase 2; Short=Poly(P)/ATP NAD kinase 2	32,1	8,97	3	5	8,37E+07	0,03	2,78E+05	0,00	12,62	4	5	2,29E+08	0,01	7,59E+05	0,00
prcB1	RecName: Full=Proteasome subunit beta 2; AltName: Full=20S proteasome beta subunit 2; AltName: Full=Proteasome core protein PrcB 2; Flags: Precursor	30,3	24,20	5	50	3,49E+08	0,13	1,24E+06	0,00	36,30	11	232	1,82E+11	9,76	6,48E+08	0,47
SAV_4896	RecName: Full=UPF0234 protein SAV_4896	18,0		0	0	0,00E+00			0,00	15,43	2	2	1,56E+08	0,01	9,65E+05	0,00
eno	RecName: Full=Enolase 1; AltName: Full=2-phospho-D-glycerate hydro-lyase 1; AltName: Full=2-phosphoglycerate dehydratase 1	45,5	10,80	3	4	1,14E+08	0,04	2,68E+05	0,00	14,08	4	7	3,13E+08	0,02	7,34E+05	0,00
oprI	RecName: Full=Major outer membrane lipoprotein; Short=Outer membrane lipoprotein I; Flags: Precursor	8,8	12,05	1	1	2,91E+08	0,11	3,51E+06	0,00		0	0	0,00E+00			0,00
	RecName: Full=50S ribosomal protein L3	22,4		0	0	0,00E+00			0,00		0	0	0,00E+00			0,00
SCO3907	RecName: Full=Single-stranded DNA-binding protein 2; Short=SSB 2; AltName: Full=Helix-destabilizing protein 2	19,9	6,03	1	1	8,94E+07	0,03	4,49E+05	0,00		0	0	0,00E+00			0,00
icd	RecName: Full=Isocitrate dehydrogenase [NADP]; Short=IDH; AltName: Full=Oxalosuccinate decarboxylase	80,0		0	0	0,00E+00			0,00	4,74	2	2	2,55E+08	0,01	3,45E+05	0,00
glmU	RecName: Full=Bifunctional protein GlmU; Includes: RecName: Full=UDP-N-acetylglucosamine pyrophosphorylase; AltName: Full=N-acetylglucosamine-1-phosphate uridyltransferase; Includes: RecName: Full=Glucosamine-1-phosphate N-acetyltransferase	49,8	2,07	1	1	2,69E+07	0,01	5,58E+04	0,00	3,73	2	2	2,10E+08	0,01	4,35E+05	0,00

Gene Name	Description	MW[kDa]	sample_Mpa_50per							sample_Cp_50per						
			Coverage	# Peptides	# PSMs	Area	Rel. Area (%)	Norm. Area	ControlQ	Coverage	# Peptides	# PSMs	Area	Rel. Area (%)	Norm. Area	ControlQ
carB	RecName: Full=Carbamoyl-phosphate synthase large chain; AltName: Full=Carbamoyl-phosphate synthetase ammonia chain	117,8	4,81	4	5	5,90E+07	0,02	5,36E+04	0,91	13,16	12	15	3,52E+08	0,02	3,20E+05	0,00
rplE	RecName: Full=50S ribosomal protein L5	20,8	18,38	3	4	8,64E+07	0,03	4,67E+05	0,00	7,57	1	2	6,12E+08	0,03	3,31E+06	0,00
	RecName: Full=Pyruvate dehydrogenase E1 component; Short=PDH E1 component	100,2		0	0	0,00E+00			0,00		0	0	0,00E+00			0,00
tig	RecName: Full=Trigger factor; Short=TF; AltName: Full=PPIase	50,6	7,56	3	5	1,73E+08	0,07	3,75E+05	0,00	9,29	4	8	5,36E+08	0,03	1,16E+06	0,00
rplL	RecName: Full=50S ribosomal protein L7/L12	12,7	11,57	1	2	8,18E+07	0,03	6,76E+05	0,00		0	0	0,00E+00			0,00
SCO3123	RecName: Full=Ribose-phosphate pyrophosphokinase; Short=RPPK; AltName: Full=Phosphoribosyl pyrophosphate synthase; Short=P-Rib-PP synthase; Short=PRPP synthase	35,2	7,72	2	2	1,25E+08	0,05	3,86E+05	0,00	12,65	3	3	2,65E+08	0,01	8,17E+05	0,00
tsf	RecName: Full=Elongation factor Ts; Short=EF-Ts	29,8	10,79	3	4	9,31E+07	0,04	3,35E+05	0,00	10,79	3	3	3,06E+08	0,02	1,10E+06	0,00
Mmcs_0970	RecName: Full=DNA-directed RNA polymerase subunit beta'; Short=RNAP subunit beta'; AltName: Full=RNA polymerase subunit beta'; AltName: Full=Transcriptase subunit beta'	146,8	3,50	4	4	6,53E+07	0,03	4,97E+04	0,02	1,29	2	2	6,56E+07	0,00	4,99E+04	0,00
SSP0976	RecName: Full=S-adenosylmethionine synthase; Short=AdoMet synthase; AltName: Full=MAT; AltName: Full=Methionine adenosyltransferase	43,9	3,52	1	2	9,26E+07	0,04	2,33E+05	0,00	3,52	1	1	4,50E+07	0,00	1,13E+05	0,18
tpiA	RecName: Full=Triosephosphate isomerase; Short=TIM; AltName: Full=Triose-phosphate isomerase	27,9	8,14	2	2	9,00E+07	0,03	3,49E+05	0,00	7,75	3	3	2,91E+08	0,02	1,13E+06	0,00
MSMEG_4699	RecName: Full=NAD-specific glutamate dehydrogenase; Short=NAD-GDH; AltName: Full=NAD(+)-dependent glutamate dehydrogenase	174,0	0,50	1	1	9,26E+07	0,04	5,81E+04	0,00		0	0	0,00E+00			0,00
murE	RecName: Full=UDP-N-acetylmuramoyl-L-alanyl-D-glutamate--2,6-diaminopimelate ligase; AltName: Full=Meso-A2pm-adding enzyme; AltName: Full=Meso-diaminopimelate-adding enzyme; AltName: Full=UDP-MurNAc-L-Ala-D-Glu:meso-diaminopimelate ligase; AltName: Full=UDP-MurNAc-tripeptide synthetase; AltName: Full=UDP-N-acetylmuramyl-tripeptide synthetase	53,2	1,78	1	1	7,84E+07	0,03	1,55E+05	0,00	4,35	2	2	2,93E+08	0,02	5,80E+05	0,00
	RecName: Full=Protein translocase subunit SecA	105,1	10,85	9	9	1,68E+08	0,06	1,79E+05	3,64	9,04	7	8	2,62E+08	0,01	2,79E+05	0,00

Gene Name	Description	MW[kDa]	sample_Mpa_50per							sample_Cp_50per						
			Coverage	# Peptides	# PSMs	Area	Rel. Area (%)	Norm. Area	ControlQ	Coverage	# Peptides	# PSMs	Area	Rel. Area (%)	Norm. Area	ControlQ
gyrB	RecName: Full=DNA gyrase subunit B	75,4	6,27	4	4	9,80E+07	0,04	1,43E+05	0,00	8,45	4	5	2,93E+08	0,02	4,27E+05	0,00
	RecName: Full=Outer membrane protein Omp38; AltName: Full=Outer membrane protein OmpA; AltName: Full=Outer membrane protein OmpAb; Flags: Precursor	38,4	6,74	3	5	1,08E+08	0,04	3,02E+05	0,00	3,09	1	2	7,19E+07	0,00	2,02E+05	0,00
glpK	RecName: Full=Glycerol kinase 3; AltName: Full=ATP:glycerol 3-phosphotransferase 3; AltName: Full=Glycerokinase 3; Short=GK 3	55,3	3,96	2	2	1,44E+08	0,06	2,85E+05	0,00	20,59	8	18	7,78E+08	0,04	1,54E+06	0,00
	RecName: Full=DNA-directed RNA polymerase subunit beta'; Short=RNAP subunit beta'; AltName: Full=RNA polymerase subunit beta'; AltName: Full=Transcriptase subunit beta'	170,8	0,46	1	1	3,09E+07	0,01	2,03E+04	0,02	0,59	1	1	1,08E+08	0,01	7,06E+04	0,00
Sfri_3056	RecName: Full=ATP synthase subunit alpha 1; AltName: Full=ATP synthase F1 sector subunit alpha 1; AltName: Full=F-ATPase subunit alpha 1	56,0	2,32	1	1	1,44E+08	0,06	2,79E+05	0,00	2,32	1	1	2,75E+08	0,01	5,32E+05	0,00
	RecName: Full=Transcription termination/antitermination protein NusG	31,8	14,63	4	5	6,04E+07	0,02	2,05E+05	0,00	15,99	4	6	1,58E+08	0,01	5,38E+05	0,00
infA	RecName: Full=Translation initiation factor IF-1	8,2	11,11	1	1	1,06E+08	0,04	1,47E+06	0,00	22,22	2	3	5,85E+08	0,03	8,13E+06	0,00
oprL	RecName: Full=Peptidoglycan-associated lipoprotein; Flags: Precursor	17,8	11,45	2	2	1,44E+08	0,06	8,69E+05	0,00		0	0	0,00E+00			0,00
sucC	RecName: Full=Succinyl-CoA ligase [ADP-forming] subunit beta-1; AltName: Full=Succinyl-CoA synthetase subunit beta-1; Short=SCS-beta-1	41,6	7,36	3	3	1,12E+08	0,04	2,84E+05	0,00	11,93	5	6	3,22E+08	0,02	8,18E+05	0,00
tsf	RecName: Full=Elongation factor Ts; Short=EF-Ts	29,8	12,95	3	4	1,13E+08	0,04	4,07E+05	0,00	12,95	3	4	3,83E+08	0,02	1,38E+06	0,00
pyrE	RecName: Full=Orotate phosphoribosyltransferase; Short=OPRT; Short=OPRTase	19,1		0	0	0,00E+00			0,00		0	0	0,00E+00			0,00
SCO2470	RecName: Full=Deoxyguanosinetriphosphate triphosphohydrolase-like protein	45,9	4,95	2	2	2,30E+08	0,09	5,41E+05	0,00	2,12	1	1	9,35E+08	0,05	2,21E+06	0,00
hmgA	RecName: Full=Homogentisate 1,2-dioxygenase; AltName: Full=Homogentisate oxygenase; AltName: Full=Homogentisic acid oxidase; AltName: Full=Homogentisicase	47,8	2,74	1	1	0,00E+00			0,00	10,50	3	9	5,01E+08	0,03	1,14E+06	0,00

Gene Name	Description	MW[kDa]	sample_Mpa_50per							sample_Cp_50per						
			Coverage	# Peptides	# PSMs	Area	Rel. Area (%)	Norm. Area	ControlQ	Coverage	# Peptides	# PSMs	Area	Rel. Area (%)	Norm. Area	ControlQ
msrA	RecName: Full=Peptide methionine sulfoxide reductase MsrA; Short=Protein-methionine-S-oxide reductase; AltName: Full=Peptide-methionine (S)-S-oxide reductase; Short=Peptide Met(O) reductase	20,1	5,68	1	1	5,14E+07	0,02	2,92E+05	0,00		0	0	0,00E+00			0,00
rpmB	RecName: Full=50S ribosomal protein L28-1	6,6	14,75	1	1	1,00E+08	0,04	1,64E+06	0,00		0	0	0,00E+00			0,00
rpsO	RecName: Full=30S ribosomal protein S15	10,8	35,79	3	4	6,99E+07	0,03	7,35E+05	0,00	35,79	3	6	2,93E+08	0,02	3,09E+06	0,00
rplE	RecName: Full=50S ribosomal protein L5	20,0	9,50	1	1	2,11E+07	0,01	1,18E+05	0,00	9,50	1	2	3,20E+08	0,02	1,79E+06	0,00
glmU	RecName: Full=Bifunctional protein GlmU; Includes: RecName: Full=UDP-N-acetylglucosamine pyrophosphorylase; AltName: Full=N-acetylglucosamine-1-phosphate uridyltransferase; Includes: RecName: Full=Glucosamine-1-phosphate N-acetyltransferase	50,0		0	0	0,00E+00			0,00	4,15	2	2	5,55E+08	0,03	1,15E+06	0,00
PPA1193	RecName: Full=S-adenosylmethionine synthase; Short=AdoMet synthase; AltName: Full=MAT; AltName: Full=Methionine adenosyltransferase	42,2	5,79	2	3	6,24E+07	0,02	1,57E+05	5,97	6,30	2	2	6,90E+07	0,00	1,74E+05	17,97
carB	RecName: Full=Carbamoyl-phosphate synthase large chain; AltName: Full=Carbamoyl-phosphate synthetase ammonia chain	117,3	0,95	1	1	9,72E+07	0,04	9,19E+04	0,00		0	0	0,00E+00			0,00
katG	RecName: Full=Catalase-peroxidase; Short=CP; AltName: Full=Peroxidase/catalase	82,4	1,32	1	1	5,53E+07	0,02	7,31E+04	0,00		0	0	0,00E+00			0,00
gltD	RecName: Full=Glutamate synthase [NADPH] small chain; AltName: Full=NADPH-GOGAT	54,8	2,03	1	1	5,91E+07	0,02	1,20E+05	0,00		0	0	0,00E+00			0,00
SCO3873	RecName: Full=DNA gyrase subunit A	94,5	6,65	4	4	3,50E+07	0,01	4,09E+04	0,00	4,20	3	4	2,90E+08	0,02	3,39E+05	0,00
rplB	RecName: Full=50S ribosomal protein L2	26,4		0	0	0,00E+00			0,00	7,23	1	1	3,93E+07	0,00	1,67E+05	0,00
rplB	RecName: Full=50S ribosomal protein L2	30,6		0	0	0,00E+00			0,00	10,39	2	3	2,65E+07	0,00	9,48E+04	0,00
SCO2848	RecName: Full=UPF0303 protein SCO2848	17,2	5,70	1	1	9,52E+07	0,04	6,02E+05	0,00	5,70	1	1	2,03E+08	0,01	1,28E+06	0,00

Gene Name	Description	MW[kDa]	sample_Mpa_50per							sample_Cp_50per						
			Coverage	# Peptides	# PSMs	Area	Rel. Area (%)	Norm. Area	ControlQ	Coverage	# Peptides	# PSMs	Area	Rel. Area (%)	Norm. Area	ControlQ
gcp	RecName: Full=tRNA N6-adenosine threonylcarbamoyltransferase; AltName: Full=t(6)A37 threonylcarbamoyladenosine biosynthesis protein TsaD; AltName: Full=tRNA threonylcarbamoyladenosine biosynthesis protein TsaD	35,4		0	0	0,00E+00			0,00		0	0	0,00E+00			0,00
carB	RecName: Full=Carbamoyl-phosphate synthase large chain; AltName: Full=Carbamoyl-phosphate synthetase ammonia chain	117,8	2,09	2	2	4,54E+07	0,02	4,12E+04	0,00	8,53	8	9	1,99E+08	0,01	1,81E+05	0,00
Mb1496	RecName: Full=UPF0051 protein Mb1496; Contains: RecName: Full=Endonuclease PI-MtuHIIP; AltName: Full=Mtu pps1 intein	94,1	3,66	3	4	6,68E+07	0,03	7,90E+04	0,00	1,30	1	2	2,93E+08	0,02	3,46E+05	0,00
	RecName: Full=Inosamine-phosphate amidinotransferase 1; AltName: Full=Aminocyclitol amidinotransferase; Short=ADT; AltName: Full=Inosamine-phosphate amidinotransferase I	38,6	4,32	1	1	3,59E+07	0,01	1,04E+05	0,00	16,43	4	4	1,46E+08	0,01	4,22E+05	0,00
rpoC	RecName: Full=DNA-directed RNA polymerase subunit beta'; Short=RNAP subunit beta'; AltName: Full=RNA polymerase subunit beta'; AltName: Full=Transcriptase subunit beta'	156,1		0	0	0,00E+00			0,00	1,84	2	2	9,92E+07	0,01	7,01E+04	4,00
	RecName: Full=Deoxyribodipyrimidine photo-lyase; AltName: Full=DNA photolyase; AltName: Full=Photoreactivating enzyme	50,4	1,98	1	1	4,49E+07	0,02	9,87E+04	0,00	7,91	3	3	9,06E+07	0,00	1,99E+05	0,00
rpoC	RecName: Full=DNA-directed RNA polymerase subunit beta'; Short=RNAP subunit beta'; AltName: Full=RNA polymerase subunit beta'; AltName: Full=Transcriptase subunit beta'	147,9	0,75	1	1	9,01E+07	0,03	6,74E+04	0,05	2,02	3	3	1,03E+08	0,01	7,73E+04	0,00
tal2	RecName: Full=Transaldolase 2	40,6	7,26	2	2	5,30E+07	0,02	1,43E+05	0,00	4,84	2	2	1,19E+08	0,01	3,19E+05	0,00
SCO3168	RecName: Full=Putative tricorn protease homolog 2	125,6	2,73	3	5	7,01E+07	0,03	5,98E+04	0,00	2,65	3	3	1,77E+08	0,01	1,51E+05	0,00
	RecName: Full=Tryptophan synthase beta chain	43,5	2,46	1	1	6,62E+07	0,03	1,63E+05	0,00	2,46	1	1	2,21E+07	0,00	5,44E+04	0,00
rplB	RecName: Full=50S ribosomal protein L2	30,6	6,16	1	3	8,74E+07	0,03	3,17E+05	0,00	6,16	1	2	1,60E+08	0,01	5,80E+05	0,00
SCO1660	RecName: Full=Glycerol kinase 1; AltName: Full=ATP:glycerol 3-phosphotransferase 1; AltName: Full=Glycerokinase 1; Short=GK 1	55,9	1,95	1	1	5,29E+07	0,02	1,03E+05	0,00	3,13	1	2	1,42E+08	0,01	2,77E+05	0,00

Gene Name	Description	MW[kDa]	sample_Mpa_50per							sample_Cp_50per						
			Coverage	# Peptides	# PSMs	Area	Rel. Area (%)	Norm. Area	ControlQ	Coverage	# Peptides	# PSMs	Area	Rel. Area (%)	Norm. Area	ControlQ
gcp	RecName: Full=tRNA N6-adenosine threonylcarbamoyltransferase; AltName: Full=t(6)A37 threonylcarbamoyladenosine biosynthesis protein TsaD; AltName: Full=tRNA threonylcarbamoyladenosine biosynthesis protein TsaD	39,1	3,21	1	2	3,22E+07	0,01	8,62E+04	0,00	3,21	1	2	1,62E+08	0,01	4,34E+05	0,00
rplT	RecName: Full=50S ribosomal protein L20	14,2	18,90	2	3	1,05E+08	0,04	8,26E+05	0,00	18,90	2	2	1,77E+08	0,01	1,39E+06	0,00
SCO1476	RecName: Full=S-adenosylmethionine synthase; Short=AdoMet synthase; AltName: Full=MAT; AltName: Full=Methionine adenosyltransferase	43,4	11,19	4	5	6,23E+07	0,02	1,55E+05	5,96	12,19	4	5	9,71E+07	0,01	2,41E+05	25,27
	RecName: Full=50S ribosomal protein L11	15,0	19,44	2	2	1,20E+08	0,05	8,33E+05	0,00	19,44	2	3	4,19E+08	0,02	2,91E+06	10,13
SCO3670	RecName: Full=Protein GrpE; AltName: Full=HSP-70 cofactor	23,9	9,33	2	2	8,70E+07	0,03	3,87E+05	0,00	9,33	2	2	2,59E+08	0,01	1,15E+06	0,00
rpoC	RecName: Full=DNA-directed RNA polymerase subunit beta'; Short=RNAP subunit beta'; AltName: Full=RNA polymerase subunit beta'; AltName: Full=Transcriptase subunit beta'	160,0		0	0	0,00E+00			0,00	1,12	1	1	2,05E+08	0,01	1,43E+05	0,00
rpmJ	RecName: Full=50S ribosomal protein L36	4,4	24,32	1	1	1,80E+07	0,01	4,85E+05	0,00		0	0	0,00E+00			0,00
infA	RecName: Full=Translation initiation factor IF-1	8,2	25,00	2	2	7,72E+07	0,03	1,07E+06	0,00	25,00	2	2	4,28E+08	0,02	5,95E+06	0,00
rplS	RecName: Full=50S ribosomal protein L19	13,1	8,62	1	1	2,39E+07	0,01	2,06E+05	0,00	14,66	3	3	3,49E+08	0,02	3,01E+06	0,00
SCO7036	RecName: Full=Argininosuccinate synthase; AltName: Full=Citrulline--aspartate ligase	52,2	2,29	1	1	1,13E+08	0,04	2,34E+05	0,00	3,33	1	2	1,33E+08	0,01	2,77E+05	0,00
rplF	RecName: Full=50S ribosomal protein L6	19,2		0	0	0,00E+00			0,00	8,38	1	1	3,69E+08	0,02	2,06E+06	0,00
ftsH	RecName: Full=ATP-dependent zinc metalloprotease FtsH	76,7	1,71	1	1	4,62E+07	0,02	6,59E+04	0,00		0	0	0,00E+00			0,00
	RecName: Full=ATP synthase subunit alpha; AltName: Full=ATP synthase F1 sector subunit alpha; AltName: Full=F-ATPase subunit alpha	57,2	4,16	2	2	8,46E+07	0,03	1,60E+05	0,20	10,02	4	6	1,40E+08	0,01	2,64E+05	0,00
rplN	RecName: Full=50S ribosomal protein L14	13,4	8,20	1	1	1,06E+08	0,04	8,71E+05	0,00	8,20	1	1	5,75E+08	0,03	4,71E+06	0,00
rplE	RecName: Full=50S ribosomal protein L5	23,8	5,71	1	1	8,57E+07	0,03	4,08E+05	0,00	5,71	1	1	3,01E+08	0,02	1,43E+06	0,00
cysA2	RecName: Full=Putative thiosulfate sulfurtransferase; AltName: Full=Rhodanese-like protein	31,0	2,89	1	1	7,76E+07	0,03	2,80E+05	0,00	7,94	2	2	5,81E+07	0,00	2,10E+05	0,00
	RecName: Full=RNA polymerase sigma factor SigA; AltName: Full=RNA polymerase principal sigma factor HrdB	56,1	6,81	3	3	6,63E+08	0,25	1,29E+06	0,00	1,95	1	1	1,01E+08	0,01	1,97E+05	0,00

Gene Name	Description	MW[kDa]	sample_Mpa_50per							sample_Cp_50per						
			Coverage	# Peptides	# PSMs	Area	Rel. Area (%)	Norm. Area	ControlQ	Coverage	# Peptides	# PSMs	Area	Rel. Area (%)	Norm. Area	ControlQ
SCO3543	RecName: Full=DNA topoisomerase 1; AltName: Full=DNA topoisomerase I; AltName: Full=Omega-protein; AltName: Full=Relaxing enzyme; AltName: Full=Swivelase; AltName: Full=Untwisting enzyme	103,5	4,31	3	3	7,79E+07	0,03	8,18E+04	0,00	1,68	1	1	8,99E+07	0,00	9,44E+04	0,00
rpsS	RecName: Full=30S ribosomal protein S19	10,1		0	0	0,00E+00			0,00		0	0	0,00E+00			0,00
murE	RecName: Full=UDP-N-acetylmuramoyl-L-alanyl-D-glutamate--2,6-diaminopimelate ligase; AltName: Full=Meso-A2pm-adding enzyme; AltName: Full=Meso-diaminopimelate-adding enzyme; AltName: Full=UDP-MurNAc-L-Ala-D-Glu:meso-diaminopimelate ligase; AltName: Full=UDP-MurNAc-tripeptide synthetase; AltName: Full=UDP-N-acetylmuramyl-tripeptide synthetase	52,8	4,15	2	2	6,78E+07	0,03	1,34E+05	0,00	4,15	2	2	1,97E+08	0,01	3,90E+05	0,00
	RecName: Full=Aspartate aminotransferase; Short=AspAT; AltName: Full=Transaminase A	42,4	4,03	1	1	3,35E+07	0,01	8,43E+04	0,00	4,03	1	1	1,38E+08	0,01	3,47E+05	0,00
	RecName: Full=S-adenosylmethionine synthase; Short=AdoMet synthase; AltName: Full=MAT; AltName: Full=Methionine adenosyltransferase	41,9	2,34	1	1	3,22E+07	0,01	8,37E+04	0,22	2,86	1	1	9,30E+07	0,00	2,42E+05	1,79
Mvan_2429	RecName: Full=(Dimethylallyl)adenosine tRNA methylthiotransferase MiaB; AltName: Full=tRNA-i(6)A37 methylthiotransferase	54,9	1,37	1	1	5,80E+07	0,02	1,14E+05	0,00	1,37	1	1	1,15E+08	0,01	2,25E+05	0,00
SCO6073	RecName: Full=Germacradienol/geosmin synthase; Includes: RecName: Full=Germacradienol/germacrene D synthase; AltName: Full=Sesquiterpene cyclase; AltName: Full=Sesquiterpene synthase; Includes: RecName: Full=Geosmin synthase	81,4	1,52	1	1	0,00E+00			0,00		0	0	0,00E+00			0,00
serS1	RecName: Full=Serine--tRNA ligase 1; AltName: Full=Seryl-tRNA synthetase 1; Short=SerRS 1; AltName: Full=Seryl-tRNA(Ser/Sec) synthetase 1	47,2		0	0	0,00E+00			0,00		0	0	0,00E+00			0,00
	RecName: Full=Chromosomal replication initiator protein DnaA	69,9	1,76	1	1	5,00E+07	0,02	8,01E+04	0,00	4,33	2	4	2,21E+08	0,01	3,54E+05	0,00
tuf-2	RecName: Full=Elongation factor Tu; Short=EF-Tu	43,4	2,79	1	2	4,54E+08	0,17	1,15E+06	0,05		0	0	0,00E+00			0,00
glmM	RecName: Full=Phosphoglucosamine mutase	46,9	6,19	2	2	4,16E+07	0,02	9,21E+04	0,00	6,19	2	2	1,82E+08	0,01	4,03E+05	0,00
glmM	RecName: Full=Phosphoglucosamine mutase	46,7	7,08	2	2	2,40E+07	0,01	5,31E+04	0,00	7,08	2	2	1,10E+08	0,01	2,43E+05	0,00
guaB1	RecName: Full=Uncharacterized oxidoreductase Mb1874c	49,9		0	0	0,00E+00			0,00		0	0	0,00E+00			0,00

Gene Name	Description	MW[kDa]	sample_Mpa_50per							sample_Cp_50per						
			Coverage	# Peptides	# PSMs	Area	Rel. Area (%)	Norm. Area	ControlQ	Coverage	# Peptides	# PSMs	Area	Rel. Area (%)	Norm. Area	ControlQ
hutU	RecName: Full=Urocanate hydratase; Short=Urocanase; AltName: Full=Imidazolonepropionate hydrolase	59,8	2,17	1	1	7,44E+07	0,03	1,34E+05	0,00	6,50	3	4	1,38E+08	0,01	2,50E+05	0,00
rplR	RecName: Full=50S ribosomal protein L18	13,6	8,66	1	1	1,44E+08	0,06	1,13E+06	0,00		0	0	0,00E+00			0,00
rpsD	RecName: Full=30S ribosomal protein S4	23,6		0	0	0,00E+00			0,00	4,41	1	2	2,51E+08	0,01	1,23E+06	0,00
	RecName: Full=DNA-directed RNA polymerase subunit beta'; Short=RNAP subunit beta'; AltName: Full=RNA polymerase subunit beta'; AltName: Full=Transcriptase subunit beta'	155,1		0	0	0,00E+00			0,00	0,57	1	1	2,35E+07	0,00	1,67E+04	1,27
rpoC	RecName: Full=DNA-directed RNA polymerase subunit beta'; Short=RNAP subunit beta'; AltName: Full=RNA polymerase subunit beta'; AltName: Full=Transcriptase subunit beta'	156,0		0	0	0,00E+00			0,00	0,57	1	1	2,35E+07	0,00	1,66E+04	0,95
Ping_3445	RecName: Full=DNA-directed RNA polymerase subunit beta'; Short=RNAP subunit beta'; AltName: Full=RNA polymerase subunit beta'; AltName: Full=Transcriptase subunit beta'	155,0		0	0	0,00E+00			0,00	0,57	1	1	2,35E+07	0,00	1,67E+04	0,95
rpoC	RecName: Full=DNA-directed RNA polymerase subunit beta'; Short=RNAP subunit beta'; AltName: Full=RNA polymerase subunit beta'; AltName: Full=Transcriptase subunit beta'	157,6		0	0	0,00E+00			0,00	0,57	1	1	2,35E+07	0,00	1,66E+04	0,99
rpoC	RecName: Full=DNA-directed RNA polymerase subunit beta'; Short=RNAP subunit beta'; AltName: Full=RNA polymerase subunit beta'; AltName: Full=Transcriptase subunit beta'	154,9		0	0	0,00E+00			0,00	0,57	1	1	2,35E+07	0,00	1,67E+04	0,99
rpoC	RecName: Full=DNA-directed RNA polymerase subunit beta'; Short=RNAP subunit beta'; AltName: Full=RNA polymerase subunit beta'; AltName: Full=Transcriptase subunit beta'	157,2		0	0	0,00E+00			0,00	0,57	1	1	2,35E+07	0,00	1,67E+04	1,53
rpoC	RecName: Full=DNA-directed RNA polymerase subunit beta'; Short=RNAP subunit beta'; AltName: Full=RNA polymerase subunit beta'; AltName: Full=Transcriptase subunit beta'	155,3		0	0	0,00E+00			0,00	0,57	1	1	2,35E+07	0,00	1,67E+04	0,99
rpoC	RecName: Full=DNA-directed RNA polymerase subunit beta'; Short=RNAP subunit beta'; AltName: Full=RNA polymerase subunit beta'; AltName: Full=Transcriptase subunit beta'	157,2		0	0	0,00E+00			0,00	0,56	1	1	2,35E+07	0,00	1,65E+04	0,00

Gene Name	Description	MW[kDa]	sample_Mpa_50per							sample_Cp_50per						
			Coverage	# Peptides	# PSMs	Area	Rel. Area (%)	Norm. Area	ControlQ	Coverage	# Peptides	# PSMs	Area	Rel. Area (%)	Norm. Area	ControlQ
RPE_3596	RecName: Full=DNA-directed RNA polymerase subunit beta'; Short=RNAP subunit beta'; AltName: Full=RNA polymerase subunit beta'; AltName: Full=Transcriptase subunit beta'	156,0		0	0	0,00E+00			0,00	0,57	1	1	2,35E+07	0,00	1,68E+04	0,34
	RecName: Full=Peptidyl-prolyl cis-trans isomerase A; Short=PPIase A; AltName: Full=Cyclophilin ScCypA; AltName: Full=Cyclophilin homolog; AltName: Full=Rotamase A	17,7	8,48	1	3	2,86E+07	0,01	1,73E+05	0,00	8,48	1	2	1,35E+08	0,01	8,19E+05	0,00
	RecName: Full=Uncharacterized protein YggP	45,8		0	0	0,00E+00			0,00		0	0	0,00E+00			0,00
dapB	RecName: Full=4-hydroxy-tetrahydrodipicolinate reductase; Short=HTPA reductase	26,3		0	0	0,00E+00			0,00	12,00	2	2	1,39E+08	0,01	5,56E+05	0,00
	RecName: Full=Putative pyrophosphorylase ModD	30,5		0	0	0,00E+00			0,00		0	0	0,00E+00			0,00
prfB	RecName: Full=Peptide chain release factor 2; Short=RF-2	41,1	6,52	2	2	5,83E+07	0,02	1,59E+05	0,00	3,80	1	1	2,52E+08	0,01	6,85E+05	0,00
	RecName: Full=Thioredoxin reductase; Short=TRXR	34,1	3,73	1	1	7,92E+07	0,03	2,46E+05	0,00	12,73	3	3	1,18E+08	0,01	3,67E+05	0,00
rplC	RecName: Full=50S ribosomal protein L3	22,7		0	0	0,00E+00			0,00	3,74	1	1	9,82E+08	0,05	4,59E+06	0,00
gpmA	RecName: Full=2,3-bisphosphoglycerate-dependent phosphoglycerate mutase; Short=BPG-dependent PGAM; Short=PGAM; Short=Phosphoglyceromutase; Short=dPGM	28,2	7,91	2	2	5,56E+07	0,02	2,20E+05	0,00	7,91	2	2	1,75E+08	0,01	6,91E+05	0,00
rpsI	RecName: Full=30S ribosomal protein S9	18,7	11,76	2	2	4,89E+07	0,02	2,88E+05	0,00	20,00	3	4	2,53E+08	0,01	1,49E+06	0,00
panB	RecName: Full=3-methyl-2-oxobutanoate hydroxymethyltransferase; AltName: Full=Ketopantoate hydroxymethyltransferase; Short=KPHMT	30,3		0	0	0,00E+00			0,00		0	0	0,00E+00			0,00
murC	RecName: Full=UDP-N-acetylmuramate--L-alanine ligase; AltName: Full=UDP-N-acetylmuramoyl-L-alanine synthetase	51,4	1,68	1	1	5,85E+07	0,02	1,23E+05	0,00	1,68	1	1	3,02E+08	0,02	6,34E+05	0,00
SCO1715	RecName: Full=Homogentisate 1,2-dioxygenase; AltName: Full=Homogentisate oxygenase; AltName: Full=Homogentisic acid oxidase; AltName: Full=Homogentisicase	48,4	2,72	1	1	0,00E+00			0,00	6,12	2	8	7,37E+08	0,04	1,67E+06	0,00
ureG	RecName: Full=Urease accessory protein UreG	21,8	5,42	1	1	3,69E+07	0,01	1,82E+05	0,00		0	0	0,00E+00			0,00
pyrH	RecName: Full=Uridylate kinase; Short=UK; AltName: Full=Uridine monophosphate kinase; Short=UMP kinase; Short=UMPK	27,0		0	0	0,00E+00			0,00	4,76	1	1	1,31E+08	0,01	5,19E+05	0,00

Gene Name	Description	MW[kDa]	sample_Mpa_50per							sample_Cp_50per						
			Coverage	# Peptides	# PSMs	Area	Rel. Area (%)	Norm. Area	ControlQ	Coverage	# Peptides	# PSMs	Area	Rel. Area (%)	Norm. Area	ControlQ
	RecName: Full=Major outer membrane lipoprotein Lpp; AltName: Full=Braun lipoprotein; AltName: Full=Murein-lipoprotein; Flags: Precursor	8,3	33,33	2	2	9,60E+07	0,04	1,23E+06	0,06		0	0	0,00E+00			0,00
rpsQ	RecName: Full=30S ribosomal protein S17	10,1		0	0	0,00E+00			0,00	10,71	1	1	1,76E+08	0,01	2,10E+06	0,00
gltX	RecName: Full=Glutamate--tRNA ligase; AltName: Full=Glutamyl-tRNA synthetase; Short=GluRS	54,9		0	0	0,00E+00			0,00		0	0	0,00E+00			0,00
M6_Spy0132	RecName: Full=DNA-directed RNA polymerase subunit beta'; Short=RNAP subunit beta'; AltName: Full=RNA polymerase subunit beta'; AltName: Full=Transcriptase subunit beta'	135,3	0,58	1	1	3,09E+07	0,01	2,55E+04	0,02	1,40	2	2	6,56E+07	0,00	5,40E+04	0,00
THEMA_02395	RecName: Full=DNA-directed RNA polymerase subunit beta'; Short=RNAP subunit beta'; AltName: Full=RNA polymerase subunit beta'; AltName: Full=Transcriptase subunit beta'	190,4		0	0	0,00E+00			0,00	0,47	1	1	2,35E+07	0,00	1,39E+04	0,00
	RecName: Full=Transcription termination factor Rho; AltName: Full=ATP-dependent helicase Rho	76,5	2,83	2	2	4,19E+07	0,02	5,93E+04	0,07	1,41	1	1	2,22E+08	0,01	3,14E+05	7,71
rplX	RecName: Full=50S ribosomal protein L24	13,4		0	0	0,00E+00			0,00		0	0	0,00E+00			0,00
tuf	RecName: Full=Elongation factor Tu; Short=EF-Tu	44,1	2,52	1	1	3,01E+08	0,12	7,58E+05	0,04	4,79	1	11	2,74E+09	0,15	6,90E+06	9,33
SCO2148	RecName: Full=Ubiquinol-cytochrome c reductase cytochrome b subunit	60,8		0	0	0,00E+00			0,00	3,12	2	3	8,50E+07	0,00	1,56E+05	0,00
hutH	RecName: Full=Histidine ammonia-lyase; Short=Histidase	52,7	4,30	2	2	3,67E+07	0,01	7,17E+04	0,00	11,52	3	3	9,48E+07	0,01	1,85E+05	0,00
mreB	RecName: Full=Rod shape-determining protein MreB	35,9		0	0	0,00E+00			0,00		0	0	0,00E+00			0,00
	RecName: Full=Glutamate synthase [NADPH] large chain; AltName: Full=Glutamate synthase subunit alpha; Short=GLTS alpha chain	165,8	0,72	1	1	9,58E+07	0,04	6,27E+04	0,00	2,75	2	2	3,61E+08	0,02	2,36E+05	0,00
	RecName: Full=dTDP-dihydrostreptose--streptidine-6-phosphate dihydrostreptosyltransferase	42,9	9,38	3	5	4,61E+07	0,02	1,20E+05	0,00	17,71	5	7	3,25E+08	0,02	8,47E+05	0,00
	RecName: Full=Uncharacterized ABC transporter ATP-binding protein Rv2477c/MT2552	61,9		0	0	0,00E+00			0,00	2,87	1	1	9,49E+07	0,01	1,70E+05	0,00
SCO4089	RecName: Full=Valine dehydrogenase; Short=ValDH	38,3	2,75	1	1	2,96E+07	0,01	8,13E+04	0,00		0	0	0,00E+00			0,00
	RecName: Full=Aminopeptidase N; AltName: Full=Alanine aminopeptidase; AltName: Full=Lysyl aminopeptidase; Short=Lys-AP	94,4	2,33	2	2	3,77E+07	0,01	4,40E+04	0,00		0	0	0,00E+00			0,00

Gene Name	Description	MW[kDa]	sample_Mpa_50per							sample_Cp_50per						
			Coverage	# Peptides	# PSMs	Area	Rel. Area (%)	Norm. Area	ControlQ	Coverage	# Peptides	# PSMs	Area	Rel. Area (%)	Norm. Area	ControlQ
atpG	RecName: Full=ATP synthase gamma chain; AltName: Full=ATP synthase F1 sector gamma subunit; AltName: Full=F-ATPase gamma subunit	32,9	2,95	1	1	4,57E+07	0,02	1,50E+05	0,00		0	0	0,00E+00			0,00
	RecName: Full=Non-haem bromoperoxidase BPO-A1; AltName: Full=BPO1; AltName: Full=Bromide peroxidase	30,5		0	0	0,00E+00			0,00	18,18	3	6	2,79E+08	0,01	1,01E+06	0,00
atpA	RecName: Full=ATP synthase subunit alpha; AltName: Full=ATP synthase F1 sector subunit alpha; AltName: Full=F-ATPase subunit alpha	55,2		0	0	0,00E+00			0,00	2,59	1	2	4,21E+08	0,02	8,38E+05	0,00
secA2	RecName: Full=Protein translocase subunit SecA 2	89,1	1,54	1	1	0,00E+00			0,00		0	0	0,00E+00			0,00
rpsH	RecName: Full=30S ribosomal protein S8	14,3		0	0	0,00E+00			0,00	21,97	2	6	3,20E+08	0,02	2,42E+06	0,00
SCO2082	RecName: Full=Cell division protein FtsZ	41,1	3,51	1	1	4,66E+07	0,02	1,17E+05	0,00	8,52	3	3	1,18E+08	0,01	2,95E+05	0,00
atpG	RecName: Full=ATP synthase gamma chain; AltName: Full=ATP synthase F1 sector gamma subunit; AltName: Full=F-ATPase gamma subunit	32,6		0	0	0,00E+00			0,00		0	0	0,00E+00			0,00
SCO4628	RecName: Full=Uncharacterized HTH-type transcriptional regulator SCO4628	29,7	8,18	2	2	8,41E+07	0,03	3,13E+05	0,00	4,09	1	1	4,46E+08	0,02	1,66E+06	0,00
lpl0457	RecName: Full=Ribosomal protein S6 modification protein	32,9	2,32	1	1	3,29E+07	0,01	1,09E+05	0,00		0	0	0,00E+00			0,00
dut	RecName: Full=Deoxyuridine 5'-triphosphate nucleotidohydrolase; Short=dUTPase; AltName: Full=dUTP pyrophosphatase	18,5	5,14	1	1	9,34E+07	0,04	5,34E+05	0,00	17,71	2	3	5,24E+08	0,03	2,99E+06	0,00
rplC	RecName: Full=50S ribosomal protein L3	24,5	5,96	1	1	3,06E+07	0,01	1,30E+05	0,00	5,96	1	2	2,98E+08	0,02	1,27E+06	0,00
gabD1	RecName: Full=Succinate-semialdehyde dehydrogenase [NADP(+)]; Short=SSADH; Short=SSDH	50,0		0	0	0,00E+00			0,00		0	0	0,00E+00			0,00
SCO1643	RecName: Full=Proteasome subunit alpha; AltName: Full=20S proteasome alpha subunit; AltName: Full=Proteasome core protein PrcA	27,9	28,74	6	8	5,46E+08	0,21	2,15E+06	1,94	51,57	24	366	3,03E+11	16,25	1,19E+09	0,71
prcA	RecName: Full=Proteasome subunit alpha; AltName: Full=20S proteasome alpha subunit; AltName: Full=Proteasome core protein PrcA	27,7	28,85	5	7	1,38E+08	0,05	5,46E+05	0,49	45,45	17	318	3,03E+11	16,25	1,20E+09	0,57
	RecName: Full=Streptomycin-6-phosphate phosphatase; Flags: Precursor	46,3	2,00	1	1	1,76E+07	0,01	3,93E+04	0,00	7,57	3	3	4,67E+07	0,00	1,04E+05	0,00

Gene Name	Description	MW[kDa]	sample_Mpa_50per							sample_Cp_50per						
			Coverage	# Peptides	# PSMs	Area	Rel. Area (%)	Norm. Area	ControlQ	Coverage	# Peptides	# PSMs	Area	Rel. Area (%)	Norm. Area	ControlQ
TTHA1120	RecName: Full=Bifunctional protein FolD; Includes: RecName: Full=Methylenetetrahydrofolate dehydrogenase; Includes: RecName: Full=Methenyltetrahydrofolate cyclohydrolase	30,6		0	0	0,00E+00			0,00		0	0	0,00E+00			0,00
BP1974	RecName: Full=NAD-dependent protein deacetylase; AltName: Full=Regulatory protein SIR2 homolog	29,9		0	0	0,00E+00			0,00		0	0	0,00E+00			0,00
rplV	RecName: Full=50S ribosomal protein L22	12,8	9,57	1	1	2,45E+07	0,01	2,13E+05	0,00	20,00	2	2	1,83E+08	0,01	1,59E+06	0,00
thrS	RecName: Full=Threonine--tRNA ligase; AltName: Full=Threonyl-tRNA synthetase; Short=ThrRS	74,5	1,37	1	1	3,36E+07	0,01	5,11E+04	0,00	1,37	1	1	8,12E+07	0,00	1,23E+05	0,00
	RecName: Full=Protein RecA; AltName: Full=Recombinase A	39,5	6,15	2	2	3,43E+07	0,01	9,17E+04	0,00		0	0	0,00E+00			0,00
Francci3_4259	RecName: Full=DNA integrity scanning protein DisA; AltName: Full=Cyclic di-AMP synthase; Short=c-di-AMP synthase; AltName: Full=Diadenylate cyclase	38,9		0	0	0,00E+00			0,00	2,51	1	1	1,12E+08	0,01	3,12E+05	0,00
alaS	RecName: Full=Alanine--tRNA ligase; AltName: Full=Alanyl-tRNA synthetase; Short=AlaRS	95,7		0	0	0,00E+00			0,00		0	0	0,00E+00			0,00
rplL	RecName: Full=50S ribosomal protein L7/L12	13,4		0	0	0,00E+00			0,00		0	0	0,00E+00			0,00
tsf	RecName: Full=Elongation factor Ts; Short=EF-Ts	29,1	7,35	2	2	6,68E+07	0,03	2,45E+05	0,00	7,35	2	4	1,12E+08	0,01	4,12E+05	0,00
	RecName: Full=Elongation factor Tu; Short=EF-Tu	43,3	20,56	7	9	3,60E+08	0,14	9,15E+05	0,02	13,71	4	4	1,85E+08	0,01	4,69E+05	0,26
FN1636	RecName: Full=30S ribosomal protein S17	9,9	9,64	1	1	8,39E+07	0,03	1,01E+06	0,00	8,43	1	1	4,40E+08	0,02	5,30E+06	0,00
gatB	RecName: Full=Aspartyl/glutamyl-tRNA(Asn/Gln) amidotransferase subunit B; Short=Asp/Glu-ADT subunit B	54,6	3,54	2	2	6,08E+07	0,02	1,20E+05	0,00	2,55	1	1	7,76E+07	0,00	1,53E+05	0,00
	RecName: Full=Adenylate cyclase; AltName: Full=ATP pyrophosphate-lyase; AltName: Full=Adenylyl cyclase	43,1		0	0	0,00E+00			0,00	5,76	2	2	5,92E+07	0,00	1,48E+05	0,00
THEMA_00180	RecName: Full=4-hydroxy-3-methylbut-2-en-1-yl diphosphate synthase; AltName: Full=1-hydroxy-2-methyl-2-(E)-butenyl 4-diphosphate synthase	37,7	2,03	1	1	3,88E+07	0,01	1,13E+05	0,00		0	0	0,00E+00			0,00
	RecName: Full=60 kDa chaperonin; AltName: Full=GroEL protein; AltName: Full=Heat shock protein 60; AltName: Full=Protein Cpn60	56,4		0	0	0,00E+00			0,00		0	0	0,00E+00			0,00

Gene Name	Description	MW[kDa]	sample_Mpa_50per							sample_Cp_50per						
			Coverage	# Peptides	# PSMs	Area	Rel. Area (%)	Norm. Area	ControlQ	Coverage	# Peptides	# PSMs	Area	Rel. Area (%)	Norm. Area	ControlQ
Noca_1763	RecName: Full=ATP synthase subunit beta; AltName: Full=ATP synthase F1 sector subunit beta; AltName: Full=F-ATPase subunit beta	52,6	2,07	1	1	1,30E+08	0,05	2,69E+05	0,00		0	0	0,00E+00			0,00
	RecName: Full=FKBP-type peptidyl-prolyl cis-trans isomerase SlyD; Short=PPIase; AltName: Full=Metallochaperone SlyD	20,8	4,59	1	1	2,66E+08	0,10	1,36E+06	0,14	72,96	8	37	4,95E+09	0,27	2,52E+07	0,40
argS	RecName: Full=Arginine--tRNA ligase; AltName: Full=Arginyl-tRNA synthetase; Short=ArgRS	65,1		0	0	0,00E+00			0,00		0	0	0,00E+00			0,00
SCO5862	RecName: Full=Transcriptional regulatory protein CutR; AltName: Full=Defective melC1 suppressor protein	23,9	12,44	2	2	2,81E+07	0,01	1,29E+05	0,00	12,90	2	3	1,34E+08	0,01	6,16E+05	0,00
	RecName: Full=Elongation factor Tu; Short=EF-Tu	43,8	2,78	1	1	3,48E+07	0,01	8,78E+04	0,00	2,78	1	1	1,45E+08	0,01	3,65E+05	0,00
dnaK	RecName: Full=Chaperone protein DnaK; AltName: Full=HSP70; AltName: Full=Heat shock 70 kDa protein; AltName: Full=Heat shock protein 70	69,4	2,16	1	1	3,87E+07	0,01	5,98E+04	0,00		0	0	0,00E+00			0,00
	RecName: Full=50S ribosomal protein L10	19,5	28,11	4	4	8,22E+07	0,03	4,44E+05	0,00	28,11	5	5	1,80E+08	0,01	9,71E+05	0,00
	RecName: Full=Alkyl hydroperoxide reductase subunit C; AltName: Full=Alkyl hydroperoxide reductase protein C22; AltName: Full=Peroxiredoxin; AltName: Full=SCRP-23; AltName: Full=Sulfate starvation-induced protein 8; Short=SSI8; AltName: Full=Thioredoxin peroxidase	20,7		0	0	0,00E+00			0,00		0	0	0,00E+00			0,00
ureG	RecName: Full=Urease accessory protein UreG	23,8	6,61	1	1	3,44E+07	0,01	1,52E+05	0,00		0	0	0,00E+00			0,00
	RecName: Full=UPF0042 nucleotide-binding protein SCO1952	32,8	3,01	1	1	1,05E+08	0,04	3,53E+05	0,00	12,37	3	5	1,41E+08	0,01	4,73E+05	0,00
eno	RecName: Full=Enolase; AltName: Full=2-phospho-D-glycerate hydro-lyase; AltName: Full=2-phosphoglycerate dehydratase	45,1	2,59	1	1	5,31E+07	0,02	1,25E+05	0,00	2,59	1	2	8,51E+08	0,05	2,00E+06	0,00
oprL	RecName: Full=Peptidoglycan-associated lipoprotein; Flags: Precursor	17,9	5,36	1	1	6,74E+07	0,03	4,01E+05	0,00		0	0	0,00E+00			0,00
	RecName: Full=dTDP-4-dehydrorhamnose 3,5-epimerase; AltName: Full=Thymidine diphospho-4-keto-rhamnose 3,5-epimerase; AltName: Full=dTDP-4-keto-6-deoxyglucose 3,5-epimerase; AltName: Full=dTDP-6-deoxy-D-xylo-4-hexulose 3,5-epimerase; AltName: Full=dTDP-L-rhamnose synthetase	21,9		0	0	0,00E+00			0,00		0	0	0,00E+00			0,00

Gene Name	Description	MW[kDa]	sample_Mpa_50per							sample_Cp_50per						
			Coverage	# Peptides	# PSMs	Area	Rel. Area (%)	Norm. Area	ControlQ	Coverage	# Peptides	# PSMs	Area	Rel. Area (%)	Norm. Area	ControlQ
	RecName: Full=6-phosphofructokinase 2; AltName: Full=Phosphofructokinase 2; AltName: Full=Phosphohexokinase 2	41,7		0	0	0,00E+00			0,00		0	0	0,00E+00			0,00
gltX	RecName: Full=Glutamate--tRNA ligase; AltName: Full=Glutamyl-tRNA synthetase; Short=GluRS	55,7	1,81	1	1	3,35E+07	0,01	6,75E+04	0,00		0	0	0,00E+00			0,00
ftsY	RecName: Full=Signal recognition particle receptor FtsY; Short=SRP receptor	36,3		0	0	0,00E+00			0,00		0	0	0,00E+00			0,00
sucC	RecName: Full=Succinyl-CoA ligase [ADP-forming] subunit beta; AltName: Full=Succinyl-CoA synthetase subunit beta; Short=SCS-beta	41,3		0	0	0,00E+00			0,00		0	0	0,00E+00			0,00
ureA	RecName: Full=Urease subunit gamma; AltName: Full=Urea amidohydrolase subunit gamma	11,1		0	0	0,00E+00			0,00	29,00	2	3	2,53E+08	0,01	2,53E+06	0,00
aspS	RecName: Full=Aspartate--tRNA ligase; AltName: Full=Aspartyl-tRNA synthetase; Short=AspRS	65,7		0	0	0,00E+00			0,00		0	0	0,00E+00			0,00
carA	RecName: Full=Carbamoyl-phosphate synthase small chain; AltName: Full=Carbamoyl-phosphate synthetase glutamine chain	39,7		0	0	0,00E+00			0,00		0	0	0,00E+00			0,00
CC_2482	RecName: Full=Non-motile and phage-resistance protein	89,5		0	0	0,00E+00			0,00		0	0	0,00E+00			0,00
	RecName: Full=Catalase-peroxidase; Short=CP; AltName: Full=Peroxidase/catalase	80,8		0	0	0,00E+00			0,00		0	0	0,00E+00			0,00
SCO5662	RecName: Full=Putative adenosine/adenine deaminase 1; AltName: Full=Adenosine aminohydrolase 1	42,4		0	0	0,00E+00			0,00	3,62	1	2	1,86E+08	0,01	4,80E+05	0,00
purH	RecName: Full=Bifunctional purine biosynthesis protein PurH; Includes: RecName: Full=Phosphoribosylaminoimidazolecarboxamide formyltransferase; AltName: Full=AICAR transformylase; Includes: RecName: Full=IMP cyclohydrolase; AltName: Full=ATIC; AltName: Full=IMP synthase; AltName: Full=Inosinicase	55,0	6,12	2	2	9,30E+06	0,00	1,78E+04	0,00	11,47	4	5	1,77E+08	0,01	3,38E+05	0,00
pheT	RecName: Full=Phenylalanine--tRNA ligase beta subunit; AltName: Full=Phenylalanyl-tRNA synthetase beta subunit; Short=PheRS	89,9		0	0	0,00E+00			0,00	1,55	1	1	1,16E+08	0,01	1,38E+05	0,00
	RecName: Full=Uncharacterized protein in hutH 5'region	25,4		0	0	0,00E+00			0,00		0	0	0,00E+00			0,00
proS1	RecName: Full=Proline--tRNA ligase 1; AltName: Full=Prolyl-tRNA synthetase 1; Short=ProRS 1	61,2		0	0	0,00E+00			0,00	4,26	2	3	1,56E+08	0,01	2,76E+05	0,00

Gene Name	Description	MW[kDa]	sample_Mpa_50per							sample_Cp_50per						
			Coverage	# Peptides	# PSMs	Area	Rel. Area (%)	Norm. Area	ControlQ	Coverage	# Peptides	# PSMs	Area	Rel. Area (%)	Norm. Area	ControlQ
dhaS	RecName: Full=Putative aldehyde dehydrogenase DhaS	53,8		0	0	0,00E+00			0,00		0	0	0,00E+00			0,00
rplI	RecName: Full=50S ribosomal protein L9	16,0		0	0	0,00E+00			0,00		0	0	0,00E+00			0,00
ftsY	RecName: Full=Signal recognition particle receptor FtsY; Short=SRP receptor	43,6		0	0	0,00E+00			0,00		0	0	0,00E+00			0,00
trpC	RecName: Full=Indole-3-glycerol phosphate synthase; Short=IGPS	28,1	4,09	1	1	0,00E+00			0,00	4,09	1	2	4,24E+08	0,02	1,57E+06	0,00
groEL	RecName: Full=60 kDa chaperonin; AltName: Full=GroEL protein; AltName: Full=Protein Cpn60	57,7		0	0	0,00E+00			0,00		0	0	0,00E+00			0,00
	RecName: Full=Glutamine--fructose-6-phosphate aminotransferase [isomerizing]; AltName: Full=D-fructose-6-phosphate amidotransferase; AltName: Full=GFAT; AltName: Full=Glucosamine-6-phosphate synthase; AltName: Full=Hexosephosphate aminotransferase; AltName: Full=L-glutamine--D-fructose-6-phosphate amidotransferase	66,9	12,81	8	8	1,77E+08	0,07	2,90E+05	0,19	11,66	5	5	1,80E+08	0,01	2,96E+05	0,77
clpB1	RecName: Full=Chaperone protein ClpB 1	95,0	2,41	2	3	3,43E+07	0,01	3,94E+04	0,00	1,26	1	1	1,88E+08	0,01	2,16E+05	0,00
ileS	RecName: Full=Isoleucine--tRNA ligase; AltName: Full=Isoleucyl-tRNA synthetase; Short=IleRS	116,8	1,05	1	1	2,30E+07	0,01	2,20E+04	0,00	1,05	1	1	5,09E+07	0,00	4,86E+04	0,00
SCO1488	RecName: Full=Bifunctional protein PyrR; Includes: RecName: Full=Pyrimidine operon regulatory protein; Includes: RecName: Full=Uracil phosphoribosyltransferase; Short=UPRTase	21,2	11,40	2	2	1,45E+07	0,01	7,50E+04	0,00		0	0	0,00E+00			0,00
Noc_2331	RecName: Full=DNA-directed RNA polymerase subunit beta; Short=RNAP subunit beta; AltName: Full=RNA polymerase subunit beta; AltName: Full=Transcriptase subunit beta	151,0	0,96	1	1	4,63E+07	0,02	3,41E+04	0,03	0,96	1	1	9,13E+07	0,00	6,72E+04	17,52
infB	RecName: Full=Translation initiation factor IF-2	108,8		0	0	0,00E+00			0,00		0	0	0,00E+00			0,00
	RecName: Full=Chaperone protein ClpB	94,1	3,03	2	3	2,48E+07	0,01	2,90E+04	0,00	3,03	2	2	1,71E+08	0,01	2,00E+05	0,00
SCO3382	RecName: Full=L-aspartate oxidase; Short=LASPO; AltName: Full=Quinolinate synthase B	61,2		0	0	0,00E+00			0,00	2,59	1	2	1,53E+08	0,01	2,65E+05	0,00
SCO1523	RecName: Full=Pyridoxal biosynthesis lyase PdxS	32,2	4,29	1	1	3,24E+07	0,01	1,07E+05	0,00	4,95	1	2	7,39E+07	0,00	2,44E+05	0,00

Gene Name	Description	MW[kDa]	sample_Mpa_50per							sample_Cp_50per						
			Coverage	# Peptides	# PSMs	Area	Rel. Area (%)	Norm. Area	ControlQ	Coverage	# Peptides	# PSMs	Area	Rel. Area (%)	Norm. Area	ControlQ
	RecName: Full=Triosephosphate isomerase; Short=TIM; AltName: Full=Triose-phosphate isomerase	26,9	3,14	1	1	2,75E+07	0,01	1,08E+05	7,43		0	0	0,00E+00			0,00
	RecName: Full=Peptidyl-prolyl cis-trans isomerase B; Short=PPIase B; AltName: Full=Cyclophilin ScCypB; AltName: Full=Rotamase B; AltName: Full=S-cyclophilin	19,0	7,43	1	1	2,07E+07	0,01	1,18E+05	0,00		0	0	0,00E+00			0,00
SCO3792	RecName: Full=Methionine--tRNA ligase; AltName: Full=Methionyl-tRNA synthetase; Short=MetRS	59,7		0	0	0,00E+00			0,00	8,18	3	3	6,90E+07	0,00	1,28E+05	0,00
rpsB	RecName: Full=30S ribosomal protein S2	28,4	4,74	1	2	2,07E+07	0,01	8,20E+04	0,00	4,74	1	1	5,81E+07	0,00	2,29E+05	0,00
ftsH	RecName: Full=ATP-dependent zinc metalloprotease FtsH 1	70,9	1,71	1	1	1,09E+07	0,00	1,69E+04	0,00		0	0	0,00E+00			0,00
SCO5208	RecName: Full=Histidinol-phosphatase; Short=HolPase; AltName: Full=Histidinol-phosphate phosphatase	29,1	9,40	2	2	5,21E+07	0,02	1,96E+05	0,00	15,41	3	5	1,57E+08	0,01	5,92E+05	0,00
	RecName: Full=Beta-lactamase; AltName: Full=Penicillinase; Flags: Precursor	33,7		0	0	0,00E+00			0,00		0	0	0,00E+00			0,00
rpoA	RecName: Full=DNA-directed RNA polymerase subunit alpha; Short=RNAP subunit alpha; AltName: Full=RNA polymerase subunit alpha; AltName: Full=Transcriptase subunit alpha	37,2		0	0	0,00E+00			0,00		0	0	0,00E+00			0,00
pyrB	RecName: Full=Aspartate carbamoyltransferase; AltName: Full=Aspartate transcarbamylase; Short=ATCase	35,6		0	0	0,00E+00			0,00		0	0	0,00E+00			0,00
uvrA	RecName: Full=UvrABC system protein A; Short=UvrA protein; AltName: Full=Excinuclease ABC subunit A	110,9	1,38	1	1	8,48E+06	0,00	8,37E+03	0,08		0	0	0,00E+00			0,00
sfsA	RecName: Full=Sugar fermentation stimulation protein homolog	26,7		0	0	0,00E+00			0,00		0	0	0,00E+00			0,00
trpB	RecName: Full=Tryptophan synthase beta chain	42,8	5,71	2	2	2,95E+07	0,01	7,32E+04	0,00	2,98	1	1	1,08E+08	0,01	2,68E+05	0,00
	RecName: Full=Protein translocase subunit SecY	47,3		0	0	0,00E+00			0,00		0	0	0,00E+00			0,00
	RecName: Full=Phosphate import ATP-binding protein PstB; AltName: Full=ABC phosphate transporter; AltName: Full=Phosphate-transporting ATPase	28,4	8,14	2	2	3,97E+07	0,02	1,54E+05	0,00		0	0	0,00E+00			0,00
	RecName: Full=Putative thioredoxin-2; Short=Trx-2	14,6		0	0	0,00E+00			0,00	6,72	3	3	1,84E+07	0,00	1,38E+05	0,00

Gene Name	Description	MW[kDa]	sample_Mpa_50per							sample_Cp_50per						
			Coverage	# Peptides	# PSMs	Area	Rel. Area (%)	Norm. Area	ControlQ	Coverage	# Peptides	# PSMs	Area	Rel. Area (%)	Norm. Area	ControlQ
SCO2950	RecName: Full=DNA-binding protein HU 1; AltName: Full=HSl	9,8	11,83	1	1	0,00E+00			0,00	11,83	1	2	5,67E+08	0,03	6,10E+06	0,00
glyA	RecName: Full=Serine hydroxymethyltransferase; Short=SHMT; Short=Serine methylase	45,2		0	0	0,00E+00			0,00		0	0	0,00E+00			0,00
proS	RecName: Full=Proline--tRNA ligase; AltName: Full=Prolyl-tRNA synthetase; Short=ProRS	49,3		0	0	0,00E+00			0,00		0	0	0,00E+00			0,00
	RecName: Full=Ribonuclease 3; AltName: Full=Antibiotic biosynthesis protein B; Short=AbsB; AltName: Full=Ribonuclease III; Short=RNase III	29,1		0	0	0,00E+00			0,00	12,68	3	3	6,16E+07	0,00	2,23E+05	0,00
	RecName: Full=Putative inosamine-phosphate amidinotransferase 2; AltName: Full=Aminocyclitol amidinotransferase; Short=ADT; AltName: Full=Inosamine-phosphate amidinotransferase II	38,2		0	0	0,00E+00			0,00		0	0	0,00E+00			0,00
	RecName: Full=Catalase	56,9	1,59	1	3	6,34E+09	2,44	1,26E+07	0,00	1,59	1	7	1,75E+10	0,94	3,48E+07	0,00
	RecName: Full=Ferric uptake regulation protein; Short=Ferric uptake regulator	16,7		0	0	0,00E+00			0,00	54,73	5	24	5,86E+09	0,31	3,96E+07	1,79
	RecName: Full=Ribosomal small subunit pseudouridine synthase A; AltName: Full=16S pseudouridylate 516 synthase; AltName: Full=16S rRNA pseudouridine(516) synthase; AltName: Full=rRNA pseudouridylate synthase A; AltName: Full=rRNA-uridine isomerase A	25,8		0	0	0,00E+00			0,00	41,13	7	20	4,39E+09	0,24	1,90E+07	1,82
	RecName: Full=Ferric uptake regulation protein; Short=Ferric uptake regulator	17,8		0	0	0,00E+00			0,00	44,52	4	21	3,23E+09	0,17	2,08E+07	1,37
mukB	RecName: Full=Chromosome partition protein MukB; AltName: Full=Structural maintenance of chromosome-related protein	169,7	0,47	1	1	4,07E+09	1,56	2,75E+06	3,25	0,47	1	1	2,42E+09	0,13	1,63E+06	0,00
	RecName: Full=Pyruvate kinase; Short=PK	50,7	2,54	1	1	3,37E+08	0,13	7,13E+05	0,00	2,54	1	3	2,11E+09	0,11	4,48E+06	0,00
NE2135	RecName: Full=Probable phosphoketolase	89,6		0	0	0,00E+00			0,00	2,53	1	4	1,87E+09	0,10	2,37E+06	0,00
	RecName: Full=Uncharacterized protein YqjI	23,4		0	0	0,00E+00			0,00	31,88	7	15	1,73E+09	0,09	8,34E+06	2,45
glyA	RecName: Full=Serine hydroxymethyltransferase; Short=SHMT; Short=Serine methylase	45,7	1,63	1	1	5,21E+08	0,20	1,21E+06	0,00	1,63	1	3	1,49E+09	0,08	3,47E+06	0,00
groEL	RecName: Full=60 kDa chaperonin; AltName: Full=GroEL protein; AltName: Full=Heat shock protein 60; AltName: Full=Protein Cpn60	58,2	1,47	1	3	4,58E+08	0,18	8,39E+05	0,08	1,47	1	1	1,48E+09	0,08	2,72E+06	0,00

Gene Name	Description	MW[kDa]	sample_Mpa_50per							sample_Cp_50per						
			Coverage	# Peptides	# PSMs	Area	Rel. Area (%)	Norm. Area	ControlQ	Coverage	# Peptides	# PSMs	Area	Rel. Area (%)	Norm. Area	ControlQ
rplM	RecName: Full=50S ribosomal protein L13	16,3		0	0	0,00E+00			0,00	4,76	1	3	1,31E+09	0,07	8,90E+06	0,00
PSHAa0182	RecName: Full=UPF0061 protein PSHAa0182	51,7		0	0	0,00E+00			0,00	9,59	1	1	1,16E+09	0,06	2,48E+06	0,00
hisS	RecName: Full=Histidine--tRNA ligase; AltName: Full=Histidyl-tRNA synthetase; Short=HisRS	52,2		0	0	0,00E+00			0,00	1,50	1	1	9,84E+08	0,05	2,11E+06	0,00
rpoA	RecName: Full=DNA-directed RNA polymerase subunit alpha; Short=RNAP subunit alpha; AltName: Full=RNA polymerase subunit alpha; AltName: Full=Transcriptase subunit alpha	37,6	3,26	1	1	1,07E+08	0,04	3,18E+05	0,00	3,26	1	1	9,36E+08	0,05	2,78E+06	0,00
PPA1994	RecName: Full=Adenylosuccinate synthetase; Short=AMPSase; Short=AdSS; AltName: Full=IMP--aspartate ligase	46,7	2,10	1	1	1,70E+08	0,07	3,98E+05	0,00	2,10	1	2	8,68E+08	0,05	2,03E+06	0,00
ECP_4208	RecName: Full=Regulator of sigma D	18,2		0	0	0,00E+00			0,00	12,66	3	3	8,40E+08	0,04	5,31E+06	2,71
infB	RecName: Full=Translation initiation factor IF-2	96,6	0,90	1	1	3,09E+08	0,12	3,48E+05	1,06	0,90	1	1	8,36E+08	0,04	9,41E+05	18,48
mukB	RecName: Full=Chromosome partition protein MukB; AltName: Full=Structural maintenance of chromosome-related protein	173,3		0	0	0,00E+00			0,00	0,46	1	1	8,03E+08	0,04	5,32E+05	0,00
	RecName: Full=Glucokinase; AltName: Full=Glucose kinase	37,7		0	0	0,00E+00			0,00	1,97	1	2	8,00E+08	0,04	2,25E+06	0,00
BruAb2_1122	RecName: Full=Putative binding protein BruAb2_1122; Flags: Precursor	34,4		0	0	0,00E+00			0,00	13,17	1	1	7,86E+08	0,04	2,46E+06	0,00
rpmB	RecName: Full=50S ribosomal protein L28	9,0	12,82	1	1	3,78E+07	0,01	4,85E+05	0,01	24,36	2	4	7,63E+08	0,04	9,78E+06	0,23
rpsS	RecName: Full=30S ribosomal protein S19	10,8		0	0	0,00E+00			0,00	15,05	1	1	7,19E+08	0,04	7,73E+06	0,09
rpsO	RecName: Full=30S ribosomal protein S15	10,3		0	0	0,00E+00			0,00	33,71	1	2	6,40E+08	0,03	7,19E+06	0,09
SCO6060	RecName: Full=UDP-N-acetylmuramate--L-alanine ligase; AltName: Full=UDP-N-acetylmuramoyl-L-alanine synthetase	47,6		0	0	0,00E+00			0,00	2,60	1	1	6,23E+08	0,03	1,35E+06	0,00
ykpA	RecName: Full=Uncharacterized ABC transporter ATP-binding protein YkpA	61,0		0	0	0,00E+00			0,00	1,30	1	1	5,84E+08	0,03	1,08E+06	0,00
rpoA	RecName: Full=DNA-directed RNA polymerase subunit alpha; Short=RNAP subunit alpha; AltName: Full=RNA polymerase subunit alpha; AltName: Full=Transcriptase subunit alpha	34,9	4,76	1	3	1,18E+08	0,05	3,74E+05	0,00	4,76	1	3	5,43E+08	0,03	1,72E+06	0,00
rplB	RecName: Full=50S ribosomal protein L2	29,8		0	0	0,00E+00			0,00	23,44	4	11	5,29E+08	0,03	1,94E+06	0,11
rplO	RecName: Full=50S ribosomal protein L15	16,0	12,58	1	1	4,48E+07	0,02	2,97E+05	0,00	19,21	2	3	4,95E+08	0,03	3,28E+06	0,00
	RecName: Full=Elongation factor G; Short=EF-G	76,5		0	0	0,00E+00			0,00	1,73	1	1	4,46E+08	0,02	6,42E+05	15,41

Gene Name	Description	MW[kDa]	sample_Mpa_50per							sample_Cp_50per						
			Coverage	# Peptides	# PSMs	Area	Rel. Area (%)	Norm. Area	ControlQ	Coverage	# Peptides	# PSMs	Area	Rel. Area (%)	Norm. Area	ControlQ
rplP	RecName: Full=50S ribosomal protein L16	15,9		0	0	0,00E+00			0,00	10,14	1	2	4,31E+08	0,02	3,13E+06	0,00
pgk	RecName: Full=Phosphoglycerate kinase	41,7		0	0	0,00E+00			0,00	4,22	1	1	4,15E+08	0,02	1,03E+06	0,00
mshD	RecName: Full=Mycothiol acetyltransferase; Short=MSH acetyltransferase; AltName: Full=Mycothiol synthase	32,9		0	0	0,00E+00			0,00	3,57	1	1	4,04E+08	0,02	1,31E+06	0,00
c2831	RecName: Full=Glutamate-pyruvate aminotransferase AlaA	45,5		0	0	0,00E+00			0,00	19,51	6	6	4,03E+08	0,02	9,96E+05	0,35
	RecName: Full=50S ribosomal protein L1	25,6	18,33	3	4	7,44E+07	0,03	3,10E+05	0,00	20,00	3	4	3,97E+08	0,02	1,65E+06	0,00
SCO3801	RecName: Full=Probable M18 family aminopeptidase 2	45,9	2,08	1	1	2,31E+07	0,01	5,35E+04	0,00	6,71	2	2	3,92E+08	0,02	9,07E+05	0,00
hemL	RecName: Full=Glutamate-1-semialdehyde 2,1-aminomutase; Short=GSA; AltName: Full=Glutamate-1-semialdehyde aminotransferase; Short=GSA-AT	45,5		0	0	0,00E+00			0,00	2,58	1	1	3,80E+08	0,02	8,91E+05	0,00
rplD	RecName: Full=50S ribosomal protein L4	23,6		0	0	0,00E+00			0,00	4,57	1	1	3,70E+08	0,02	1,69E+06	0,00
	RecName: Full=GTPase obg; AltName: Full=GTP-binding protein obg	51,0	3,77	1	2	0,00E+00			0,00	11,30	3	4	3,49E+08	0,02	7,30E+05	0,00
	RecName: Full=Phosphate-binding protein PstS; Short=PBP; Flags: Precursor	37,3	2,33	1	1	2,70E+08	0,10	7,84E+05	0,00	2,33	1	1	3,46E+08	0,02	1,01E+06	0,00
hemL	RecName: Full=Glutamate-1-semialdehyde 2,1-aminomutase; Short=GSA; AltName: Full=Glutamate-1-semialdehyde aminotransferase; Short=GSA-AT	45,3		0	0	0,00E+00			0,00	22,54	7	8	3,42E+08	0,02	8,03E+05	0,12
SCO4079	RecName: Full=Phosphoribosylformylglycinamidine synthase 2; AltName: Full=Phosphoribosylformylglycinamidine synthase II; Short=FGAM synthase II	79,8	1,33	1	1	2,03E+07	0,01	2,70E+04	0,00	2,53	2	2	3,28E+08	0,02	4,37E+05	0,00
	RecName: Full=Uncharacterized protein YffL	25,1	3,29	1	2	4,02E+08	0,15	1,89E+06	0,00	3,29	1	1	3,24E+08	0,02	1,52E+06	0,00
plsX	RecName: Full=Phosphate acyltransferase; AltName: Full=Acyl-ACP phosphotransacylase; AltName: Full=Acyl-[acyl-carrier-protein]--phosphate acyltransferase; AltName: Full=Phosphate-acyl-ACP acyltransferase	36,2		0	0	0,00E+00			0,00	2,67	1	1	3,23E+08	0,02	9,57E+05	0,00
pfk	RecName: Full=6-phosphofructokinase 2; AltName: Full=Phosphofructokinase 2; AltName: Full=Phosphohexokinase 2	39,5	4,92	1	1	0,00E+00			0,00	4,92	1	1	3,00E+08	0,02	8,20E+05	0,00

Gene Name	Description	MW[kDa]	sample_Mpa_50per							sample_Cp_50per						
			Coverage	# Peptides	# PSMs	Area	Rel. Area (%)	Norm. Area	ControlQ	Coverage	# Peptides	# PSMs	Area	Rel. Area (%)	Norm. Area	ControlQ
HI0441	RecName: Full=Ribosomal RNA large subunit methyltransferase J; AltName: Full=23S rRNA (adenine(2030)-N6)-methyltransferase; AltName: Full=23S rRNA m6A2030 methyltransferase; AltName: Full=ORFJ	32,2	4,63	1	1	7,02E+07	0,03	2,50E+05	0,00	4,63	1	1	2,88E+08	0,02	1,02E+06	0,00
ribB	RecName: Full=3,4-dihydroxy-2-butanone 4-phosphate synthase; Short=DHBP synthase	23,7		0	0	0,00E+00			0,00	20,18	1	1	2,74E+08	0,01	1,26E+06	0,00
ilvC	RecName: Full=Ketol-acid reductoisomerase; AltName: Full=Acetohydroxy-acid isomeroreductase; AltName: Full=Alpha-keto-beta-hydroxylacyl reductoisomerase	36,8		0	0	0,00E+00			0,00	2,65	1	1	2,56E+08	0,01	7,54E+05	0,00
	RecName: Full=Aconitate hydratase	101,1		0	0	0,00E+00			0,00	1,18	1	1	2,51E+08	0,01	2,69E+05	0,00
	RecName: Full=4-hydroxy-tetrahydrodipicolinate reductase; Short=HTPA reductase	25,7		0	0	0,00E+00			0,00	5,31	1	1	2,41E+08	0,01	9,83E+05	0,00
	RecName: Full=FKBP-type peptidyl-prolyl cis-trans isomerase SlyD; Short=PPIase; AltName: Full=Metallochaperone SlyD	21,0		0	0	0,00E+00			0,00	12,82	2	6	2,30E+08	0,01	1,18E+06	0,02
	RecName: Full=tRNA (guanine-N(7)-)-methyltransferase; AltName: Full=tRNA (guanine(46)-N(7))-methyltransferase; AltName: Full=tRNA(m7G46)-methyltransferase	27,3		0	0	0,00E+00			0,00	9,21	2	2	2,21E+08	0,01	9,23E+05	0,07
rplB	RecName: Full=50S ribosomal protein L2	29,8		0	0	0,00E+00			0,00	5,11	1	2	2,19E+08	0,01	7,99E+05	0,22
def1	RecName: Full=Peptide deformylase 1; Short=PDF 1; AltName: Full=Polypeptide deformylase 1	24,1		0	0	0,00E+00			0,00	7,87	1	1	2,12E+08	0,01	9,84E+05	0,00
	RecName: Full=NAD-dependent malic enzyme; Short=NAD-ME	51,5		0	0	0,00E+00			0,00	3,77	1	1	2,11E+08	0,01	4,42E+05	0,00
Acel_0306	RecName: Full=50S ribosomal protein L3	23,5		0	0	0,00E+00			0,00	4,50	1	1	2,11E+08	0,01	9,50E+05	0,00
	RecName: Full=GTP cyclohydrolase 1; AltName: Full=GTP cyclohydrolase I; Short=GTP-CH-I	24,8		0	0	0,00E+00			0,00	13,51	2	2	2,09E+08	0,01	9,41E+05	1,54
	RecName: Full=Chaperone protein DnaK; AltName: Full=HSP70; AltName: Full=Heat shock 70 kDa protein; AltName: Full=Heat shock protein 70	69,1	15,99	8	8	1,09E+08	0,04	1,71E+05	0,03	15,99	9	10	2,08E+08	0,01	3,26E+05	0,08
	RecName: Full=Soluble pyridine nucleotide transhydrogenase; Short=STH; AltName: Full=NAD(P)(+) transhydrogenase [B-specific]	51,5	54,72	18	120	6,03E+09	2,32	1,30E+07	0,10	9,87	2	2	2,06E+08	0,01	4,41E+05	0,46
rpsO	RecName: Full=30S ribosomal protein S15	10,3		0	0	0,00E+00			0,00	10,11	1	1	2,05E+08	0,01	2,30E+06	0,00

Gene Name	Description	MW[kDa]	sample_Mpa_50per							sample_Cp_50per						
			Coverage	# Peptides	# PSMs	Area	Rel. Area (%)	Norm. Area	ControlQ	Coverage	# Peptides	# PSMs	Area	Rel. Area (%)	Norm. Area	ControlQ
gyrB	RecName: Full=DNA gyrase subunit B	90,1		0	0	0,00E+00			0,00	1,24	1	1	2,02E+08	0,01	2,50E+05	11,10
	RecName: Full=50S ribosomal protein L17	14,4		0	0	0,00E+00			0,00	7,87	1	1	1,94E+08	0,01	1,52E+06	0,10
	RecName: Full=30S ribosomal protein S19	10,4		0	0	0,00E+00			0,00	16,30	1	1	1,77E+08	0,01	1,93E+06	0,04
efp	RecName: Full=Elongation factor P; Short=EF-P	20,6		0	0	0,00E+00			0,00	10,11	1	2	1,75E+08	0,01	9,29E+05	0,00
	RecName: Full=Serine hydroxymethyltransferase; Short=SHMT; Short=Serine methylase	44,5	2,21	1	1	5,22E+07	0,02	1,28E+05	0,00	2,21	1	1	1,66E+08	0,01	4,09E+05	0,00
	RecName: Full=Succinate dehydrogenase flavoprotein subunit	64,4	9,52	5	5	8,39E+07	0,03	1,43E+05	0,04	7,65	4	4	1,66E+08	0,01	2,82E+05	0,42
ackA	RecName: Full=Acetate kinase; AltName: Full=Acetokinase	43,2		0	0	0,00E+00			0,00	4,44	1	1	1,66E+08	0,01	4,10E+05	0,00
dnaK	RecName: Full=Chaperone protein DnaK; AltName: Full=HSP70; AltName: Full=Heat shock 70 kDa protein; AltName: Full=Heat shock protein 70	69,4	2,80	2	2	3,23E+07	0,01	5,03E+04	0,02	2,80	3	3	1,66E+08	0,01	2,58E+05	0,15
yrbI	RecName: Full=3-deoxy-D-manno-octulosonate 8-phosphate phosphatase KdsC; AltName: Full=KDO 8-P phosphatase	19,4		0	0	0,00E+00			0,00	3,89	1	1	1,65E+08	0,01	9,18E+05	0,00
	RecName: Full=3-oxoacyl-[acyl-carrier-protein] synthase 2; AltName: Full=3-oxoacyl-[acyl-carrier-protein] synthase II; AltName: Full=Beta-ketoacyl-ACP synthase II; Short=KAS II	43,0		0	0	0,00E+00			0,00	3,39	1	1	1,61E+08	0,01	3,91E+05	0,67
	RecName: Full=ATP synthase subunit beta; AltName: Full=ATP synthase F1 sector subunit beta; AltName: Full=F-ATPase subunit beta	50,3		0	0	0,00E+00			0,00	17,39	5	6	1,60E+08	0,01	3,48E+05	0,64
rpsC	RecName: Full=30S ribosomal protein S3	26,1	9,87	2	2	9,26E+07	0,04	3,98E+05	0,01	21,03	3	3	1,59E+08	0,01	6,84E+05	0,06
	RecName: Full=30S ribosomal protein S3	26,0	9,87	2	2	9,26E+07	0,04	3,98E+05	0,01	21,03	3	3	1,59E+08	0,01	6,84E+05	0,06
ddl	RecName: Full=D-alanine--D-alanine ligase; AltName: Full=D-Ala-D-Ala ligase; AltName: Full=D-alanylalanine synthetase	32,6		0	0	0,00E+00			0,00	3,29	1	1	1,59E+08	0,01	5,24E+05	0,00
	RecName: Full=Tyrosine recombinase XerD	34,2		0	0	0,00E+00			0,00	11,41	4	4	1,59E+08	0,01	5,34E+05	3,05
tkt	RecName: Full=Transketolase; Short=TK	75,5		0	0	0,00E+00			0,00	1,29	1	1	1,56E+08	0,01	2,23E+05	0,00
	RecName: Full=Prolyl tri/tetrapeptidyl aminopeptidase; Short=PTP-SM; AltName: Full=Tripeptidyl aminopeptidase; Short=SM-TAP; Flags: Precursor	53,7		0	0	0,00E+00			0,00	2,52	1	1	1,55E+08	0,01	3,26E+05	0,00

Gene Name	Description	MW[kDa]	sample_Mpa_50per							sample_Cp_50per						
			Coverage	# Peptides	# PSMs	Area	Rel. Area (%)	Norm. Area	ControlQ	Coverage	# Peptides	# PSMs	Area	Rel. Area (%)	Norm. Area	ControlQ
ppsC	RecName: Full=Plipastatin synthase subunit C; AltName: Full=Peptide synthase 3; Includes: RecName: Full=ATP-dependent glutamate adenylase 2; Short=GluA 2; AltName: Full=Glutamate activase 2; Includes: RecName: Full=ATP-dependent alanine/valine adenylase; Short=Ala/ValA; AltName: Full=Alanine/valine activase	287,3		0	0	0,00E+00			0,00	0,67	1	1	1,55E+08	0,01	6,07E+04	0,00
mesJ	RecName: Full=tRNA(Ile)-lysidine synthase; AltName: Full=tRNA(Ile)-2-lysyl-cytidine synthase; AltName: Full=tRNA(Ile)-lysidine synthetase	36,2	3,77	1	1	1,64E+07	0,01	4,76E+04	0,00	3,77	1	1	1,50E+08	0,01	4,34E+05	0,00
	RecName: Full=UPF0234 protein Mmcs_0777	18,2	4,91	1	1	2,02E+07	0,01	1,24E+05	0,00	12,27	2	2	1,49E+08	0,01	9,13E+05	0,00
argS	RecName: Full=Arginine--tRNA ligase; AltName: Full=Arginyl-tRNA synthetase; Short=ArgRS	64,7	1,88	1	1	5,89E+07	0,02	1,00E+05	0,00	1,88	1	1	1,49E+08	0,01	2,54E+05	0,00
dapF	RecName: Full=Diaminopimelate epimerase; Short=DAP epimerase	30,0		0	0	0,00E+00			0,00	4,50	1	1	1,45E+08	0,01	5,03E+05	0,00
SCO0527	RecName: Full=Cold shock protein ScoF	7,2		0	0	0,00E+00			0,00	25,37	1	1	1,44E+08	0,01	2,14E+06	0,00
dnaK	RecName: Full=Chaperone protein DnaK; AltName: Full=HSP70; AltName: Full=Heat shock 70 kDa protein; AltName: Full=Heat shock protein 70	68,4	1,42	1	1	5,19E+07	0,02	8,19E+04	0,03	1,42	1	1	1,43E+08	0,01	2,26E+05	0,11
	RecName: Full=Ferredoxin	11,7	31,43	2	3	0,00E+00			0,00	31,43	2	2	1,42E+08	0,01	1,35E+06	0,00
rplB	RecName: Full=50S ribosomal protein L2	30,5	4,68	1	1	6,56E+06	0,00	2,36E+04	0,00	4,68	1	2	1,41E+08	0,01	5,08E+05	0,05
SCO4179	RecName: Full=UPF0678 fatty acid-binding protein-like protein SCO4179	21,7	12,04	2	2	6,28E+07	0,02	3,29E+05	0,00	4,71	1	1	1,39E+08	0,01	7,27E+05	0,00
Rru_A0931	RecName: Full=Aldehyde dehydrogenase	55,4		0	0	0,00E+00			0,00	2,96	1	1	1,38E+08	0,01	2,73E+05	0,00
dnaK	RecName: Full=Chaperone protein DnaK; AltName: Full=HSP70; AltName: Full=Heat shock 70 kDa protein; AltName: Full=Heat shock protein 70	68,4	3,92	2	2	3,64E+07	0,01	5,71E+04	0,02	3,92	2	2	1,38E+08	0,01	2,17E+05	0,09
SCO2155	RecName: Full=Probable cytochrome c oxidase subunit 1-alpha; AltName: Full=Cytochrome aa3 subunit 1-alpha; AltName: Full=Cytochrome c oxidase polypeptide I-alpha	64,1	1,90	1	1	4,99E+07	0,02	8,63E+04	0,00	1,90	1	1	1,37E+08	0,01	2,37E+05	0,00
	RecName: Full=Uridylate kinase; Short=UK; AltName: Full=Uridine monophosphate kinase; Short=UMP kinase; Short=UMPK	25,2		0	0	0,00E+00			0,00	3,75	1	1	1,36E+08	0,01	5,69E+05	0,00

Gene Name	Description	MW[kDa]	sample_Mpa_50per							sample_Cp_50per						
			Coverage	# Peptides	# PSMs	Area	Rel. Area (%)	Norm. Area	ControlQ	Coverage	# Peptides	# PSMs	Area	Rel. Area (%)	Norm. Area	ControlQ
ureC	RecName: Full=Urease subunit alpha; AltName: Full=Urea amidohydrolase subunit alpha	59,6	1,25	1	1	7,79E+07	0,03	1,39E+05	0,00	1,25	1	1	1,35E+08	0,01	2,40E+05	0,00
	RecName: Full=60 kDa chaperonin; AltName: Full=GroEL protein; AltName: Full=Protein Cpn60	57,3	2,01	1	1	2,16E+07	0,01	3,95E+04	0,00	5,29	1	1	1,34E+08	0,01	2,44E+05	1,87
rplM	RecName: Full=50S ribosomal protein L13	16,0		0	0	0,00E+00			0,00	14,08	1	1	1,30E+08	0,01	9,12E+05	0,06
thrS	RecName: Full=Threonine--tRNA ligase; AltName: Full=Threonyl-tRNA synthetase; Short=ThrRS	74,2		0	0	0,00E+00			0,00	4,26	2	2	1,29E+08	0,01	1,96E+05	0,00
thrB	RecName: Full=Homoserine kinase; Short=HK; Short=HSK	31,3		0	0	0,00E+00			0,00	3,61	1	1	1,28E+08	0,01	4,18E+05	0,00
xerC	RecName: Full=Tyrosine recombinase XerC	33,8		0	0	0,00E+00			0,00	4,70	1	1	1,22E+08	0,01	4,10E+05	1,28
clpC	RecName: Full=Negative regulator of genetic competence ClpC/MecB	90,1		0	0	0,00E+00			0,00	3,33	2	2	1,22E+08	0,01	1,51E+05	0,00
murC	RecName: Full=UDP-N-acetylmuramate--L-alanine ligase; AltName: Full=UDP-N-acetylmuramoyl-L-alanine synthetase	48,0		0	0	0,00E+00			0,00	2,59	1	1	1,18E+08	0,01	2,55E+05	0,00
SCO5212	RecName: Full=3-phosphoshikimate 1-carboxyvinyltransferase 2; AltName: Full=5-enolpyruvylshikimate-3-phosphate synthase 2; Short=EPSP synthase 2; Short=EPSPS 2	45,8		0	0	0,00E+00			0,00	4,79	1	1	1,13E+08	0,01	2,57E+05	0,00
	RecName: Full=Elongation factor G; Short=EF-G	77,5	2,84	1	1	2,50E+07	0,01	3,55E+04	0,18	2,84	1	1	1,12E+08	0,01	1,59E+05	2,34
fusA	RecName: Full=Elongation factor G; Short=EF-G	79,3	2,82	1	1	2,50E+07	0,01	3,52E+04	0,38	2,82	1	1	1,12E+08	0,01	1,58E+05	3,89
PPA2219	RecName: Full=Serine--tRNA ligase; AltName: Full=Seryl-tRNA synthetase; Short=SerRS; AltName: Full=Seryl-tRNA(Ser/Sec) synthetase	46,5		0	0	0,00E+00			0,00	3,77	1	1	1,05E+08	0,01	2,48E+05	0,00
gatA	RecName: Full=Glutamyl-tRNA(Gln) amidotransferase subunit A; Short=Glu-ADT subunit A	52,7	2,00	1	1	4,13E+07	0,02	8,25E+04	0,00	2,00	1	1	1,05E+08	0,01	2,09E+05	0,00
SCO1570	RecName: Full=Argininosuccinate lyase; Short=ASAL; AltName: Full=Arginosuccinase	50,9	3,37	1	1	3,42E+07	0,01	7,20E+04	0,00	7,37	3	3	1,03E+08	0,01	2,17E+05	0,00
SAV_6025	RecName: Full=Probable cytosol aminopeptidase; AltName: Full=Leucine aminopeptidase; Short=LAP; AltName: Full=Leucyl aminopeptidase	51,9	4,87	2	2	2,53E+07	0,01	4,93E+04	0,00	2,92	1	2	9,95E+07	0,01	1,94E+05	0,00
	RecName: Full=HIT-like protein HinT; AltName: Full=Purine nucleoside phosphoramidase	13,2	10,92	1	1	3,38E+07	0,01	2,84E+05	0,00	31,93	3	3	9,77E+07	0,01	8,21E+05	0,58

Gene Name	Description	MW[kDa]	sample_Mpa_50per							sample_Cp_50per						
			Coverage	# Peptides	# PSMs	Area	Rel. Area (%)	Norm. Area	ControlQ	Coverage	# Peptides	# PSMs	Area	Rel. Area (%)	Norm. Area	ControlQ
	RecName: Full=Bifunctional polymyxin resistance protein ArnA; AltName: Full=Polymyxin resistance protein PmrI; Includes: RecName: Full=UDP-4-amino-4-deoxy-L-arabinose formyltransferase; AltName: Full=ArnAFT; AltName: Full=UDP-L-Ara4N formyltransferase; Includes: RecName: Full=UDP-glucuronic acid oxidase, UDP-4-keto-hexauronic acid decarboxylating; AltName: Full=ArnADH; AltName: Full=UDP-GlcUA decarboxylase; AltName: Full=UDP-glucuronic acid dehydrogenase	74,2	32,88	19	42	1,37E+09	0,53	2,07E+06	0,21	4,55	3	3	9,76E+07	0,01	1,48E+05	0,30
arnA	RecName: Full=Bifunctional polymyxin resistance protein ArnA; Includes: RecName: Full=UDP-4-amino-4-deoxy-L-arabinose formyltransferase; AltName: Full=ArnAFT; AltName: Full=UDP-L-Ara4N formyltransferase; Includes: RecName: Full=UDP-glucuronic acid oxidase, UDP-4-keto-hexauronic acid decarboxylating; AltName: Full=ArnADH; AltName: Full=UDP-GlcUA decarboxylase; AltName: Full=UDP-glucuronic acid dehydrogenase	74,3	27,58	16	36	1,37E+09	0,53	2,07E+06	0,21	4,55	3	3	9,76E+07	0,01	1,48E+05	0,30
	RecName: Full=Streptomycin biosynthesis protein StrG	23,1	6,53	1	1	0,00E+00			0,00	6,53	1	1	9,64E+07	0,01	4,84E+05	0,00
	RecName: Full=Histidine biosynthesis bifunctional protein HisB; Includes: RecName: Full=Histidinol-phosphatase; Includes: RecName: Full=Imidazoleglycerol-phosphate dehydratase; Short=IGPD	40,3	12,11	3	3	2,46E+07	0,01	6,94E+04	0,04	6,76	2	2	9,60E+07	0,01	2,70E+05	0,31
	RecName: Full=Histidine biosynthesis bifunctional protein HisB; Includes: RecName: Full=Histidinol-phosphatase; Includes: RecName: Full=Imidazoleglycerol-phosphate dehydratase; Short=IGPD	40,1	12,11	3	3	2,46E+07	0,01	6,94E+04	0,04	6,76	2	2	9,60E+07	0,01	2,70E+05	0,31
hemL	RecName: Full=Glutamate-1-semialdehyde 2,1-aminomutase; Short=GSA; AltName: Full=Glutamate-1-semialdehyde aminotransferase; Short=GSA-AT	44,4		0	0	0,00E+00			0,00	2,59	1	1	9,28E+07	0,00	2,19E+05	0,00
add	RecName: Full=Adenosine deaminase; AltName: Full=Adenosine aminohydrolase	36,4		0	0	0,00E+00			0,00	6,91	2	2	9,06E+07	0,00	2,72E+05	0,45

Gene Name	Description	MW[kDa]	sample_Mpa_50per							sample_Cp_50per						
			Coverage	# Peptides	# PSMs	Area	Rel. Area (%)	Norm. Area	ControlQ	Coverage	# Peptides	# PSMs	Area	Rel. Area (%)	Norm. Area	ControlQ
murC	RecName: Full=UDP-N-acetylmuramate--L-alanine ligase; AltName: Full=UDP-N-acetylmuramoyl-L-alanine synthetase	50,1		0	0	0,00E+00			0,00	6,72	1	1	8,79E+07	0,00	1,85E+05	0,00
folE	RecName: Full=GTP cyclohydrolase 1; AltName: Full=GTP cyclohydrolase I; Short=GTP-CH-I	22,3		0	0	0,00E+00			0,00	7,96	1	1	8,49E+07	0,00	4,23E+05	0,00
SCO2127	RecName: Full=Uncharacterized protein SCO2127	20,1	4,71	1	1	2,78E+07	0,01	1,46E+05	0,00	4,71	1	1	8,15E+07	0,00	4,27E+05	0,00
	RecName: Full=Phospho-2-dehydro-3-deoxyheptonate aldolase; AltName: Full=3-deoxy-D-arabino-heptulosonate 7-phosphate synthase; AltName: Full=DAHP synthase; AltName: Full=Phospho-2-keto-3-deoxyheptonate aldolase	2,2	50,00	1	1	3,80E+07	0,01	2,11E+06	0,00	50,00	1	1	7,81E+07	0,00	4,34E+06	0,00
SCO3412	RecName: Full=UPF0145 protein SCO3412	11,3	10,38	1	1	3,33E+07	0,01	3,14E+05	0,00	10,38	1	1	7,77E+07	0,00	7,33E+05	0,00
rpsF	RecName: Full=30S ribosomal protein S6	11,2		0	0	0,00E+00			0,00	34,38	2	2	7,70E+07	0,00	8,02E+05	0,00
	RecName: Full=UDP-N-acetylglucosamine--N-acetylmuramyl-(pentapeptide) pyrophosphoryl-undecaprenol N-acetylglucosamine transferase; AltName: Full=Undecaprenyl-PP-MurNAc-pentapeptide-UDPGlcNAc GlcNAc transferase	38,8	3,87	1	1	0,00E+00			0,00	3,87	1	1	7,21E+07	0,00	1,99E+05	0,00

Gene Name	Description	MW[kDa]	sample_Mpa_50per							sample_Cp_50per						
			Coverage	# Peptides	# PSMs	Area	Rel. Area (%)	Norm. Area	ControlQ	Coverage	# Peptides	# PSMs	Area	Rel. Area (%)	Norm. Area	ControlQ
	RecName: Full=Multifunctional 2-oxoglutarate metabolism enzyme; AltName: Full=2-hydroxy-3-oxoadipate synthase; Short=HOA synthase; Short=HOAS; AltName: Full=2-oxoglutarate carboxy-lyase; AltName: Full=2-oxoglutarate decarboxylase; AltName: Full=Alpha-ketoglutarate decarboxylase; Short=KG decarboxylase; Short=KGD; AltName: Full=Alpha-ketoglutarate-glyoxylate carboligase; Includes: RecName: Full=2-oxoglutarate dehydrogenase E1 component; Short=ODH E1 component; AltName: Full=Alpha-ketoglutarate dehydrogenase E1 component; Short=KDH E1 component; Includes: RecName: Full=Dihydrolipoyllysine-residue succinyltransferase component of 2-oxoglutarate dehydrogenase complex; AltName: Full=2-oxoglutarate dehydrogenase complex E2 component; Short=ODH E2 component; Short=OGDC-E2; AltName: Full=Dihydrolipoamide succinyltransferase	136,9	0,64	1	1	8,99E+07	0,03	7,24E+04	0,00	0,64	1	1	6,62E+07	0,00	5,32E+04	0,00
kgd	RecName: Full=Multifunctional 2-oxoglutarate metabolism enzyme; AltName: Full=2-hydroxy-3-oxoadipate synthase; Short=HOA synthase; Short=HOAS; AltName: Full=2-oxoglutarate carboxy-lyase; AltName: Full=2-oxoglutarate decarboxylase; AltName: Full=Alpha-ketoglutarate decarboxylase; Short=KG decarboxylase; Short=KGD; AltName: Full=Alpha-ketoglutarate-glyoxylate carboligase; Includes: RecName: Full=2-oxoglutarate dehydrogenase E1 component; Short=ODH E1 component; AltName: Full=Alpha-ketoglutarate dehydrogenase E1 component; Short=KDH E1 component; Includes: RecName: Full=Dihydrolipoyllysine-residue succinyltransferase component of 2-oxoglutarate dehydrogenase complex; AltName: Full=2-oxoglutarate dehydrogenase complex E2 component; Short=ODH E2 component; Short=OGDC-E2; AltName: Full=Dihydrolipoamide succinyltransferase	140,0	1,26	2	2	6,57E+07	0,03	5,18E+04	0,00	0,63	1	1	6,62E+07	0,00	5,21E+04	0,00

Gene Name	Description	MW[kDa]	sample_Mpa_50per							sample_Cp_50per						
			Coverage	# Peptides	# PSMs	Area	Rel. Area (%)	Norm. Area	ControlQ	Coverage	# Peptides	# PSMs	Area	Rel. Area (%)	Norm. Area	ControlQ
	RecName: Full=Valine--pyruvate aminotransferase; AltName: Full=Alanine--valine transaminase; AltName: Full=Transaminase C	46,7		0	0	0,00E+00			0,00	10,55	3	3	6,59E+07	0,00	1,58E+05	0,23
	RecName: Full=Probable glycerophosphoryl diester phosphodiesterase 1; Short=Glycerophosphodiester phosphodiesterase 1	29,9		0	0	0,00E+00			0,00	3,65	1	1	6,35E+07	0,00	2,32E+05	0,00
Francci3_3707	RecName: Full=ATP synthase subunit beta; AltName: Full=ATP synthase F1 sector subunit beta; AltName: Full=F-ATPase subunit beta	52,3		0	0	0,00E+00			0,00	4,38	1	1	6,27E+07	0,00	1,31E+05	0,00
SCO1818	RecName: Full=Tyrosine--tRNA ligase; AltName: Full=Tyrosyl-tRNA synthetase; Short=TyrRS	46,3		0	0	0,00E+00			0,00	3,32	1	1	6,14E+07	0,00	1,46E+05	0,00
Mnod_5503	RecName: Full=Protein RecA; AltName: Full=Recombinase A	38,9		0	0	0,00E+00			0,00	3,03	1	1	5,83E+07	0,00	1,61E+05	0,00
	RecName: Full=2-oxoglutarate dehydrogenase E1 component; AltName: Full=Alpha-ketoglutarate dehydrogenase	105,0	19,40	16	25	5,74E+08	0,22	6,15E+05	0,26	3,64	3	3	5,63E+07	0,00	6,04E+04	0,22
	RecName: Full=Dihydrolipoyl dehydrogenase; AltName: Full=Dihydrolipoamide dehydrogenase; AltName: Full=E3 component of pyruvate and 2-oxoglutarate dehydrogenases complexes; AltName: Full=Glycine cleavage system L protein	50,7	15,61	6	7	7,89E+07	0,03	1,66E+05	0,02	11,81	3	3	5,54E+07	0,00	1,17E+05	0,21
topA	RecName: Full=DNA topoisomerase 1; AltName: Full=DNA topoisomerase I; AltName: Full=Omega-protein; AltName: Full=Relaxing enzyme; AltName: Full=Swivelase; AltName: Full=Untwisting enzyme	104,0		0	0	0,00E+00			0,00	0,74	1	1	5,29E+07	0,00	5,59E+04	0,00
tolA	RecName: Full=Protein TolA	39,8		0	0	0,00E+00			0,00	2,15	1	1	4,95E+07	0,00	1,33E+05	0,00
	RecName: Full=dTDP-4-dehydrorhamnose reductase; AltName: Full=dTDP-4-keto-L-rhamnose reductase; AltName: Full=dTDP-6-deoxy-L-lyxo-4-hexulose reductase; AltName: Full=dTDP-6-deoxy-L-mannose dehydrogenase; AltName: Full=dTDP-L-rhamnose synthase	32,2	8,55	2	2	2,16E+07	0,01	7,11E+04	0,00	3,95	1	1	4,85E+07	0,00	1,60E+05	0,00
SCO3649	RecName: Full=Fructose-bisphosphate aldolase; Short=FBP aldolase; Short=FBPA; AltName: Full=Fructose-1,6-bisphosphate aldolase	36,9		0	0	0,00E+00			0,00	3,79	1	1	4,79E+07	0,00	1,40E+05	0,00
hisC2	RecName: Full=Putative phenylalanine aminotransferase	38,7		0	0	0,00E+00			0,00	5,57	1	1	4,76E+07	0,00	1,33E+05	0,00

Gene Name	Description	MW[kDa]	sample_Mpa_50per							sample_Cp_50per						
			Coverage	# Peptides	# PSMs	Area	Rel. Area (%)	Norm. Area	ControlQ	Coverage	# Peptides	# PSMs	Area	Rel. Area (%)	Norm. Area	ControlQ
SCO5425	RecName: Full=Phosphate acetyltransferase; AltName: Full=Phosphotransacetylase	74,0		0	0	0,00E+00			0,00	3,44	2	2	4,41E+07	0,00	6,32E+04	0,00
	RecName: Full=Rod shape-determining protein MreB	36,9		0	0	0,00E+00			0,00	3,46	1	1	4,16E+07	0,00	1,20E+05	0,04
mreB	RecName: Full=Rod shape-determining protein MreB	37,4		0	0	0,00E+00			0,00	3,42	1	1	4,16E+07	0,00	1,19E+05	0,07
yobI	RecName: Full=Uncharacterized membrane protein YobI	140,5		0	0	0,00E+00			0,00	0,83	1	1	3,94E+07	0,00	3,28E+04	0,00
SCO2562	RecName: Full=Elongation factor 4; Short=EF-4; AltName: Full=Ribosomal back-translocase LepA	68,3		0	0	0,00E+00			0,00	2,57	1	1	3,63E+07	0,00	5,83E+04	0,00
trpS	RecName: Full=Tryptophan--tRNA ligase; AltName: Full=Tryptophanyl-tRNA synthetase; Short=TrpRS	37,8		0	0	0,00E+00			0,00	2,90	1	1	3,56E+07	0,00	1,03E+05	0,00
	RecName: Full=Protein PmbA	48,3		0	0	0,00E+00			0,00	6,00	2	2	3,53E+07	0,00	7,85E+04	0,65
	RecName: Full=dTDP-glucose 4,6-dehydratase	35,6		0	0	0,00E+00			0,00	4,57	1	1	3,46E+07	0,00	1,05E+05	0,00
hisE	RecName: Full=Phosphoribosyl-ATP pyrophosphatase; Short=PRA-PH	9,9		0	0	0,00E+00			0,00	12,22	1	1	3,25E+07	0,00	3,61E+05	0,00
ilvC	RecName: Full=Ketol-acid reductoisomerase; AltName: Full=Acetohydroxy-acid isomeroreductase; AltName: Full=Alpha-keto-beta-hydroxylacyl reductoisomerase	36,9		0	0	0,00E+00			0,00	3,34	1	1	2,81E+07	0,00	8,55E+04	0,00
	RecName: Full=Anti-sigma F factor antagonist; AltName: Full=Stage II sporulation protein AA	13,3		0	0	0,00E+00			0,00	7,69	1	1	2,73E+07	0,00	2,33E+05	0,00
	RecName: Full=Anaerobic glycerol-3-phosphate dehydrogenase subunit A; Short=G-3-P dehydrogenase	58,9		0	0	0,00E+00			0,00	2,77	1	1	2,55E+07	0,00	4,70E+04	0,69
	RecName: Full=Formate dehydrogenase-O major subunit; AltName: Full=Aerobic formate dehydrogenase major subunit; AltName: Full=FDH-Z subunit alpha; AltName: Full=Formate dehydrogenase-O subunit alpha; Flags: Precursor	112,5		0	0	0,00E+00			0,00	1,77	1	1	2,53E+07	0,00	2,49E+04	0,47
	RecName: Full=Uncharacterized protein YeiR	36,1	14,33	4	4	6,72E+07	0,03	2,05E+05	0,04	3,66	1	1	2,26E+07	0,00	6,90E+04	0,12
	RecName: Full=2-isopropylmalate synthase; AltName: Full=Alpha-IPM synthase; AltName: Full=Alpha-isopropylmalate synthase	54,7		0	0	0,00E+00			0,00	2,99	1	1	1,91E+07	0,00	3,81E+04	0,00
clpB	RecName: Full=Chaperone protein ClpB	95,8		0	0	0,00E+00			0,00	0,93	1	1	1,77E+07	0,00	2,06E+04	2,04

Gene Name	Description	MW[kDa]	sample_Mpa_50per							sample_Cp_50per						
			Coverage	# Peptides	# PSMs	Area	Rel. Area (%)	Norm. Area	ControlQ	Coverage	# Peptides	# PSMs	Area	Rel. Area (%)	Norm. Area	ControlQ
	RecName: Full=cAMP-activated global transcriptional regulator CRP; AltName: Full=Catabolite activator protein; Short=CAP; AltName: Full=Catabolite gene activator; AltName: Full=cAMP receptor protein; Short=CRP; AltName: Full=cAMP regulatory protein	23,6		0	0	0,00E+00			0,00	5,71	1	1	1,37E+07	0,00	6,54E+04	0,00
rplM	RecName: Full=50S ribosomal protein L13	16,4		0	0	0,00E+00			0,00	7,48	1	1	1,14E+07	0,00	7,77E+04	0,00
sthA	RecName: Full=Soluble pyridine nucleotide transhydrogenase; Short=STH; AltName: Full=NAD(P)(+) transhydrogenase [B-specific]	51,5	15,70	6	28	1,57E+09	0,60	3,38E+06	0,04		0	0	0,00E+00			0,00
lwe1048	RecName: Full=UPF0358 protein lwe1048	10,7	8,60	1	1	7,70E+08	0,30	8,28E+06	0,00		0	0	0,00E+00			0,00
kup2	RecName: Full=Probable potassium transport system protein kup 2	80,5	1,49	1	1	6,90E+08	0,26	9,37E+05	0,00		0	0	0,00E+00			0,00
	RecName: Full=Soluble pyridine nucleotide transhydrogenase; Short=STH; AltName: Full=NAD(P)(+) transhydrogenase [B-specific]	51,5	9,59	4	19	6,68E+08	0,26	1,42E+06	0,02		0	0	0,00E+00			0,00
	RecName: Full=Soluble pyridine nucleotide transhydrogenase; Short=STH; AltName: Full=NAD(P)(+) transhydrogenase [B-specific]	51,3	9,23	4	17	6,68E+08	0,26	1,43E+06	0,02		0	0	0,00E+00			0,00
lpxD	RecName: Full=UDP-3-O-acylglucosamine N-acyltransferase	35,7	4,41	1	1	5,94E+08	0,23	1,75E+06	0,00		0	0	0,00E+00			0,00
	RecName: Full=Trigger factor; Short=TF; AltName: Full=PPIase	48,2	26,62	11	15	3,95E+08	0,15	9,15E+05	0,01		0	0	0,00E+00			0,00
	RecName: Full=DNA polymerase III subunit tau; AltName: Full=DNA polymerase III subunit gamma	71,1	9,49	6	8	2,85E+08	0,11	4,43E+05	0,09		0	0	0,00E+00			0,00
cyoE	RecName: Full=Protoheme IX farnesyltransferase; AltName: Full=Heme B farnesyltransferase; AltName: Full=Heme O synthase	35,2	3,00	1	1	2,33E+08	0,09	7,01E+05	0,00		0	0	0,00E+00			0,00
sucA	RecName: Full=2-oxoglutarate dehydrogenase E1 component; AltName: Full=Alpha-ketoglutarate dehydrogenase	106,7	2,25	2	3	2,10E+08	0,08	2,25E+05	0,28		0	0	0,00E+00			0,00
rpmA	RecName: Full=50S ribosomal protein L27	8,7	8,64	1	1	1,93E+08	0,07	2,38E+06	0,00		0	0	0,00E+00			0,00
ppnK	RecName: Full=Probable inorganic polyphosphate/ATP-NAD kinase; Short=Poly(P)/ATP NAD kinase	32,2	2,30	1	1	1,92E+08	0,07	6,32E+05	0,00		0	0	0,00E+00			0,00

Gene Name	Description	MW[kDa]	sample_Mpa_50per							sample_Cp_50per						
			Coverage	# Peptides	# PSMs	Area	Rel. Area (%)	Norm. Area	ControlQ	Coverage	# Peptides	# PSMs	Area	Rel. Area (%)	Norm. Area	ControlQ
	RecName: Full=Acetylornithine deacetylase; Short=AO; Short=Acetylornithinase; AltName: Full=N-acetylornithinase; Short=NAO	42,3	15,14	5	7	1,70E+08	0,07	4,43E+05	0,07		0	0	0,00E+00			0,00
aceE	RecName: Full=Pyruvate dehydrogenase E1 component; Short=PDH E1 component	100,8	1,13	1	1	1,49E+08	0,06	1,68E+05	0,05		0	0	0,00E+00			0,00
zwf	RecName: Full=Glucose-6-phosphate 1-dehydrogenase; Short=G6PD	56,0	1,43	1	1	1,38E+08	0,05	2,81E+05	10,38		0	0	0,00E+00			0,00
	RecName: Full=Cell division protein FtsA	45,3	2,62	1	1	1,31E+08	0,05	3,12E+05	0,03		0	0	0,00E+00			0,00
MXAN_7260	RecName: Full=CRISPR-associated protein Cas4/endonuclease Cas1 fusion	62,7	1,23	1	1	1,21E+08	0,05	2,13E+05	0,00		0	0	0,00E+00			0,00
	RecName: Full=Probable diguanylate cyclase YfiN; Short=DGC	46,0	3,19	1	1	1,09E+08	0,04	2,67E+05	0,00		0	0	0,00E+00			0,00
purU	RecName: Full=Formyltetrahydrofolate deformylase; AltName: Full=Formyl-FH(4) hydrolase	31,9	14,64	3	3	9,98E+07	0,04	3,56E+05	0,03		0	0	0,00E+00			0,00
rpsM	RecName: Full=30S ribosomal protein S13	14,4	6,35	1	1	9,23E+07	0,04	7,33E+05	0,00		0	0	0,00E+00			0,00
	RecName: Full=Soluble pyridine nucleotide transhydrogenase; Short=STH; AltName: Full=NAD(P)(+) transhydrogenase [B-specific]	50,8	1,51	1	7	8,63E+07	0,03	1,86E+05	2,09		0	0	0,00E+00			0,00
groEL	RecName: Full=60 kDa chaperonin; AltName: Full=GroEL protein; AltName: Full=Protein Cpn60	57,9	1,28	1	1	8,33E+07	0,03	1,52E+05	0,03		0	0	0,00E+00			0,00
	RecName: Full=Uricase; AltName: Full=Urate oxidase; Short=AgUOX	33,8	2,98	1	1	7,59E+07	0,03	2,51E+05	0,00		0	0	0,00E+00			0,00
tig	RecName: Full=Trigger factor; Short=TF; AltName: Full=PPIase	48,2	1,61	1	1	7,43E+07	0,03	1,71E+05	0,01		0	0	0,00E+00			0,00
hslO	RecName: Full=33 kDa chaperonin; AltName: Full=Heat shock protein 33 homolog; Short=HSP33	32,5	4,11	1	1	7,10E+07	0,03	2,43E+05	0,02		0	0	0,00E+00			0,00
	RecName: Full=Acyl carrier protein; Short=ACP	8,7	12,82	1	1	6,96E+07	0,03	8,93E+05	0,00		0	0	0,00E+00			0,00
katA	RecName: Full=Vegetative catalase	54,8	1,86	1	1	6,09E+07	0,02	1,26E+05	0,00		0	0	0,00E+00			0,00
RPE_3195	RecName: Full=Aliphatic sulfonates import ATP-binding protein SsuB	30,5	2,85	1	1	5,91E+07	0,02	2,10E+05	0,00		0	0	0,00E+00			0,00
	RecName: Full=Pyruvate dehydrogenase E1 component; Short=PDH E1 component	99,6	8,57	6	6	5,90E+07	0,02	6,65E+04	0,02		0	0	0,00E+00			0,00
	RecName: Full=Ribonuclease E; Short=RNase E	118,1	1,13	1	1	5,89E+07	0,02	5,56E+04	0,04		0	0	0,00E+00			0,00
	RecName: Full=Probable DNA endonuclease SmrA	21,5	16,58	3	3	5,83E+07	0,02	3,12E+05	0,10		0	0	0,00E+00			0,00

Gene Name	Description	MW[kDa]	sample_Mpa_50per							sample_Cp_50per						
			Coverage	# Peptides	# PSMs	Area	Rel. Area (%)	Norm. Area	ControlQ	Coverage	# Peptides	# PSMs	Area	Rel. Area (%)	Norm. Area	ControlQ
nudC	RecName: Full=NADH pyrophosphatase	29,7	20,23	4	6	5,75E+07	0,02	2,24E+05	0,11		0	0	0,00E+00			0,00
ZMO0402	RecName: Full=Ribosomal RNA large subunit methyltransferase E; AltName: Full=23S rRNA Um2552 methyltransferase; AltName: Full=rRNA (uridine-2'-O-)-methyltransferase	24,3	3,17	1	1	5,33E+07	0,02	2,41E+05	0,00		0	0	0,00E+00			0,00
	RecName: Full=Sensory transduction protein regX3	24,8	4,85	1	1	5,27E+07	0,02	2,32E+05	0,00		0	0	0,00E+00			0,00
	RecName: Full=Helicase IV; AltName: Full=75 kDa helicase	77,9	9,80	6	6	4,92E+07	0,02	7,19E+04	0,07		0	0	0,00E+00			0,00
phoH	RecName: Full=PhoH-like protein	37,7	2,29	1	1	4,91E+07	0,02	1,41E+05	0,00		0	0	0,00E+00			0,00
	RecName: Full=Outer membrane protein A; AltName: Full=Outer membrane protein II*; Flags: Precursor	37,2	3,76	1	1	4,87E+07	0,02	1,41E+05	0,02		0	0	0,00E+00			0,00
gldA	RecName: Full=Glycerol dehydrogenase; Short=GDH; Short=GLDH	38,7	2,72	1	1	4,80E+07	0,02	1,31E+05	0,20		0	0	0,00E+00			0,00
carB	RecName: Full=Carbamoyl-phosphate synthase large chain; AltName: Full=Carbamoyl-phosphate synthetase ammonia chain	125,8	0,77	1	1	4,77E+07	0,02	4,10E+04	0,00		0	0	0,00E+00			0,00
pgi	RecName: Full=Glucose-6-phosphate isomerase 2; Short=GPI 2; AltName: Full=Phosphoglucose isomerase 2; Short=PGI 2; AltName: Full=Phosphohexose isomerase 2; Short=PHI 2	60,6	1,64	1	1	4,67E+07	0,02	8,48E+04	0,00		0	0	0,00E+00			0,00
dnaJ	RecName: Full=Chaperone protein DnaJ	41,0	6,12	2	2	4,40E+07	0,02	1,17E+05	0,01		0	0	0,00E+00			0,00
lysK	RecName: Full=Lysine--tRNA ligase; AltName: Full=Lysyl-tRNA synthetase; Short=LysRS	63,5	1,55	1	1	4,37E+07	0,02	7,53E+04	0,00		0	0	0,00E+00			0,00
	RecName: Full=Primosomal protein N'; AltName: Full=ATP-dependent helicase PriA; AltName: Full=Replication factor Y	81,6	5,74	4	4	4,25E+07	0,02	5,80E+04	0,08		0	0	0,00E+00			0,00
	RecName: Full=Galactitol-1-phosphate 5-dehydrogenase	37,4	6,07	2	2	3,79E+07	0,01	1,09E+05	0,02		0	0	0,00E+00			0,00
argR	RecName: Full=Arginine repressor	17,7	5,14	1	1	3,53E+07	0,01	2,02E+05	0,00		0	0	0,00E+00			0,00

Gene Name	Description	MW[kDa]	sample_Mpa_50per							sample_Cp_50per						
			Coverage	# Peptides	# PSMs	Area	Rel. Area (%)	Norm. Area	ControlQ	Coverage	# Peptides	# PSMs	Area	Rel. Area (%)	Norm. Area	ControlQ
glnD	RecName: Full=Bifunctional uridylyltransferase/uridylyl-removing enzyme; Short=UTase/UR; AltName: Full=Bifunctional [protein-PII] modification enzyme; AltName: Full=Bifunctional nitrogen sensor protein; Includes: RecName: Full=[Protein-PII] uridylyltransferase; Short=PII uridylyltransferase; Short=UTase; Includes: RecName: Full=[Protein-PII]-UMP uridylyl-removing enzyme; Short=UR	102,3	3,82	3	3	3,25E+07	0,01	3,65E+04	0,06		0	0	0,00E+00			0,00
	RecName: Full=Granaticin polyketide synthase putative ketoacyl reductase 1; AltName: Full=ORF5	28,4	2,94	1	1	3,06E+07	0,01	1,13E+05	0,00		0	0	0,00E+00			0,00
SAV_4389	RecName: Full=Probable M18 family aminopeptidase 2	46,0	2,31	1	1	2,92E+07	0,01	6,77E+04	0,00		0	0	0,00E+00			0,00
ECP_2325	RecName: Full=NADH-quinone oxidoreductase subunit C/D; AltName: Full=NADH dehydrogenase I subunit C/D; AltName: Full=NDH-1 subunit C/D	68,2	5,70	3	3	2,82E+07	0,01	4,74E+04	0,02		0	0	0,00E+00			0,00
aceE	RecName: Full=Pyruvate dehydrogenase E1 component; Short=PDH E1 component	99,5	1,13	1	1	2,69E+07	0,01	3,05E+04	0,01		0	0	0,00E+00			0,00
	RecName: Full=Pyruvate formate-lyase 1-activating enzyme; AltName: Full=Formate-C-acetyltransferase-activating enzyme 1; AltName: Full=PFL-activating enzyme 1	28,2	4,47	1	1	2,61E+07	0,01	1,06E+05	0,05		0	0	0,00E+00			0,00
	RecName: Full=Outer membrane porin F; Flags: Precursor	36,5	3,49	1	1	2,29E+07	0,01	6,66E+04	0,00		0	0	0,00E+00			0,00
gltA	RecName: Full=Citrate synthase	48,0	2,58	1	1	2,21E+07	0,01	5,17E+04	0,07		0	0	0,00E+00			0,00
dgt	RecName: Full=Deoxyguanosinetriphosphate triphosphohydrolase; Short=dGTP triphosphohydrolase; Short=dGTPase	59,3	4,36	2	2	2,20E+07	0,01	4,35E+04	0,01		0	0	0,00E+00			0,00
uvrC	RecName: Full=UvrABC system protein C; Short=Protein UvrC; AltName: Full=Excinuclease ABC subunit C	70,4	1,29	1	1	2,18E+07	0,01	3,53E+04	0,00		0	0	0,00E+00			0,00

Gene Name	Description	MW[kDa]	sample_Mpa_50per							sample_Cp_50per						
			Coverage	# Peptides	# PSMs	Area	Rel. Area (%)	Norm. Area	ControlQ	Coverage	# Peptides	# PSMs	Area	Rel. Area (%)	Norm. Area	ControlQ
	RecName: Full=Bifunctional uridylyltransferase/uridylyl-removing enzyme; Short=UTase/UR; AltName: Full=Bifunctional [protein-PII] modification enzyme; AltName: Full=Bifunctional nitrogen sensor protein; Includes: RecName: Full=[Protein-PII] uridylyltransferase; Short=PII uridylyltransferase; Short=UTase; Includes: RecName: Full=[Protein-PII]-UMP uridylyl-removing enzyme; Short=UR	102,3	2,37	2	2	2,09E+07	0,01	2,36E+04	0,04		0	0	0,00E+00			0,00
	RecName: Full=Lipoyl synthase; AltName: Full=Lip-syn; Short=LS; AltName: Full=Lipoate synthase; AltName: Full=Lipoic acid synthase; AltName: Full=Sulfur insertion protein LipA	36,0	2,80	1	1	2,07E+07	0,01	6,46E+04	0,01		0	0	0,00E+00			0,00
	RecName: Full=Catalase HPII; AltName: Full=Hydroxyperoxidase II	84,1	4,78	3	3	1,97E+07	0,01	2,62E+04	0,12		0	0	0,00E+00			0,00
	RecName: Full=Aconitate hydratase 1; Short=Aconitase 1; AltName: Full=Citrate hydro-lyase 1	97,6	0,90	1	1	1,96E+07	0,01	2,20E+04	0,00		0	0	0,00E+00			0,00
pheT	RecName: Full=Phenylalanine--tRNA ligase beta subunit; AltName: Full=Phenylalanyl-tRNA synthetase beta subunit; Short=PheRS	90,1	1,33	1	1	1,94E+07	0,01	2,34E+04	0,00		0	0	0,00E+00			0,00
rbfA	RecName: Full=Ribosome-binding factor A	16,5	5,10	1	1	1,94E+07	0,01	1,24E+05	0,00		0	0	0,00E+00			0,00
Pnap_3468	RecName: Full=Multifunctional CCA protein; Includes: RecName: Full=CCA-adding enzyme; AltName: Full=CCA tRNA nucleotidyltransferase; AltName: Full=tRNA CCA-pyrophosphorylase; AltName: Full=tRNA adenylyl-/cytidylyl-transferase; AltName: Full=tRNA nucleotidyltransferase; AltName: Full=tRNA-NT; Includes: RecName: Full=2'-nucleotidase; Includes: RecName: Full=2',3'-cyclic phosphodiesterase; Includes: RecName: Full=Phosphatase	46,8	3,54	1	1	1,91E+07	0,01	4,51E+04	0,00		0	0	0,00E+00			0,00
groEL	RecName: Full=60 kDa chaperonin; AltName: Full=GroEL protein; AltName: Full=Protein Cpn60	57,0	1,47	1	1	1,67E+07	0,01	3,06E+04	0,00		0	0	0,00E+00			0,00
rplL	RecName: Full=50S ribosomal protein L7/L12	12,5	8,26	1	1	1,63E+07	0,01	1,34E+05	0,00		0	0	0,00E+00			0,00
thyX	RecName: Full=Thymidylate synthase ThyX; Short=TS; Short=TSase	27,8	4,47	1	1	1,62E+07	0,01	6,60E+04	0,00		0	0	0,00E+00			0,00

Gene Name	Description	MW[kDa]	sample_Mpa_50per							sample_Cp_50per						
			Coverage	# Peptides	# PSMs	Area	Rel. Area (%)	Norm. Area	ControlQ	Coverage	# Peptides	# PSMs	Area	Rel. Area (%)	Norm. Area	ControlQ
	RecName: Full=Exodeoxyribonuclease 7 small subunit; AltName: Full=Exodeoxyribonuclease VII small subunit; Short=Exonuclease VII small subunit	8,9	12,50	1	1	1,53E+07	0,01	1,92E+05	0,01		0	0	0,00E+00			0,00
ispG	RecName: Full=4-hydroxy-3-methylbut-2-en-1-yl diphosphate synthase; AltName: Full=1-hydroxy-2-methyl-2-(E)-butenyl 4-diphosphate synthase	40,8	3,16	1	1	1,35E+07	0,01	3,56E+04	0,00		0	0	0,00E+00			0,00
	RecName: Full=Oligoribonuclease	22,1	6,97	1	1	1,29E+07	0,00	6,40E+04	0,00		0	0	0,00E+00			0,00
	RecName: Full=50S ribosomal protein L7/L12; AltName: Full=L8	12,3	9,92	1	1	1,15E+07	0,00	9,51E+04	0,03		0	0	0,00E+00			0,00
	RecName: Full=Deoxyguanosinetriphosphate triphosphohydrolase; Short=dGTP triphosphohydrolase; Short=dGTPase	59,5	1,39	1	1	9,93E+06	0,00	1,97E+04	0,01		0	0	0,00E+00			0,00

ABSTRACT

Für das langfristige Überleben von *M. tuberculosis* im Wirt ist das Proteasom essentiell, wahrscheinlich sowohl durch den Abbau von Proteinen, die durch reaktive Stickstoffspezies beschädigt wurden als auch durch einen bisher unbekannten Prozeß. Das Proteasom ist daher ein vielversprechendes Ziel für zukünftige Anti-Tuberkulosemedikamente. Die Struktur des mycobakteriellen Protasoms ist nur teilweise geklärt, wobei die des zentralen proteolytischen Komplexes (dem *core particle*, CP) gut erforscht ist, die der apikalen AAA+-ATPase Mpa, besonders an den Bindungsstellen zu CP, weniger. Die Prozesse bei der Assemblierung des Mpa-CP-Komplexes sind ebenfalls nicht vollständig bekannt. Studien zeigten daß Mpa direkt an CP weder *in vivo* noch *in vitro* bindet, was die Existenz eines zusätzlichen, unidentifizierten Faktors nahelegt. Diese Arbeit versuchte, Konditionen, in denen sich der Mpa-CP-Komplex zusammenfügt und stabil bleibt, zu klären.

Photocrosslinking-Experimente mit Peptiden, die der C-terminalen CP-bindenden Domäne von Mpa entsprachen sowie mit dem kompletten Mpa-Protein, die beide die photoreaktive Aminosäure *p*-Benzoylphenylalanin enthielten, zeigten, daß die Interaktion zwischen Mpa und CP verläßlich *in vitro* reproduziert werden kann. Der Einfluß des Crosslinks auf die Entfaltungsfähigkeit von Mpa, die Proteaseaktivität des CPs, sowie die Frage, ob Mpa und CP *in vivo* aneinander binden, wurden ebenfalls untersucht. Die Ergebnisse deuten darauf hin daß die Bindung von Mpa und CP *in vivo* unter den verwendeten Bedingnungen nicht stattfindet und möglicherweise von einem zusätzlichen unbekannten, mit Mpa und/oder dem *core particle* interagierenden Faktor abhängt.

ABSTRACT

For long-term survival in the host, the proteasome of *M. tuberculosis* has been shown to be essential, likely through the removal of proteins damaged by reactive nitrogen species as well as by some as-yet unknown mechanism. This makes the mycobacterial proteasome a promising target for future anti-tuberculosis drugs. Its structure has only been partially resolved, with that of the central proteolytic complex (the core particle, CP) being well-understood but that of the apical AAA-ATPase Mpa/ARC, especially where it binds to CP, less so. The assembly of the complex is unclear as well. Previous studies have shown that Mpa does not bind to CP either *in vitro* or *in vivo*, suggesting that there must be some additional unidentified factor. This study attempted to clarify the conditions in which the complex assembles and remains stable.

Photocrosslinking experiments with peptides equivalent to the C-terminal CP-binding domain of Mpa as well as the full length Mpa protein, both containing the photoreactive amino acid *p*-Benzoylphenylalanine, showed that the interaction between Mpa and CP can be reliably reproduced *in vitro*. Further experiments were conducted to test whether the crosslinking of the complex would influence either the unfoldase activity of Mpa or the proteolytic activity of CP, as well as whether Mpa and CP would bind *in vivo.* The results indicate that binding does not occur *in vivo* under the chosen conditions and could depend on an additional, unidentified factor interacting with Mpa and/or the core particle.

CURRICULUM VITAE

2015: Master of Science in Molecular Biology with a specialization in structural biology at the University of Vienna

2013 – 2014: Master's thesis for the Clausen Group of the Institute of Molecular Biology, Vienna

2012 – 2013: Research Technician at the Clausen Group of the Institute of Molecular Biology, Vienna

2012: Bachelor of Science in Microbiology and Genetics from the University of Vienna

2012: Intern at the Research and Development Center of Biomin GmbH

2011: Intern at the Clinical Department of Virology at the Vienna General Hospital

2010: Intern at the Department of Microbiology of Ferring AG, Kiel, Germany

2009: Intern at Baxter AG, Department of Quality Assurance

2006 – 2007: Certified assistant paramedic with the Red Cross Vienna as part of alternative civil service

2003: Graduated from AHS Perchtoldsdorf